

**Creation of cellular models and functional investigation of *PARK2*
Copy Number Variants (CNVs) associated with
Attention-Deficit/Hyperactivity Disorder (ADHD)**

Dissertation

zur Erlangung des Doktorgrades

der Naturwissenschaften

vorgelegt beim Fachbereich 15

der Johann Wolfgang Goethe -Universität

in Frankfurt am Main

von

Viola Stella Palladino

aus Assisi (Perugia), Italien

Frankfurt 2019

(D 30)

vom Fachbereich 15 der

Johann Wolfgang Goethe - Universität als Dissertation angenommen.

Dekan: Prof. Dr. Sven Klimpel

Gutachter

Gutachterin: Jun. Prof. Michaela Müller-McNicoll, PhD

Gutachter: Prof. Dr. med. Andreas Reif

Datum der Disputation:

INDEX

INDEX	I
LIST OF FIGURES	V
LIST OF TABLES	VI
DECLARATION/ EHRENWÖRTLICHE ERKLÄRUNG	VII
ZUSAMMENFASSUNG	VIII
ABSTRACT	1
1 INTRODUCTION	4
1.1 ATTENTION-DEFICIT/HYPERACTIVITY DISORDER (ADHD)	4
1.1.1 Childhood and adult ADHD.....	5
1.1.2 Symptoms and comorbidities	7
1.1.3 Treatment.....	9
1.1.4 Genetics of ADHD	11
1.1.4.1 Genetic contribution	11
1.1.4.2 Environmental Risk factors- Nicotine exposure.....	12
1.1.4.3 Epigenetic	14
1.1.5 <i>PARK2</i> Copy Number Variations and ADHD.....	14
1.2 PARKIN RBR E3 UBIQUITIN PROTEIN LIGASE (PARK2)	17
1.2.1 <i>PARK2</i> : physiological function	17
1.2.2 <i>PARK2/PINK1</i> : Mitochondria quality control.....	19
1.2.3 <i>PARK2</i> and autosomal early-onset Parkinson’s Disease	20
1.2.4 Involvement of <i>PARK2</i> in ADHD: mitochondrial dysfunctions and oxidative stress	21
1.3 CELLULAR MODELS FOR PSYCHIATRIC AND NEURODEVELOPMENTAL DISORDERS	23
1.3.1 Human dermal fibroblast (HDF)	23
1.3.2 The advent of hiPSC and hiPSC-derived neurons: implications for neurodevelopmental and psychiatric research	24
1.3.2.1 Technique workflow	25
1.3.2.2 Neural Induction	26
1.3.2.3 Applications, advantages and limitations	26
1.3.3 Focus on available ADHD models	27
1.3.4 Focus on available <i>PARK2</i> models	28
1.4 AIMS AND EXPERIMENTAL DESIGN	31

1.4.1	PART 1: creation and validation of aADHD cellular model systems	31
1.4.2	PART2: Phenotyping	33
1.4.2.1	Evaluation of patho-phenotypes connected with ADHD/ <i>PARK2</i> CNVs in HDF and HiPSC after stress exposure.....	33
1.4.2.2	Evaluation of nicotine effects on HiPSC-derived dopaminergic neurons from aADHD patients	34
2	METHODS	36
2.1	Patients recruitment, psychiatric evaluation and neurological assessment	36
2.2	Cell culture methods.....	36
2.2.1	Generation and maintenance of human dermal fibroblasts	36
2.2.1.1	Cell counting, viability and doubling time.....	37
2.2.2	Fibroblast transfection for HiPSC generation	38
2.2.3	HiPSC cultures maintenance.....	38
2.2.3.1	Embryoid bodies assay.....	39
2.2.4	Neural induction and maintenance of HiPSC-derived dopaminergic neurons	39
2.2.5	Treatments	40
2.3	Genetic methods	40
2.3.1	DNA extraction	40
2.3.2	<i>PARK2</i> TaqMan Copy Number assay	41
2.3.3	Genotyping by Illumina Infinium Omni2.5-8 Bead Array.....	41
2.4	RNA methods.....	42
2.4.1	RNA extraction.....	42
2.4.2	Two step Reverse Transcription PCR (RT-PCR)	42
2.4.3	Quantitative RT-PCR (RT-qPCR)	43
2.4.3.1	RT-qPCR.....	43
2.4.3.2	<i>PARK2</i> pre-amplification and TaqMan Gene Expression assay.....	44
2.4.4	RNA-Sequencing	44
2.5	Microscopy methods	45
2.5.1	Live staining	45
2.5.2	Immunofluorescence for pluripotency markers, embryonic germs layers differentiation and neuronal markers.....	45
2.5.3	Immunofluorescence for mitochondrial network morphology.....	46
2.6	Protein methods.....	46
2.6.1	Protein extraction and measurement	46
2.6.2	<i>PARK2</i> protein concentration by enzyme-linked immunosorbent assay (ELISA)	47
2.6.3	DOPAMINE levels by ELISA	48
2.7	Assays for energy impairment and oxidative stress	48
2.7.1	ATP production	48
2.7.2	Oxygen consumption	49
2.7.3	ROS production.....	50
2.8	Data analysis and statistics	50
2.8.1	Data analysis for mitochondrial network morphology (macro)	50
2.8.2	Statistics.....	51
3	RESULTS.....	52

3.1	Summary of sample size	52
3.2	Neurological and psychiatric assessment.....	53
3.3	<i>PARK2</i> genotyping	56
3.4	Creation and validation of the models.....	59
3.4.1	Human dermal fibroblasts (HDFs)	59
3.4.2	Human induced pluripotent stem cells (HiPSC).....	60
3.4.2.1	<i>Expression of pluripotency markers</i>	62
3.4.2.2	<i>Pluripotency ability</i>	63
3.4.2.3	<i>Absence of viral vector</i>	65
3.4.2.4	<i>Genetic variations and relatedness</i>	65
3.4.3	HiPSC-derived dopaminergic neurons	68
3.4.3.1	<i>Expression of dopaminergic neurons markers</i>	69
3.4.3.2	<i>Dopamine levels</i>	72
3.5	Evaluation of patho-phenotypes connected with ADHD/<i>PARK2</i> CNVs in HDF and HiPSC after nutrient deprivation	74
3.5.1	<i>PARK2</i> gene expression	74
3.5.2	<i>PARK2</i> protein expression	75
3.5.3	Hypothesis driven gene expression analysis	77
3.5.4	Energy impairment and oxidative stress	83
3.5.5	Mitochondrial network morphology	88
3.6	Evaluation of nicotine effects on HiPSC-derived dopaminergic neuron from aADHD patients	93
3.6.1	Hypothesis free gene expression analysis (RNA-Sequencing).....	93
3.6.2	<i>PARK2</i> gene expression	98
3.6.3	<i>PARK2</i> protein expression	99
4	DISCUSSION.....	100
4.1	ADHD/<i>PARK2</i> CNV carriers used in the study do not show early signs of PD	100
4.2	HiPSC and HiPSC-derived neurons were positive for all the <i>bona fide</i> characterization tests performed without genotype differences	101
4.3	Evaluation of patho-phenotypes connected with ADHD/<i>PARK2</i> CNVs in HDF and HiPSC after stress exposure	103
4.3.1	ADHD/ <i>PARK2</i> CNV carriers show different <i>PARK2</i> protein levels but not gene expression.....	104
4.3.2	ADHD/ <i>PARK2</i> CNV carriers show lower levels of cellular ATP and extracellular oxygen consumption rates compared to controls	106
4.3.3	The amount of reactive oxygen species (ROS) is influenced by the stressors but not by genotype .	107
4.3.4	The mitochondrial network morphology is influenced by starvation stress but not by genotype ...	108
4.4	Evaluation of nicotine effects on HiPSC-derived dopaminergic neurons from aADHD patients.....	109
4.5	Limitations of the study and future perspectives	112
5	CONCLUSIONS.....	114
6	APPENDIX	116

6.1	List of antibodies used in this study	116
6.2	List of primers used in this study	118
6.3	List of abbreviations	119
7	BIBLIOGRAPHY	121
8	ACKNOWLEDGMENTS.....	135
9	CURRICULUM VITAE	136
10	LIST OF PUBLICATIONS	140

LIST OF FIGURES

Figure 1 Experimental design part 1: creation and validation of aADHD model systems.	32
Figure 2 Experimental design Part 2: phenotyping of ADHD/ <i>PARK2</i> CNVs model systems.....	35
Figure 3 Chromosome 6 ideogram and SNP array analysis of the <i>PARK2 locus</i> for the ADHD/ <i>PARK2</i> CNVs carriers	58
Figure 4 Human dermal fibroblast doubling time and viability	59
Figure 5 HiPSC morphological changing during transfection protocol	61
Figure 6 HiPSCs expression of pluripotency- specific markers by RT-PCR	62
Figure 7 HiPSCs expression of pluripotency-specific markers by Immunofluorescence.	63
Figure 8 Embryoid bodies assay	64
Figure 9 SeV detection RT-PCR.....	65
Figure 10 Copy Number Variants plot.....	66
Figure 11 Genetic relatedness matrix.	67
Figure 12 Neural Induction factors and media timeline	68
Figure 13 Morphological changes during the neural Induction.....	69
Figure 14 Neuronal maturation time-course analysis by quantitative RT-PCR (RT-qPCR).....	71
Figure 15 Immunofluorescence staining in mature HiPSC-derived dopaminergic neurons	72
Figure 16 Dopamine concentration in mature HiPSC-derived dopaminergic neuron.	73
Figure 17 <i>PARK2</i> gene expression in HDF in baseline condition and after nutrient deprivation stress.	74
Figure 18 <i>PARK2</i> protein levels in HDF.....	76
Figure 19 <i>PARK2</i> protein levels in HiPSC	77
Figure 20 Hypothesis driven gene expression analysis in blood samples.....	78
Figure 21 Hypothesis driven gene expression analysis in HDF..	80
Figure 22 Hypothesis driven gene expression analysis in HiPSC.....	82
Figure 23 ATP production in HDF	84
Figure 24 Basal oxygen consumption rates in HDF.....	86
Figure 25 ROS production in HDF.....	87
Figure 26 Mitochondrial network staining in HDF and HiPSC.....	89
Figure 27 Mitochondrial network aspect ratio and form factor in HDF in baseline conditions and after starvation stress.	90
Figure 28 Mitochondrial network aspect ratio and form factor in HiPSC in baseline conditions and after starvation stress.	92
Figure 29 Volcano Plots of differentially regulated genes.	95
Figure 30 Gene ontology enrichment analysis of upregulated DEGs after Nicotine acute treatment.	96
Figure 31 Venn diagram of DEGs.....	96
Figure 32 <i>PARK2</i> protein expression in HiPSC-derived dopaminergic neurons after nicotine treatment	99

LIST OF TABLES

Table 1 Genotype for the <i>PARK2</i> locus and demographic data of the donors used in this study.	52
Table 2 Demographic data and neurological assessment.....	54
Table 3 Psychiatric assessment of ADHD patients used in the study.	55
Table 4 <i>PARK2</i> genotyping by Duplex TaqMan CNV assay.....	57
Table 5 Statistics summary of <i>PARK2</i> gene expression in HDF.	75
Table 6 Statistics summary of hypothesis driven gene expression in blood samples.	79
Table 7 Statistics summary of hypothesis driven gene expression analysis in HDF.	81
Table 8 Statistics summary of hypothesis driven gene expression analysis in HiPSC.....	82
Table 9 Summary of the samples used for RNA sequencing.....	94
Table 10 List of genes differentially regulated after nicotine exposure.	97
Table 11 <i>PARK2</i> gene expression in baseline and after nicotine treatment in immature and mature HiPSC-derived dopaminergic neurons.....	98
Table 12: List of antibodies used in this study	116
Table 13: List of primers used in this study.....	118

DECLARATION/ EHRENWÖRTLICHE ERKLÄRUNG

I, Viola Stella Palladino born on 25.02.1989 in Assisi (Perugia-Italy), hereby declare that my Doctoral Thesis “Creation of cellular models and functional investigation of *PARK2* Copy Number Variants (CNVs) associated with Attention-Deficit/ Hyperactivity Disorder (ADHD)” conducted at the Department of Psychiatry, Psychosomatic Medicine and Psychotherapy, University Hospital Frankfurt, under the supervision of Prof. Dr. med. Andreas Reif and Jun. Prof. Michaela Müller-McNicoll with essential support and guidance by PD Dr. med. Sarah Kittel-Schneider, when not explicitly stated, is result of my own work. I did not receive any help or support from commercial consultants. All sources and materials applied are listed and specified in the thesis. Furthermore, I confirm that this thesis has not been submitted as part of another examination process at any German or foreign university neither in identical nor in similar form.

Place, Date

Signature

Hiermit erkläre Ich, Viola Stella Palladino, geboren am 25.02.1989 in Assisi (Perugia, Italien), dass ich die im Fachbereich Biowissenschaften an der Johann Wolfgang Goethe-Universität in Frankfurt am Main eingereichte Dissertation mit dem Titel “Creation of cellular models and functional investigation of *PARK2* Copy Number Variants (CNVs) associated with Attention-Deficit/ Hyperactivity Disorder (ADHD)” in der Klinik für Psychiatrie, Psychosomatik und Psychotherapie Universitätsklinikum Frankfurt unter Betreuung und Anleitung von Prof. Dr. med. Andreas Reif und Jun. Prof. Michaela Müller-McNicoll mit wesentlicher Unterstützung und Anleitung durch PD Dr. med. Sarah Kittel-Schneider ohne sonstige Hilfe selbst durchgeführt und bei der Abfassung der Arbeit keine anderen als die in der Dissertation angeführten Hilfsmittel benutzt habe. Ich habe bisher an keiner in- oder ausländischen Universität ein Gesuch um Zulassung zur Promotion eingereicht. Die vorliegende Arbeit wurde bisher nicht als Dissertation eingereicht.

Ort, Datum

Unterschrift

ZUSAMMENFASSUNG

HINTERGRUND: Entwicklungspsychiatrische Erkrankungen wie die Aufmerksamkeitsdefizits-/Hyperaktivitätsstörung (ADHS) des Erwachsenenalters, können Erkrankungen sein, welche die Betroffenen lebenslang in ihrer psychosozialen Funktion beeinträchtigen und Einfluss auf die gesamte Gesellschaft haben. ADHS ist eine klinisch sehr heterogene Erkrankung, welche nach dem amerikanischen Klassifikationssystem für Erkrankungen DSM-5 in drei Untergruppen eingeteilt werden kann (vorwiegend unaufmerksam, vorwiegend hyperaktiv und gemischt) und sich bei den betroffenen Individuen sehr stark unterscheidet hinsichtlich des Schweregrads der Symptome und des Ausmaßes an funktioneller Beeinträchtigung (American Psychiatric Association, 2013). In der Allgemeinbevölkerung liegt die Prävalenz bei schätzungsweise 4 bis 7% der Kindern und bei 2,5 bis 3,4 % der Erwachsenen weltweit (Polanczyk, Willcutt, Salum, Kieling, & Rohde, 2014; J. A. Ramos-Quiroga, Nasillo, Fernández-Aranda, Casas, & Casas, 2014). Es wird angenommen, dass zumindest 15 % der Kinder, welche mit ADHS diagnostiziert werden, die Vollaussprägung der Erkrankung bis zum 25. Lebensjahr zeigen und bei weiteren ca. 40% kann nur von einer teilweisen Remission gesprochen werden, d.h. es bestehen immer noch Symptome, welche die Betroffenen beeinträchtigen können (Franke et al., 2018).

Trotz zahlreicher Bemühungen diese häufige Erkrankung zu erforschen, ist die Ätiologie immer noch nicht komplett aufgeklärt. Deswegen gibt es eine steigende Nachfrage nach Krankheitsmodellen, welche helfen sollen, die kausalen Mechanismen der Erkrankung zu verstehen und parallel auch dazu dienen sollen, neue und effektivere Behandlungsverfahren zu erforschen.

Die neueste Entwicklung und Verbesserung der Generierung von humanen induzierten pluripotenten Stammzellen (*human induced pluripotent stem cells*, hiPSC) eröffnet eine ganz neue Ära der Modellierung von Erkrankungen. Mit dieser Technologie ist es möglich fast jedes schon differenzierte Gewebe in einen pluripotenten Status zurückzusetzen und dann die Differenzierung in ein anderes spezifisches Gewebe zu induzieren. Da die genetische Information des Patienten, welcher der Spender des Gewebes ist, erhalten bleibt, kann die

hiPSCs Technologie zum einen nützlich sein um patienten-generierte Gewebe zu untersuchen, die schwer zu erhalten sind vom lebenden Spender, wie zum Beispiel neuronale Zellen, zum anderen ergibt sich so die Möglichkeit patienten-generierte zellbasierte Medikamenten-Screening Methoden zu entwickeln (N. Liang et al., 2017).

Die Identifizierung von Pathomechanismen psychiatrischer Erkrankungen ist verkompliziert durch die multifaktorielle Genese psychiatrischer Störungen, welche sowohl genetische als auch Umweltfaktoren beinhaltet (Brikell, Kuja-Halkola, & Larsson, 2015; Franke et al., 2018).

Neue Schätzungen gehen davon aus, dass die genetische Komponente bei der ADHS zwischen 70 und 80% liegt (Brikell et al., 2015). Umweltfaktoren erklären vermutlich so um die 22% der Varianz der ADHS (Faraone et al., 2005; Nikolas & Burt, 2010; Franke et al., 2018). Viele Studien haben mit unterschiedlichen Herangehensweisen die Assoziation von verschiedenen Umwelt-Risikofaktoren mit ADHS untersucht. Die meisten Studien fokussierten sich auf die prä-, peri- und postnatale Periode und untersuchten verschiedene Substanzen oder Noxen, welche die Gehirnentwicklung negativ beeinflussen könnten (Banerjee, Middleton, & Faraone, 2007). Einer der an den besten replizierten Risikofaktoren für eine kindliche ADHS ist Rauchen der Mutter während der Schwangerschaft. Insbesondere aktives Rauchen der Mutter wurde mehrfach als assoziiert gezeigt mit einem erhöhten Risiko ein Kind mit ADHS zu bekommen (Motlagh et al., 2011; Rodriguez & Bohlin, 2005; Sagiv, Epstein, Bellinger, & Korrick, 2013; Schwenke et al., 2018). Ob dieser Zusammenhang allerdings kausal ist, ist noch Gegenstand der Diskussion.

Anfänglich wurden als genetische Risikofaktoren der ADHS, wie auch anderer psychiatrischer Erkrankungen, häufige Genvarianten untersucht, wie Einzelbasenpolymorphismen (*single nucleotide polymorphisms*, SNPs). In letzter Zeit wurden auch durch die Entwicklung von Scanning-Methoden des gesamten Genoms auch vermehrt rare Varianten hinsichtlich ihres Beitrags zur Krankungsentstehung untersucht, wie zum Beispiel so genannte Kopienanzahlvarianten (*copy number variants*, CNVs). Diese sind große genomische strukturelle Variationen, welche Deletionen, Duplikationen, Triplikationen und Translokationen umfassen im Vergleich zu einem Referenzgenom (Stankiewicz & Lupski, 2010). Ein vermehrtes Gesamt-Vorkommen von seltenen CNVs wurde sowohl in kindlichen als auch Erwachsenen-ADHS Stichproben berichtet (Guyatt et al., 2018; J.-A. Ramos-Quiroga et al., 2014).

Es wurde die Hypothese aufgestellt, dass das genetische Risiko der ADHS durch ein so genanntes polygenetisches Belastungsgrenzen Modell (*polygenetic liability threshold model*) am besten erklärt wird. In diesem Modell wird davon ausgegangen, dass bei betroffenen Individuen mit seltenen großen CNVs eine geringe Anzahl an häufigen genetischen Varianten ausreicht um dann eine ADHS zu entwickeln (J Martin, O'Donovan, Thapar, Langley, & Williams, 2015). Eine genomweite Analyse seltener CNVs von Jarick und Kollegen fand CNVs im *PARK2* Locus als assoziiert mit ADHS (Jarick et al., 2014). Das codierte Protein, *PARK2*, zusammen mit seinem Interaktionspartner *PINK1*, spielt eine Rolle in der Regulation des so genannten Mitochondrien-Qualitätskontrollsystems (*mitochondria quality control*, MQC). Damit zusammen hängen Mechanismen wie Mitophagie, Fusion und Fission, Biogenese und mitochondrialer Transport und zudem scheint *PARK2* in zellulärer Energiebalance und oxidativer Stressantwort involviert zu sein (Scarffe L.A., Stevens D.A., Dawson V.L., 2015).

Das Hauptziel dieser Studie ist die Identifizierung von krankheitsspezifischen zellulären Phänotypen bei adulter ADHS. Um dieses Ziel zu erreichen, haben wir Zellmodelle von ADHS Patienten generiert, welche die seltenen *PARK2* CNVs tragen, welche in der vorangegangenen Studie als mit der Erkrankung assoziiert beschrieben worden waren. Die Hypothese war, dass seltenere Genvarianten mit einem stärker ausgeprägten zellulären Phänotyp einhergehen könnten. Zudem wollten wir die Nützlichkeit und Machbarkeit von Zellmodellen bei entwicklungspsychiatrischen Erkrankungen belegen.

METHODEN: Der erste Teil der Studie war auf die Generierung und Validierung der Zellmodelle der ADHS fokussiert. In Rahmen dieses Projekts wurden drei verschiedenen Zellmodelle generiert: humane Hautfibroblasten (*human dermal fibroblast*, HDF), humane induzierte pluripotente Stammzellen (*human induced pluripotent stem cells*, hiPSCs) und daraus differenzierte dopaminerge neuronale Zellen (*hiPSC-derived dopaminergic neurons*). Begonnen wurde von einer größeren Kohorte von 12 Probanden, von denen HDF erhalten werden konnten. Von diesen wurden dann sechs Spender für die Generierung von hiPSC und dopaminergem Neurone ausgewählt: drei adulte ADHS *PARK2* CNV Risikoträger, (ein Duplikationsträger und zwei Deletionsträger, 1 Nicht-Risikogenvariantenträger mit ADHS und zwei gesunde Kontrollen).

Zunächst wurden die Techniken und Protokolle der hiPSC Gewinnung und Differenzierung in dopaminerge Neurone optimiert.

Dann wurde eine Reihe von Validierungstests durchgeführt um zu zeigen, dass die hiPSC tatsächlich pluripotente Zellen sind und die daraus differenzierten neuronale Zellen auch funktionale dopaminerge Neurone sind. Diese Tests werden als *bona fide* Charakterisierung bezeichnet. Für jede hiPSC Linie wurden drei verschiedene Klone untersucht um Varianz durch die Reprogrammierungsmethode auszuschließen bzw. zu minimieren. Bei allen Zelllinien und klonalen Linien konnten gezeigt werden, dass diese *bona fide* hiPSC sind mithilfe von morphologischen Analysen, RT-PCR, Immunofluoreszenz, Embryoid Body Assay und dem so genannten molekularen Karyotypisieren. Auch die aus den hiPSC differenzierten dopaminergen Neurone konnten als *bona fide* bestätigt werden mittels Immunofluoreszenz, RT-qPCR und Messung von Dopamin-Konzentration.

Der zweite Teil des Projekts zielte auf die Evaluierung des zellulären Phänotyps ab und hier sollte untersucht werden, ob die ADHS *PARK2* Variantenträger im Vergleich mit den gesunden Kontrollen bzw. ADHS Nicht-Risikovariantenträgern eine spezifischen zellulären Phänotyp zeigen würden. Das MQC System zum Beispiel kann unter normalen Bedingungen funktionieren, aber wenn es zu Störungen der zellulären Homöostase kommt, könnte man potentielle Dysfunktionen besser beobachten können (Pickrell & Youle, 2015). Daher wurden in der vorliegenden Studie verschiedenen Stressoren eingesetzt um potentiell vorhandene Dysregulationen des mitochondrialen Systems gegebenenfalls besser ausgeprägt sehen zu können. Zum einen unterzogen wir die Zellen einem Nährstoffentzug („Hungerversuch“), was eine Form des metabolischen Stresses darstellt, bei dem schon gezeigt wurde, dass er zu einem Anstieg der *PARK2* Expression führt (Klinkenberg et al., 2012). Zum anderen wählten wir die pharmakologische Behandlung mit Carbonyl-Cyanid-m-Chlorophenyl-Hydrazine (CCCP), welches ein Ionophor ist, dass durch Depolarisierung der mitochondrialen Membran *PINK1* Akkumulation triggert (Yamano, Matsuda, & Tanaka, 2016). Wir führten dann eine Reihe von Untersuchungen durch mit einem Fokus auf mitochondrialer Funktion und Energiemetabolismus (ATP Produktion, basale Sauerstoffverbrauchsrate, ROS Vorrat) sowie der *PARK2* Protein- und Genexpression bei den ADHS *PARK2* Trägern im Vergleich zu gesunden Kontrollen und ADHS Nicht-Risikovariantenträgern unter den verschiedenen oben genannten Stressoren.

Nachdem wir einen möglichen zellulären Phänotyp in den Fibroblasten und hiPCS identifiziert hatten, widmeten wir uns dem dopaminergen neuronalen Zellmodell, was natürlich für die ADHS als zerebrale Erkrankung die größte Relevanz hat. Wir untersuchten die Effekte von Nikotinexposition, weil Nikotin während der Schwangerschaft einer der an den besten replizierten Risikofaktoren ist, bezüglich des Risikos ein Kind mit ADHS zu bekommen. Daher exponierten wir hiPSC-generierte dopaminerge Neurone mit Nikotin-Konzentrationen, wie sie zum einen während des akuten Rauchens auftreten, zum anderen um zu modellieren, wie es ist, wenn Mütter kontinuierlich rauchen während der Schwangerschaft, im Folgenden als „akute“ und „chronische“ Nikotinexposition benannt (Lomazzo et al., 2011) (Srinivasan et al., 2016). Es wurde dann die PARK2 Protein Expression und die gesamte Genexpression mittels RNA Sequenzierung analysiert.

ERGEBNISSE: Eine neurologische Untersuchung auf Frühwarnzeichen einer Parkinsonerkrankung zeigte keine Auffälligkeiten bei den ADHS/PARK2 CNVs Trägern und damit keine Hinweise auf eine Komorbidität mit einer früh beginnenden Parkinson Erkrankung.

Die Zelllinien, die in dieser Studie generiert wurden, bestanden alle Charakterisierungstests als *bona fide* Stammzellen. Die hiPSC zeigten eine typische ES-ähnliche (embryonale Stammzell-ähnliche) Morphologie in der lichtmikroskopischen Untersuchung und exprimierten Pluripotenzmarker sowohl auf RNA- (DPPA5, SRY, SOX2, NANOG, POU5F1) als auf Protein-Ebene (TRA-1-60, SSEA4, POU5F1). Zudem waren die hiPSC in der Lage sich spontan in zelluläre Derivate der drei Keimblätter zu differenzieren (Endoderm, Ektoderm, Mesoderm). Genetische Analysen der hiPSC Klone bestätigten, dass keine zusätzlichen CNVs im genetischen Locus von Interesse durch die Reprogrammierungsmethode dieser Studie entstanden waren. Zudem zeigte sich kein genereller signifikanter Anstieg an CNVs im Vergleich zu den Fibroblasten der Spender und eine hohe genetische Verwandtschaft (*relatedness*) zwischen den hiPSC und den Fibroblasten vom selben Spender.

Die hiPSC-generierten dopaminergen Neuronen zeigten eine nervenzellen-artige Morphologie und Genexpression von neuronalen Markern eher unreiferer Stadien (LMX1B, NEUROD1, EN1, RBFOX3). Nach weiterer Reifung konnte gezeigt werden, dass hiPSC-generierte Neurone mit Immunfluoreszenzmikroskopie positiv markiert werden konnten für einen neuron-

spezifischen Marker (TUBB3) und einen spezifischen dopaminergen Marker (TH). Zudem konnten Dopamin-Konzentrationen sowohl im extrazellulären Medium als auch in intrazellulären Fraktionen gemessen werden.

In keiner der Charakterisierungsuntersuchungen, welche in Rahmen des vorliegenden Projekts durchgeführt wurden, konnte ein Unterschied zwischen den verschiedenen Genotypen festgestellt werden, was anders ist als in früheren Untersuchungen mit Zelllinien von Parkinson Patienten mit *PARK2* Mutationen (Shaltouki et al., 2015). Daher kann aus unseren Ergebnissen geschlussfolgert werden, dass die *PARK2* CNVs in unseren Zelllinien wohl nicht mit der dopaminergen Differenzierung interferieren.

Wir konnten allerdings anderweite Unterschiede zwischen den verschiedenen Zelllinien zeigen, zum einen konnten unterschiedliche *PARK2* Proteinkonzentrationen nach Nährstoffentzug bei den Zelllinien der ADHS/*PARK2* CNVs Trägern (HDF und hiPSC) gemessen werden, die *PARK2* Genexpression war jedoch nicht signifikant unterschiedlich.

Zudem zeigten die Zelllinien (HDF und hiPSC) der ADHS/*PARK2* CNV Träger niedrigere Konzentrationen an zellulärem ATP und eine geringere basale Sauerstoffverbrauchsrate im Vergleich zu Zellen von gesunden und ADHS Nichttrisikovariantenträgern sowohl bei der Baseline-Bedingung als auch nach 24h Nährstoffentzug.

Unserer Versuche mit den Fibroblasten der verschiedenen Spender geben Hinweise, dass sowohl die Gesamtmenge an reaktiver Sauerstoff-Spezies (ROS) als auch die mitochondriale Netzwerkmorphologie zwar von den verschiedenen Stressoren beeinflusst werden aber nicht vom Genotyp. Diese Ergebnisse passen zu unserer hypothesen-getragenen Genexpressionsanalyse, welche vorher durchgeführt wurde. Fibroblasten der ADHS/*PARK2* CNV Träger zeigten eine gesteigerte Genexpression von NAD(P)H Quinon Dehydrogenase1 (NQO1) nach Nährstoffentzug. *NQO1* spielt eine protektive Rolle bei oxidativem Stress und damit der Produktion von Radikalen und könnte daher einen kompensatorischen Mechanismus erklären bei den Risikoträgern, was dann dazu führt, dass es keine Unterschiede zu den Kontrollen bei der Gesamtmenge an ROS gab (Ross & Siegel, 2017).

Die Auswertung der Nikotineffekte der hiPSC-generierten dopaminergen Neurone der adulten ADHS Patienten zeigte keine Effekte auf *PARK2* Protein Konzentrationen und Genexpression. Die Analyse differentiell exprimierter Gene (DEGs) zwischen ADHS/ *PARK2* CNVs Trägern mit

den Wildtypkontrollen in den jeweiligen Bedingungen zeigte eine Reihe differentiell exprimierter Gene. Die hiPSC-generierten neuronalen Zellen der ADHS/*PARK2* CNV Träger zeigten nach Nikotinexposition insbesondere Gene angereichert (Gene Ontology Enrichment Analyse) in Signalwegen, welche mit der Regulation vom Zellwachstum assoziiert sind. Um die Genotyp-spezifischen Einflüsse von den nur durch Nikotin-induzierten Veränderungen der Genexpression auseinanderhalten zu können, analysierten wir die Gene genauer, die signifikant herauf- oder herunterreguliert waren sowohl nach akuter und chronischer Nikotinexposition aber nicht in der Baseline-Bedingung. Wir identifizierten 11 Gene, die nach beiden Nikotinexpositionen differentiell reguliert waren, zwei von diesen spielen eine Rolle in der Energieproduktion und oxidativer Stressantwort (*C1QTNF3* und *CART*) und drei sind in Prozessen der extrazellulären Matrix und Zelladhäsion involviert (*MAFAP1*, *PCDHGA6*, *COL5A1*).

SCHLUSSFOLGERUNG: Die vorliegende Studie gibt erste Hinweise auf einen beeinträchtigten mitochondrialen Stoffwechsel in Zellmodellen von adulten ADHS Patienten, welche seltene CNVs im *PARK2* Locus tragen. In den letzten Jahren wurden mehrfach mitochondriale Dysfunktionen mit der Ätiologie von verschiedenen psychiatrischen und neurodevelopmentalen Erkrankungen in Verbindung gebracht (McCann & Ross, 2018). Zudem wurde ein generell gesteigerter oxidativer Stress und insuffiziente Antwort auf oxidative Stressschädigung bei sowohl Kindern als auch Erwachsenen mit ADHS beschrieben (Joseph, Zhang-James, Perl, & Faraone, 2015) (Lopresti, 2015). Die teilweise beeinträchtigten Mitochondrienfunktionen könnten zur Störung der normalen Gehirnplastizität und zellulären Resistenz insbesondere in sehr sensitiven Zeitfenstern der Gehirnentwicklung führen. Zudem zeigen unsere ersten Ergebnisse bezüglich Nikotinexposition, als gut bekannter pränataler Umwelt-Risikofaktor für ADHS, Hinweise für eine besondere Empfindlichkeit der *PARK2* CNV Trägern diesbezüglich in Prozessen, welche in Regulation von Zellwachstum involviert sind sowie extrazellulärer Matrixkomposition und Zelladhäsion. Neuronale Zellreifung und Bildung von funktionierenden neuronalen Verbindungen und funktionellen Synapsen wird erreicht durch ein komplexes Zusammenspiel zwischen extrazellulären Matrix-Glykoproteinen und Zelladhäsionsmolekülen (Washbourne et al., 2004), daher passen unsere Befunde zu ADHS als entwicklungspsychiatrischer Erkrankung,

Verschiedene vorherige Studien haben Hinweise für eine abnormale Gehirnkonnektivität bei ADHS erbracht (Gehricke et al., 2017). Zukünftige Experimente werden zeigen, ob die Beeinträchtigungen des mitochondrialen Energiemetabolismus auch in den hiPSC-generierten dopaminergen neuronalen Zellen zu finden sind und ob diese ebenfalls auf die Nikotinexposition reagieren.

Zusammenfassend zeigte die vorliegende Studie ein neues Zellmodellsystem um die Ätiopathogenese der ADHS assoziiert mit seltenen CNVs im *PARK2* Locus zu erforschen. Zudem kann die Identifizierung eines krankheitsrelevanten Phänotyps in diesem Zellmodell in der Zukunft hilfreich sein um neue pharmakologische Therapiemethoden zu testen.

ABSTRACT

BACKGROUND: Attention-Deficit/Hyperactivity Disorder (ADHD) is one of the most common neurodevelopmental disorders worldwide. As described in the DSM-5, ADHD is clinically heterogeneous with three main subtypes; predominant hyperactive, predominant attention deficit and combined. The severity of symptoms widely differs among the patients and interferes with the person functioning, negatively impacting social and occupational activities (American Psychiatric Association, 2013). Despite the many efforts, the etiology of the disorder is still unclear. Therefore, there is an increasing demand of models that would help elucidating the causative mechanisms of the disorder and, in parallel, would be valuable tools to discover new and effective treatments. The main goal of the study is the identification of disease specific cellular phenotypes related to Attention-Deficit/Hyperactivity Disorder (ADHD) in cellular models from patients carrying rare copy number variants (CNVs) in the *PARK2* locus that have been previously associated with ADHD (Elia et al., 2010; Jarick et al., 2014).

METHODS: Human dermal fibroblast (HDF) cultures were obtained from skin punches and reprogrammed into human induced pluripotent stem cells (HiPSC) and successively induced to differentiate into HiPSC-derived dopaminergic neurons. Both HiPSC and HiPSC-derived neurons, were proven to be *bona fide* models by morphological analysis, RT-PCR, RT-qPCR, immunofluorescence, embryoid body assay, molecular karyotyping and dopamine level quantification. A total of six donors were selected for HiPSC and dopaminergic neuron generation: 3 adult ADHD *PARK2* CNV risk carriers (1 duplication and 2 deletion carriers, 1 ADHD non-risk CNV variant carrier and 2 healthy controls).

We conducted stress-response experiments (nutrient deprivation and CCCP administration) that are well known to increase *PARK2* expression, on both fibroblasts and HiPSC. After assessing *PARK2* gene and protein expression levels, we evaluated the gene expression of genes that are involved with different processes orchestrated by *PARK2*. We then performed a series of assays with a special focus on mitochondrial function and energy metabolism (ATP

production, basal oxygen consumption rates, ROS abundance) and evaluated changing in the mitochondrial network morphology.

To evaluate the effect of nicotine exposure, one of the best replicated prenatal risk factors for having a child later on diagnosed with ADHD, we treated HiPSC-derived dopaminergic neurons with smoking-relevant nicotine concentrations and evaluated PARK2 protein expression after treatment and gene expression by RNA sequencing.

RESULTS: The cell models created in this study passed all the characterization tests required to assess whether the lines can be considered *bona fide* models without underlying genotype differences. The evaluation of patho-phenotypes connected with ADHD/*PARK2* CNVs in HDF and HiPSC showed that, although *PARK2* gene expression was unchanged, ADHD/*PARK2* CNV carriers show different *PARK2* protein levels possibly implying the presence of different post-transcriptional processes. ADHD/*PARK2* CNV carriers show lower levels of ATP production and basal oxygen consumption rates compared to controls, a result in line with what was already reported in ADHD cybrids cells model (Verma et al., 2016). Our experiments indicate that both the amount of reactive oxygen species (ROS) and the mitochondrial network morphology is influenced by the treatment but not by the genotype. The evaluation of nicotine effects on HiPSC-derived dopaminergic neuron from aADHD patients showed no effects on *PARK2* protein levels and gene expression. ADHD/*PARK2* CNVs carriers show gene ontology enrichment in modules connected with the regulation of cell growth after nicotine acute treatment. Additionally, genes connected with energy production & oxidative stress response and extracellular matrix & cell adhesion were significantly differentially expressed after nicotine treatments.

CONCLUSIONS: This study points out the presence of impairment of mitochondrial energetics in cellular models derived from adult ADHD patients carrying rare CNVs within the *PARK2* locus. In the last years, several studies have linked mitochondrial impairments to the etiology of psychiatric and neurodevelopmental disorders (McCann & Ross, 2018) and reported an overall increase of oxidative stress or insufficient response to oxidative damage both in children and adults with ADHD (Joseph, Zhang-James, Perl, & Faraone, 2015; Lopresti, 2015). Additionally, different groups have underlined an abnormal brain connectivity in ADHD patients in their work (Gehricke et al., 2017). Our preliminary investigation of the effects of a

well-known prenatal risk factor for ADHD, nicotine gestation exposure, point out a susceptibility of the *PARK2* CNVs carriers in processes involved in regulation of cell growth and in proteins connected with extracellular matrix composition and cell-adhesion molecules, all factors necessary for neuronal maturation and formation of proper neural connections (Washbourne et al., 2004). In conclusion, this study presents novel and fully validated cellular model systems to study the etiopathogenesis of ADHD based on rare CNVs in the *PARK2 locus*. Moreover, the identification of disease-relevant phenotypes in the model might be helpful in the future for testing new alternative medications.

1 INTRODUCTION

Neurodevelopmental and psychiatric disorders, such as Attention-Deficit/Hyperactivity Disorder (ADHD), can be lifelong conditions that affect strongly the personal life of the patient and have an impact of society itself. As the name suggests, core features of ADHD are hyperactive-impulsive traits and inattentive symptoms. In the present chapter the heterogeneous spectrum of symptoms and comorbid disorders of both the childhood and adult form of ADHD will be discussed. Additionally, the available options for treatment will be presented and an overview of the complex genetic panorama of the disorder will be given, with a special focus on the available knowledge of the pure genetic contribution and the known environmental risk factors to develop the disease. Finally, the importance of copy number variants (CNVs) in the genetic of ADHD and the association between CNVs within the *PARK2 locus* and ADHD will be displayed.

1.1 ATTENTION-DEFICIT/HYPERACTIVITY DISORDER (ADHD)

ADHD is characterized by being clinically heterogeneous with a large spectrum of symptoms and severity. This is the reason why the core diagnostic criteria have been refined over the years and vary across the different versions of the diagnostic manuals. In the clinical practice, ADHD is usually diagnosed following the diagnostic criteria of the International Classification of Mental and Behavioral Disorders 10th revision (ICD-10) published by the World Health Organization (WHO) or, more often, the Diagnostic and Statistical Manual for Mental Disorders (DSM) (American Psychiatric Association, 2013). The latest edition of the DSM (DSM-5) requires that inattention and/or hyperactivity/impulsivity is shown persistently for at least 6 months and interferes with the person functioning or development, negatively impacting social and academic/occupational activities (American Psychiatric Association, 2013). Moreover, the symptoms must have begun prior to age 12 (in the previous version the age was set at 6) and interfere with the normal functioning in 2 or more settings. ADHD can be further divided into 3 main subtypes: primarily hyperactive/impulsive, primarily inattentive,

and combined type (American Psychiatric Association, 2013). In the clinical practice ADHD diagnosis is made by diagnostic interviews with rating scales questionnaires tailored for the age and adapted for the country, such as The Diagnostic Interview for adults ADHD (DIVA 2.0). For adult ADHD self-report questionnaires are used as, for example, the Adult ADHD Self-Report Scale (ASRS-v1.1 from the WHO), Conners' Adult ADHD Rating Scale for DSM-IV (CAARS) (Christiansen et al., 2012). Additionally, to assess the childhood symptomatology retrospectively, Wender-Utah Rating Scale is used (WURS-k) (Retz-Junginger et al., 2002). Furthermore, written reports about behavior at school are valuable information. To capture specific symptoms of adult ADHD like emotional dysregulation and disorganization, the Wender-Reimherr-Interview is usually used (WRI) (Rösler et al., 2006).

For diagnosing childhood ADHD, teacher and parent ratings are mandatory because self-report is only possible from adolescence on. However, also for the diagnosis of adult ADHD it is very important to get reports from family members, friends or colleagues at work because ADHD patients themselves tend to underestimate the symptom severity (Subcommittee on Attention-Deficit/Hyperactivity Disorder et al., 2011). Additionally, to exclude a somatic cause of the symptoms, the medical history needs to be captured, routine blood results are needed including thyroid function as well as a neurological and medical examination. To exclude epilepsy an EEG should be done at least once, as well before starting the medication. If there are neurological soft signs, a cerebral MRI should be conducted. To exclude other psychiatric disorders as a cause of the symptoms, an extensive psychiatric anamnesis should be done by an experienced psychiatrist.

1.1.1 Childhood and adult ADHD

Although a large proportion of the general population still believes that ADHD is mainly a childhood disorder (cADHD), a great number of population-based analysis and longitudinal follow-up studies have shown that ADHD is also present in adults (aADHD) (Faraone & Biederman, 2016).

The general population prevalence of ADHD in the childhood has been estimated to be around 4% to 7% (Spencer, Biederman, & Mick, 2007)(Polanczyk et al., 2014). In the adult population ADHD prevalence rates are believed to be between 2.5% and 3.4%, as reported by meta-

analysis (J. A. Ramos-Quiroga et al., 2014) (Simon, Czobor, Bálint, Mészáros, & Bitter, 2009) (Fayyad et al., 2007).

It has been estimated that at least 15% of children diagnosed with ADHD will continue to retain a full diagnosis by the age of 25 (“persistent ADHD”) from the other 85%, just 50% will have a complete remission (“remitted ADHD”) whereas the other half will show just a partial remission and continue to experience impairing symptoms (Faraone, Biederman, & Mick, 2006; Franke et al., 2018). In this regard, it must be pointed out that, until the publication of the 5th edition of the DSM in 2013, ADHD in adults was still diagnosed using the childhood criteria and this could have misled the estimations in adults.

The symptomatology of ADHD seems to slightly vary according to the age. Whereas young children show hyperactive-impulsive traits more prominently, ADHD patients suffer more of inattentive symptoms, such as forgetfulness and difficulty in paying attention to details and organizing tasks and activities (Katzman, Bilkey, Chokka, Fallu, & Klassen, 2017). As reported in a recent review by Franke and colleagues, patients that meet the ADHD diagnostic criteria after the age of 12 can be further divided into two main groups (Franke et al., 2018). The first group, classified as “acquired or secondary ADHD”, shows a high rate of correlation between the insurgence of ADHD symptoms and an event of traumatic brain injury (TBI) (Schachar, Park, & Dennis, 2015). The second part is composed by “idiopathic ADHD”. Although it has been suggested that the adult form is not necessarily a continuation of childhood ADHD (Moffitt et al., 2015), it is still in debate if ADHD arises *de novo* in adulthood. In fact this might be due to a pre-existence of a sub-threshold ADHD in the childhood that, although present was not impairing enough to be diagnosed (Faraone & Biederman, 2016) (Franke et al., 2018).

It is still unclear how and why some children “grow out” of ADHD in the adulthood. During the last decade different theories have been proposed that can be summarized into two main models. The “normalization model”, is based mostly on results from studies that report no significant difference in cognitive control, functional connectivity and prefrontal cortical morphology between previously affected and never affected, suggesting that the remission is due to the convergence towards a more typical brain structure and function (Shaw et al., 2015). The second model, the “compensation model”, suggests the recruitment of new compensatory brain systems (Francx et al., 2015). Recently Sudre and colleagues proposed

that both mechanism could occur in “remitted ADHD” patients possibly at different levels in diverse brain areas (Sudre, Mangalmurti, & Shaw, 2018).

As already mentioned, ADHD is an extremely heterogeneous disorder and, not only the prevalence of the type of symptoms but also the gender prevalence, seems to differ depending on the age range. In fact, in childhood and adolescence the patients population is mainly composed by male (80%), whereas in the adult population the gender ratio decrease to nearly 1:1 (Kooij et al., 2010). Although it might be hypothesized that males could have a tendency to “grow out” from the disorder during adulthood, a systematic review of the literature does not pin point the gender as being associated with the persistence or remittance of ADHD symptoms (Caye et al., 2016) nor a higher burden of common ADHD risk variants was found in females affected (Joanna Martin et al., 2018). Therefore, this discrepancy in gender ratio between child and adult ADHD might be due to a under identification and underdiagnosis of female ADHD patients in young age. This might be connected with the fact that females with ADHD are reported to have more inattentive symptoms rather than hyperactive ones when compared with males or because of the co-existence of other psychiatric disorders. Both factors might therefore complicate the diagnosis of ADHD (Skogli, Teicher, Andersen, Hovik, & Øie, 2013).

1.1.2 Symptoms and comorbidities

ADHD patients present pronounced functional and psychosocial difficulties that have a profound personal and societal cost. Stringently, the core symptoms underlying neuropsychological processes are: impaired inhibition and memory (Ossmann & Mulligan, 2003), decision making (Mowinckel, Pedersen, Eilertsen, & Biele, 2015), executive functioning (Boonstra, Oosterlaan, Sergeant, & Buitelaar, 2005) as well as dysregulation in the default-mode network. Emotional dysregulation is a common feature too, especially in adult ADHD patients (Retz, Stieglitz, Corbisiero, Retz-Junginger, & Rösler, 2012).

ADHD affects many aspects of the everyday and professional life. Many studies have shown an association between ADHD and educational difficulties, such as lower grades, high rates of retention, lower rates of graduation (Galéra, Melchior, Chastang, Bouvard, & Fombonne, 2009; Wilens & Dodson, 2004). The difficulties persist also later on in life, with ADHD patients

presenting higher rates of unemployment, difficulties in maintaining jobs and general financial problems (Biederman et al., 2006). On a social interaction level, it has been demonstrated that ADHD patients show also impaired relationships (Minde et al., 2003; Seo et al., 2014). Additionally, research has shown an increased risk taking behaviour (Barkley, Murphy, Dupaul, & Bush, 2002) as well as pathological gambling (L. Jacob, Haro, & Koyanagi, 2018) and lower life expectancy (Dalsgaard, Ostergaard, Leckman, Mortensen, & Pedersen, 2015) with an increased involvement in transport accident (Z. Chang, Lichtenstein, D'Onofrio, Sjölander, & Larsson, 2014) and suicide (Ljung, Chen, Lichtenstein, & Larsson, 2014). A recent work by Du Reitz and colleagues, has analyzed if the polygenic risk scores obtained by the latest mega genome-wide association study (GWAS) on ADHD (Demontis et al., 2017) predicts genetic association with one of the previously mentioned outcomes. They found that polygenic risk for clinically diagnosed ADHD predicts higher tendency to be prone to psychological stress, risk-taking, alcohol and nicotine use, anxiety and depressive disorders, BMI, and lower general cognitive ability in an adult population sample (Du Rietz et al., 2018).

ADHD patients often show other comorbid psychiatric disorders such as substance use disorder, disruptive and antisocial behavior, anxiety disorders, major depression and bipolar disorder (Franke et al., 2018; Sobanski et al., 2007). Substance use disorder (SUD) seems to be comorbid regardless the age of the ADHD patient: ADHD adolescents have an early onset and increased use of alcohol, nicotine and illegal drugs (Charach, Yeung, Climans, & Lillie, 2011) and drug abuse or dependency has been reported to be increased in ADHD in comparison to general population as well (Buchmann et al., 2009; Jacob et al., 2007). Disruptive and antisocial behavior such as oppositional defiant disorder (ODD), and conduct disorder (CD) seems to have a high rate of comorbidity in children and adolescents ranging from 25% up to 80% (Rösler et al., 2004). Anxiety disorder, major depression and bipolar disorders are significantly comorbid in adult ADHD patients (Jacob et al., 2007; Meinzer et al., 2013). Moreover, about 50% of the adult ADHD patients can be diagnosed with personality disorders and recent research hints at a shared genetic basis of ADHD and borderline personality disorder (BPS) (Matthies & Philipsen, 2014; Moukhtarian, Mintah, Moran, & Asherson, 2018).

ADHD shares as well a strong comorbidity with another neurodevelopmental disorder, autism spectrum disorder (ASD). It has been estimated that 20 up to 50% of children diagnosed with ADHD also meet criteria of ASD (Rommelse, Geurts, Franke, Buitelaar, & Hartman, 2011).

Accounting for this strong comorbidity, the latest DSM edition allows the comorbid diagnosis of both the disorders. Although ASD-ADHD has been mainly studied in children recent data support that the comorbidity is still present in the adult population (Hartman, Geurts, Franke, Buitelaar, & Rommelse, 2016) and that could be linked to genetic and familiar factors and relatives of individuals with ASD are at higher risk of developing ADHD (Ghirardi et al., 2018).

1.1.3 Treatment

A large amount of literature shows how the symptoms of ADHD can be treated relatively effectively in both children and adults. Treatments for ADHD can be divided into two broad categories, pharmacological treatments and non-pharmacological treatments based mostly on cognitive-behavioral therapy, psychoeducation and behavioral training and most importantly parent training. It has been shown that a multimodal approach shows a significant improvement of the core ADHD symptoms, however, stimulant therapy has been proven in several studies to have the best efficacy in treating the core symptoms and is in this indication clearly superior to non-pharmacological treatments (Philipsen et al., 2015). Nevertheless, psychotherapy (cognitive behavioral psychotherapy) and psychoeducation are effective in helping the ADHD patients cope with their symptoms. The efficacy of methods like neurofeedback is still not clear enough (Razoki, 2018) so that the current German S3 guidelines cannot recommend neurofeedback (<https://www.awmf.org/leitlinien/detail/II/028-045.html>).

Pharmacological treatments for ADHD can be further divided into stimulants medications, usually the first line of treatment (such as methylphenidate, mixed amphetamine salts, and lisdexamfetamine dimesylate) and non-stimulant medication (such as atomoxetine, guanfacine and clonidine) (Katzman et al., 2017). Methylphenidate (MPH) (known with the trade name Ritalin, Medikinet, Concerta, Tranquilyn...) is the drug most widely used in ADHD treatment and its use is officially approved for both in adults and children in most European countries (Ramos-Quiroga et al., 2013). However, in Germany only two long-acting methylphenidate formulations are approved to initiate the treatment in adult patients (Ritalin adult, Medikinet adult). Although there might be an overestimation of amphetamine efficacy due to the experimental design, meta-analysis of the current literature has proven that amphetamines reduce the severity of ADHD symptoms in adults in the short term (Castells,

Blanco-Silvente, & Cunill, 2018). However, about 20% to 50% of adults patients are believed to be non- or partial-responders to stimulant medication due to insufficient symptom reduction or inability to tolerate adverse effects and consequently, there is pressing demand for alternative medication (Torgersen, Gjervan, & Rasmussen, 2008).

The chemical structure of amphetamines is extremely similar to the ones of catecholamine neurotransmitters, such as dopamine (DA) and noradrenaline (NE) and explains why they act as competitive substrate for the monoamine reuptake transporters, DAT (dopamine transporter), NET (noradrenaline transporter), and SERT (5-HT transporter) (Heal, Smith, Gosden, & Nutt, 2013). Although the exact mechanism of action of amphetamine is not completely understood, the end point effect of amphetamine administration is an increase level of DA and NE at the synaptic cleft. This might be due to the inhibition or the inversion of the transport direction of DAT, inhibition of the vesicular monoamine transporter 2 (VMAT-2), increase in exocytosis of vesicles containing DA or inhibition of catecholamine metabolism through catechol-O-methyltransferase and monoamine oxidase (COMT) activity inhibition (Castells et al., 2018; Heal et al., 2013). Additionally, some studies point out that amphetamines also interact with glutamate and opioid systems (Faraone, 2018).

Similarly to amphetamines, methylphenidate administration causes an increase of synaptic availability of both DA and NE (J Zhu & Reith, 2008). In fact, MPH acts as an indirect DA agonist that binds to the DAT and NET and blocks the inward transport of DA and NE into the presynaptic terminal (Héron, Costentin, & Bonnet, 1994). Additionally, MPH administration causes a redistribution of VMAT-2 (Riddle, Hanson, & Fleckenstein, 2007). Although MPH drug formulations usually contain a 1:1 racemic mixture of MPH enantiomers, data show a stronger pharmacological potency of the d-threo-MPH enantiomer (Srinivas, Hubbard, Korchinski, & Midha, 1993).

It has been demonstrated that both methylphenidate and amphetamines in general act in brain regions, such as the corticostriatal systems, that influence cognition and executive functions. Specifically they are involved in regions previously associated with emotional regulation, decision making and reward, all processes dysregulated in ADHD patients (Faraone, 2018).

1.1.4 Genetics of ADHD

Neurodevelopmental disorders, such as ADHD or ASD are believed to be due to a combination of genetic and environmental factors as well as epigenetic modifications. Over the years different genetic approaches such as classical family and twin studies, candidate genes association studies and genome wide association studies (GWAS) have investigated the genetic contribution to the disorder. The genetic contribution to childhood and adolescent ADHD is believed to be between 0.7 and 0.8, as reported by meta-analysis of multiple large-scale twin studies (Nikolas & Burt, 2010). The estimation of adult ADHD genetic heritability varies across the studies but estimates show values similar to the one of cADHD (Brikell et al., 2015). The environmental component of the risk of ADHD seems to be lower than the true genetic one and is believed to explain about the 22% of ADHD variance (Faraone et al., 2005; Franke et al., 2018; Nikolas & Burt, 2010).

1.1.4.1 Genetic contribution

Although, as reported, environmental factors and epigenetic mechanisms have a role in the etiopathogenesis of the disorder, it has been shown a strong genetic component in children affected of ADHD with heritability rates of about 75% (Faraone & Mick, 2010). Reviewing of the recent literature on the genetic component of adult ADHD shows differences in the estimated heritability among the studies. This effect is most likely due the symptoms self-rating system used, where adult ADHD patient might underestimate the severity of symptoms; therefore, it has been proposed that the heritability of aADHD might actually be similar to the one of cADHD (Bonvicini, Faraone, & Scassellati, 2016; Brikell et al., 2015).

In the last decades a total of seven genome wide linkage studies have been conducted on ADHD (Franke et al., 2018). Those analysis have identified different genetic loci possibly involved (5p13, 14q12, and 17p11) and some gene candidates such as *PARK2*, *SLC6A3*, *DRD4*, *DRD5*, *SLC6A4*, *HTR1B*, *SNAP-25*, *DIRAS2*, *LPHN3* and *NOS1*, mainly involved in neurotransmission and/or functionally related genes or pathways (Arcos-Burgos et al., 2010; Hawi et al., 2015; Reif et al., 2012). Findings among the studies show a very little replication or overlap that might be explained by the strong heterogeneity and multifactorial nature of the disorder; extremely large effects might be needed in order to surpass the threshold of genome-wide significance. This is the reason why Demontis and colleagues have performed a super large genome-wide association meta-analysis of all prior GWAS studies achieving

therefore large end numbers (20,183 ADHD cases and 35,191 controls). By using this approach, they identified 12 independent loci that surpass genome-wide significance (Demontis et al., 2017).

To explain and quantify the contribution of the thousands risk-variants under covered by the GWAS studies on psychiatric disorders, the concept of polygenic risk scores was introduced (International Schizophrenia Consortium et al., 2009). The polygenic risk score, also known as genome wide score, reflects the sum of all known known risk alleles weighted for the known risk of the variant itself (Zheutlin & Ross, 2018). This allows to estimate the contribution of variants that exert small effects to ADHD phenotype and it has been shown that predicts both hyperactivity and inattention traits in the general population (Hamshere et al., 2013) and autism spectrum disorder (Joanna Martin, Hamshere, Stergiakouli, O'Donovan, & Thapar, 2014).

1.1.4.2 Environmental Risk factors- Nicotine exposure

Several diverse studies have investigated the association of different risk factors with ADHD. Most of the studies have focused on the pre-, peri- and postnatal periods and have indicated a number of substances or events that could affect the typical neurodevelopment (Banerjee et al., 2007).

It has been reported that pre- and perinatal risk factors related to the mother behavior during pregnancy are positively associated with a higher risk of a child later diagnosed with ADHD. Proves of an association with ADHD are reported in regards of gestational alcohol exposure (Mick, Biederman, Faraone, Sayer, & Kleinman, 2002) and illegal drug use (Sagiv et al., 2013). Additionally, it has been suggested that maternal stress (Rodriguez & Bohlin, 2005; Van den Bergh & Marcoen, 2004) and obstetric problems during pregnancy (Tole et al., in revision, 2018) could also play a role as ADHD risk factors. Post-natal risk factors have been suggested to be a low Apgar score (a measure of the physical condition of the new-born) at 5 minutes (Li, Olsen, Vestergaard, & Obel, 2011) (Schwenke et al., 2018), not-on-term birth (Silva, Colvin, Hagemann, & Bower, 2014), low birth weight (Halmøy, Klungsoyr, Skjærven, & Haavik, 2012) and being highly crybabies (Tole et al., in revision, 2018).

Active nicotine exposure during pregnancy has been repeatedly demonstrated to be associated with ADHD and is one of the best replicated risk factor for this disorder (Motlagh et al., 2011; Rodriguez & Bohlin, 2005; Sagiv et al., 2013; Schwenke et al., 2018). As for many

environmental risk-factors, it is difficult to disentangle the pure risk-factor contribution from other additive and/or concomitant effects. In fact, maternal smoking might be a consequence of the presence of a pre-existent or concomitant risk factor such as for example an increased level of maternal stress. At the same time, the presence of risk factor itself may actually be due to an underlying genetic cause (Ficks & Waldman, 2009). In fact, mother affected from ADHD or with a genetic predisposition to impulsive tendency, show high levels of nicotine consumption (McClernon & Kollins, 2008).

Nicotine, a natural alkaloid contained in tobacco leaves, is rapidly absorbed systemically during smoking (Benowitz and Jacob 1984); after a puff, high levels of nicotine reach the brain in 10–20 seconds, producing rapid behavioral reinforcement (Benowitz 1990). Nicotine, and its lactam derivative cotinine, binds to brain tissues with high affinity, and the receptor binding capacity is increased in smokers compared with non-smokers (Breese et al. 1997; Perry et al. 1999). Additionally, by crossing the placental barrier, nicotine can be transferred from the maternal circulation to the fetus (Jauniaux, Gulbis, Acharya, Thiry, & Rodeck, 1999; Pastrakuljic et al., 1998; Tiesler & Heinrich, 2014). Many studies have underlined a wide range of adverse health effect in the newborn, such as low weight at birth, preterm delivery, sudden infant death syndrome, after both active smoking behavior by the mother and passive smoking exposure (DiFranza, Aligne, & Weitzman, 2004; Salmasi, Grady, Jones, & McDonald, 2010). A large number of studies have investigated the association between gestational exposure to nicotine and ADHD as summarized by many reviews on the topic (Linnet et al., 2003; Tiesler & Heinrich, 2014) that concluded that most studies reported an increased risk for the development of such problems in children of smoking mothers, some even showing a dose–response effect in the association. On a GxE level, fetal nicotine exposure has been connected with oppositional and hyperactive-impulsive symptoms and ADHD diagnosis in children carrying a genetic risk variant for ADHD, the *DAT1* VNTR genotype and the *DAT1* 9-repeat allele (Kahn et al., 2003; Neuman et al., 2007). Interesting, mouse subject to a prolonged prenatal nicotine exposure show the full range of ADHD-associated behavioral phenotypes, decrease in cingulate cortical volume and radial thickness and a low dopamine turnover in the frontal cortex (Jinmin Zhu et al., 2012; Jinmin Zhu et al., 2017).

Subjects whose mother smoked during pregnancy, show reduced grey matter volume in the cerebral cortex, smaller volume of the corpus callosum and thinning in the frontal, temporal and parietal regions (Bublitz & Stroud, 2012). Reduced volume of the corpus callosum and

cerebellum was also observed in children with ADHD, thereby providing a potential link between in utero exposure to smoke and ADHD (Krain & Castellanos, 2006).

1.1.4.3 Epigenetic

Several of the abovementioned environmental risk factors are believed to be involved in epigenetic modifications. It is to be noted that epigenetic changes might have a greater impact during key developmental time points, a notion that fits well with the prevalence of pre- and peri-natal risk factor associated with ADHD (Mill & Petronis, 2008). In fact, in these susceptible time windows of brain development are characterized by a high mitotic activity when the environmentally induced epigenetic changes are more likely to be propagated to the cell progeny (Spiers et al., 2015). Epigenetic modification include cytosine methylation in CpG-islands associated with gene silencing and chromatin compaction; histone modification such as histone acetylation, methylation, and phosphorylation and small interfering RNA (siRNA) that can suppress the activity of specific genes via targeted RNA interference (RNAi) (Mill & Petronis, 2008).

To support this hypothesis, a recent study by Wilmot and colleagues has shown an increases CpG methylation in peripheral tissue of male children with ADHD. Enrichment analysis suggested involvement of gene sets (*VIPR2* and *MYT1L*) linked to inflammatory processes and modulation of monoamine and cholinergic neurotransmission (Wilmot et al., 2016). Sequentially Walton and colleagues performed a genome wide analysis of DNA methylation from ADHD patient blood samples. They report an association of ADHD trajectories at birth for multiple genomic locations (*SKI*, *ZNF544*, *ST3GAL3* and *PEX2*) but none of those genes maintained an association at the age of 7 (Walton et al., 2017).

1.1.5 *PARK2* Copy Number Variations and ADHD

In the last years many efforts have been made to understand the genetic basis of complex diseases such ADHD. The common disease common variant (CDCV) hypothesis postulates that common genetic variations with allele frequency of 45% that show low penetrance in the common population are the main genetic drivers to the disease (Hawi et al., 2015). This hypothesis explains the initial genetic approach to the investigation of the genetic

contribution that was mainly based on candidate genes studies. The advancement in technologies and the advent of large GWAS allowed the advancement an alternative hypothesis, the common disease rare variant (CDRV) hypothesis. As the name suggests, it postulates that multiple rare variations ($\leq 5\%$ frequency) when combined together significantly affect the risk for common conditions (Hawi et al., 2015).

The development of comparative genomic hybridization (CGH) and next generation sequencing has allowed the discovery of copy number variations (CNVs). CNVs are large genomic structural variations with sizes ranging from kilobases (kb) to megabases (mb), and comprise deletions, duplications, triplications and translocations in comparison to a reference genome (Stankiewicz & Lupski, 2010). They are believed to account for about 13% of the human genome and could arise more frequently than single nucleotide polymorphisms (SNPs): it has been found that 70% of individuals carry at least one rare CNV and that copy number gains are more common than deletions (Ruderfer et al., 2016). CNVs can be inherited or arise *de novo* and both recombination- and replication-based mechanisms are believed to be causal of CNV formation (Stankiewicz & Lupski, 2010).

CNVs are thought to play a role in several neuropsychiatric and neurodevelopmental diseases (Lew, Kellermayer, Sule, & Szigeti, 2018; Takumi & Tamada, 2018) although the exact mechanism by which CNVs affect the phenotype is still unclear. It has been proposed that it could involve gene dosage effects, positional effects or it could unmask a recessive mutation of the remaining allele in case of deletion CNVs. Additionally, they could delete regulatory elements or disrupting coding sequences (Stankiewicz & Lupski, 2010).

Several studies have investigated if an increase in the overall rare CNV burden was present in ADHD patients. This hypothesis has been confirmed both in young ADHD populations (Guyatt et al., 2018; Martin et al., 2015; Stergiakouli et al., 2012; Williams et al., 2010) and in adults (Lesch et al., 2011; J.-A. Ramos-Quiroga et al., 2014). It has been proposed that the risk for ADHD follows a polygenic liability threshold model, in which individuals with rare large CNVs require a lower number of multiple common genetic risk variants for developing ADHD (Martin et al., 2015).

CNVs in the *PARK2* locus were first reported in an American cohort (Elia et al., 2010). Some years later, a genome-wide analysis of rare CNVs carried out by Jarick and colleagues, has pinpointed *PARK2* as a candidate gene in ADHD (Jarick et al., 2014). Locus-specific association

tests for an overrepresentation of CNVs identified *PARK2* as only genome-wide significant genomic region (*locus* chr6: 162 659 756—162 767 019 - NCBI36/hg18). The study used 489 young ADHD patients and 1285 controls Caucasian (plus replication group of 461 ADHD and 1063 controls) and found among the ADHD patients 5 CNVs deletions and 11 duplications carriers into the coding region (exon 2 or exon 3) of *PARK2*. Additionally, the study reports an increased length of rare CNVs in the ADHD sample compared to the controls, as already suggested by the literature. The same gene has also been proposed to be a candidate for ASD, a neurodevelopmental disorder that often co-occurs in ADHD patients as described above (Yin et al., 2016).

1.2 PARKIN RBR E3 UBIQUITIN PROTEIN LIGASE (PARK2)

Rare CNVs within the *PARK2 locus* have been associated with Attention-Deficit/Hyperactivity Disorder (ADHD) by genome-wide analysis (Jarick et al., 2014) (Elia et al., 2010). In the following chapter the biological functions of the Parkin RBR E3 Ubiquitin Protein Ligase (PARK2), a major regulator of the mitochondria quality control system (MQC), will be discussed. This information will help to draw and understand the hypothetical basis used to plan the experimental activity of the present study. Additionally, the available data of the connection between the biological functions of PARK2 and relevant phenotypes that characterize ADHD will be introduced.

1.2.1 PARK2: physiological function

PARK2 alternatively known as *PRKN* or *Parkin RBR E3 Ubiquitin Protein Ligase*, spans 1.380 kb and contains 12 exons (Asakawa et al., 2001; Kitada et al., 1998). To date, many *PARK2* splice transcripts have been described and have been demonstrated to be differentially expressed in tissue and cells (La Cognata et al., 2014; Scuderi, La Cognata, Drago, Cavallaro, & D'Agata, 2014). These multiple *PARK2* splice variants potentially encode for a large range of distinct protein isoforms with different and molecular architectures structures. This gene encodes for a particular type of E3 ubiquitin ligase. In fact, this enzyme is part of the class of Ring Between Ring Domain Proteins (RBR domain proteins), characterized by the ability of transferring ubiquitin molecules received by E2 proteins directly to their own RBR domain, forming another high energy thioester intermediate (Marín, 2009). Structurally, the enzyme is composed by 4 Zinc coordinating domains: RING0, RING1, IBR and RING2. In its auto-inhibited form, the Cys431 site for the thioester formation within the RING 1 domain, is occluded by a linker region called repressor element (Pickrell & Youle, 2015).

One of the most studied *PARK2* partner is the Ser/Thr protein kinase PINK1. Thanks to its unique structure, with an N-terminal mitochondrial targeting domain and three insertional loops within its catalytic domain, the protein is addressed to the outer mitochondrial membrane (OMM) (Kazlauskaite & Muqit, 2015). Under steady state conditions, PINK1 is imported, first by the TIM and then the TOM complex, inside the organelle and cleaved by the mitochondrial processing peptidase MPP (Greene et al., 2012) and the rhomboid protease

PARL (Meissner, Lorenz, Weihofen, Selkoe, & Lemberg, 2011). The regulation of this mechanism is under control of a large protease complex named SPY complex (Wai et al., 2016). This generates a 52 KDa N-terminal deleted form of PINK that is then released in the cytosol for degradation by the Ubiquitin Proteasome System (UPS) (Yamano & Youle, 2013). When the cell is perturbed by specific events that cause loss of the mitochondrial membrane potential, the import and cleavage process is inhibited and PINK1 becomes stable and active on the OMM (Yamano, Matsuda, & Tanaka, 2016). The presence of PINK1 on the OMM is sufficient and necessary for the recruitment and activation of cytosolic PARK2 by phosphorylation. PINK1 in fact phosphorylates PARK2 and Ubiquitin (Ub) at their Ser65 residues (McWilliams & Muqit, 2017). Phospho-ubiquitin binds with high affinity phosphorylated PARK2 inducing an allosteric change that activates the PARK2 enzymatic activity and thus recruitment of E2 ubiquitin-conjugating enzymes (Wauer, Simicek, Schubert, & Komander, 2015). PARK2 is then able to target several proteins expressed on the mitochondrial surface and cytoplasm for degradation both by ubiquitylating substrates *de novo* and elongating pre-existing Ub chains (Hang, Thundiyil, & Lim, 2015). To date, more than thirty-six substrates of PARK2 solely on the OMM have been identified (Sarraf et al., 2013)(McWilliams & Muqit, 2017). It has been shown that PARK2 forms mostly non-canonical K6 and K11-linked chains and in a lower rate K48 and 63-linked chains. The latter seem to be involved in p62 recruitment whereas the other forms seem to be linked with the Reticulum-associated degradation of the OMM proteins (Pickrell & Youle, 2015). It has also been suggested that an initial phosphorylation of various PARK2 substrates, like Mfn2, vDACs or Miro, by PINK1 could prime them to act like docking sites resulting in a positive autoregulation feedback (McWilliams & Muqit, 2017) (Scarffe et al., 2015).

Many studies have been carried out to comprehend what influences the interaction between PARK2 and PINK1. The general accepted model sees this interplay as an internal sensor system for disparate cellular homeostasis perturbations (Pickrell & Youle, 2015). Specifically, acting together, PARK2 and PINK1 exert a strong role in the mitochondria quality control (MQC) in a series of subsequent events set in place by the cell to overcome a disturbance of the internal homeostasis. To date, several genetic and environmental stressors have been proven to trigger PINK1 accumulation in experimental conditions. Those spread from different pharmacological reagents capable of depolarizing the mitochondrial membrane potential (CCCP, oligomycin combined with antimycin A, valinomycin or KillerRed) to genetic changes

linked with the mitochondrion itself (genetic loss of *Mfn1* and *Mfn2*, dysfunctional mitochondria complex I, mtDNA mutations) (Narendra, Tanaka, Suen, & Youle, 2008; Y. Wang, Nartiss, Steipe, McQuibban, & Kim, 2012). Interestingly the same effect seems to be achieved also by ornithine transcarbamylase (Δ OTC), that normally activates the mitochondrial unfolded protein response (UPR) (Jin & Youle, 2013).

1.2.2 PARK2/PINK1: Mitochondria quality control

As already introduced, the interaction between PINK1 and PARK2 seems to play a pivotal role in disparate mitochondrial dynamics like, mitophagy, fusion and fission, biogenesis and transport exerting thus a strong effect on the mitochondrial quality control (MQC) (Scarffe et al., 2015).

The ubiquitin chains attached by PARK2 to the proteins on the OMM can initiate a process known as mitophagy. This event occurs both as a steady state maintenance tool and as a resource to adjust the bioenergetic efficiency after a stress condition like starvation or hypoxia (Altman & Rathmell, 2012). In fact, in this way, the cell can prevent the accumulation of damaged mitochondria and reactive oxygen species (ROS) increase and at the same time generate intracellular nutrients. Mitophagy initiation shares some effectors with the autophagy pathway. Recent studies confirmed that also for mitophagy two pathways can be followed probably depending on the activator stimulus; a canonical pathway (Atg5-Atg7 dependent) and an alternative one (Atg5-atg7 independent) (Hirota et al., 2015). Both lead to the clustering of Ub-tagged mitochondria at the perinuclear area, growth of a surrounding membrane and finally fusion with lysosome for degradation (Tanida, Ueno, & Kominami, 2008). The formation of the auto-phagophore requires the recruitment of several receptors on the mitochondrial surface such as NBR1, NDP52, OPTN, p62/ SQSTM1, TAX1BP1 and TOLLIP essential for PINK1/PARK2 mitophagy (Yamano et al., 2016).

Additionally, it has been proven that PARK2 indirectly influences mitochondrial biogenesis by acting as an upstream regulator of PGC-1 α , a transcriptional coactivator required for the activation of several transcription factors necessary for mitochondrial biogenesis. This effect is carried out by PARK2 ubiquitination, and thus down regulation, of PARIS, the major repressor of PGC-1 α (Hang et al., 2015; Shin et al., 2011).

The MQC plays a strong role especially for long-living and terminally differentiated cells. In the case of neurons, where mitochondria could reside very far from the soma, PINK1/PARK2 might help in the arrest of their mobility through the axon and thus quarantine of the damaged organelle (Ashrafi, Schlehe, LaVoie, & Schwarz, 2014). Mitochondrial transport plays an important role especially in cells, like neurons, where localized energy and calcium buffering is required. On the OMM two proteins, Miro1 and Miro2, participate in the mitochondrial axon and dendritic transport by coupling the organelle to kinesin and dynein-dependent transport pathway. Miro1 is a specific target of the PINK1/PARK2 system and is subject to a rapid ubiquitination leading to transport arrest (S. Liu et al., 2012; X. Wang et al., 2012).

Although results from different studies are not univocal, PARK2 has been implicated in the process of apoptosis. Diverse evidences show both a pro-apoptotic and an anti-apoptotic role of PARK2 suggesting that its contribution could be stressor- and environmental- dependent (Altman & Rathmell, 2012). Some studies demonstrated that anti-apoptotic members of the Bcl-2 family are present on the OMM and inhibit PARK2 translocation on the mitochondrial surface and PARK2 seems to indirectly promote apoptosis by tagging Mcl-1 for degradation (Hollville, Carroll, Cullen, & Martin, 2014; C. Zhang et al., 2014). On the other hand PARK2 is able to inhibit the translocation of the pro-apoptotic Bax protein to the same organelle and elicit protection from apoptosis via the NF-KB pathway (Müller-Rischart et al., 2013). PARK2 overexpression seems to have a protective effect against stress induced apoptosis and it was shown to be a repressor of p53 (da Costa et al., 2009).

Additionally, several PARK2/PINK1 substrates are located at the endoplasmic reticulum-mitochondria (ER-M) interface, an area extremely important for calcium homeostasis. Genetic loss of PARK2 exacerbates ER-M juxtaposition and leads to aberrant calcium transfer (Gautier et al., 2016).

1.2.3 PARK2 and autosomal early-onset Parkinson's Disease

PARK2 was first identified as causative gene for young-onset Parkinson's disease (PD) (Matsumine et al., 1997). Over the years many different mutations in *PARK2* have been found to be associated with PD including homozygous and heterozygous point mutations. Although the localization of the mutations appears to be scattered throughout the gene, more mutations were found in exon 2,7 and 12 (Hattori & Mizuno, 2017). The autosomal early-onset

Parkinson disease is characterized by rigidity, bradykinesia, and resting tremor. Differently from other forms of PD, the onset usually occurs between ages 20 and 40 years with an average age of onset in the early thirties (Brüggemann & Klein, 1993).

1.2.4 Involvement of PARK2 in ADHD: mitochondrial dysfunctions and oxidative stress

As already reported in the previous chapter, on a genetic level evidence of an association of CNVs within the *PARK2 locus* and ADHD has been reported (Jarick et al., 2014). To evaluate a possible association between PARK2 and ADHD it is also worth investigating the pathways PARK2 is involved in and their potential role in ADHD.

Some studies have already shown impairment of mitochondrial functions in other neurodevelopmental disorders, such as ASD, where a general mitochondrial dysfunction is believed to be present in 30 to 40% of affected children (Giulivi et al., 2010; Morris & Berk, 2015; Rossignol & Frye, 2012). In regard of ADHD, a recent innovative study conducted by Verma and colleagues strongly suggested mitochondrial dysfunctions in the etiology of this disorder. By using ADHD cybrids cell models they showed lower levels of oxygen consumption and ATP production together with by increased levels of superoxide radicals (Verma et al., 2016). Interesting, a study using young rats found a decrease in the activity of complexes I, II, III and IV in the hippocampus, prefrontal cortex, striatum and cerebral cortex after acute or chronic administration of methylphenidate, one of the standard treatments for ADHD (Fagundes et al., 2010). Additionally, sporadic mtDNA mutations and increase in oxidative markers have been reported in ADHD patients (Marazziti et al., 2012). Mitochondria are an important source of reactive oxygen species (ROS) and reactive nitrogen species (RNS) (Murphy, 2009). The brain is one of the organs with the highest oxygen requirements and presents a high lipid concentration. This would suggest that could be one of the most sensitive targets of oxidative damage. Under non-pathological conditions, the presence of ROS is buffered by antioxidant balancing systems. Over the last decade, different studies have focused their attention on the contribution of oxidative stress in ADHD patients. Being cellular models for this disorder limited and just recently available, research has focused on oxidative markers found in ADHD-patient derived tissues as reviewed in (Lopresti, 2015). Given the heterogeneity of the biological samples used, inconsistency of marker tested, different sample

selection and probably population used, findings are sometimes contradictory (Lopresti, 2015). In spite of it, most of the study report an increase of oxidative stress and insufficient response to oxidative damage both in children and adults with ADHD (Joseph et al., 2015). Interestingly, it has been reported that methylphenidate administration increases antioxidant defense mechanisms (Guney et al., 2015) and overall antioxidant therapy has a positive effect on ADHD symptoms (Bloch & Qawasmi, 2011; Garcia et al., 2013). It is still in debate if these findings are an artefact due to other concomitant factors such as diet or comorbid medical conditions. This is one of the reasons at the base for the need of developing standardized, reproducible and characterized ADHD cellular models that could help in understanding if oxidative damage or related pathway are a phenotypical feature of ADHD.

1.3 CELLULAR MODELS FOR PSYCHIATRIC AND NEURODEVELOPMENTAL DISORDERS

The use of animal and cellular models has greatly contributed to the understanding of the biological bases of many diseases as well to develop treatments. A good model for neurodevelopmental psychiatric disorders should show a face validity (similar symptoms), predictive validity (similar response to human to a known medication) and construct validity (similar biological mechanism underpinning the human disorder) (de la Peña et al., 2017; Willner, 1986). For complex disorder, such as ADHD, where the understanding of the etiopathogenesis is still lacking, the construct validity criteria still fails to be fulfilled thus complicating the achievement of a good model.

The last century has seen the arouse of the use of cellular models to understand and treat neuropsychiatric disorders. In fact, different types of patient-derived cells have been proven to be a valuable tool for examining cellular, molecular, metabolic and pathophysiological states *in vitro*. In this chapter the last advancement on the field of disease cellular modelling will be reported with a special focus on different types of cell models such as human dermal fibroblasts (HDF), human induced pluripotent stem cells (HiPSC) and HiPSC-derived neuronal cells that will be employed in the present study. In the last part of the chapter the state of art evidenced on ADHD models and on models based on PARK2 mutants will be presented.

1.3.1 Human dermal fibroblast (HDF)

Patient-derived human dermal fibroblast (HDF) cultures are an easy and accessible way of studying certain aspects of a disease and in the last decades have shown their utility in neuropsychiatric research (Kálmán, Garbett, Janka, & Mirnics, 2016). Different studies on diverse neuropsychiatric conditions have proven HDF cultures to be suitable for studying transduction, redox homeostasis, circadian rhythms and gene per environment interactions (Vangipuram, Ting, Kim, Diaz, & Schüle, 2013). HDF are relatively easy to obtain from small skin biopsies and easy to maintain and propagate without further genetic manipulations. Furthermore, they can be stored for years in liquid nitrogen and form highly homogenous fibroblast cultures that maintain genetic stability (Hänzelmann et al., 2015). Although HDF

cultures have many advantages some limitations need to be taken into consideration both regarding the choice of donor and the effect of culturing. First of all, it has been shown that the age of the donor has a strong effect on cell viability and senescence thus influencing many cellular processes (Peterson & Goldman, 1986; Waldera-Lupa et al., 2014). Moreover, it has been demonstrated that *in vitro* cellular ageing has important consequences on mitotic, protein and transcription level (Maier et al., 2007; Sprenger et al., 2010) and HDF start to show senescence after passage 21 (Hänzelmann et al., 2015). On the other hand, it has been proven that the use of early passaging HDF is not advisable since the culture are still not homogenous and that the patient's dietary, hormonal and medication effect disappear just after the 5th passage (Auburger et al., 2012). Hence, to gather consistent and reproducible findings from HDF studies it is important to choose carefully case-control age matches and use cells at a similar *in vitro* passage that has to be between 5 and 20 (Kálmán et al., 2016).

1.3.2 The advent of HiPSC and HiPSC-derived neurons: implications for neurodevelopmental and psychiatric research

The recent development and improvement of human induced pluripotent stem cells (HiPSC) has opened a whole new era for cellular modelling. In fact, this technology allows the conversion of any already differentiated tissue in a pluripotent state that can be then directed in a specific cell type. It is easy to foresee how this can facilitate the study of biological samples that are extremely hard to obtain by other means, such as human neurons. Moreover, this technique allows to maintain the whole genetic make-up of the patient in a non-invasive and ethical manner. This limitless patient-derived cells source can be used to model human disease, screen drugs, and even generate tissues for transplantation (N. Liang et al., 2017).

The technique was pioneered by the group of Shinya Yamanaka in 2006: in a ground breaking paper they demonstrated that iPSC could be generated by introducing just four factors, *Oct3/4*, *Sox2*, *c-Myc*, and *Klf4* in mouse fibroblast cells (Takahashi & Yamanaka, 2006) and one year later in human fibroblast cultures (Takahashi et al., 2007). These cells exhibit functional properties similar to human embryonic stem cells (hESCs); they are self-renewable and can differentiate into any cell type in the human body (pluripotency).

1.3.2.1 Technique workflow

In the last decade the iPSC technique has been refined by several different laboratories. Although details may vary according to the protocol used, the technique follows three main steps: (i) first the initial culture is established, (ii) then the cells are induced to iPSCs, (iii) finally the cells are characterized and expanded (Singh, Kalsan, Kumar, Saini, & Chandra, 2015).

- (i) The most common cell type as the starting material for reprogramming process are easy-to-obtain cells such as skin dermal fibroblasts, peripheral blood cells, renal epithelial cells from urine and keratinocytes (N. Liang et al., 2017).
- (ii) To date several different transduction methods are available that range from exogenous addition of small molecules, mRNA Transfection, PiggyBac or viral vectors (Malik & Rao, 2013). The transduction method may influence parameters such as efficiency, velocity and quality of the reprogramming. Although the DNA integrating delivery systems show a higher efficiency, they might interfere with the host genome and cause multiple insertional mutagenesis. Among the non-integrating viral vectors, the ones based on the Sendai virus, a negative-sense single-stranded RNA virus ((-)ssRNA virus), are the mostly used. Although more difficult to work with and with an efficiency of about 1%, the replication of transgenes occurs in the cytoplasm without possible genomic integration and after about 10 cell passaging the virus appears to be completely lost (Lim et al., 2015).
- (iii) Once the putative colonies of HiPSC start to appear they need to fulfil certain criteria in order to be considered *bona fide* HiPSC and thus used for further applications (Martí et al., 2013). HiPSC colonies can be characterized by different morphological and physiochemical methods. On a morphological level, HiPSC are similar to hESCs and characterized by round shape, large nucleolus, and low cytoplasm whereas colonies are tightly packed adherent monolayers with sharp edges. Further, HiPSC may be defined on the basis of expression of different cell surface proteins (SSEA-4, alkaline phosphatase) and transcription factors *POU5F1*, *SOX2*, *NANOG* related to pluripotency (Chan et al., 2009). The pluripotency can be demonstrated both *in vivo*, by the teratoma assay where HiPSC inoculated in an immunodeficient mice generate a teratoma (a type of tumor made up of several different types of tissue), or *in vitro* by the embryoid bodies assay. This assay takes advantage of the fact that spherical iPSC aggregates grown in suspension (embryoid bodies, EBs) will spontaneously differentiate into cells of all three embryonic germ lineages. Additionally,

HiPSC must display a normal karyotype and show a high rate of genetic similarity with the cellular source (Singh et al., 2015).

1.3.2.2 Neural Induction

Once the HiPSC have been proven to be *bona fide* they can be induced to become a specific cellular type. This “directed differentiation”, as well as the HiPSC technology itself, is still recent and the protocols are still in development and refinement especially for generating specific subtypes of neurons. Generally, neural induction (NI) can be promoted by either inclusion of growth factors that promote neural differentiation or withdrawal of those that prevent it (LaMarca, Powell, Akbarian, & Brennand, 2018). Additionally, a number of starting culturing methods have been proposed, such as embryoid bodies, cultivation of HiPSC on stromal feeders or feeder-free cultivation (Lim et al., 2015). In the case of HiPSC-derived midbrain dopaminergic neurons, the majority of the recent protocols are based on a combination of the pioneering work of Chambers and Kriks (Chambers et al., 2009; Kriks et al., 2011). They first showed how two inhibitors of SMAD signaling, Noggin and SB431542, are sufficient to induce rapid and complete neural conversion (Chambers et al., 2009) whereas the second demonstrated that caudalization can be achieved by activation of Wnt signaling and that sonic hedgehog (shh) and fibroblast growth factor 8 (FGF-8) direct the cells toward a ventral mesencephalic fate (Kriks et al., 2011). As for the HiPSC, also the HiPSC-derived neuron must be proven to be *bona fide* neurons by morphological and neuron-specific markers analysis.

1.3.2.3 Applications, advantages and limitations

Many different studies can be carried out by taking advantage of HiPSC-derived cellular models. For example, morphological, histological, physiological and transcriptional characteristics of HiPSC-derived cells can be studied in vitro by gene expression profiling (RNA sequencing or RNA microarray), chromatin studies (chip sequencing), and proteomic analyses. Specific analyses can be further applied on HiPSC-derived neurons that assess changing in morphology, spine density, connectivity as well as electrophysiology (Adegbola, Bury, Fu, Zhang, & Wynshaw-Boris, 2017).

The applications of this technology can be divided into two interconnected paths: on one hand it represents a method for studying the pathology itself, on the other it can be used as platform to develop treatments. In fact, the main objective of iPSC studies is the identification of disease specific cellular phenotypes (patho-phenotypes) and subsequently assess if they can be rescued by therapeutic intervention (Prilutsky et al., 2014). One of the main advantages of disease modelling

by HiPSC technology is that it recapitulates the pathologic condition and takes into account the whole donor genomic make-up *in vitro*. Moreover, it represents a non-invasive and ethic method and infinite source of starting material that can be used to originate a variety of cell types and subtypes (Singh et al., 2015). HiPSC have a great relevance for studying neurodevelopmental disorder: they in fact are suitable for generating cells expressed during embryonic development that are normally not available for *in vitro* testing. This technology is now believed to be a revolutionary method in drug discovery: patient-specific iPSC platforms are a valid tool for preclinical screening and validation of candidate drugs and they can reveal safety, efficacy and responsiveness across a spectrum of genetically different human patients.

Although extremely promising, this technique has still some limitations that would need to be addressed by implementing the protocols in the future. In fact, there is still a large heterogeneity in culture, reprogramming and induction techniques that makes difficult to compare results from different laboratories (LaMarca et al., 2018). Additionally, it has to be reported that heterogeneity might be present also from HiPSC clones deriving from the same patient (Adegbola et al., 2017). In fact, formation of random CNVs has been reported after cell reprogramming especially when the line is still young (Ronen & Benvenisty, 2012). This is the reason why HiPSC studies should be conducted using multiple clones per donor that are over 10 passages of culturing. Moreover the increase of total CNVs burden and genetic correlation to the source should be assessed by DNA sequencing (Flaherty & Brennand, 2017). Additionally, when possible, it should be considered to create control isogenic cell lines by targeted genetic manipulation of HiPSC sequence-specific designed zinc finger nucleases (ZFNs) or transcription activator-like effector nucleases (TALENs) (Aigner, Heckel, Zhang, Andreae, & Jagasia, 2014)

1.3.3 Focus on available ADHD models

The creation of animal models for a complex disorder such as ADHD is complicated by the fact that the exact etiopathogenesis of the disorder is still unclear and thus is not easy to fulfil the face validity criteria (de la Peña et al., 2017). To date, five highly validated transgenic animal models of ADHD have been proposed; the *Dat*-KO mouse, Coloboma-mutant or *Snap25*-mutant mouse, *Nk1r*-KO mouse, *Trβpv*-KO mouse, *P35*-KO mouse, as reviewed in (de la Peña et al., 2017). On a behavioral level, they display impulsivity, inattention and hyperactivity and the latest is ameliorated by amphetamine or methylphenidate treatment. All of them present alteration of

the dopaminergic system. Although the many efforts, data from a recent systematic study suggests a very little contribution of animal research in the understanding of ADHD (Carvalho, Crespo, Bastos, Knight, & Vicente, 2016).

It is interesting to note that a recently developed mouse model, obtained by prenatal nicotine exposure, shows the full range of ADHD associated behavioral phenotypes, including working memory deficit, attention-deficit and impulsive-like behavior and has thus been proposed as possible preclinical model for ADHD (Jinmin Zhu et al., 2017). The same model shows selective decrease in cingulate cortical volume and radial thickness and a low dopamine turnover in the frontal cortex (Jinmin Zhu et al., 2012). More stringently, a single administration of a therapeutic equivalent dose of methylphenidate causes a decrease in all the ADHD-like symptoms (Jinmin Zhu et al., 2017).

Moving to the cellular level, an interesting ADHD cellular model was created by Verma and colleagues. The generated ADHD cybrids cells, a transgenic cell model that allows to study only the contribution of patient's derived mitochondria, showing lower levels of ATP production and oxygen consumption and increased levels of superoxide radicals in the ADHD lines compared to controls (Verma et al., 2016).

In regard of innovative HiPSC based cellular models, literature search shows the creation of two independent HiPSC lines related to ADHD. Recently, it has been reported the creation of a HiPSC line from an ADHD patient carrying a duplication of *SLC2A3*, a gene encoding neuronal glucose transporter-3 (GLUT3) (Jansch et al., 2018). Sochacki and colleagues reports the generation of 3 HiPSC lines from ADHD patient from urine samples but they do not present any genetic information about the patients (Sochacki, Devalle, Reis, Mattos, & Rehen, 2016). To the best of our knowledge, none of the abovementioned models report an investigation of the cellular phenotype.

1.3.4 Focus on available PARK2 models

As already mentioned, mutations in *PARK2* were first discovered as causative of a small percentage of young-onset Parkinson's disease patients (Matsumine et al., 1997). This is the reason why available *PARK2* models were mainly generated and evaluated with a focus on potential pathomechanisms of Parkinson's Disease.

Surprisingly, *Park2* knock out mice do not represent a robust model for this disease (Perez & Palmiter, 2005). In fact, they do not show impairment of the motor system (Goldberg et al., 2003; Perez & Palmiter, 2005; Rial et al., 2014), olfactory changes or dopaminergic neuron degeneration in any area (Kurtenbach, Wewering, Hatt, Neuhaus, & Lübbert, 2013). The extensive phenotypic characterization of these animals could be useful to try to understand if there is a link with neurodevelopmental disorders like ADHD. Interestingly, most of the studies showed effects on cognitive and working memory traits: *Park2* KO mice have impaired habituation and exploratory activity in a new environment (Itier et al., 2003; Stichel et al., 2007) and exhibit a worse performance on object location (Rial et al., 2014). Additionally, they perform worse than controls in a Y-maze (Rial et al., 2014) and show less spontaneous alternation in a T-maze. Although tests that represent the core features of ADHD have not been carried out on *Park2* KO mice, it is interesting to note that this line shows impairments in working memory, as seen in other ADHD-like mouse lines. No paper reporting testing for social behavior or impulsivity was found and thus it is difficult to make further speculations about the hypothetical role of this model and ADHD.

Several HiPSC lines have been created using samples from donors with various types of CNVs and mutations within the *PARK2* locus (Xu et al., 2016). All the donors were diagnosed with Parkinson's disease whereas currently no HiPSC study has been carried out with ADHD/*PARK2* CNVs donors. The creation of human midbrain dopaminergic neurons from these stem cells underlined an impairment in this neurotransmitter system with an increase of DA release from terminals accompanied by low DA reuptake and a lower number of DAT (Jiang et al., 2012). The same cells show a diminished degree of neuronal process complexity, measured by different features like length, number of terminals and branch points, probably due to a concomitant instability in microtubules (Ren et al., 2015). In a complex study, Shaltouki and colleagues demonstrated that the rate of DA differentiation from *PARK2* mutation carrier HiPSC is lower than in controls (Shaltouki et al., 2015). Most of the studies have found impairment in mitochondrial morphology (Imaizumi et al., 2012a; Shaltouki et al., 2015) and complex I activity (Zanon et al., 2017) together with an increase in the presence of ROS and a decrease of anti-oxidative pathways (K. H. Chang et al., 2016; Suzuki et al., 2016). The latter group also demonstrated an impairment in mitophagy. It should be pointed out that just one of these studies provided a control for the effects of reprogramming HiPSCs (i.e. isogenic cells lines) whereas none reported a multiclonal analysis of each stem cell line. Moreover, the protocols

used for the neural induction vary from study to study and this could affect the efficiency of differentiation and make comparisons difficult. However, it is interesting to notice that the features reported by these studies can be also linked with ADHD phenotypes. Nevertheless more uniform studies and with a special focus on ADHD features are needed (DallaVecchia&Mortimer&Palladino, 2018).

1.4 AIMS AND EXPERIMENTAL DESIGN

The main goal of the study is the identification of disease specific cellular phenotypes related to Attention-Deficit/Hyperactivity Disorder (ADHD). To achieve this aim we have generated cellular models from patients carrying rare *PARK2* Copy Number Variants (CNVs) associated with ADHD (Jarick et al., 2014) and then evaluated different phenotypical aspect that could have been impaired.

The project might thus be divided in two main interconnected and dependent parts; the creation and validation of the models used (Human dermal fibroblasts -HDF-, human induced pluripotent stem cells -HiPSCs- and HiPSC-derived dopaminergic neurons) and the evaluation of the presence of pathological phenotypes (patho-phenotypes).

1.4.1 PART 1: creation and validation of aADHD cellular model systems

The first part of the study was focused on the creation and validation of the cellular models (Figure 1). In this study, three different cellular models were generated: Human dermal fibroblast (HDF), human induced pluripotent stem cells (HiPSCs) and HiPSC-derived dopaminergic neurons. Starting from a larger initial cohort (n=12), a total of six donors were selected for HiPSC and dopaminergic neuron generation: 3 adult ADHD *PARK2* CNV risk carriers (1 duplication carrier [PARK2CNV_DUP/ADHD] and 2 deletion carriers [PARK2CNV_DEL_A/ADHD] and [PARK2CNV_DEL_B/ADHD], 1 non-risk CNV variant carrier diagnosed with ADHD [WT / ADHD] and 2 healthy controls [WT_A/HEALTHY] and [WT_B / HEALTHY].

First, we optimized the technique and protocols to generate HiPSC and to induce them to differentiate into HiPSC-derived dopaminergic neurons. Then, we performed a series of assays to demonstrate the validity of the model, a process known as *bona fide* characterization. For each HiPSC line we decided to evaluate 3 clones in order to avoid possible confounding effects due to the reprogramming technique. All the cell lines and the clones were assessed to be *bona fide* HiPSC by morphological analysis, RT-PCR, immunofluorescence, embryoid body

assay and molecular karyotyping and *bona fide* HiPSC-derived dopaminergic neurons by immunofluorescence, RT-qPCR, and dopamine levels quantification.

This part of the project: (i) supports the validity of the models created (ii) presents a human model to study the etiopathogenesis of ADHD.

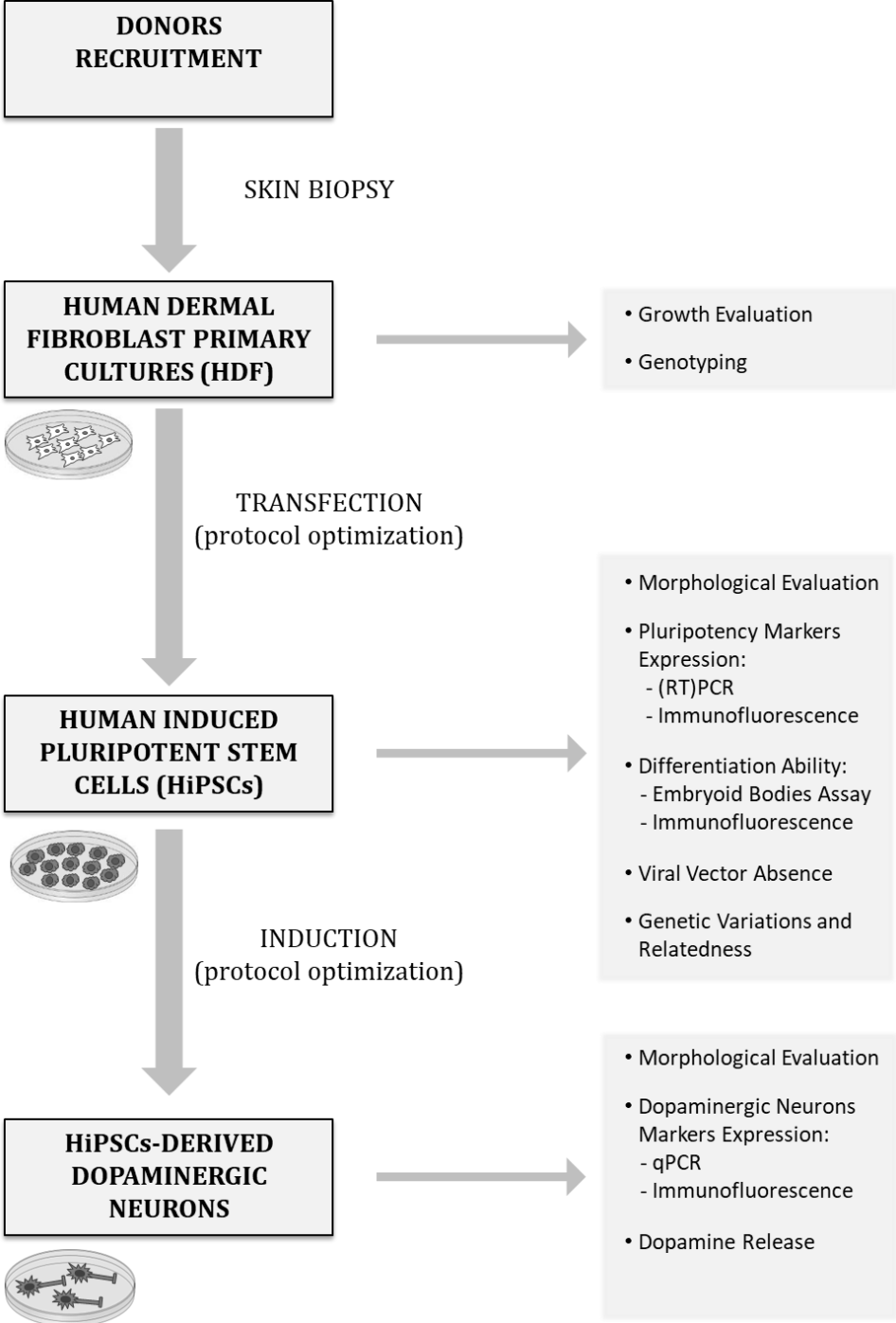


Figure 1 Experimental design part 1: creation and validation of *aADHD* model systems. Overview of the workflow followed to generate the three different cellular models (Human dermal fibroblast (HDF), human induced pluripotent stem cells (HiPSC) and HiPSC-derived dopaminergic neurons) used in the study and list of the *bona fide* characterization tests performed.

1.4.2 PART2: Phenotyping

The second part of the project was aimed on evaluating the cellular phenotype (Figure 2) and to establish if a patho-phenotype in ADHD/*PARK2* CNVs carriers compared to WT controls was present. The effects of *PARK2* mutations have been extensively studied in PD patients but, to the best of our knowledge, no data are available regarding the functional consequences of *PARK2* CNVs associated with ADHD.

1.4.2.1 *Evaluation of patho-phenotypes connected with ADHD/PARK2 CNVs in HDF and HiPSC after stress exposure*

In a preliminary study, we assessed if alterations in gene expression of *PARK2* related genes were already visible in peripheral cells such as blood cells and if *PARK2* gene expression was altered in fibroblast by using a larger donor' sample (n=12). We then decided to perform a closer evaluation of the phenotype in a selected group of the previous sample. Taking into consideration that *PARK2* together with *PINK1* plays a pivotal role in orchestrating mitochondrial dynamics especially after perturbation of the cellular homeostasis, we decided to evaluate if differences were exacerbated under cellular stress conditions. We thus applied a nutrient deprivation paradigm (starvation stress) on the HDF and HiPSC cultures and pharmacological depolarization of the mitochondrial membrane potential with the ionophore Carbonyl cyanide m-chlorophenyl hydrazine (CCCP) known to trigger *PINK1* accumulation (Yamano et al., 2016). We then performed a series of assays with a special focus on mitochondrial function and energy metabolism and on *PARK2* protein expression. These experiments can help to discern if: (i) alteration are still visible also in peripheral cell such as fibroblasts, (ii) alteration are present already in an early developmental stage (HiPSC). In fact, it has been reported that *PINK1*, the main interaction partner of *PARK2*, has a role in the control of cell fate plasticity and maintenance of pluripotency (Vazquez-Martin et al., 2016a). (iii) draw the basis to assess whether a patho-phenotype is present and direction subsequent experiments.

1.4.2.2 Evaluation of nicotine effects on HiPSC-derived dopaminergic neurons from aADHD patients

Once we pinpointed the presence of phenotypic differences between ADHD/*PARK2* CNV carriers and healthy controls we moved to the evaluation of a model, HiPSC-derived neurons, that more closely represent the disease. We decide to evaluate the effect of nicotine exposure, one of the best replicated environmental risk factors for having a child later on diagnosed with ADHD. We thus treated HiPSC-derived dopaminergic neurons with smoking-relevant nicotine concentrations mirroring “binging episodes” and “continuous consumption” (namely “acute” and “chronic” treatment) (Lomazzo et al., 2011; Srinivasan et al., 2016). We evaluated *PARK2* protein expression after treatment and gene expression by RNA sequencing. In this part of the project we aimed to: (i) evaluate if the presence of *PARK2* CNVs conveys a different susceptibility to ADHD-risk associated factors such as nicotine compared to controls. (ii) Evaluate if HiPSC-derived dopaminergic neurons, a model that mirrors more closely the anatomical region connected with the disease, originated from the ADHD/*PARK2* CNV carriers show the same patho-phenotypic characteristics we have reported in HDF and HiPSC.

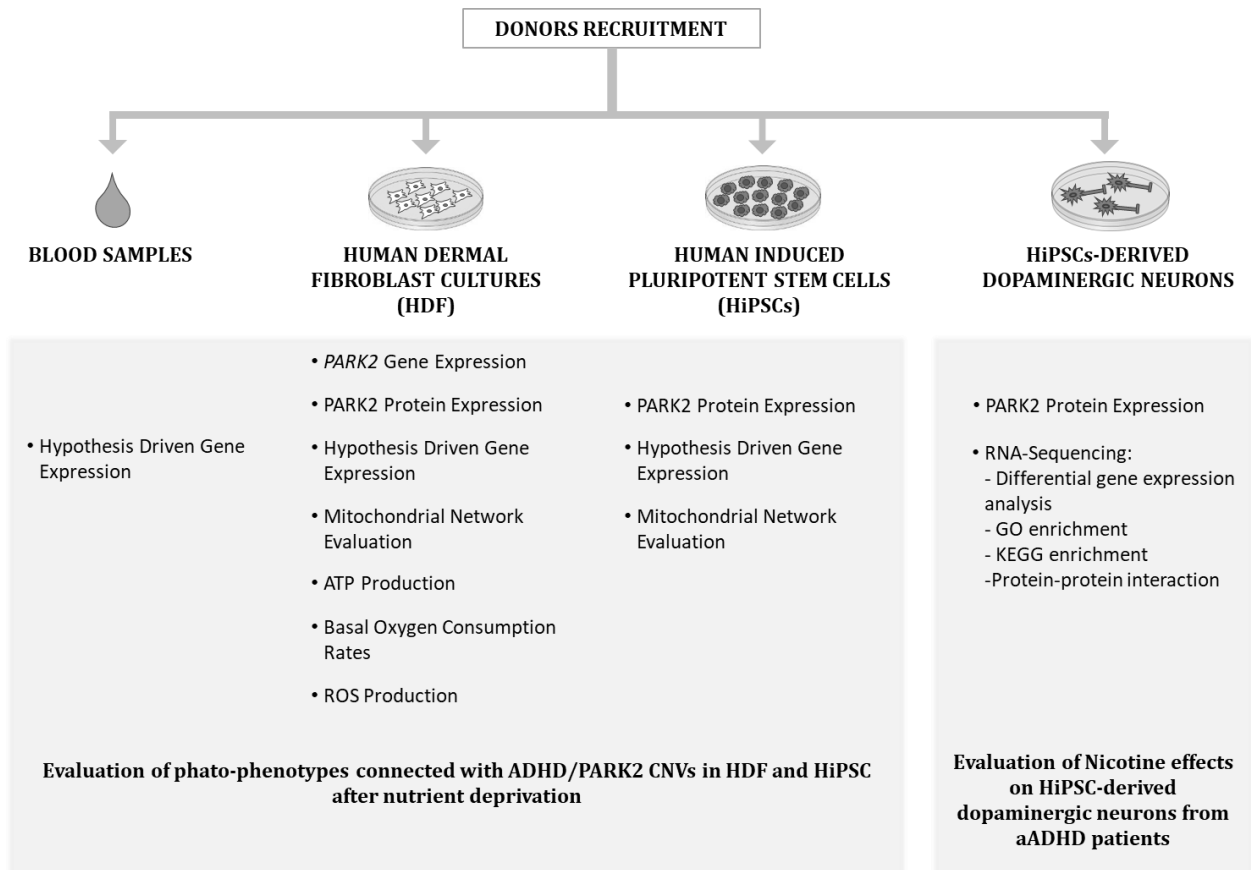


Figure 2 *Experimental design Part 2: phenotyping of ADHD/*PARK2* CNVs model systems.* Overview of the assays performed on the different cellular models generated. In the first part of the experiments we evaluated the presence of patho-phenotypes connected with ADHD/*PARK2* CNVs in HDF and HiPSC after nutrient deprivation. In the second part of the experiments we evaluated the effects of ADHD-risk factor nicotine on HiPSC-derived dopaminergic neuron from aADHD patients.

2 METHODS

2.1 PATIENTS RECRUITMENT, PSYCHIATRIC EVALUATION AND NEUROLOGICAL ASSESSMENT

Donors were recruited in 2012 and 2013 at the Department of Psychiatry, Psychosomatics and Psychotherapy, University of Würzburg (Germany) among patients from a previously published sample (Jarick et al., 2014) and age and sex-matched hospital staff. Extensive and comprehensive psychiatric assessment was performed by two experienced physicians (Prof.Dr.med Andreas Reif and PD Dr.med. Sarah Kittel-Schneider). ADHD was diagnosed by assessing the childhood symptomatology with the “retrospective German short form of Wender Utah Rating Scale” (WURS-k) whereas adulthood symptoms were measured by “Conners Adult ADHD Rating Scales” (CAARS) following the DSM-IV criteria. Exclusion criteria for controls were a history of psychiatric disorders and acute and chronic infectious diseases and severe neurological or internal diseases for patients. Given the association of *PARK2* with an early-onset autosomal form of Parkinson’s Disease, all donors were also neurologically examined. Early signs of Parkinson's disease were examined by Unified Parkinson's Disease Rating Scale (PDRS), Non-Motor Symptom assessment scale for Parkinson’s disease (PD NMS) and sniffing test (olfactory function). Additionally, to evaluate dopaminergic neurons degeneration, the *substantia nigra* volume was measured by ultrasound.

2.2 CELL CULTURE METHODS

2.2.1 Generation and maintenance of human dermal fibroblasts

Human dermal fibroblasts were obtained from donor’s skin biopsies. Skin punches of 3 mm² were performed by a certified physician (PD Dr. med. Sarah Kittel-Schneider) under local anesthesia and stored overnight in DPBS/ Gentamicin (1 µg/ml) (Life Technologies).

The biopsy was washed five times with DPBS, subcutaneous fat tissue was removed, and samples were incubated for 16 hours at 4°C in Dispase solution (2.4 U/ml, PAN Biotech). The sample was washed 3 times with DPBS, the epidermis layer was removed with forceps and the sample incubated with Collagenase (500 U/ml, Serva) for 45 min at 37°C. Samples were centrifuged for 5 min at 1200 rpm and washed with DMEM/10% FBS and Gentamicin (1 µg/ml) (Life Technologies). Dermal samples were seeded in a 25cm² flask (Sarstedt) in 1.5ml of DMEM/10% FBS/ Gentamicin (1µl/ml) for expansion.

Fibroblasts were maintained and feed every other day in Dulbecco's Modified Eagle Medium (DMEM) supplemented with 10% Fetal Bovine Serum (FBS) (Life Technologies).

When cells reached confluence, fibroblasts were detached by Trypsin/EDTA (PANBiotech) incubation. Backup samples were frozen in liquid nitrogen in FBS containing 10% DMSO (Applichem). All fibroblast lines used in the experimental part of this study were between passage 5 and 13 and passage matched with each other.

2.2.1.1 Cell counting, viability and doubling time

For all experiments, cell counting and viability (ratio between live cells and dead cell) was assessed with EVE automated cell counter (NanoEnTek). Shortly, 10 µL of cellular suspension was mixed with 10 µL of 0.4% trypan blue stain (Nano Entek) and loaded on an EVE Cell counting slide and measured within 3 minutes. Instrument setting (sensitivity, minimum and maximum cell size, circularity) were calibrated according to the cell type measured (Fibroblasts, HiPSC, DA neurons). Measurements were done in duplicate and total cell number, number of dead cells and number of viable cells and viability expressed as percentage was reported.

To evaluate differences in growth due to the genotype we measured the HDF cell number and viability in all the lines for 4 subsequent passages (from P3 to P7). The fibroblast doubling time was calculated by the following formula (Roth, 2016):

$$\text{Doubling Time} = \frac{\text{DURATION} * \text{LOG}(2)}{\text{LOG}(\text{FINAL CONCENTRATION}) - \text{LOG}(\text{INITIAL CONCENTRATION})}$$

2.2.2 Fibroblast transfection for HiPSC generation

Six HDF lines were selected for generating HiPSC: 3 adult ADHD *PARK2* CNV risk carriers (1 duplication carrier [PARK2CNV_DUP/ADHD] and 2 deletion carriers [PARK2CNV_DEL_A/ADHD] and [PARK2CNV_DEL_B/ADHD]), 1 non-risk CNV variant carrier diagnosed with ADHD [WT/ADHD] and 2 healthy controls [WT_A/HEALTHY] and [WT_B/HEALTHY].

Fibroblast at early passage (mean P6) were seeded in a 24-well plate at a density of 4×10^4 cells per well and transfected with CytoTune-Ips 2.0 Sendai Reprogramming Kit (Invitrogen) with a vector MOI of KOS=9, hc-Myc=9, hKlf4=6. Fibroblast were incubated with the viral vectors for 24h in “Fibroblast medium”: DMEM, 10% FBS, 1% MEM Non-Essential Amino Acids 100x, 55 μ M 2-Mercaptoethanol (Life Technologies). On day 7 after transfection, cells were plated on Gelatin (Merck Millipore) coated 6-well plates with CF-1 Mouse Embryonic Fibroblasts (MEF) feeder cells (2.5×10^5 cells/well) at different densities (2.5×10^4 , 5×10^4 , 1×10^5). From the day after on cells were fed daily with “IPSC medium”: KnockOut DMEM/F-12, 20% KnockOut Serum Replacement, 1% MEM Non-Essential Amino Acids 100x, 55 μ M 2-Mercaptoethanol (Life Technologies). After about 2 weeks, the first putative HiPSC colonies were manually picked detaching the colony from the surrounding with a needle (Becton Dickinson GmbH) and transferred on Matrigel coated 48-well plates for clone expansion in mTeSR1, 10 μ M Y-27632 (StemCell Technologies).

2.2.3 HiPSC cultures maintenance

HiPSCs were cultured on Matrigel matrix coated plates (Corning), feed daily with mTeSR1 (StemCell Technologies) and maintained in an incubator at 37°C and 5% CO₂. Cells were split 1:2 ratio one day before reaching confluence using ReLeSR as large colonies clumps (StemCell Technologies). Several clones were picked from the same line and expanded. After every day morphological monitoring (evaluation of HiPSC morphology by light microscopy) 3 best looking clones were chosen for each line and after passage 12 used for *bona fide* characterization. Backup samples were frozen in liquid nitrogen in KnockOut Serum Replacement, 10% DMSO (Applichem).

2.2.3.1 Embryoid bodies assay

Embryoid Bodies (EBs) were generated plating 1.0×10^7 cells as single cell suspension on AggreWell 400Ex plate in AggreWell Formation Medium, 10 μ M Y-27632 (Stem Cell Technologies). When spherical aggregates with distinct borders were visible (24 to 36 hours after seeding), EBs were harvested and plated in suspension culture on ultra-low-adhesion plates (Corning). EBs were fed every 2 days interval with AggreWell Formation Medium until day 11, then with “EB maintenance medium”: DMEM/F-12, 10%KnockOut Serum Replacement, 1%MEM Non-Essential Amino Acids 100x, 0.1 mM 2-Mercaptoethanol, L-glutamine (Life Technologies). After two weeks EBs were seeded onto Matrigel-coated coverslips and cultured for 6 days.

2.2.4 Neural induction and maintenance of HiPSC-derived dopaminergic neurons

HiPSC were seeded as single cell suspension (3.6×10^4 cells per cm^2) in mTeSR1, 10 μ M Y-27632. From day 1 to day 5 cells were feed with “KSR differentiation medium”: DMEM, 15% KnockOut Serum Replacement, GlutaMAX-I Supplement 100x 2 mM, β -mercaptoethanol 10 μ M (Life Technologies) then it was gradually switched to “N2 differentiation media”: DMEM, 100X N2 Supplement (Life Technologies) and from day 12 on with “B27 differentiation medium”: Neurobasal Plus Medium, B-27 Plus Supplement (50X), GlutaMAX-I Supplement 100x 2 mM (Life Technologies). A different combination of factors was added every day (see Figure 13): LDN193189 100nM, CHIR99021 3 μ M, Purmorphamine 2 μ M (Miltenyi Biotech), FGF8 50ng/ml (Bio-technie), SB431542 10 μ M (Bertinpharma), SAG 0.25 μ M (Millipore), BDNF 10ng/ml, GDNF 10ng/ml, TGF β 3 1ng/ml (Immunotools), ascorbic acid 0.2mM (Sigma Aldrich), DAPT 10nM (ABSOURCE Diagnostics GmbH), cAMP bucladesine 0.1 mM (Cayman). On day 20 cells were harvested by Accutase incubation (StemCell Technologies) and counted: part was frozen in liquid nitrogen in STEMdiff Neural Progenitor Freezing Medium (StemCell Technologies) as same-batch back-up; the other part was plated at a density of 2×10^5 cells per cm^2 on poly-L-ornithine hydrobromide (15 μ g/ml), laminin (5 μ g/ml) fibronectin (4 μ g/ml) coated plates (Sigma Aldrich). Medium was changed every other day and the cells were considered to have reached maturity at day 50.

2.2.5 Treatments

For experimental procedures cells were randomly assigned to the different treatment groups. Cells were matched to have a similar passage number. Before treatment culture were washed twice with DPBS.

For experiments involving HDF 3 groups were created: “baseline group” cultured with plain DMEM 10%FBS; “starvation group” that underwent serum nutrient deprivation for 24 h (just DMEM) and “CCCP group” (DMEM 10% FBS, 10 μ M carbonyl cyanide 3-chlorophenylhydrazone (Sigma Aldrich) for 24 h). For experiments involving HiPSC similar groups were created. The “baseline group” was cultured in mTeSR1 complete medium; the “starvation group” was cultured only with mTeSR1 basal medium for 24 h and the “CCCP group” was cultured with mTeSR1 complete medium, 10 μ M CCCP for 24 h.

For the evaluation of the effect of the ADHD-risk factor nicotine HiPSC-derived dopaminergic neurons were divided in 5 experimental groups: “baseline immature neurons” and “baseline mature neurons” cultured with B27 complete Medium, “nicotine chronic group” supplemented with 0.4 μ M nicotine for 7 days, “nicotine acute immature neurons group” “nicotine acute mature neurons group” supplemented with 5 μ M nicotine for the 24 hours prior to harvesting. The term “mature” or “immature” neurons refers to neurons respectively harvested at day 45 and 60 of neural induction. Nicotine (Sigma Aldrich) was dissolved in B27 complete medium. Concentrations were chosen after literature search to resemble human blood/CSF nicotine concentration following an episode of binge smoking (acute) or continuous cigarette (chronic) consumption (Lomazzo et al., 2011; Srinivasan et al., 2016) (Lomazzo et al., 2011) (Srinivasan et al., 2016).

2.3 GENETIC METHODS

2.3.1 DNA extraction

Genomic DNA was extracted from blood samples, fibroblasts and HiPSCs. For blood samples, DNA was isolated from EDTA-monovettes by de-salting method (Miller, Dykes, & Polesky, 1988) whereas DNA from fibroblast and HiPSC was isolated with DNeasy kit (Quiagen)

according to the manufacturer protocol. DNA concentration and quality were assessed by spectrophotometric measurement (Infinite 200 PRO -Tecan).

2.3.2 *PARK2* TaqMan Copy Number assay

Quantitative detection of genomic copy number changes in the *PARK2 locus* was performed with TaqMan Copy Number Assays (Applied Biosystems, Darmstadt, Germany, assay Hs03615859_cn at chr6: 162696987 +/- 50 bp) following the manufacturer recommendations and as described in (Jarick et al., 2014). Briefly, blood and fibroblast gDNA samples with an A260/A280 ratio greater than 1.7 (Infinite 200 PRO-Tecan) were diluted in nuclease-free water to a concentration of 5 ng/ μ L. PCR amplification was performed in LightCycler 2.0 (Lifescience-Roche) on a 384-well plate. Measurements were performed in quadruplicate. Data analysis was performed by Dr. Heike Weber (Department of Psychiatry, Psychotherapy and Psychosomatic Medicine, University Hospital Würzburg, Würzburg, Germany) by using CopyCaller Software (PN 4412907).

2.3.3 Genotyping by Illumina Infinium Omni2.5-8 Bead Array

gDNA from 6 selected fibroblasts lines and 3 respective HiPSC clones was analyzed by Illumina Infinium Omni2.5-8 bead array at the Institute of Human Genetics, LIFE&BRAIN GmbH, University Bonn. Data analysis was performed by Dr. Andreas Chiocchetti (Department of Child and Adolescent Psychiatry and Psychotherapy, University Hospital Frankfurt, Frankfurt, Germany).

SNP calling was performed using the GenomeStudio 2.0 software and the GenTrain-Algorithm 2.0 with a GenCall-Threshold of 0.2. All samples had a SNP-call rate above 99%. Genetic variations in the HiPSC lines were evaluated analysing the CNV present in each line. CNVs were called implementing the CNVision pipeline based on the LogR and BAF scores exported from the FinalReport exports from GenomeStudio. CNVs were considered valid if larger than 15kb, if spanning more than 15 SNPs and if at least two out of three algorithms implemented in the CNVision pipeline confirmed the presence. CNV annotation was performed using the BAMotate algorithm.

Genetic Relatedness among HiPSC clones and fibroblast source was evaluated. SNP based relatedness-analysis to confirm lineage identity was performed on the pedigree export format (Genome studio plink plug-in) using plink v 1.9 and the IBD function -genome function. Visualization is based on the PI_HAT score.

2.4 RNA METHODS

2.4.1 RNA extraction

Blood samples from the different donors were collected in PAXgene Blood RNA Tubes and RNA extracted with PAXgene Blood RNA Kit IVD (Quiagen) according to the manufacturer protocol.

To obtain RNA from cell cultures, cells were detached by Accutase (Stemcell) incubation for 5 minutes. The reaction was stopped by addition of 2 mL DMEM. Cells were centrifugated for 5 minutes at 600g, washed with 1 mL DPBS and centrifuged again. Pellet was resuspended in 1 mL RNAprotect Cell Reagent (Qiagen) and stored at -20°C until the isolation of the RNA. Total RNA was isolated using RNeasy-Plus Mini Kit (Qiagen) according to manufacturer's instructions.

RNA was firstly quantified using NanoQuant Plate (Tecan) measuring the absorbance at 260 and 280nm wavelength with the Infinite M200 PRO microplate reader (Tecan) and RNA concentration was adjusted to be below 500 ng/μL. RNA quality, absence of gDNA contamination and a more accurate estimation of RNA concentration was assessed using the Standard Sensitivity RNA Analysis Kit with Fragment Analyzer (Advanced Analytical). RNA with RQN >9 and a 28S/26S ratio above 1.5 was used for further applications.

500 ng/μL of RNA was synthesized into cDNA by using the iScript Synthesis Kit (Biorad) for following applications.

2.4.2 Two step Reverse Transcription PCR (RT-PCR)

For all the Reverse Transcription PCR (RT-PCR) used in this study primers were purchased from Eurofins Medigenomix at a concentration of 100 pmol/μl and designed with NCBI Primer-

Blast. Primer sequences are reported in Table 11. Amplification was performed in 25 μ l total volume reaction with primers diluted 1:10, 100mM dNTPs, 10xTaq Reaction Buffer, Taq Polymerase (all Biozym) in a Mastercycler nexus X2 (Eppendorf). Amplicons were separated on 2-3% agarose gel and imaged with myECL Imager (Thermo Fisher Scientific).

2.4.3 Quantitative RT-PCR (RT-qPCR)

2.4.3.1 RT-qPCR

Primers were designed with NCBI Primer-Blast to be intron spanning with the size of intron greater than 1 kbp, primer sequences are reported in Table 11. Primers were checked for hairpins (QC cutoff $-2 \leq \Delta G \leq 2$; $T_m < 40^\circ\text{C}$) as well as homo- and heterodimers ($\Delta G \geq -8$) using the IDT Oligo Analyzer tool (<https://eu.idtdna.com/calc/analyzer>).

RT-qPCR was performed on 384-well-plates with an automated pipetting robot (Biomek NX-Beckman Coulter). The total reaction volume was 10 μ l in a formulation of: 1 μ l cDNA, 1 μ l primer mix (10 pmol/ μ l) 3 μ l RNase-free water, 5 μ l FastStart Essential DNA (Roche). Plates were read in LightCycler 2.0 (Lifescience-Roche).

Prior to the sample run, a standard curve for each primer was created using quadruplicate measurement of 10-fold serial pooled cDNA dilutions. The absence of primer dimers or unspecific products was confirmed by melting curve analysis with LightCycler 480 SW 1.5.1 (Lifescience-Roche). Primer efficiency and linearity of the amplification were evaluated by Genex ver6 (Biomcc).

For each experiment a minimum of four different reference genes were included (Hs_HPRT1, Hs_SDHA, Hs_ALAS1, Hs_TBP). The best reference genes to be used for normalization were chosen according the lowest M-values obtained using the geNorm feature and lowest SD scores NormFinder of Genex ver6 (Biomcc). After gene expression normalization with the best reference genes, relative quantities (fold change, also known as fold difference) were averaged to the percentage of gene expression or using the WT baseline control group as arbitrary reference level ($\Delta\Delta\text{C}_q$ approach) depending on the experiment and then converted in Log₂ scale.

2.4.3.2 *PARK2* pre-amplification and TaqMan Gene Expression assay

Given the low gene expression of *PARK2*, samples subsequently used for *PARK2* gene expression evaluation were pre-amplified. Pre-amplification of the target genes was performed with TaqMan PreAmp Master Mix Kit (ThermoFisher Scientific) according to the manufacturer protocol. The total reaction volume was 25µl in a formulation of: 12.5 µl TaqMan PreAmp Mastermix, 6.25 µl TaqMan PreAmp Pool, 6.25 µl 100 ng cDNA sample. TaqMan PreAmp Pool was obtained by combining 10 µl of each probe (*PARK2*, *B2M*, *YWHAZ*, *POLR2A*, *SDHA*) with TE buffer as suggested by the manufacturer. The preamplification reaction was performed Mastercycler nexus X2 (Eppendorf) with the following settings: 95°C 10 minutes, (95°C 15 seconds, 60°C 4minutes) x14 cycles, 99°C 10 minutes. The products were diluted 1:20 and used for the subsequent TaqMan Gene Expression assay. Total volume of the reaction was 10 µl: 0.5 µl TaqMan Gene Expression assay, 2.5 µl diluted pre-amplified cDNA products, 5 µl TaqMan Gene Expression MasterMix, 2 µl nuclease-free water. The plate was run in LightCycler 2.0 (Lifescience-Roche) with the following settings: 50°C 2 minutes, 95°C 10 minutes, (95°C 15 seconds, 60°C 60 seconds) x14 cycles. Predesigned primer and probe sets used in the assay for the target gene (*PARK2*) and reference genes (*B2M*, *YWHAZ*, *POLR2A*, *SDHA*) are reported in Table 1. Data analysis was performed as described above.

2.4.4 RNA-Sequencing

RNA samples were analyzed by Novogene (HK) Company Limited, Hong Kong according to the company's protocols. Briefly, quality control (QC) of total RNA was assessed by Nanodrop, Agarose Gel Electrophoresis, Agilent 2100. Library was constructed enriching mRNA with oligo(dT) beads, fragmented randomly in fragmentation buffer, followed by cDNA synthesis using random hexamers and reverse transcriptase. After first-strand synthesis, a custom second-strand synthesis buffer (Illumina) was added with dNTPs, RNase H and Escherichia coli polymerase I to generate the second strand by nick-translation followed by a round of purification, terminal repair, A-tailing, ligation of sequencing adapters, size selection and PCR enrichment. Library QC was performed by Qubit 2.0 fluorometer (Life Technologies), before checking insert size on an Agilent 2100 and quantifying to greater accuracy by quantitative PCR (Q-PCR) (library activity >2 nM). Raw data obtained from Illumina analysis of the libraries

were transformed to sequenced reads by base calling. QC was performed in regard of Error Rate and A/T/G/C Content Distribution. Data were filtered to remove reads containing adapters or reads of low quality. Mapping to Reference Genome was built using Bowtie v2.2.3 and paired-end clean reads were aligned to the reference genome using TopHat v2.0.12. Gene expression levels were estimated by FPKM method. Differential expression analysis of two conditions/groups was performed using the DESeq R package (1.18.0). Gene Ontology (GO) enrichment analysis of differentially expressed genes was implemented by the Goseq R package, in which gene length bias was corrected. GO terms with corrected P-value less than 0.05 were considered significantly enriched by differential expressed genes.

2.5 MICROSCOPY METHODS

Cells were monitored daily by using a light microscopy microscope (Primo Vert, Zeiss) equipped with a digital camera (AxioCam ICc5, Zeiss).

2.5.1 Live staining

Early HiPSC clone selection was performed after live staining for alkaline phosphatase expression with Alkaline Phosphatase Live Stain (Life Technologies) directly on the transfected fibroblasts. Staining was performed according to manufacturer instruction. Briefly, cells were washed and incubated with 1.5 μ l of AP Live Staining 500x per ml in DMEM for 30 minutes. Cultured were washed twice with DMEM and imaged with a fluorescent microscopy equipped with a standard FITC filter (Leica). Glowing colonies were manually picked and transferred in new culture ware for single clone expansion.

2.5.2 Immunofluorescence for pluripotency markers, embryonic germs layers differentiation and neuronal markers

For all immunofluorescence staining used in this study, cultures were grown on 12 mm diameter glass coverslips (Marienfeld GmbH&Co) in 24 well plates and fixed with 4% paraformaldehyde (Sigma Aldrich) for 30 minutes. Cells were washed three times with DPBS

and permeabilized with 0.2% Triton-X in DPBS (Sigma Aldrich) for the HiPSC or 1% Saponin in DPBS (Sigma Aldrich) for EBs for 15 min at RT. Cells were washed three times with DPBS and blocked by incubation for 30 minutes at RT with 3% BSA in DPBS (Sigma Aldrich). Primary antibodies (see Table 12 for a complete list of primary and secondary antibodies and dilutions used in this study) were added directly into the blocking solution and incubated overnight at 4°C. Cells were washed three times with DPBS and secondary antibodies were incubated for 1 hour at RT. Coverslip were mounted on glass slides with ProLong Diamond Antifade Mountant with DAPI (Life Technologies). Slides were imaged with a fluorescence microscope with ApoTome function (Axio Observer.Z1, Zeiss).

2.5.3 Immunofluorescence for mitochondrial network morphology

Cells were grown on coverslips 12mm diameter glass coverslips (Marienfeld GmbH&Co) in 24 well plates. Mitochondria were stained with 400 nM MitoTracker Red CMXRos (ThermoFisher Scientific) diluted in prewarmed feeding medium (DMEM 10%FBS for fibroblasts and mTeSR1 complete medium for HiPSC) for 30 min at 37°C in the dark. Cells were washed three times with DPBS and fixed in with 4% paraformaldehyde (Sigma Aldrich) in DPBS for 15 minutes at room temperature. Cells were washed three times with DPBS and nuclei stained with 20µl/per well of NucBlue Fixed Cell Stain (ThermoFisher Scientific) during the last wash step and incubated for 5 minutes. Cells were washed three times with DPBS and coverslips were fixed on glass slides with ProLong Diamond Antifade Mountant (Life Technologies) for imaging with Zeiss Axio Observer.Z1 microscope with ApoTome function (Zeiss).

2.6 PROTEIN METHODS

2.6.1 Protein extraction and measurement

Cells were harvested by trypsin incubation for fibroblasts, accutase incubation for HiPSC and HiPSC-derived Neurons, and centrifuged for 5 minutes at 400 g. Cell pellet was washed in DPBS, pelleted again (400 g for 5 min), lysed in Pierce Lysis Buffer supplemented with 10 µl/ml Halt Protease and Phosphatase Inhibitor Cocktail (Thermo Scientific) and incubated for 10 min

on ice with occasional mixing. For the fibroblast cultures, cell pellet was additionally homogenized using pestle homogenizer (Schuett-Biotec). Homogenized lysate was centrifuged at 13.000 g for 10 min at 4°C. To separate from cell debris, the lysate was transferred to a new tube. To prevent loss of activity and protein destabilization during freeze-thaw and storing period, Protein Stabilizing Cocktail 4x (Thermo Scientific) was added.

Protein concentration was measured by colorimetric assay using Precision Red Advanced Protein Assay Reagent (Cytoskeleton Inc). Measurement was carried out on clear bottom dark sides 96-well plate (Greiner, 655090) and absorbance measured at 600 nm wavelength using Infinite M200 PRO microplate reader (Tecan). The values were measured in duplicates, averaged and corrected by subtraction of the background value. Protein concentration was extrapolated by interpolation with a standard curve performed with known serial dilutions of BSA (Sigma Aldrich).

2.6.2 PARK2 protein concentration by enzyme-linked immunosorbent assay (ELISA)

PARK2 protein concentration was measured with Human Parkin SimpleStep ELISA Kit (Abcam). Shortly, 50 µl of sample containing 1000 µg of total cellular protein extract was loaded in each well. 50 µl of the antibody cocktail was added to each well and the plate sealed and incubated for 1 hour at room temperature on a plate shaker set to 400 rpm. After washing 3 times the wells with Wash Buffer PT to remove unbound material, 100 µL of TMB Substrate was added to each well and incubated for 10 minutes in the dark on a plate shaker (400 rpm) generating blue coloration. The reaction was stopped by addition of 100 µL of Stop Solution completing any color change from blue to yellow. The plate was shake for one additional minute to mix. Endpoint reading of Optical Density (OD) at 450 nm was performed on Infinite M200 PRO microplate reader (Tecan). For every assay, 8 standards with known concentration of human PARK2 obtained from extract of HEK293T Cells overexpressing human parkin was included. Samples and standards were measured in duplicate and data are the average value of in two independent experiments. The calculated minimal detectable dose of PARK2 with this kit is 9.7 pg/mL according to the manufacturer's information.

2.6.3 DOPAMINE levels by ELISA

Dopamine concentration was measured on mature HiPSC-derived dopaminergic neurons. Intracellular dopamine concentration was measured using total protein extracts obtained as described above whereas extracellular concentration was assessed using conditioned media. Cells were washed with DPBS and B27 complete media added, after 2 days a total of 1 ml of conditioned media was collected from 10 randomly chosen well and centrifuged at 3000 rpm at 4°C for 10 minutes. Supernatant was then used for ELISA assay and additionally the total protein concentration in the conditioned media was measured as described in 2.6.1. Dopamine levels were measured in duplicates with human dopamine (DA) ELISA Kit (Cusabio) by adding 50 µl of standard or sample, 50 µl of HRP-conjugate, 50µl antibody per well. Plates were then incubated for 1 hour at 37°C on a plate shaker set to 200 rpm. Wells were washed 3 times with wash buffer and 50 µl of substrate A and 50 µl of substrate B added to each well. Sealed plates were incubated for 15 minutes at 37°C on a plate shaker set to 200 rpm. The reaction was stopped by adding 50 µl of stop solution to each well and mixing on a plate shaker set to 200 rpm for 1 min. Endpoint reading of optical density (OD) at 450 nm was performed on Infinite M200 PRO microplate reader (Tecan). Standards with known concentration of dopamine were included in every experiment and a standard curve created using the free software CurveExpert 1.4. After averaging the duplicate measurement and correct for blank readings, extracellular dopamine concentration was derived by interpolation with the standard curve. Extracellular dopamine levels were corrected for 10000 µg/ml total protein loaded. Both conditioned media and total cellular protein extract from fibroblast was used as negative control and led to below threshold of detection dopamine levels.

2.7 ASSAYS FOR ENERGY IMPAIRMENT AND OXIDATIVE STRESS

2.7.1 ATP production

Fibroblast were seeded at a concentration of 20000 cells per well on black sided 96-well plates with clear bottom (Greiner Bio one) after being counted twice by EVE Automated Cell Counter (NanoEnTek). Cells were allowed to adhere for 4 hours and then the treatments were applied

in a total volume per well of 100 μ L. Given a possible interaction with luminescence reading, DMEM without phenol red (Thermofisher scientific) was used.

ATP production was measured with ATPlite Luminescence Assay System (PerkinElmer) according to manufacturer's instructions and as described in (Mortiboys et al., 2009). Briefly, to lyse the cells and stabilizes the ATP, 50 μ L of mammalian cell lysis solution per well was added, plate sealed with dark foil and shake for 5 minutes in an orbital shaker at 700 rpm. Then, plates were incubated for 5 minutes with 50 μ L substrate solution with continuous orbital shaking. After short spin down the plates were allowed to dark adapt in the reader for 10 minutes, luminescence was read with Plate reader Infinite 200 PRO (Tecan). Settings used were: temperature 24°C \pm 4°C, 50 ms integration time, 150 ms settle time, automatic attenuation. Output reading is given in RLU (Relative Luminescence Units). All readings were blank subtracted. Samples were measured in triplicate and data presented are the average of 2 independent experiments.

2.7.2 Oxygen consumption

Fibroblast lines were seeded at a concentration of 50000 cells per well on black sided 96-well plates with clear bottom (Greiner Bio one) after being counted by EVE Automated Cell Counter (NanoEnTek). Cells were allowed to adhere for 4 hours and then the treatments were applied for 24h in a total volume per well of 200 μ L, DMEM without phenol red (Thermofisher scientific) was used. Basal extracellular oxygen consumption rate (OCR) was measured with the extracellular O₂ consumption assay (Abcam) as suggested by the manufacturer. Shortly, 10 μ l extracellular O₂ consumption reagent was added in each well and sealed with 100 μ l high sensitivity mineral oil. Fluorescence was measured with plate reader Infinite 200 PRO (Tecan). Settings used were: temperature 37°C \pm 4°C, 30 μ s delay time, 100 μ s gate time, 380nm/650 nm ex/em wavelength. Measurement were performed every 2 minutes interval for 90 minutes. Output reading is given in RFU (Relative Fluorescence Units). All readings were blank subtracted. Samples were measured in triplicate and data presented are the average of 2 independent experiments. Experiments were performed conjunctly with Lukas Frank, bachelor student.

2.7.3 ROS production

As for the previous assay, fibroblasts were counted twice with EVE Automated Cell Counter (NanoEnTek), seeded on a sided 96-well plates with clear bottom (Greiner Bio one) at a concentration of 20000 cells per well and allowed to adhere for 4 hours and then treatments were applied. Reactive oxygen species abundance was measured with DCFDA/H2DCFDA - Cellular Reactive Oxygen Species Detection Assay Kit (ABCAM) using a modified protocol suggested by the manufacturer for 24h treatments. The assay uses the cell permeant reagent 2',7' -dichlorofluorescein diacetate (DCFDA), a fluorogenic dye that measures hydroxyl, peroxy and other ROS activity within the cell. 40 minutes before the completion of the 24hours treatments used in this study, 100 μ L DCFDA was added to each test well and incubated for 40 minutes at 37°C. End point fluorescence reading was carried out in Plate reader Infinite 200 PRO (Tecan). Settings used were: temperature 37°C \pm 4°C, 50 ms integration time, 150 ms settle time, automatic attenuation, Ex/Em wavelength = 485/535 nm. Output reading is given in RFU (relative fluorescence units). Fold difference in ROS levels was calculated against Wild Type baseline after background subtraction. Tert-Butyl Hydrogen Peroxide (TBHP) 55 mM was used as positive control for the assay. Samples were measured in duplicate. Given a possible interaction with luminescence reading, DMEM without phenol red (Thermofisher scientific) was used.

2.8 DATA ANALYSIS AND STATISTICS

2.8.1 Data analysis for mitochondrial network morphology (macro)

Analysis of the mitochondrial morphology was performed as described in (Burbulla & Krüger, 2012) with minor adjustments. Two macros were created for semi-automated analysis by Fiji ImageJ software (Wayne Rasband; National Institutes of Health, USA). RGB Images were converted in 8-bit images, and channels spitted. Region of interest (ROI) were manually drawn to include a single cell, in case of fibroblast, or the whole picture, in case of HiPSC, by transforming the red-channel image in Fire Look-up Table (LUT). A second macro was runt on the ROI selection to reduce unspecific noise (Despekle), imaged was then convolved and

automatic threshold (Intermodes) set. Shape descriptors values for each single mitochondrion present in each cell were then obtained by selecting the “analyze particles” function with measurement redirected to the original unprocessed image. Mean values were then calculated as well as the AR (aspect ratio): $\text{major_axis}/\text{minor_axis}$ and FF (Form factor): $[\text{perimeter}^2/(4\pi \times \text{area})]$ on a Excel spreadsheet. 15 different selected fibroblasts for each line (90 cells total) from two independent experiments were analyzed for the fibroblast lines whereas for the HiPSC lines, analysis was run on 6 pictures as whole for each line/condition (36 in total). Statistical analysis was performed on the mean value for each line/condition.

```
Macro 1 : Run ("Duplicate...", "title=duplicate");run("Split Channels");selectWindow("duplicate (blue)");close();selectWindow("duplicate (green)");close();selectWindow("duplicate (red)");run("Duplicate...", "title=[for lut]");run("Fire");
```

```
Macro 2: run("Despeckle");run("Convolve...", "text1=[-1 -1 -1 -1 -1\n-1 -1 -1 -1 -1\n-1 -1 24 -1 -1\n-1 -1 -1 -1 -1\n-1 -1 -1 -1 -1\n] normalize");run("Auto Threshold", "method=Intermodes white");
```

2.8.2 Statistics

Data were analyzed with IBM SPSS Statistics 22 software (IBM). For each experiment, data were tested for normal distribution and fit to parametric testing assumption and one-way ANOVA or two-way ANOVA (univariate analysis of variance) were used. In case data were not normally distributed, non-parametric tests (Kruskal-Wallis test or Mann-Whitney test) were performed. If statistical analysis showed significant difference, Post-hoc testing was performed (Tukey HD or Dunn's test). Additionally, effect size was calculated (Cohen's d or Partial eta squares). If a different trend was shown by the *PARK2* CNV duplication carrier from the deletion one, CNVs carriers were considered as separate groups. Diagnosis was also tested as independent variable for each test. The level of significance was set at $p=.05$. Graphs were plotted designed using GraphPad Prism 5.01. Standard curves were created using the free software CurveExpert 1.4.

3 RESULTS

3.1 SUMMARY OF SAMPLE SIZE

In the first initial screening tests, a total of 12 lines deriving from human donors were used, 4 *PARK2* CNV carriers affected by ADHD, 4 *PARK2* wild types affected by ADHD and 4 *PARK2* wild types non-affected (Table 1). Participants were carefully chosen to be age and sex matched. This sample set was used for gene expression analysis in blood samples and in human dermal fibroblast cultures. A subset of this sample cohort was used both for generating HiPSC and HiPSC-derived neurons and to conduct the subsequent experiments included in the study. Therefore, 6 HiPSC and HiPSC-derived dopaminergic neurons lines were generated in our facility, three *PARK2* CNV carriers affected by ADHD, one *PARK2* wild type affected by ADHD and two *PARK2* wild types non-affected. For technical reasons one of WT healthy lines had to be dismissed later and was substituted by a *PARK2* WT HiPSC line generated from commercially available human foreskin fibroblasts (PromoCell) that was kindly obtained from the lab of Prof. Edenhofer, Institute of Genomic, Stem cell biology and Regenerative Medicine, Innsbruck.

<i>PARK2</i> GENOTYPE	TYPE OF <i>PARK2</i> CNV	DIAGNOSIS	Sex	Age	Ethnicity	Line name in this study
*CNV	Deletion	ADHD	female	43	Caucasian	PARK2CNV_DEL_A/ADHD
*CNV	Deletion	ADHD	male	47	Caucasian	PARK2CNV_DEL_B/ADHD
*CNV	Duplication	ADHD	female	48	Caucasian	PARK2CNV_DUP /ADHD
CNV	Duplication	ADHD	female	28	Caucasian	
WT	Wildtype	ADHD	female	48	Caucasian	
WT	Wildtype	ADHD	female	41	Caucasian	
WT	Wildtype	ADHD	male	46	Caucasian	
*WT	Wildtype	ADHD	female	30	Caucasian	WT /ADHD
WT	Wildtype	HEALTHY	male	46	Caucasian	
*WT	Wildtype	HEALTHY	female	27	Caucasian	WT_A/HEALTHY
*WT	Wildtype	HEALTHY	female	39	Caucasian	WT_B/HEALTHY
WT	Wildtype	HEALTHY	female	42	Caucasian	

Table 1 Genotype for the *PARK2* locus and demographic data of the donors used in this study. Lines marked with * were used to generate HiPSC and HiPSC-derived dopaminergic neurons.

3.2 NEUROLOGICAL AND PSYCHIATRIC ASSESSMENT

Patients and healthy controls were subject of a comprehensive neuropsychiatric assessment (Table 2) (Prof. Dr.med Andreas Reif and PD Dr. med.Sarah Kittel-Schneider). ADHD was diagnosed following the DSM-IV criteria whereas the presence of and ADHD symptomatology already in the childhood was assessed by the retrospective German short form of the Wender Utah Rating Scale (WURS-k).

Given the association of *PARK2* genetic variation with an early onset form of Parkinson's disease (arouse of symptoms mean age 30), patients were also neurologically tested. Average age in the cohort was forty years old ($M=40.417$; $SD=7.833$). None of the participant had above threshold diagnosis scores in any of the Parkinson's disease specific tests performed. Independent-samples t-test was used to assess difference in the neurological scores. No significant difference between ADHD/*PARK2* CNV carriers and WT was found in "Unified Parkinson's Disease Rating Scale" (UPDRS) scores, scores from the "Non Motor Symptoms Parkinson's questionnaire" (PD NMS), Olfactory function measured by Sniffin' Sticks olfactory test, volume of *substantia nigra* measured by ultrasound. When assessing difference based on diagnosis, we found a higher score ($t_{(7)} = -2.51$, $p = .04$, $d = 1.25$) on the PD NMS in ADHD patients compared to controls which were very likely due to the comorbidity with major depression in some of the patients and the ADHD core symptoms itself.

This data, plus the fact that *PARK2* mutation are associated with an autosomal early-onset Parkinson's disease with onset at about 30 years, suggest that the *PARK2* CNVs present in our cohort of ADHD patients are rather not correlated with PD. However, as the participants were still relatively young at sampling, late-onset PD could occur later in life, therefore for future studies participants might be contacted again for follow-up investigation.

demographic data										Neurological assessment			
PARK2 GENOTYPE	TYPE OF PARK2 CNV	DIAGNOSIS	Sex	Age	IQ	Smoker	UPDRS	PD NMS	Sniffing sticks	S. nigra right cm²	S. nigra left cm²		
WT	Wildtype	HEALTHY	female	42	94	NO	14	6	8	0,11	0,10		
WT	Wildtype	HEALTHY	female	39	136	YES	0	0	10	0,10	0,15		
WT	Wildtype	HEALTHY	female	27	118	NO	1	1	11	0,13	0,14		
WT	Wildtype	HEALTHY	Male	46	112	YES	3	1	9	0,19	0,13		
WT	Wildtype	ADHD	female	30	107	YES	26	63	11	0,10	0,07		
WT	Wildtype	ADHD	Male	46	97	NO	5	11	10	0,11	0,09		
WT	Wildtype	ADHD	female	41	136	NO	10	5	11	0,10	0,12		
WT	Wildtype	ADHD	female	48	124	NO	5	3	11	0,12	0,24		
CNV	Duplication	ADHD	female	48	101	NO	12	94	9	0,11	0,09		
CNV	Duplication	ADHD	female	28	104	NO	2	8	11	0,14	0,10		
CNV	Deletion	ADHD	male	47	130	NO	14	47	10	0,11	0,09		
CNV	Deletion	ADHD	Female	43	118	NO	3	22	10	0,08	0,15		

Table 2 Demographic data and neurological assessment.

In the first part of the table demographic data of the sample cohort used in the study is reported. Neurological assessment was performed by: “Unified Parkinson’s Disease Rating Scale” (UPDRS), “Non Motor Symptoms Parkinson’s questionnaire” (PD NMS), “Sniffing Sticks olfactory test”, volume of Substantia Nigra (cm²) measured by ultrasound

PARK2 GENOT YPE	TYPE OF PARK2 CNV	DSM-IV diagnostic criteria ADULTHOOD		DSM-IV diagnostic criteria CHILDHOOD		ADHD Subtype	sum score WUR S-k	Major Depressi on
		Inatte ntion	Hyperactivity/ Impulsivity	Inatte ntion	Hyperactivity/ Impulsivity			
WT	Wildtype	8	8	8	8	combined	80	YES
WT	Wildtype	5	7	5	3	predominantly hyperactive	54	NO
WT	Wildtype	7	6	8	7	combined	80	NO
WT	Wildtype	8	7	9	3	combined	62	YES
CNV	Duplication	8	6	6	3	combined	52	YES
CNV	Duplication	9	4	8	0	predominantly inattentive	55	NO
CNV	Deletion	7	9	6	8	combined	79	YES
CNV	Deletion	6	5	6	1	predominantly inattentive	47	YES

Table 3 *Psychiatric assessment of ADHD patients used in the study.*

Psychiatric assessment was performed by following the DSM-IV diagnostic criteria for Inattention and Hyperactivity/ Impulsivity symptoms both during adulthood and childhood. The scores were used to establish which ADHD subtype was shown by the patients (predominantly hyperactive, predominantly inattentive or combined). the presence of and ADHD symptomatology already in the childhood was additionally assessed by the “retrospective German short form of Wender Utah Rating Scale” (WURS-k). Comorbidity with Major Depression is reported on the last column.

3.3 *PARK2* GENOTYPING

PARK2 CNV status was first investigated by Duplex TaqMan CNV assay from gDNA extracted from blood and fibroblast samples in Würzburg and then replicated in Frankfurt. The analysis, (Dr. Heike Weber, Department of Psychiatry, Psychotherapy and Psychosomatic Medicine, University Hospital Würzburg, Germany), showed the presence of *PARK2* CNV duplication in 2 ADHD patients and deletion in other 2 ADHD patients (Table 3).

Successively, the lines that were chosen for HiPSC generation and HiPSC-derived dopaminergic neurons induction were subject to a more accurate genotyping by Illumina Infinium Omni2.5-8 bead array (Institute of Human Genetics, LIFE&BRAIN GmbH, University Bonn) that confirmed *PARK2* CNVs in all three patients spanning exon 2 of transcript NM_004562 (Figure 3) (*PARK2* CNV hg19 position: PARK2CNV_DEL_A/ADHD chr6:162737426-162882874; PARK2CNV_DUP/ADHD chr6:162719417- 162914986; PARK2CNV_DEL_B/ADHD chr6:162757115-163004064). Bioinformatic analysis was performed by Dr. Andreas Chiocchetti (Department of Child and Adolescent Psychiatry, University Hospital Frankfurt, Germany).

PARK2 GENOTYPE	TYPE OF PARK2 CNV	DIAGNOSIS	gDNA SOURCE	CN Calculated	CN Predicted	Confidence	 Z-Score 	Replicates Analyzed
CNV	Deletion	ADHD	BLOOD	0.98	1	> 0.99	0.11	3
			FIBRO	1.13	1	> 0.99	0.26	4
CNV	Deletion	ADHD	BLOOD	1.02	1	> 0.99	0.61	4
			FIBRO	0.99	1	> 0.99	0.07	4
CNV	Duplication	ADHD	BLOOD	2.61	3	0.86	0.77	4
			FIBRO	2.74	3	< 0.50	0.41	4
CNV	Duplication	ADHD	BLOOD	1.7	2	> 0.99	1.37	4
			FIBRO	2.6	3	0.8	0.67	3
WT	Wildtype	ADHD	BLOOD	1.95	2	> 0.99	0.07	4
WT	Wildtype	ADHD	BLOOD	1.89	2	> 0.99	0.04	3
WT	Wildtype	ADHD	BLOOD	2.06	2	> 0.99	0.62	4
WT	Wildtype	ADHD	BLOOD	2.05	2	> 0.99	0.44	3
WT	Wildtype	HEALTHY	BLOOD	1.97	2	> 0.99	0.1	4
			FIBRO	1.88	2	> 0.99	0.34	4
WT	Wildtype	HEALTHY	BLOOD	1.92	2	> 0.99	0.06	3
			FIBRO	2.18	2	0.96	0.1	3
WT	Wildtype	HEALTHY	BLOOD	2.24	2	0.94	0.21	4
			FIBRO	2.06	2	0.99	0.02	4
WT	Wildtype	HEALTHY	BLOOD	2.34	2	0.84	0.37	4
			FIBRO	1.91	2	> 0.99	0.34	4
*WT	Wildtype	HEALTHY	IPSC	1.93	2	> 0.99	0.36	4

Table 4 *PARK2* genotyping by Duplex TaqMan CNV assay.

The assay was performed from gDNA extracted from blood and fibroblast samples when available. The table shows the copy number (CN) present in the *PARK2* locus (chr6: 162696987 +/- 50 bp) as well as the confidence and Z-scores. The last column reports how many of the 4 replicates used for each line were included in the analysis.

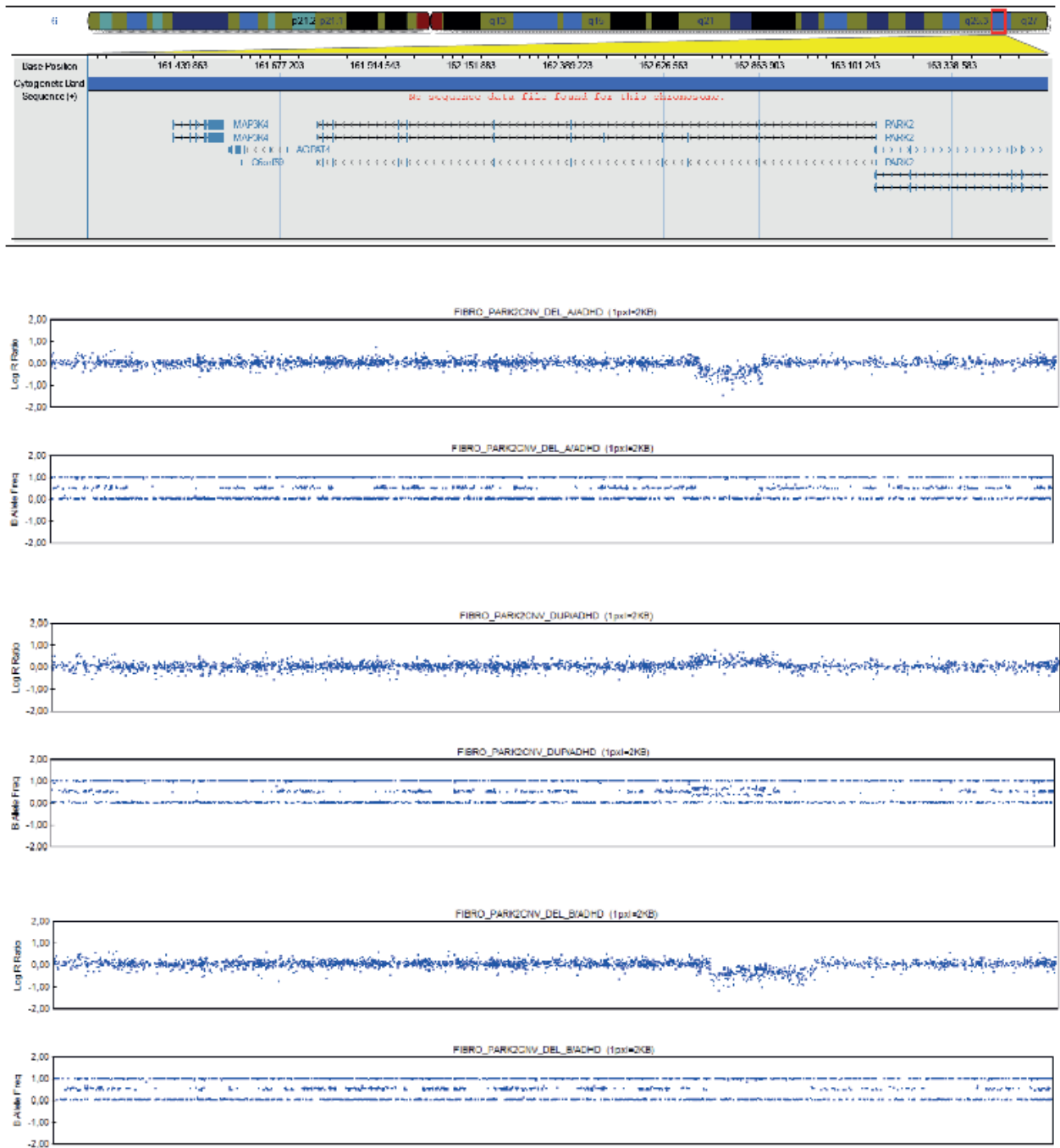


Figure 3 Chromosome 6 ideogram and SNP array analysis of the *PARK2* locus for the ADHD/*PARK2* CNVs carriers. LogR ratio and B-allele frequencies (BAF of *PARK2* CNV carriers) for the 3 *PARK2* CNVs carrier lines. *PARK2* CNV hg19 position: *PARK2*CNV_DEL_A/ADHD chr6:162737426-162882874; *PARK2*CNV_DUP /ADHD chr6:162719417-162914986; *PARK2*CNV_DEL_B/ADHD chr6:162757115-163004064).

3.4 CREATION AND VALIDATION OF THE MODELS

3.4.1 Human dermal fibroblasts (HDFs)

Fibroblast primary cultures were successfully generated from all donors. As discussed in the introduction, when using this cell type care must be taken to in vitro cellular ageing that might affect several biological processes and fibroblast growth itself (Sprenger et al., 2010). Therefore, we assessed if differences in doubling time and viability were present in our lines measuring the cell number for 4 consecutive passages (Figure 4). Our analysis did not show any significant difference due to the genotype in the doubling time of the fibroblast cultures ($t_{(4)} = -0.99$, $p = .926$), CNV carriers ($M=2.995$; $SD=1.497$) and WT ($M=2.901$; $SD=0.698$) and in the viability, expressed as a percentage of live cell on the total number of cells ($t_{(4)} = 0.563$, $p = .620$), CNV carriers ($M=92.000$; $SD=2.828$) and WT ($M=94.000$; $SD=2.000$). This confirmed that the fibroblast lines generated in our laboratory had comparable growth rates and viability.

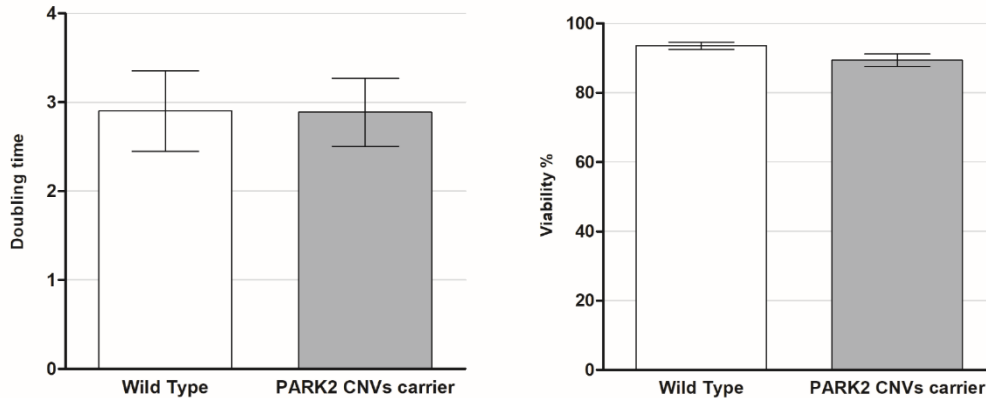


Figure 4 Human dermal fibroblast doubling time and viability.

Cells were measured in duplicate for 4 consecutive passages (from P3 to P7). Doubling time was calculated as $(\text{duration} * \text{Log}(2)) / (\text{Log}(\text{Final Concentration}) - \text{Log}(\text{Initial Concentration}))$. Viability (ratio between live cells and dead cell) was expressed as percentage. Statistical analysis did not show significant differences. Data are shown as mean \pm SEM.

3.4.2 Human induced pluripotent stem cells (HiPSC)

HiPSC obtained from fibroblast primary cultures were extensively and comprehensively characterized to prove the generation of *bona fide* HiPSC. We validated 3 clones for each line generated in order to exclude any possible confounding effect due to the reprogramming technique.

Human dermal fibroblast (Figure 5.A) at mean passage 6 were cultured and transfected with CytoTune-Ips 2.0 Sendai Reprogramming Kit (Invitrogen). After about 2 weeks, the first putative HiPSC colonies started to emerge as multilayer aggregates (Figure 5.B). The expression of Alkaline Phosphatase (AP) was used as first screening tool to discriminate between early correctly reprogrammed clones (Figure 5.C). In humans, AP is known to be expressed at high levels in pluripotent stem cell types such as embryonic stem cells and induced pluripotent stem cells (Singh et al., 2015). Fluorescent colonies were manually picked and transferred for single clone expansion (Figure 5.D). After about 6 passages the clones started to show a homogeneous morphology. HiPSC are characterized by a peculiar hESC-like morphology: round shaped and compact colonies with sharp and distinct borders, tightly packed cells with high nuclear-to-cytoplasm ratio (Figure 5.E). All the clones picked from the different cell lines were monitored by light microscopy, just HiPSC that showed above 90% of hESC-like morphology were used for the subsequent *bona fide* HiPSC validation.

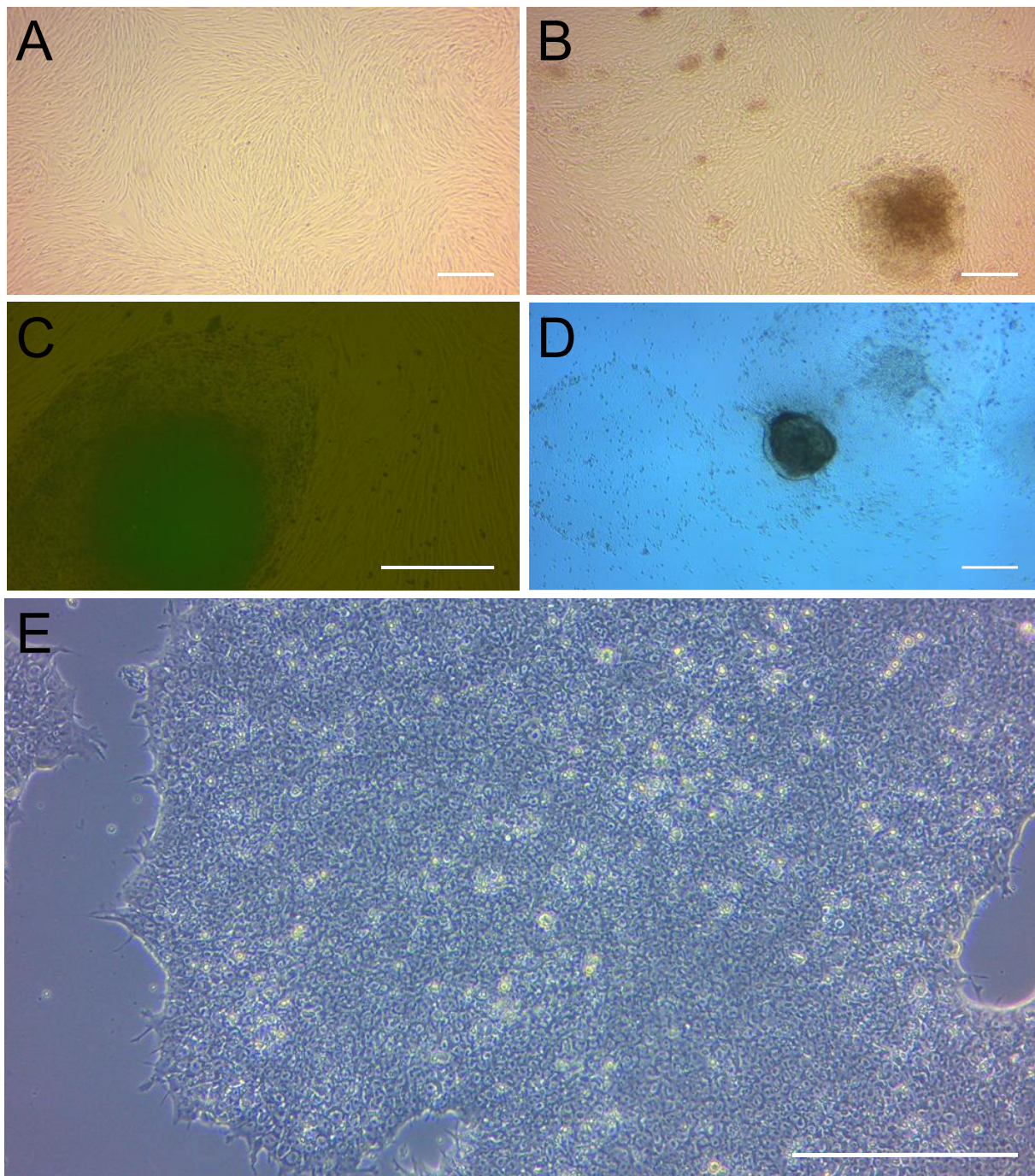


Figure 5 *HiPSC morphological changing during transfection protocol.*

(A) Light microscopy images of human dermal fibroblasts five passages after being isolated from skin biopsy.

(B) First putative HiPSCs colonies after 17 days from transfection.

(C) Live fluorescence images of Alkaline Phosphatase positive HiPSC colonies.

(D) Putative HiPSC colony manually separated from the non-reprogrammed fibroblasts and plated singularly for single clone expansion.

(E) Typical HiPSC morphology of stable HiPSC clones: compact colonies with sharp and distinct borders, round shaped tightly packed cells with high nuclear-to-cytoplasm ratio. Scale bars equal to 100 μm .

3.4.2.1 Expression of pluripotency markers

We assessed the expression of HiPSC-specific markers by RT-PCR and by immunofluorescence.

All tested HiPSC clones showed expression of developmental pluripotency associated 5 (DPPA5 also known as ESG1), SRY-box 2 (SOX2), nanog homeobox (NANOG), POU class 5 homeobox 1 (POU5F1 also known as OCT3; OCT4) that were absent in the fibroblast source lines. Glyceraldehyde-3-phosphate dehydrogenase (GAPDH) expression was used as positive control (Figure 6).

Additionally, all tested clones stained positive for the cellular surface pluripotency markers such as podocalyxin like Protein 1 (TRA-1-60 also known as PODXL) and stage-specific embryonic antigen 4 (SSEA4), and for the nuclear marker POU5F1 (also known as OCT3; OCT4) (Figure 6).

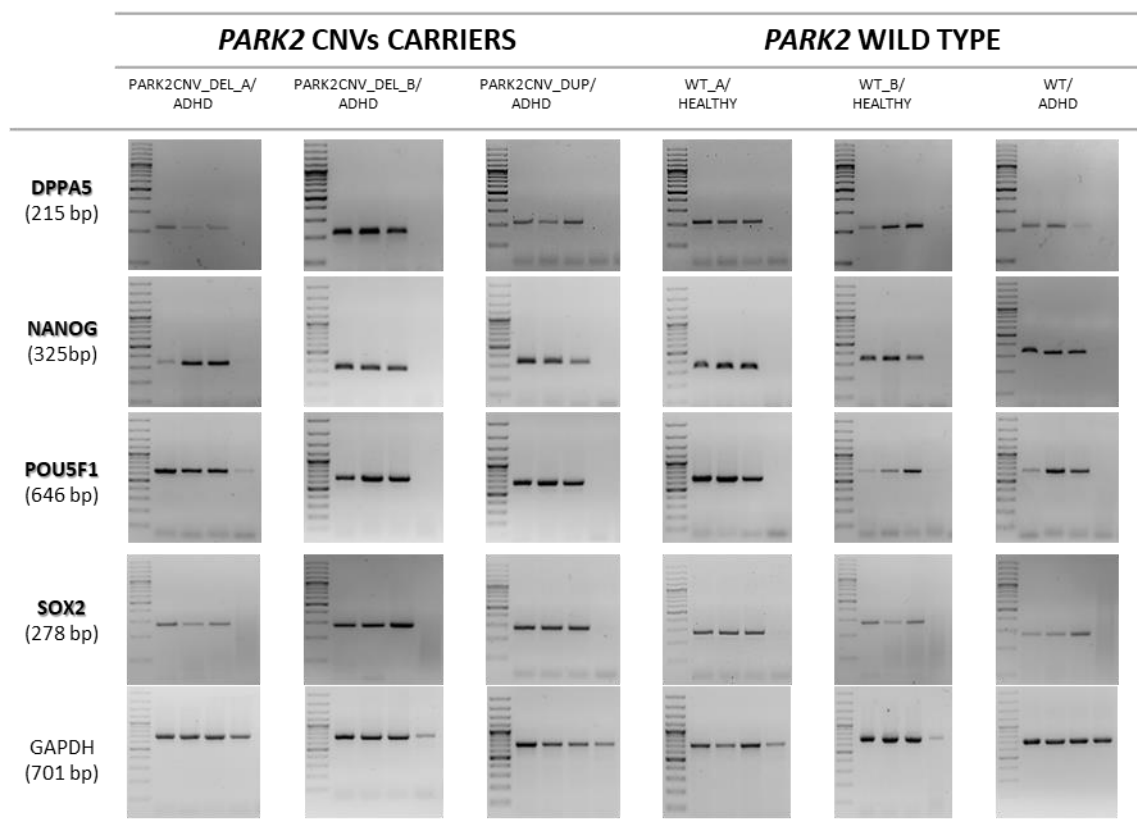


Figure 6 HiPSCs expression of pluripotency- specific markers by RT-PCR.

Three clones from each generated iPSC line (first 3 lanes) showed expression of the pluripotency markers DPPA5, SOX2, NANOG, and POU5F1 by RT-PCR. These markers were not expressed by the fibroblast line they were derived from (fourth lane). GAPDH expression (housekeeping gene) was used as RT-PCR positive control.

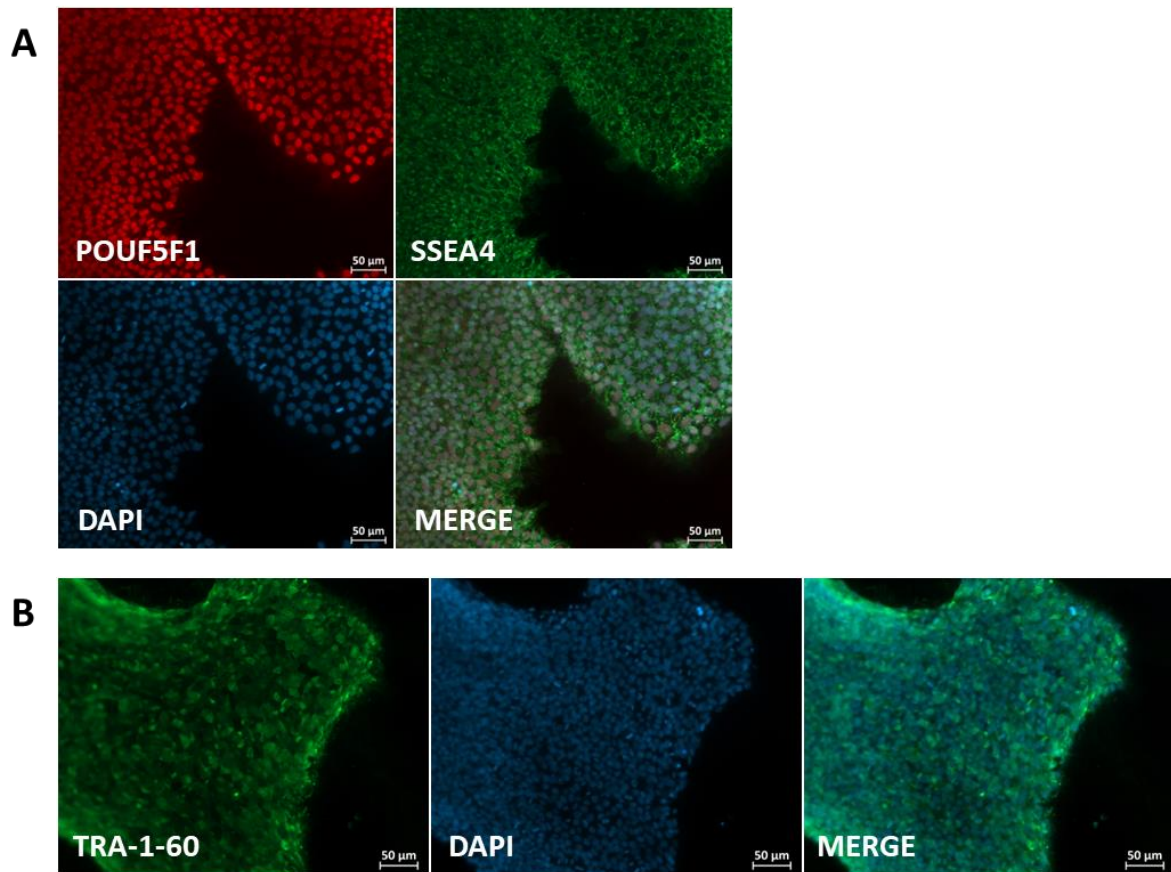


Figure 7 *HiPSCs expression of pluripotency-specific markers by Immunofluorescence.*

Representative pictures iPSC immunostaining for pluripotency factors POU5F1 (red), SSEA4 (green), TRA-1-60 (green). Cell nucleus was stained with DAPI. 3 clones for each line were evaluated. Scale bars 50 µm.

3.4.2.2 Pluripotency ability

Pluripotent stem cells should be able to generate a plethora of different cell types by definition. Allowing the growth as spherical three dimensional aggregates, called embryoid bodies (EBs), is it possible to assess if the iPSCs are able to spontaneously differentiate into cellular derivatives of all three embryonic germ layers. After 3 weeks of spontaneous differentiation, the EBs were immunostained. We report in all HiPSC tested expression of mesodermal (alpha smooth muscle actin, α -SMA; SMA), ectodermal (neuron-specific tubulin beta 3 class III, TUBB3 also known as TUJ1) and Endodermal (alpha fetoprotein (AFP) markers (Figure 8).

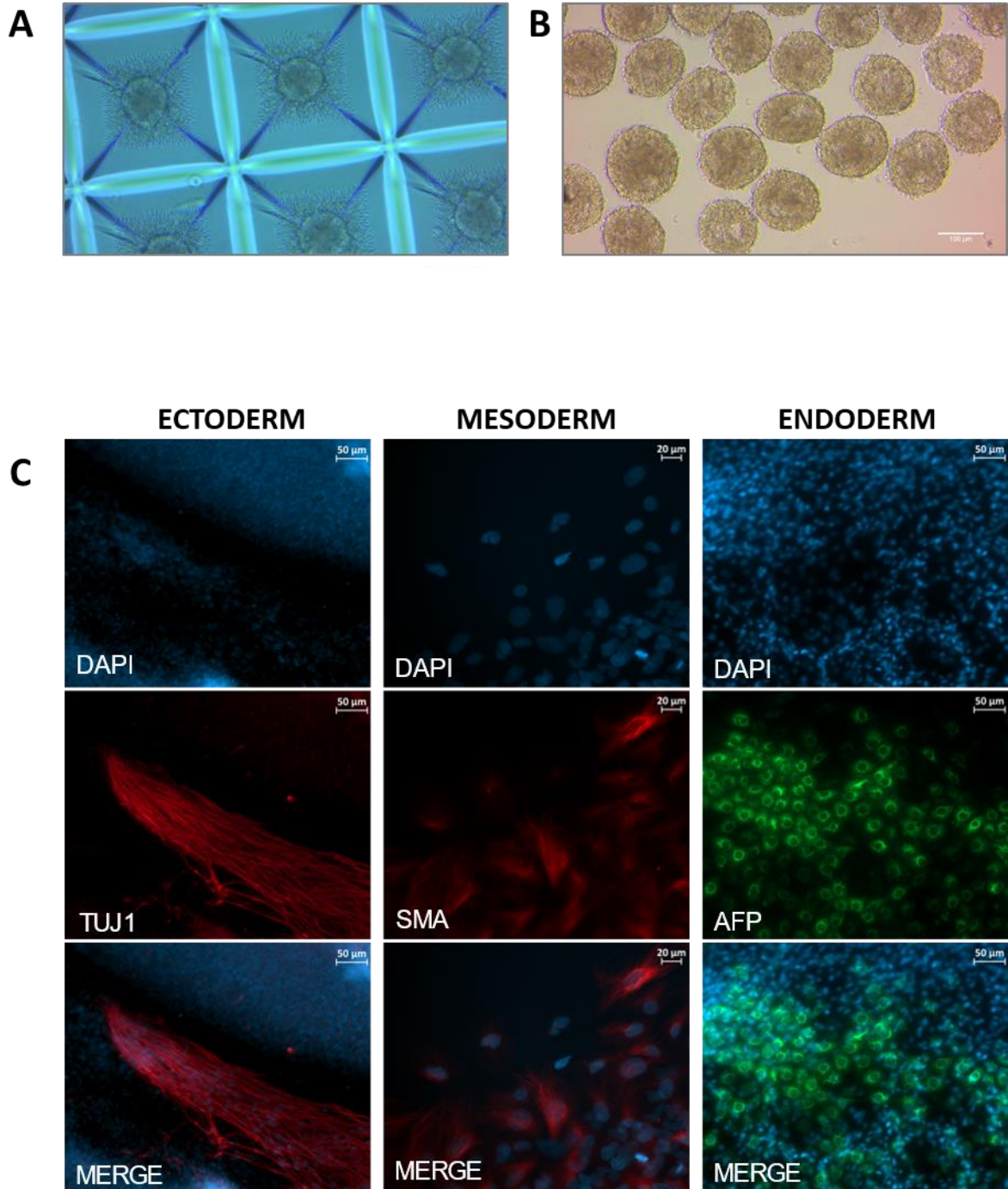


Figure 8 *Embryoid bodies assay.*

(A) The formation of spherical aggregates (EBs) was promoted by culturing a single cell suspension of HiPSC in conical wells (AggreWell 400Ex plate). After 1-day EBs with clear sharp borders are visible.

(B) Embryoid bodies (8-days old) in suspension culture maintain their spherical structure with distinct borders.

(C) After 3 weeks of spontaneous differentiation, EBs were positive for mesodermal (alpha smooth muscle actin, SMA -red), ectodermal (neuron-specific tubulin beta 3 class III, TUBB3 also known as TUJ1- red) and Endodermal (alpha fetoprotein (AFP- green) markers. Cell nucleus was stained with DAPI (blue). 3 clones for each line were evaluated.

3.4.2.3 Absence of viral vector

Fibroblast cultures were transduced into HiPSC with a non-integrative method using a vector based on the Sendai virus, a negative-sense single-stranded RNA virus (-ssRNA virus). In this case the replication of transgenes occurs in the cytoplasm without genomic integration (Lim et al., 2015). We proved that the reprogramming viral vector was no longer present in the HiPSC cultures after passage 12 thus confirming the safety of the produced cells and the absence of the viral vector that could interfere with the subsequent neural induction (Figure 9).

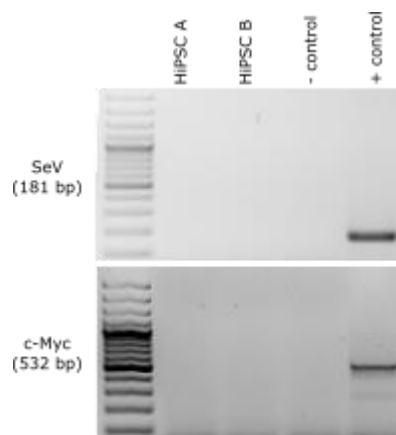


Figure 9 *SeV detection RT-PCR.*

About 1–2 months after gene transduction HiPSCs were free of Sendai (SeV) reprogramming vectors. Both SeV and c-Myc primers contains SeV genome specific sequences. Positive control was obtained from freshly transfected cells. Product were run on 2-3% agarose gel and imaged.

3.4.2.4 Genetic variations and relatedness

As mentioned in the introduction, a drawback of HiPSC techniques is that the reprogramming itself might introduce the formation of random CNVs (Ronen & Benvenisty, 2012). Therefore, we analyzed the presence of CNVs in the HiPSC clones obtained from the fibroblast cultures. The so called “molecular karyotype” was obtained from Illumina Infinium Omni2.5-8 bead array performed by LIFE&BRAIN GmbH, University Bonn (Dr. Per Hoffmann) whereas bioinformatic analysis was performed by Dr. Andreas Chiochetti (Department of Child and Adolescent Psychiatry and Psychotherapy, University Hospital Frankfurt, Germany).

The analysis of DNA anomalies is shown in the CNVs plot (Figure 10). We report no introduction of additional CNVs on the *PARK2* locus object of the study in the HiPSC clones. HiPSC showed no overall significant increase in CNVs compared to the fibroblast source and

the lines showed a high rate of genetic proximity (relatedness) with their cellular source as displayed by the relatedness matrix (Figure 11).

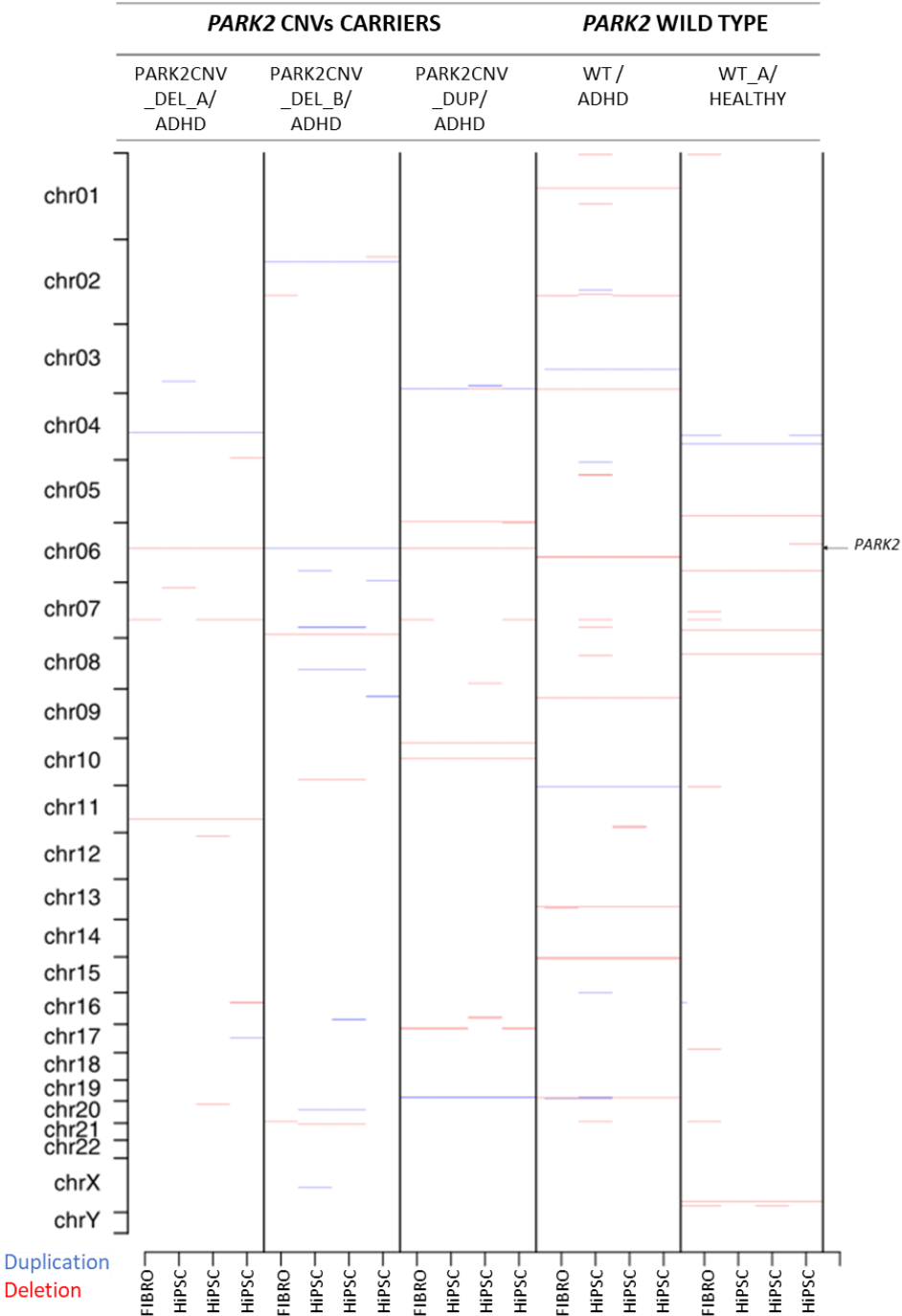


Figure 10 Copy Number Variants plot.
 The CNV plot graphically shows the acquisition or loss of CNV in 3 HiPSC clones for each line compare to the fibroblast source line. CNV duplications are displayed in blue, CNV deletions are displayed in red. CNVs were considered valid if larger than 15kb, if spanning more than 15 SNPs and if at least two out of three algorithms implemented in the CNVision pipeline confirmed the presence. Overall, cells did not show a significant increase in CNVs burden. Moreover, we show that no additional CNVs were introduced on the *PARK2* locus (black arrow) in the HiPSC clones during the cellular reprogramming.

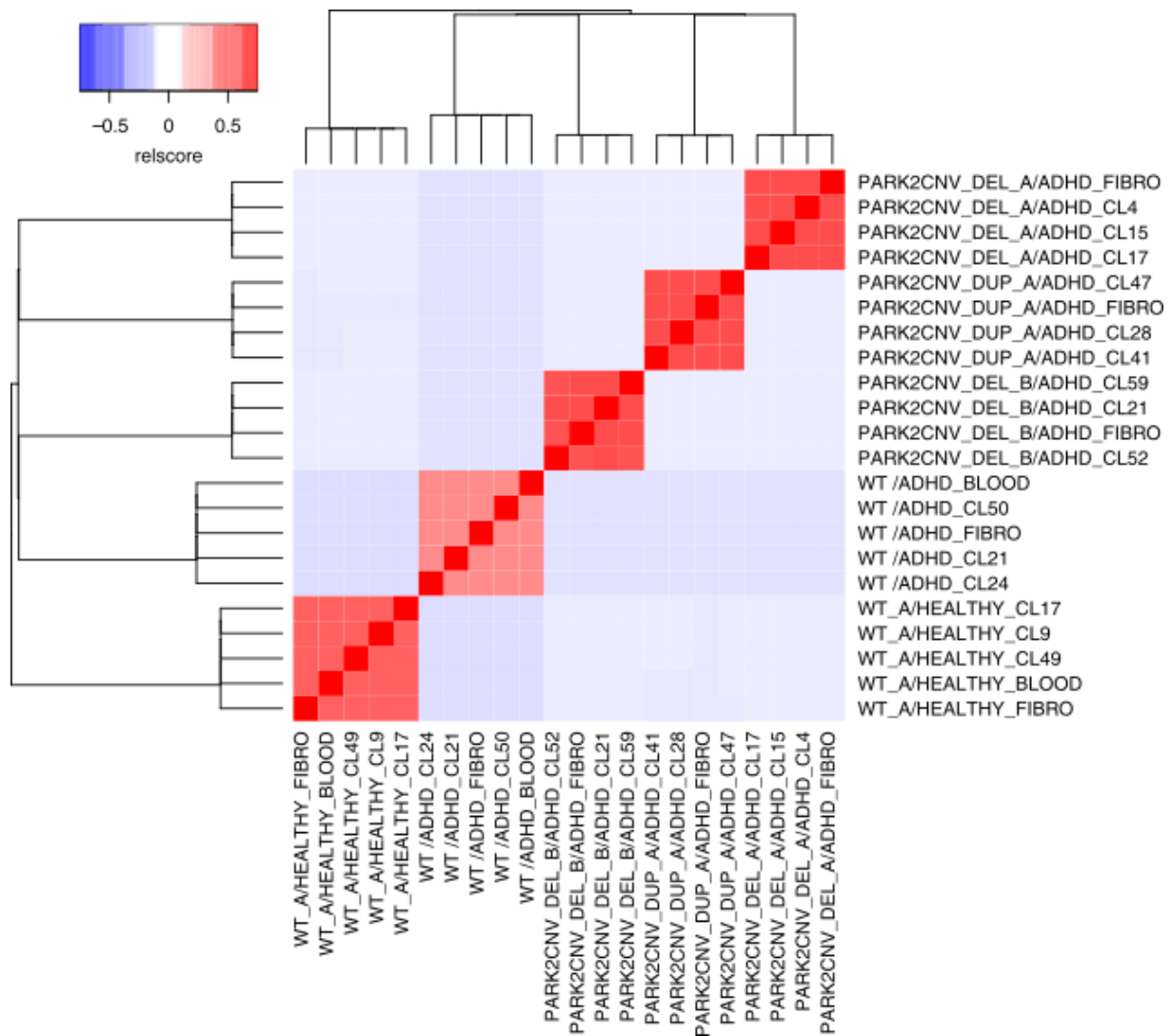


Figure 11 Genetic relatedness matrix.

Heatmap and dendrogram representing the genetic relatedness among HiPSC clones and fibroblast source. SNP based relatedness-analysis was performed using plink v 1.9 and the IBD function -genome function. Visualization is based on the PI_HAT score. A high relatedness score is represented by stronger shades of red whereas low relatedness scores are represented by stronger shades of blue. All the HiPSC clones showed a high rate of genetic similarity with their cellular source line.

3.4.3 HiPSC-derived dopaminergic neurons

Once the HiPSC generated in our laboratory were proven to be *bona fide* hiPSC they were induced to differentiate into midbrain dopaminergic neurons. As reported in the introduction, there are several different methods that can be followed for the induction. We choose a recent method (Xia et al., 2016) based on the “Dual SMAD Inhibition” and “Floor Plate Induction” (Chambers et al., 2009; Kriks et al., 2011). The original method was subject to minor modifications and consisted of the sequential addition of different factors and trophic media to the cultures (Figure 12).

During the neural induction protocol strong and consistent morphological changings were observed in all the cultures, independently from the genotype (Figure 13). In fact, after about 2 weeks of culture, cells shifted from a round shape typical of HiPSC to a more elongated and bipolar shape. By 20 days, extensive fine process formation was observed. Going through the induction, cells acquired a multipolar morphology characteristic of neurons, with extensive development of long and branched processes. Clustering of cell bodies and fiber bundles were frequently observed. After 50 days of culture cells are considered to be mature dopaminergic neurons.

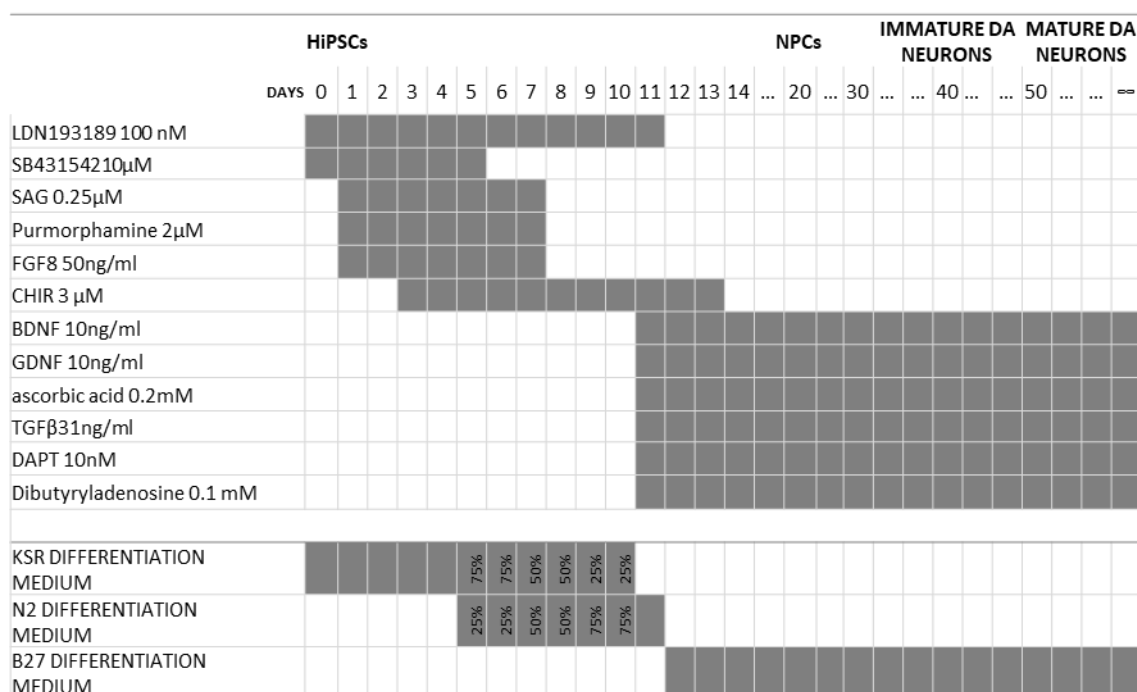


Figure 12 Neural Induction factors and media timeline.

Neural induction of the HiPSC to HiPSC-derived dopaminergic neurons was achieved by the sequential addition of different factors and trophic media to the cultures. Cells differentiate first in neural progenitor cells (NPCs) and then in dopaminergic neurons. Neurons are considered to be mature after 50 days of the protocol. The protocol was based on (Xia et al., 2016) with minor modifications.

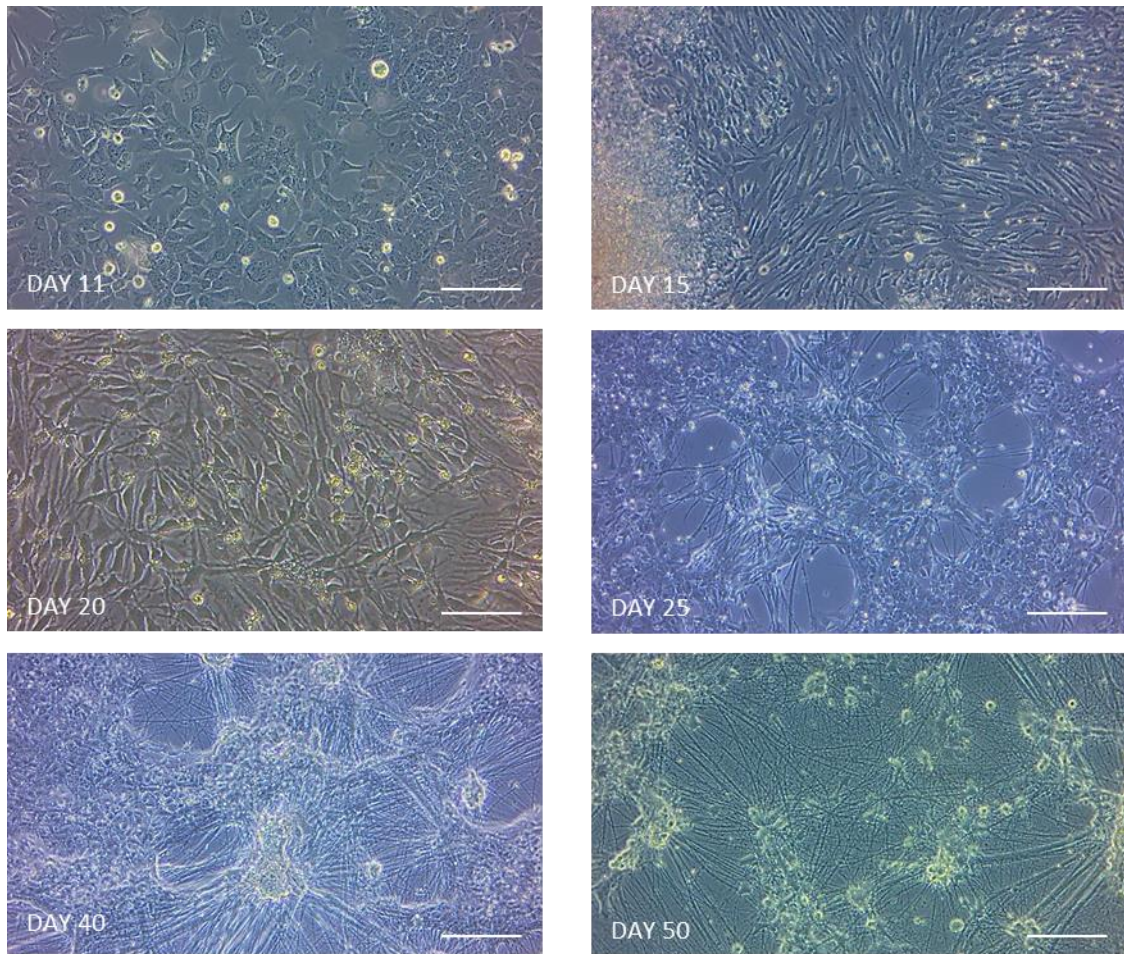


Figure 13 *Morphological changes during the neural Induction.*

During the neural induction protocol strong morphological changes were observed in all the cultures. HiPSC lose their round morphology and acquire a more elongated and bipolar shape during the first 2 weeks of Induction (day 11 to 20). As the maturation proceeds, cells acquired a multipolar morphology characteristic of neurons, with extensive development of long and branched processes. Clustering of cell bodies was frequently observed. The process was observable in all the lines used in this study, independently from the genotype. Scale bars equal to 100 μm .

3.4.3.1 Expression of dopaminergic neurons markers

As for the HiPSC, also the HiPSC -derived neuronal cells must be proven to be *bona fide* neurons by morphological and neuron-specific markers analysis.

We assessed the maturation of the HiPSC into HiPSC -derived dopaminergic neurons by a time course analysis of the expression of dopaminergic neurons related genes. We compared the gene expression by quantitative RT-PCR (qRT-PCR) in RNA harvested from the HiPSC lines before the starting of the induction protocol, from the cultures after 45 day of induction (immature neurons) and after 60 days of induction (mature neurons).

As expected, we found expression of *POU5F1* (also known as *OCT3/4*), a pluripotency-associated marker, just in the HiPSC samples. This suggests that the neural induction protocol restricts the cell fate to a differentiated cellular type. We report no or very low expression of the tested dopaminergic markers in the HiPSC samples. We report a significantly higher expression of *LMX1B* ($t_{(4)} = 6.581, p = 0.003, d = 5.375$) in the immature neurons ($M = 4.790; SD = 0.788$) compared to the mature ones ($M = 1.534; SD = 0.336$). This is consistent with the fact that *LMX1B* is required in the early stages of DA progenitors, primarily due to its essential role for the induction of mature dopaminergic neurons (Deng et al., 2011) (Andersson et al., 2006b). A similar result was found when assessing *NEUROD1* expression, a marker for general immature neurons. *NEUROD1* is a member of the family of pro-neural genes, which functions during embryonic neurogenesis as an essential neuronal differentiation factor (Pataskar et al., 2016). Immature neurons had a significantly higher expression ($t_{(4)} = 3.965, p = 0.017, d = 2.784$) of *NEUROD1* ($M = 4.586; SD = 1.335$) compared to mature neurons ($M = 1.725; SD = 0.575$). *EN1* expression normally starts early in the dopaminergic neurons maturation and is maintained throughout the adulthood (Hegarty, Sullivan, & O’Keeffe, 2013). Consistent to that we did not find any significant difference between immature ($M = 2.273; SD = 2.461$) and mature neurons ($M = 2.566; SD = 3.172$). *RBFOX3* codes for the neuronal nuclei antigen NeuN, a widely used marker for post-mitotic neurons. Surprisingly, we found *RBFOX3* expression also in the HiPSC samples ($M = 2.549; SD = 0.624$), an unexpected effect that was reported also by other researchers working with HiPSC. We report a significant differential RNA expression of *RBFOX3* among the 3 cellular stages ($F_{(2,11)} = 4.466, p = 0.038$) and between immature ($M = 3.263; SD = 0.04$) and mature ($M = 2.086; SD = 0.76$) neurons ($t_{(7)} = 3.011, p = 0.020, d = 1.938$).

Taken together, the results from this gene expression time course analysis support the restriction of the pluripotency as the induction goes on and the expression of neuron and dopaminergic neurons markers consistent with the developmental stage of the cell taken into exam.

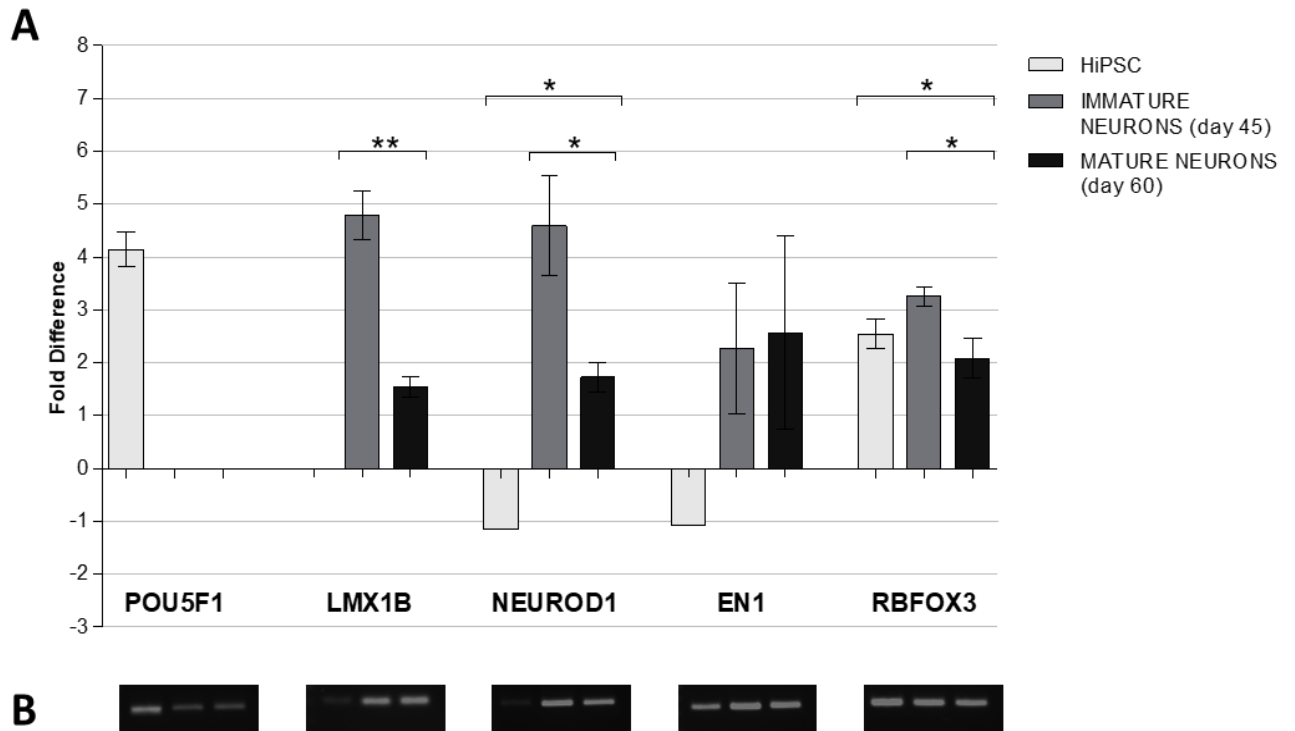


Figure 14 Neuronal maturation time-course analysis by quantitative RT-PCR (RT-qPCR).

(A) We assessed the maturation of the HiPSC into HiPSC-derived dopaminergic neurons by a time course analysis of the expression of dopaminergic neurons related genes. We compared the gene expression from the HiPSC lines before the starting of the Induction protocol, from the cultures after 45 day of Induction (immature neurons) and after 60 days of induction (mature neurons). POU5F1= Pluripotency-associated marker; Lmx1b= marker for early stages of DA progenitors; NEUROD1= marker for general immature neurons; EN1= marker for dopaminergic neurons; RBFOX3= marker for post-mitotic neurons with expression also in HiPSCs.

(B) Electrophoresis run of the RT-qPCR products. Data are shown as mean \pm SEM. One unit represents two-fold difference. Level of significance was set at $p < .05$. * $p \leq .05$, ** $p \leq .01$, and *** $p \leq .001$.

Additionally, immunocytochemical analysis of the differentiated DA neuron-like cells was performed on all the cell lines. HiPSC-derived dopaminergic neurons stained positive for the general neuron-specific marker TUBB3 and for another marker more specifically expressed in DA neurons (Figure 15) such as tyrosine hydroxylase (TH).

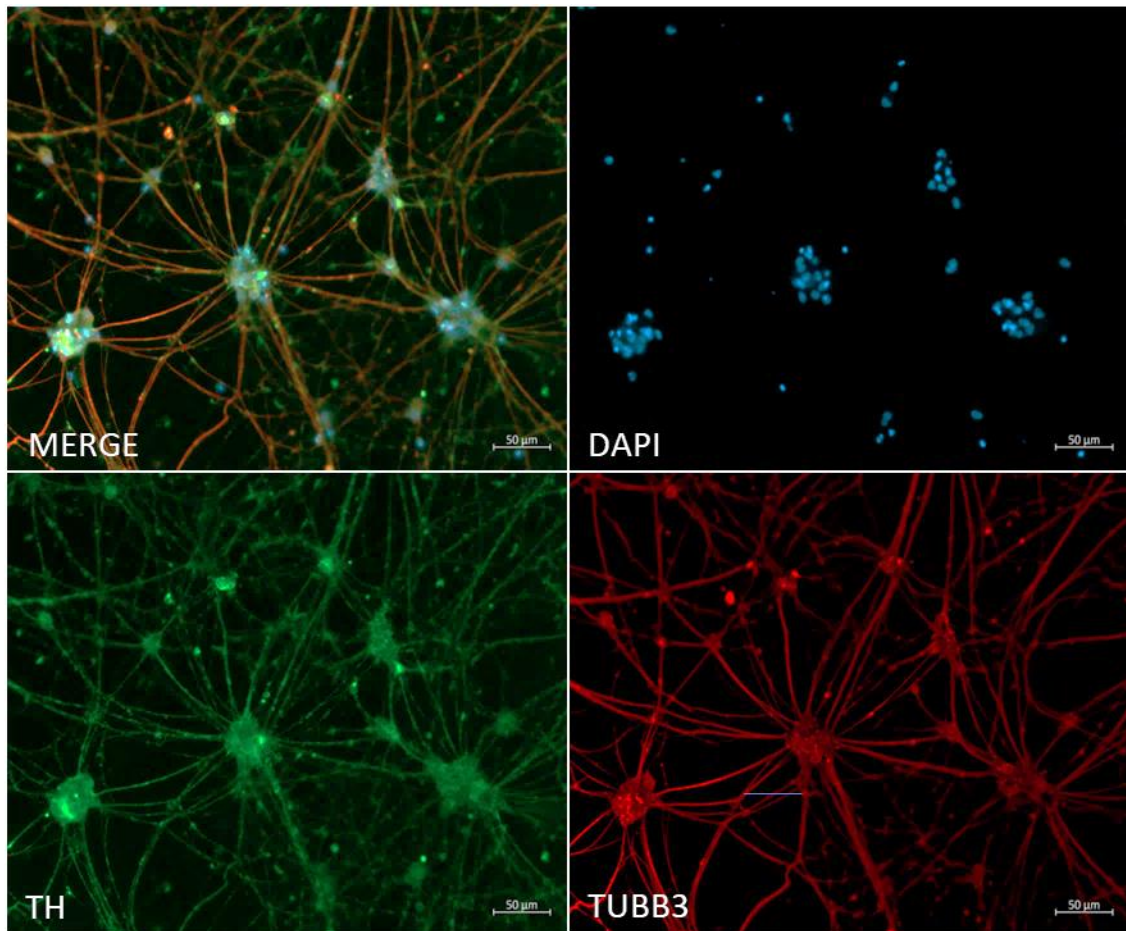


Figure 15 *Immunofluorescence staining in mature HiPSC-derived dopaminergic neurons.* Immunocytochemical analysis of the differentiated DA neuron-like cells was performed on all the cell lines differentiated with our protocol. DA neuron-like cells stained positive for the general neuron-specific marker TUBB3 and for tyrosine hydroxylase (TH), a specific DA neurons marker. Scale bars 50 µm.

3.4.3.2 Dopamine levels

Extracellular and intracellular dopamine levels in mature HiPSC-derived dopaminergic neurons cultures were measured by ELISA assay. Extracellular dopamine levels were measured using the conditioned media in basal conditions. Conditioned media was harvested from mature neurons at day 60 (Figure 16 A). Intracellular dopamine levels were measured using the total protein extract from HiPSC-derived dopaminergic neurons at day 60.

Statistical analysis did not show any significant difference due to the genotype in the extracellular and intracellular dopamine levels at day 60. These results suggest first that neurons are producing dopamine, consistent with the use of an induction protocol that directions the cells towards a dopaminergic subtype, and second that neurons are functionally

active, given that a detectable amount of dopamine in the conditioned media correlates with active dopamine release.

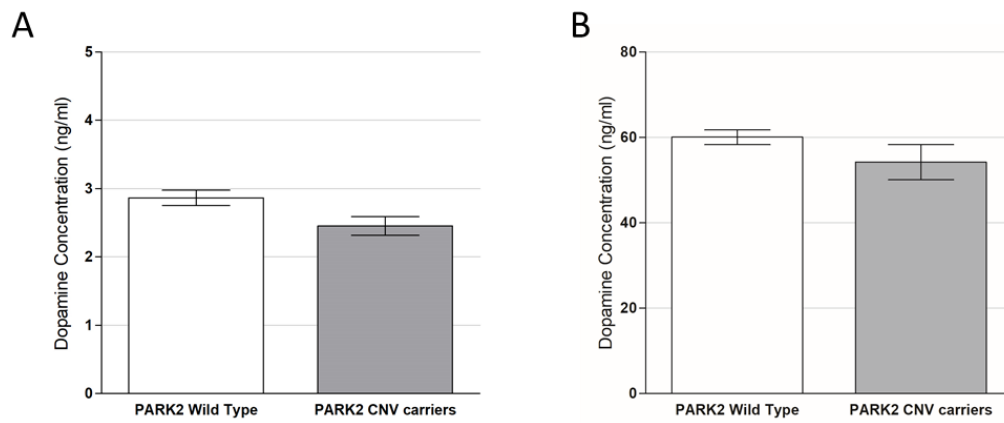


Figure 16 Dopamine concentration in mature HIPSC-derived dopaminergic neurons. (A) Extracellular dopamine concentration (ng/ml) measured in conditioned media. (B) Intracellular dopamine levels (ng/ml) detected in 1000 μ g/ml of total cellular protein extract. Statistical analysis did not show any significant difference due to the genotype in the extracellular and intracellular dopamine levels at day 60. Data are shown as mean \pm SEM.

3.5 EVALUATION OF PATHO-PHENOTYPES CONNECTED WITH ADHD/*PARK2* CNVs IN HDF AND HiPSC AFTER NUTRIENT DEPRIVATION

3.5.1 *PARK2* gene expression

In our initial preliminary analysis, we evaluated whether *PARK2* gene expression was differentially regulated in human dermal fibroblasts according to their genotype and/or after nutrient deprivation (starvation) (Figure 17).

Initially, an independent-sample t tests was run for each treatment separately, to evaluate statistical differences due to the genotype or the diagnosis. In both conditions we did not find a significant difference in *PARK2* gene expression considering either the genotype or the diagnosis (Table 4). Sequentially, a two-way ANOVA was conducted to examine the effects of the genotype and the treatment. Statistical analysis did not show a significant interaction between genotype and treatment ($F_{(1,20)}=1.252$, $p= .276$) in *PARK2* gene expression.

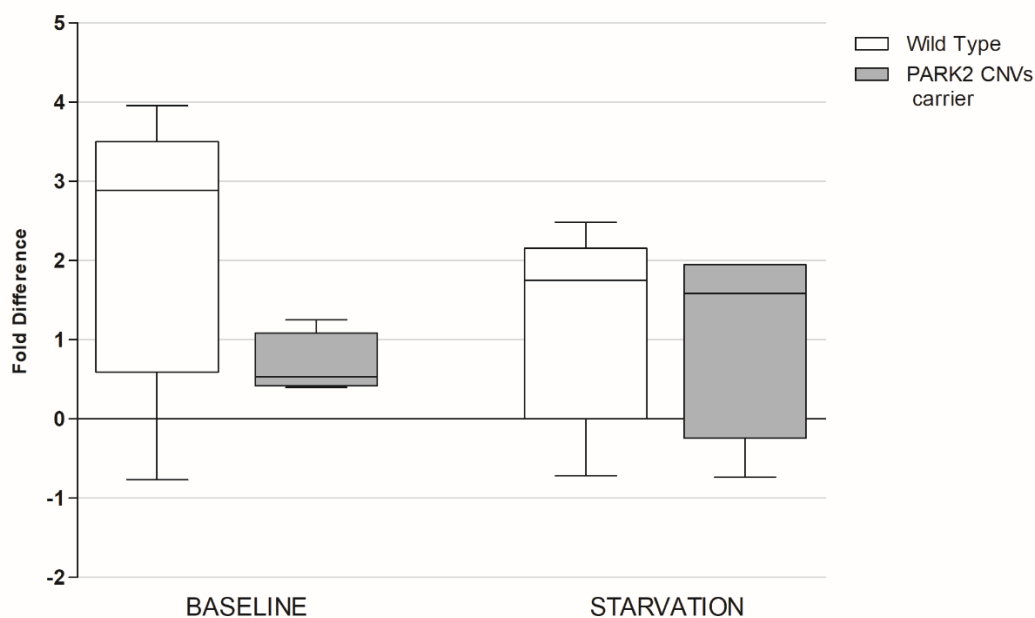


Figure 17 *PARK2* gene expression in HDF in baseline condition and after nutrient deprivation stress.

After gene expression normalization with the best reference genes, relative quantities (fold difference) were averaged to the percentage of gene expression and then converted in Log₂ scale. One unit represents two-fold difference. Statistical analysis did not reveal any significant difference. Data presented were obtained from one experiment with a total of 12 HDF lines (4 ADHD/*PARK2* CNV carriers, 4 ADHD/ *PARK2* WT and 4 HEALTHY /*PARK2* WT). Data are shown as mean \pm SEM.

Treatment	Variable	Mean	Std. Dev	Std. Err	t	df	p-value	
baseline	genotype	WT	2.201	1.717	0.607	1.712	10	0.118
		CNV	0.678	0.390	0.195			
	diagnosis	HEALTHY	2.239	2.089	1.045	0.838	10	0.422
		ADHD	1.420	1.331	0.471			
starvation	genotype	WT	1.309	1.232	0.436	0.280	10	0.785
		CNV	1.096	1.267	0.634			
	diagnosis	HEALTHY	1.317	1.404	0.702	0.155	10	0.880
		ADHD	1.198	1.172	0.415			

Table 5 Statistics summary of *PARK2* gene expression in HDF.

T-test and descriptive statistics of the HDF samples used to evaluate *PARK2* gene expression in baseline condition and after nutrient deprivation stress (N=12). Mean values of RNA fold difference expression are displayed. Statistical analysis by Student's t-test did not show significant differences. WT=Wild Type; CNV= *PARK2* CNV carrier; Std. Dev= standard deviation; Std. Err= Standard error of the mean; t= t value; df= degrees of freedom; p-value= probability value. Level of significance was set at p=.05.

3.5.2 *PARK2* protein expression

We evaluated *PARK2* protein levels both in HDF and HiPSCs lines in baseline conditions, after 24 hours of nutrient deprivation and after 24h treatment with 10 μ M carbonyl cyanide 3-chlorophenylhydrazone (CCCP). The same total protein concentration was loaded in each test and the abundance of *PARK2* protein in the total cellular extract was evaluated by Enzyme-Linked Immunosorbent Assay (ELISA) by interpolation with a standard curve with known *PARK2* concentrations.

A univariate analysis of variance was conducted to assess genotype and treatment effects on *PARK2* concentration in human dermal fibroblast lines (Figure 18). The analysis revealed a significant effect of the genotype ($F_{(1, 12)} = 5.592$, $p=.036$, $\eta_p^2=.318$) and significant effect of treatment ($F_{(2, 12)} = 9.233$, $p=.004$, $\eta_p^2=.606$) but not a significant interaction between the two fixed factors. Post hoc comparisons using the Tukey HSD on the treatment effect indicated that the difference was mainly driven by baseline condition vs. CCCP (Tukey HSD $p=.004$) and CCCP vs. starvation treatment (Tukey HSD $p=.021$). Additionally, after 24h of nutrient deprivation, we found a significant difference between ADHD/*PARK2* CNV carriers and WT ($U=.00$, $p=.05$, Dunn's Post Hoc test $p=.05$) suggesting that fibroblasts from CNVs carriers have a lower amount of *PARK2* protein after nutrient deprivation stress compared to WT lines.

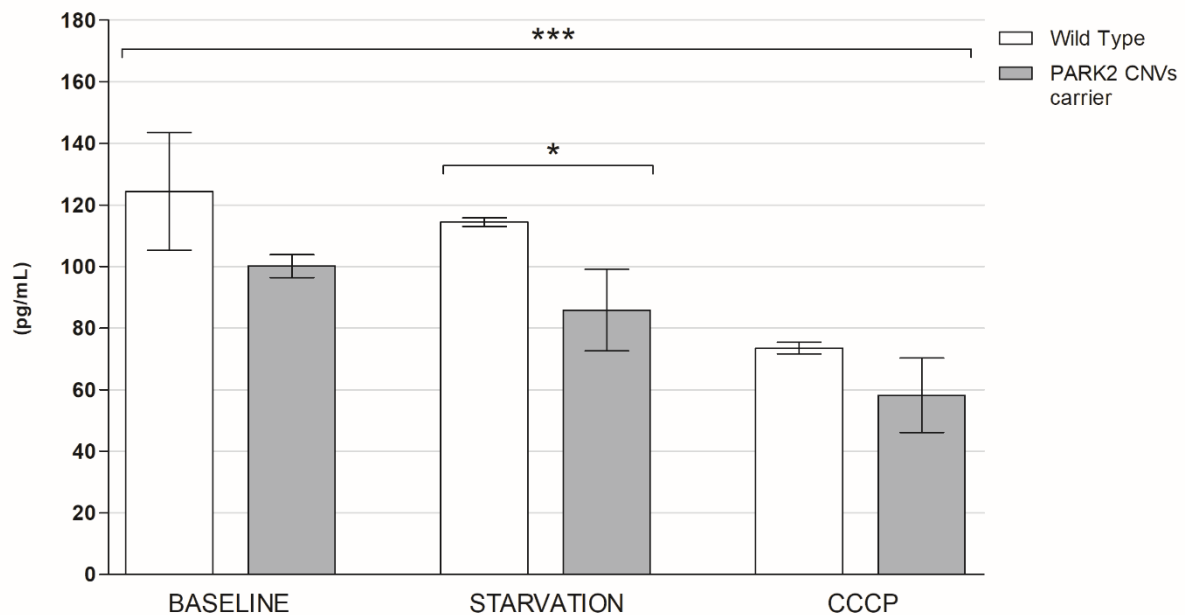


Figure 18 *PARK2* protein levels in HDF.

PARK2 protein concentration (pg/ml) in fibroblast lines in basal conditions, after 24h starvation stress and after 24 h treatment with 10 μ M CCCP. Statistical analysis by univariate analysis of variance revealed a significant effect of the genotype ($F_{(1,12)} = 5.592, p=.036, \eta_p^2=.318$) and treatment ($F_{(2,12)} = 9.233, p=.0004, \eta_p^2=.606$) mainly driven by baseline condition vs. CCCP (Tukey HSD $p=.004$) and CCCP vs. starvation treatment (Tukey HSD $p=.021$). ADHD/*PARK2* CNV carriers show significantly lower *PARK2* protein concentration after 24h of nutrient deprivation compared to WT ($U= .00, p=.05, \text{Dunn's Post Hoc test } p=.05$). Sample size=6 (3 ADHD/*PARK2* CNV carriers, 1 ADHD/ *PARK2* WT and 2 HEALTHY /*PARK2* WT). Data are shown as mean protein concentration \pm SEM. Level of significance was set at $p=.05$. * $p \leq .05$, ** $p \leq .01$, and *** $p \leq .001$.

The quantification of *PARK2* protein levels on HiPSC samples (Figure 19) revealed a significant effect of the genotype ($F_{(1,12)} = 19.830, p=.001, \eta_p^2=.623$), of the treatment ($F_{(2,12)} = 18.407, p<.0001, \eta_p^2=.754$) and of the interaction between the two factors ($F_{(1,12)} = 5.228, p=.023, \eta_p^2=.466$). Post hoc testing for the treatment showed a significant effect both of baseline vs. starvation (Tukey HSD $p<.0001$) and baseline vs. CCCP (Tukey HSD $p=.007$). An independent-samples t-test conducted for each treatment separately and showed a significant difference due to the genotype in baseline conditions. This result suggests that HiPSC lines from ADHD/*PARK2* CNV carriers have lower levels of *PARK2* compared to controls ($t_{(4)} = -3.717, p=.021, d=3.034$).

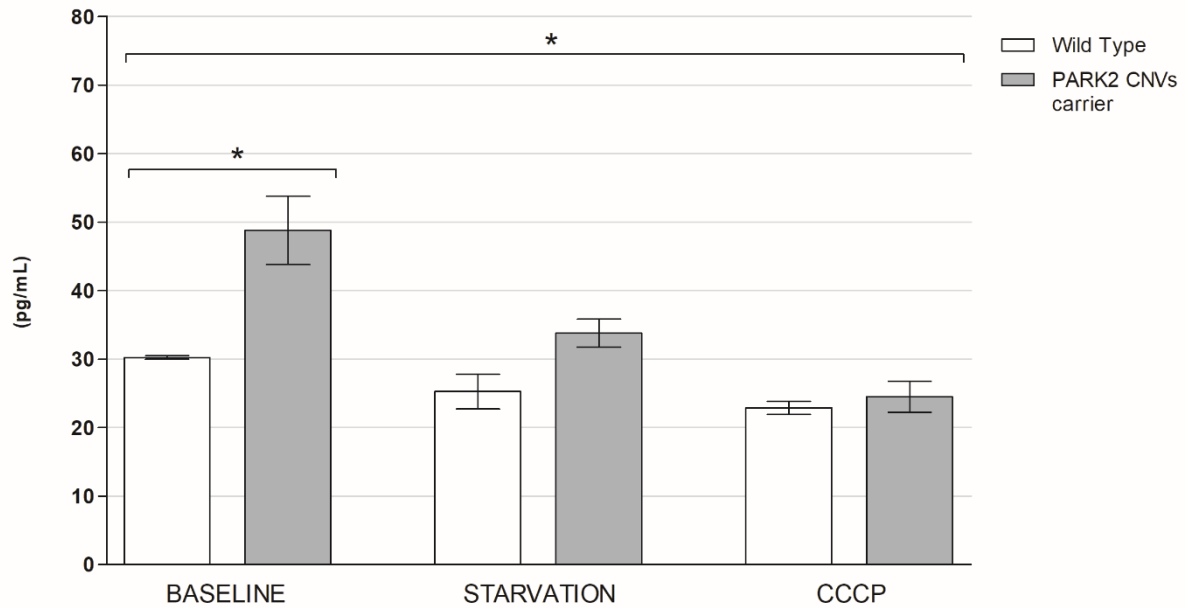


Figure 19 *PARK2* protein levels in HiPSC.

PARK2 protein concentration (pg/ml) in HiPSC lines in basal conditions, after 24h starvation stress and after 24h treatment with 10 μ M CCCP. Univariate analysis of variance showed a significant effect of the genotype ($F_{(1, 12)} = 19.830$, $p = .001$, $\eta_p^2 = .623$), of the treatment ($F_{(2, 12)} = 18.407$, $p < .000$, $\eta_p^2 = .754$) and of the interaction between the two factors ($F_{(1, 12)} = 5.228$, $p = .023$, $\eta_p^2 = .466$). Post-hoc testing for the treatment showed a significant effect both of baseline vs. starvation (Tukey HSD $p < .0001$) and baseline vs. CCCP (Tukey HSD $p = .007$). An independent-samples t-test show that HiPSC lines from ADHD/*PARK2* CNV carriers have lower levels of *PARK2* compared to controls in baseline conditions ($t_{(4)} = -3.717$, $p = .021$, $d = 3.034$). Sample size=6 (3 ADHD/*PARK2* CNV carriers, 1 ADHD/*PARK2* WT and 2 HEALTHY/*PARK2* WT). Data are shown as mean \pm SEM. Level of significance was set at $p = .05$. * $p \leq .05$, ** $p \leq .01$, and *** $p \leq .001$.

3.5.3 Hypothesis driven gene expression analysis

Representative genes known to have connections with *PARK2* biological functions were selected after reviewing of the available literature (Scarffe L.A., Stevens D.A., Dawson V.L., 2015). We evaluated the expression of genes connected with oxidative stress (*TP53*, *NQO1*, and *NFE2L2*), ubiquitin pathway (*UBE3A*, *UBB*, *UBC*, and *ATXN3*) and with mitochondrial quality control features (*PINK1*, *MFN2*, and *ATG5*). We thus assessed if the genotype had influences in the gene expression of these targets in different cellular models: blood samples, HDF and HiPSC. In the cellular models we additionally evaluated if the gene expression was influenced by the application of 24 hours nutrient deprivation paradigm.

As an initial screening, we evaluated if the gene expression of selected genes related to *PARK2* biological functions was deregulated already in peripheral and easy-to obtain tissues.

Therefore, we assessed the gene expression of ubiquitin pathway related genes (*UBC*, *UBB*, *UBE3A*, *ATXN3*) and of the main interaction partner of *PARK2* (*PINK1*) on RNA extracted from blood samples (Figure 20). Our analysis did not reveal any statistically significant difference when testing for genotype or for diagnosis (Table 3).

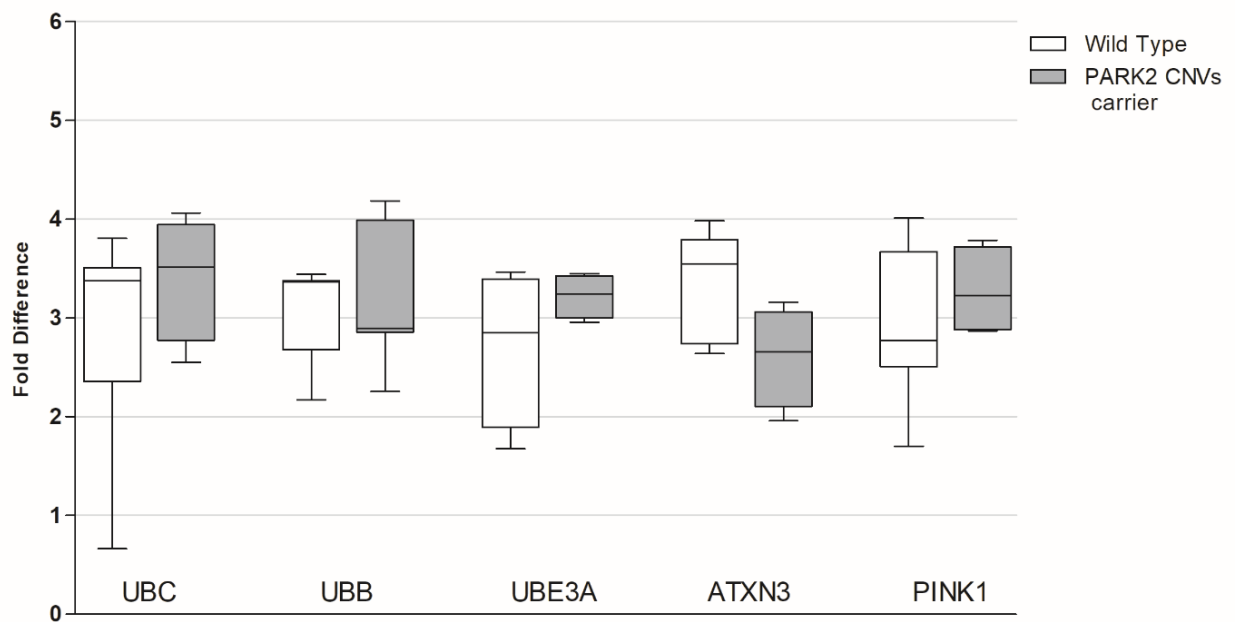


Figure 20 Hypothesis driven gene expression analysis in blood samples.

Expression of genes involved in the ubiquitin pathway and of *PARK2* interaction partner *PINK1* was evaluated by RT-qPCR. Samples were measured in triplicate, normalized to the expression of *ALAS1* and *SDHA* and ΔCq values averaged to the percentage of gene expression and Log_2 converted. One unit represents two-fold difference. Statistical analysis did not reveal any significant difference. Sample size=12 (4 ADHD/*PARK2* CNV carriers, 4 ADHD/ *PARK2* WT and 4 HEALTHY /*PARK2* WT). Data are shown as mean \pm SEM.

Gene	Genotype	Mean	Std. Dev	p-value	Gene	Diagnosis	Mean	Std. Dev	p-value
UBC	WT	2.926	1.144	0.468	UBC	HEALTHY	2.315	1.447	0.080
	CNV	3.409	0.631			ADHD	3.464	0.471	
UBB	WT	3.093	0.482	0.625	UBB	HEALTHY	3.165	0.329	0.885
	CNV	3.224	0.223			ADHD	3.126	0.458	
UBE3A	WT	3.199	0.687	0.310	UBE3A	HEALTHY	2.719	0.309	0.323
	CNV	2.711	0.791			ADHD	3.194	0.861	
ATXN3	WT	3.330	0.538	0.056	ATXN3	HEALTHY	2.974	0.407	0.728
	CNV	2.608	0.502			ADHD	3.120	0.738	
PINK1	WT	2.920	0.778	0.429	PINK1	HEALTHY	2.764	0.316	0.314
	CNV	3.277	0.448			ADHD	3.213	0.791	

Table 6 Statistics summary of hypothesis driven gene expression in blood samples.

The table reports the mean values of the gene expression fold difference, the descriptive statistics and p-values from student's t tests both for the genotype (right side of the chart) and for the diagnosis (left side) as independent variable. Statistical analysis did not show significant differences. Sample size=12. WT=Wild Type; CNV= *PARK2* CNV carrier; Std. Dev= standard deviation; p-value= probability value. Level of significance was set at p=.05.

Subsequently, we investigated the gene expression in the fibroblast and HiPSC cultures in baseline conditions and after nutrient deprivation.

A univariate analysis of variance among the fibroblast samples (Figure 21 and Table 5) with fixed factors genotype and treatment showed a significant effect of the genotype for *NQO1* ($F_{(1,8)} = 9.488$, $p = .018$, $\eta_p^2 = .575$) and *UBB* ($F_{(1,8)} = 7.316$, $p = .027$, $\eta_p^2 = .478$) and a significant effect of treatment for *MFN2* ($F_{(1,8)} = 10.341$, $p = .012$, $\eta_p^2 = .564$). Student's t test performed in each separate treatment revealed a significant difference due to the genotype in baseline for *ATG5* ($t_{(4)} = -3.283$, $p = .046$, $d = 3.374$) and after starvation for *NQO1* ($t_{(4)} = -5.906$, $p = .004$, $d = 4.824$) both suggesting that *PARK2* CNVs carrier have a higher expression of these genes compared to WT.

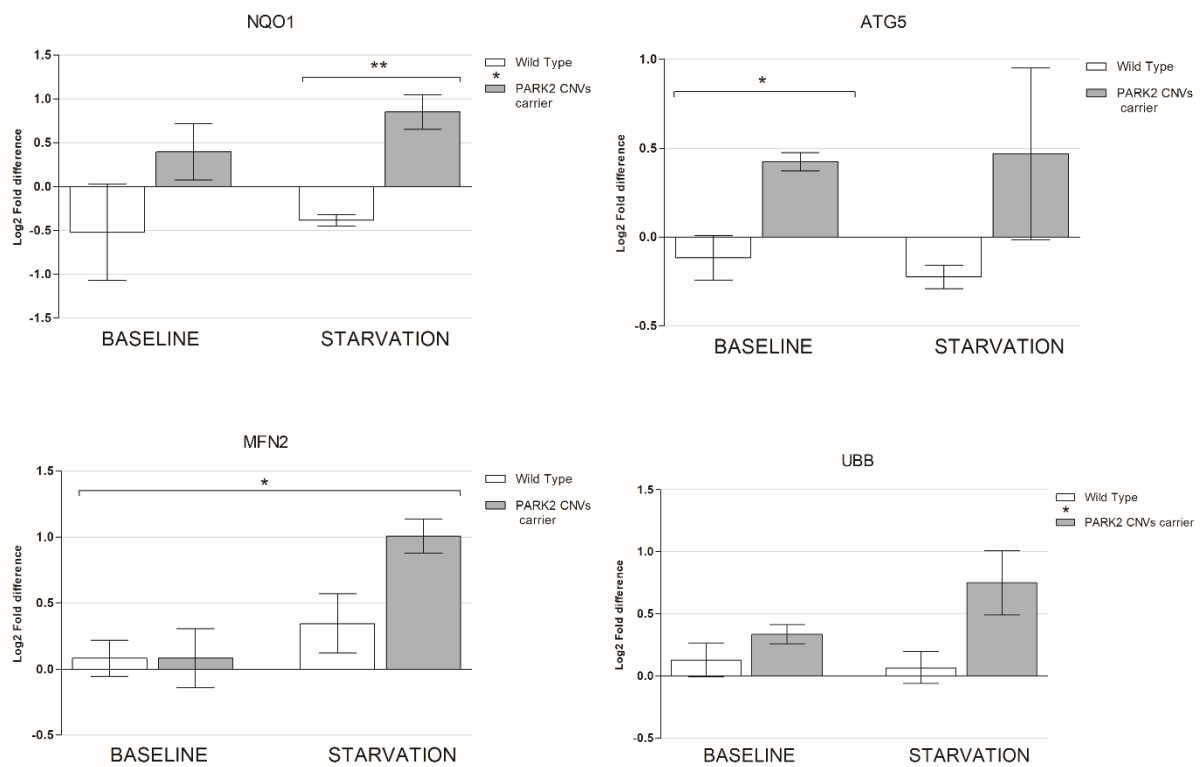


Figure 21 Hypothesis driven gene expression analysis in HDF.

Gene expression in basal conditions and after nutrient deprivation was evaluated by RT-qPCR. Samples were measured in duplicate normalized to the expression of housekeeping genes, averaged to the expression of HEALTHY /PARK2 WT in baseline conditions and ΔCq values Log₂ converted. One unit represents two-fold difference. Sample size=6 (3 ADHD/PARK2 CNV carriers, 1 ADHD/ PARK2 WT and 2 HEALTHY /PARK2 WT). Data are shown as mean \pm SEM. Level of significance was set at $p=.05$. * $p \leq .05$, ** $p \leq .01$, and *** $p \leq .001$.

		Baseline			Starvation					
		Mean	SD	p-value	Mean	SD	p-value	p-value GENOTYPE	p-value TREATMENT	p-value GENOTYPE xTREATMENT
Hs_ATXN3	WT	0.185	0.359	0.641	0.302	0.230	0.404	.354	.467	.836
	CNV	0.350	0.439		0.559	0.417				
Hs_UBB	WT	0.128	0.235	0.256	0.067	0.222	0.078	.027	.315	.187
	CNV	0.336	0.136		0.751	0.451				
Hs_UBC	WT	0.090	0.234	0.326	0.415	0.279	0.776	.398	.210	.704
	CNV	-0.341	0.626		0.248	0.906				
Hs_UBE3A	WT	-0.123	0.214	0.875	-0.232	0.245	0.155	.215	.320	.163
	CNV	-0.167	0.399		0.430	0.608				
Hs_NFE2L2	WT	0.145	0.259	0.264	-0.105	0.245	0.569	.502	.840	.194
	CNV	-0.294	0.526		0.043	0.334				
Hs_NQO1	WT	-0.522	0.950	0.307	-0.382	0.113	0.004	.018	.422	.665
	CNV	0.395	0.455		0.851	0.343				
Hs_TP53	WT	0.040	0.134	0.763	0.075	0.343	0.242	.473	.213	.262
	CNV	-0.066	0.551		0.533	0.465				
Hs_ATG5	WT	-0.117	0.215	0.046	-0.225	0.115	0.229	.068	.915	.798
	CNV	0.424	0.073		0.468	0.838				
Hs_MFN2	WT	0.081	0.240	0.997	0.345	0.390	0.063	.111	.012	.112
	CNV	0.083	0.387		1.008	0.224				
Hs_PINK1	WT	0.020	0.149	0.335	-0.218	0.139	0.351	.220	.693	.513
	CNV	0.161	0.166		0.221	0.709				

Table 7 Statistics summary of hypothesis driven gene expression analysis in HDF.

The table reports the descriptive statistics and p-values from student's t tests with genotype as independent variable as well as the p-value for the univariate analysis of variance (right side of the chart). Mean values of RNA fold difference expression are displayed. Significant p-values are highlighted in bold. WT=Wild Type; CNV= *PARK2* CNV carrier; SD= standard deviation; p-value= probability value. Level of significance was set at p=.05.

For the HiPSCs samples (Figure 22 and Table 6), univariate analysis of variance with fixed factors genotype and treatment shows a significant general effect of the genotype for UBB expression ($F_{(1, 8)} = 9.505$, $p=.015$, $\eta_p^2=.543$), *PARK2* CNVs carrier show lower expression of UBB after 24 hours starvation stress ($t_{(4)} = 3.406$, $p = .027$, $d=2.703$).

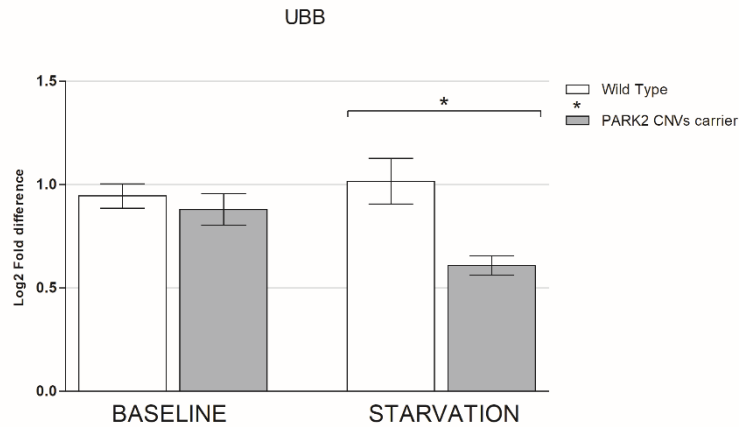


Figure 22 Hypothesis driven gene expression analysis in HiPSC.

Gene expression of UBB in basal conditions and after nutrient deprivation was evaluated by RT-qPCR. Samples were measured in duplicate, averaged to the expression of HEALTHY /PARK2 WT in baseline conditions and normalized to the expression of ALAS1 and HPRT1 and ΔCq values log2 converted. One unit represents two-fold difference. Sample size=6 (3 ADHD/PARK2 CNV carriers, 1 ADHD/ PARK2 WT and 2 HEALTHY /PARK2 WT). Data are shown as mean \pm SEM. Level of significance was set at $p=.05$. * $p \leq .05$, ** $p \leq .01$, and *** $p \leq .001$.

		Baseline			Starvation					
		Mean	SD	p-value	Mean	SD	p-value	p-value GENOTYPE	p-value TREATMENT	p-value GENOTYPE xTREATMENT
Hs_ATXN3	WT	1.060	0.262	0.640	1.039	0.262	0.758	.566	.976	.862
	CNV	0.948	0.279		0.979	0.178				
Hs_UBB	WT	0.945	0.102	0.534	1.016	0.192	0.027	.015	.229	.056
	CNV	0.879	0.132		0.607	0.080				
Hs_UBC	WT	1.085	0.190	0.186	1.093		0.776	.392	.903	.921
	CNV	0.719	0.349		0.802	0.778				
Hs_UBE3A	WT	0.926	0.146	0.388	1.258	0.306	0.692	.473	.058	.971
	CNV	1.035	0.131		1.379	0.387				
Hs_NFE2L2	WT	1.522	0.878	0.505	0.749	0.117	0.202	.264	.509	.862
	CNV	3.604	4.846		2.289	1.746				
Hs_NQO1	WT	1.017	0.263	0.629	0.780	0.073	0.375	.343	1.000	.828
	CNV	1.865	2.112		2.101	1.650				
Hs_TP53	WT	1.631	1.067	0.415	2.113	0.402	0.404	.259	.444	.678
	CNV	2.273	0.601		2.419	0.403				
Hs_ATG5	WT	1.199	0.380	0.384	0.666	0.152	0.132	.124	.680	.981
	CNV	3.504	4.074		2.906	2.046				
Hs_MFN2	WT	5.060	6.668	0.379	1.692	0.535	0.304	.280	.345	.611
	CNV	16.879	19.617		6.205	4.625				
Hs_PINK1	WT	1.737	1.198	0.441	2.099	0.314	0.708	.699	.731	.440
	CNV	2.694	1.528		1.772	1.020				

Table 8 Statistics summary of hypothesis driven gene expression analysis in HiPSC.

The table reports the descriptive statistics and p-values from student's t tests with genotype as independent variable as well as the p-value for the univariate analysis of variance. Significant values are highlighted in bold. WT=Wild Type; CNV= PARK2 CNV carrier; SD= standard deviation; p-value= probability value. Level of significance was set at $p=.05$.

3.5.4 Energy impairment and oxidative stress

Given the biological association of PARK2 with mitochondrial dynamics, we evaluated if the fibroblast lines showed genotype dependent effects with respect to energy impairment and oxidative stress.

The total cellular ATP abundance was measured in baseline conditions, after 24 hours starvation stress and after treatment with 10 μ M CCCP for 24 hours (Figure 23). Data reported are mean values of two independent tests; fold difference was calculated against WT in baseline conditions. An univariate analysis of variance (ANOVA) revealed a significant effect of the genotype ($F_{(1, 12)} = 16.924$, $p=.001$, $\eta_p^2=.585$) and of the treatment ($F_{(2, 12)} = 40.877$, $p<.0001$, $\eta_p^2=.872$) and a trend towards significance for the interaction between the 2 variables ($F_{(2, 12)} = 3.102$, $p=.082$, $\eta_p^2=.341$). Post-hoc testing confirms a significant difference between baseline and starvation and CCCP treatment (all Tukey HSD $p=.0001$) and of starvation against CCCP treatment (Tukey HSD $p=.010$). The cellular content of ATP was depending from the genotype both in baseline conditions ($t_{(4)} = 3.834$, $p =.019$, $d=3.129$) and after starvation stress ($t_{(4)} = 9.821$, $p =.001$, $d=7.947$) whereas CCCP treatment did not show genotype differences ($t_{(4)} = 0.415$, $p =.699$). Cell lines derived from ADHD/PARK2 CNV showed lower levels of ATP compared to controls both in basal conditions (CNV carriers: $M=.649$; $SD=.132$; wild types: $M=1.00$; $SD=.088$) and after 24-hour starvation (CNV carriers: $M=.170$; $SD=.037$; wild types $M=.384$; $SD=.009$).

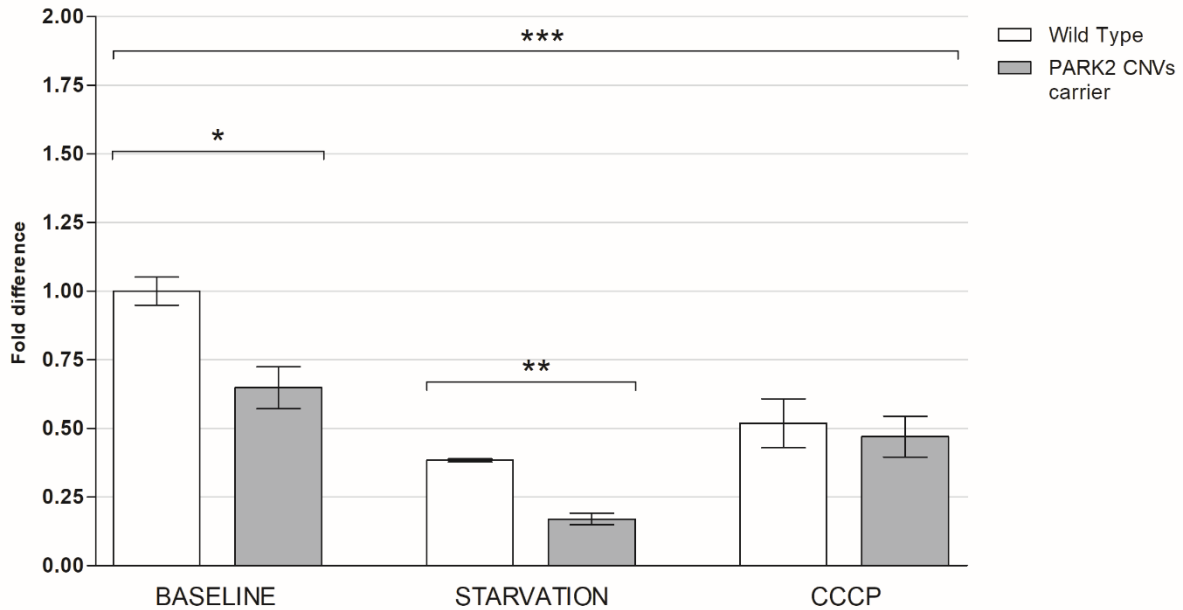


Figure 23 ATP production in HDF.

Cellular ATP content was evaluated in baseline conditions after 24 hours starvation stress and after treatment with 10 μ M CCCP for 24 hours. Fold difference was calculated against WT in baseline conditions. An univariate analysis of variance revealed a significant effect of the genotype ($F_{(1, 12)} = 16.924$, $p = .001$, $\eta^2 = .585$), treatment ($F_{(2, 12)} = 40.877$, $p < .0001$, $\eta^2 = .872$) and a trend towards significance for the interaction between the 2 variables ($F_{(2, 12)} = 3.102$, $p = .082$, $\eta^2 = .341$). Post-hoc test confirms a significant difference between baseline and starvation and CCCP treatment (all Tukey HSD $p = .0001$) and of starvation against CCCP treatment (Tukey HSD $p = .010$). ADHD/PARK2 CNV HDF lines showed lower levels of ATP compared to controls both in basal conditions ($t_{(4)} = 3.834$, $p = .019$, $d = 3.129$) (CNV carriers: $M = .649$; $SD = .132$; wild types: $M = 1.00$; $SD = .088$) and after 24-hour starvation ($t_{(4)} = 9.821$, $p = .001$, $d = 7.947$) (CNV carriers: $M = .170$; $SD = .037$; wild types $M = .384$; $SD = .009$). Data reported are mean values of two independent tests with samples measured in triplicate. Data are shown as mean \pm SEM. Level of significance was set at $p = .05$. * $p \leq .05$, ** $p \leq .01$, and *** $p \leq .001$.

Given the association between ATP production and oxygen consumption, we assessed the basal extracellular oxygen consumption rate (OCR) in the fibroblast lines in baseline conditions and after 24h starvation stress (Figure 24). We measured the fluorescence signal deriving from the ability of oxygen to quench the excited state of extracellular O₂ consumption reagent used in the assay. The higher the respiration of the sample, the higher the phosphorescence signal. The output was measured every two minutes intervals for a total of 90 minutes.

The time course recording was arbitrarily divided in 3 intervals of 30 minutes each (I_{0-30} , I_{30-60} , I_{30-90}). Student's test was run in each interval to uncover whether the genotype had an effect in the basal OCR. Statistical analysis revealed a persistent significant difference due to the genotype both in baseline conditions (I_{0-30} : $t_{(4)} = 3.292$, $p = .030$, $d = 2.692$, $r = .803$; I_{30-60} : $t_{(4)} = 4.054$, $p = .015$, $d = 3.310$, $r = .856$; I_{30-90} : $t_{(4)} = 3.675$, $p = .0321$, $d = 3.001$, $r = .832$) and after

starvation stress (l_{0-30} : $t_{(4)}=6.224$, $p=.003$, $d= 5.082$, $r=.931$; l_{30-60} : $t_{(4)}=4.351$, $p=.012$, $d= 3.553$, $r=.871$; l_{30-90} $t_{(4)}=3.842$, $p=.018$, $d= 3.337$, $r=.843$). Fibroblasts derived from ADHD patients carrying *PARK2* CNVs showed lower rates of extracellular oxygen consumptions compared to WT in all the intervals both in baseline conditions (l_{0-30} : CNV carriers (M=36.056; SD=.106), Wild types (M=38.493; SD=1.276); l_{30-60} : CNV carriers (M=35.026; SD=.068), Wild types (M=37.859; SD=1.209); l_{30-90} : CNV carriers (M=34.841; SD=.293), Wild types (M=37.626; SD=1.279) and after starvation stress(l_{0-30} : CNV carriers (M= 34.938; SD=1.267), wild types (M= 39.160; SD=1.398); l_{30-60} : CNV carriers (M= 33.907; SD=1.296), wild types (M= 36.970; SD=1.527); l_{30-90} : CNV carriers (M= 33.593; SD=1.427), wild types (M= 35.430; SD=1.265).

Therefore, according to our data, fibroblasts derived from ADHD patients carrying *PARK2* CNVs show constant lower rates of extracellular oxygen consumption compared to WT both in baseline and after starvation stress.

To test whether time had an effect on the fluorescence recorded, we performed a repeated measures ANOVA on RFU recorded in the intervals. In baseline condition we found a significant effect of the time ($F_{(2,8)}= 71.024$, $p<.0001$), but not of the interaction time x genotype, suggesting a general decline in fluorescence signal due to the use-up of the reagent over time, that was not different according to the genotype. The same time response was found for the samples subjected to 24-h starvation ($F_{(2,14)}= 411.536$, $p<.0001$) but in this case the decline was higher in wild type lines most likely because of the higher rates of oxygen consumption compared to the *PARK2* CNVs carriers ($F_{(2,14)}= 88.790$, $p < .0001$).

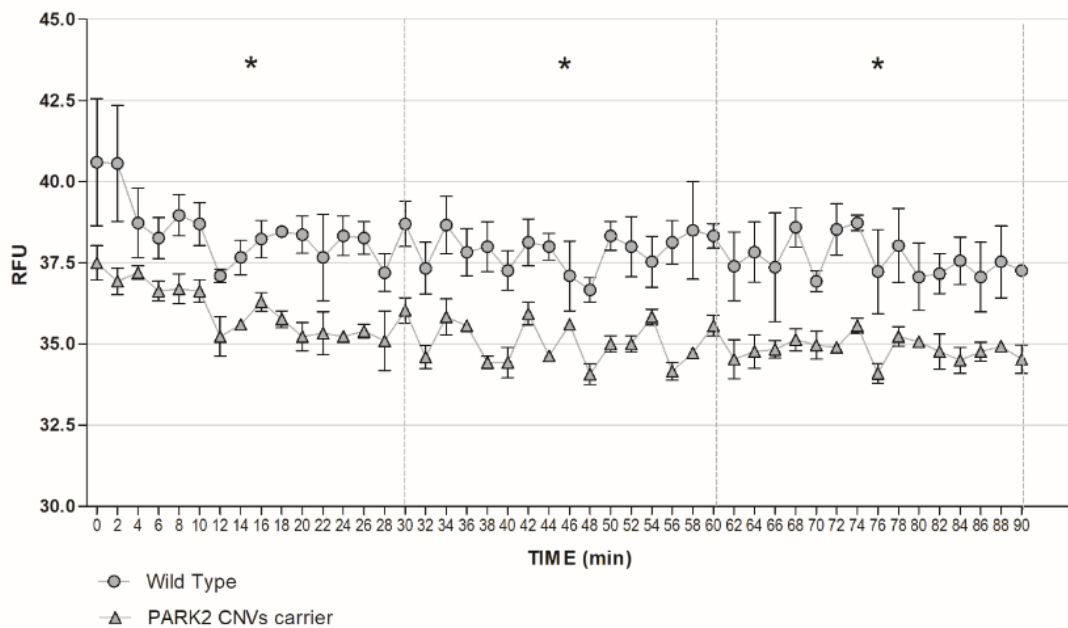
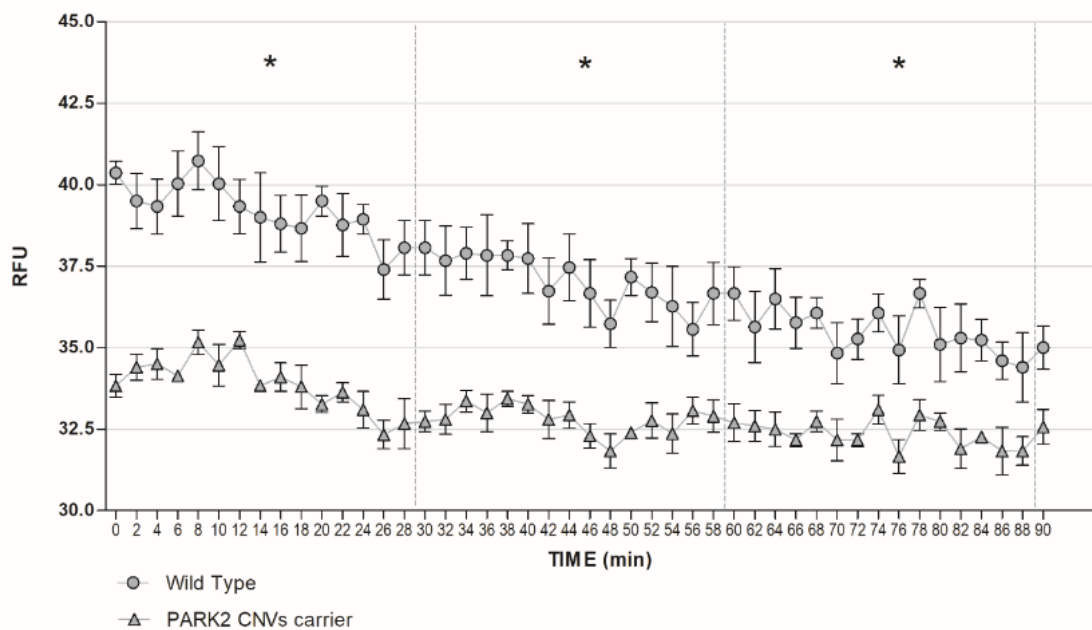
A**B**

Figure 24 Basal oxygen consumption rates in HDF.

Basal OCR was evaluated both in baseline (A) and after nutrient deprivation stress (B). Fluorescence (RFU- y-axis) signal, that directly correlates with the respiration, was recorded every two minutes for 90 minutes. Data presented are the mean of two independent experiments with samples measured in triplicate. Data are shown as mean \pm SEM. ANOVAs were calculated. Level of significance was set at $p=0.05$. * $p \leq 0.05$, ** $p \leq 0.01$, and *** $p \leq 0.001$.

Finally, we evaluated whether the different genotypes in this study, had a different response in the production of cellular reactive oxygen species (ROS) (Figure 25).

ROS measurement revealed a significant effect of the treatment ($F_{(2, 12)} = 55.208$, $p < .0001$, $\eta_p^2 = .902$) but no genotype ($F_{(1, 12)} = 2.183$, $p = .165$, $\eta_p^2 = .154$) or interaction effects ($F_{(2, 12)} = .768$, $p = .485$, $\eta_p^2 = .114$). Specifically, main difference on the treatment variable was between baseline treatment and starvation (Tukey HSD $p < .0001$) and baseline and CCCP (Tukey HSD $p < .000$). The increased amount of ROS under starvation ($M = 2.441$; $SD = .262$) and CCCP ($M = 2.268$; $SD = .064$) treatment compared to baseline ($M = 1.397$; $SD = .184$) fits well with existing literature that report how stress treatments leads to an increase of cellular ROS. We do not report a significant difference in ROS response between starvation and CCCP (Tukey HSD $p = .274$) that suggest that both treatments are powerful cellular stressors.

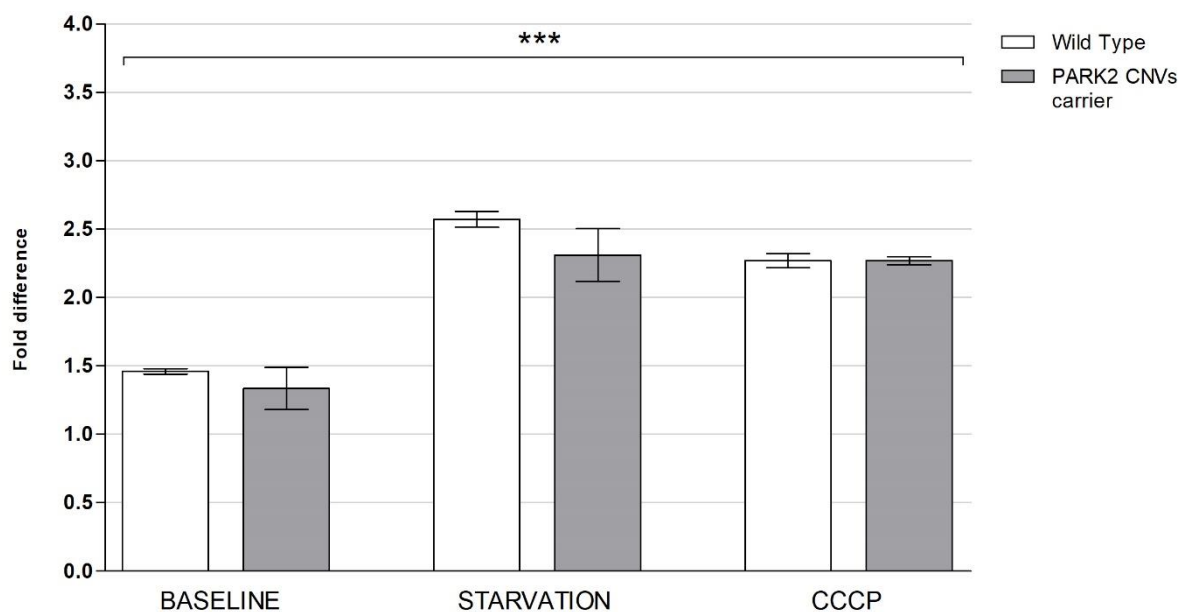


Figure 25 ROS production in HDF.

Cellular reactive oxygen (ROS) abundance was measured indirectly by measuring the fluorescence of the oxidized form of DCFDA/H₂DCFDA. Output reading is given in RFU (relative fluorescence units). Fold difference in ROS levels was calculated against wild type baseline after background subtraction. Univariate analysis of variance revealed a significant effect of the treatment ($F_{(2, 12)} = 55.208$, $p < .0001$, $\eta_p^2 = .902$) but no genotype or interaction effects. Main difference on the treatment variable was between baseline treatment and starvation (Tukey HSD $p < .0001$) and baseline and CCCP (Tukey HSD $p < .000$). Data are shown as mean \pm SEM. Level of significance was set at $p = .05$. * $p \leq .05$, ** $p \leq .01$, and *** $p \leq .001$.

3.5.5 Mitochondrial network morphology

We evaluated the presence of morphological changes in the mitochondrial network of fibroblasts and HiPSC lines derived from ADHD patients carrying CNVs within the *PARK2* gene and wild type controls under two different conditions, baseline and starvation (Figure 26). In both cases, two main parameters were considered: the aspect ratio (AR) that describes mainly the shape of the mitochondria (a value of 1 corresponds to a perfect circle, higher values to a more elongated shapes) and form factor (FF) that evaluates the mitochondrial network branching where high values represent a more tubular network and lower a more fragmented one (Mortiboys et al., 2009; Zanellati et al., 2015).

In regard of the fibroblast lines, an univariate analysis of variance revealed a significant effect of treatment for both the indexes (AR: $F_{(1, 12)} = 14.318$, $p=.009$, $\eta_p^2=.705$; FF: $F_{(1, 12)} = 16.532$, $p=.007$, $\eta_p^2=.734$) and an almost significant interaction of the genotype with the treatment in regard of the mitochondrial branching (FF: $F_{(2, 12)} = 4.842$, $p=.056$, $\eta_p^2=.617$). This suggests that the starvation stress promoted a more fragmented branching with more spherical shape (AR: $M=2.182$; $SD=.253$; FF: $M=2.311$; $SD=.096$) compared to baseline (AR: $M=2.723$; $SD=.447$; FF: $M=2.613$; $SD=.348$). Descriptively, we point out that in baseline conditions, the CNV duplication carrier show a more elongated mitochondrial shape and tubular branching compared to CNVs deletion carriers and WTs.

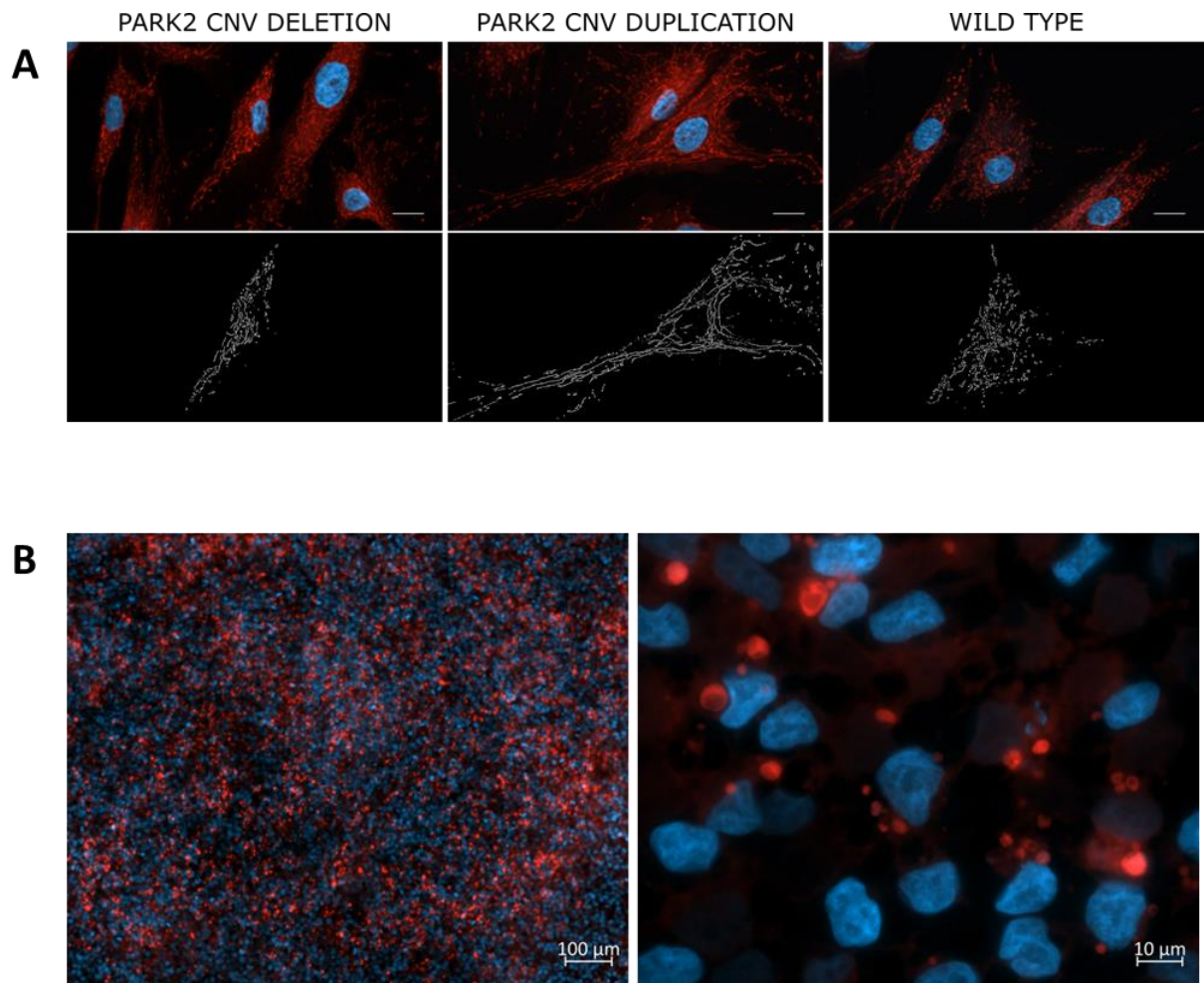


Figure 26 Mitochondrial network staining in HDF and iPSC.

(A) Representative pictures of mitochondrial staining with MitoTracker Red CMXRos in fibroblast lines in baseline conditions and mask of the semi-automated digital image analysis (Fiji/ImageJ) illustrating the different type of network morphology analysis. From the pictures is it possible to appreciate an example of a tubular elongated mitochondrial shape (ADHD/ *PARK2* CNV duplication carrier) and a fragmented round-shaped mitochondrial network (HEALTHY/*PARK2* wild type). Scale bars 100 μm .

(B) Representative pictures of mitochondrial staining with MitoTracker Red CMXRos in iPSC lines in baseline conditions at two different magnifications. As reported by the literature, iPSC mitochondria show a perinuclear distribution, low number and round shape.

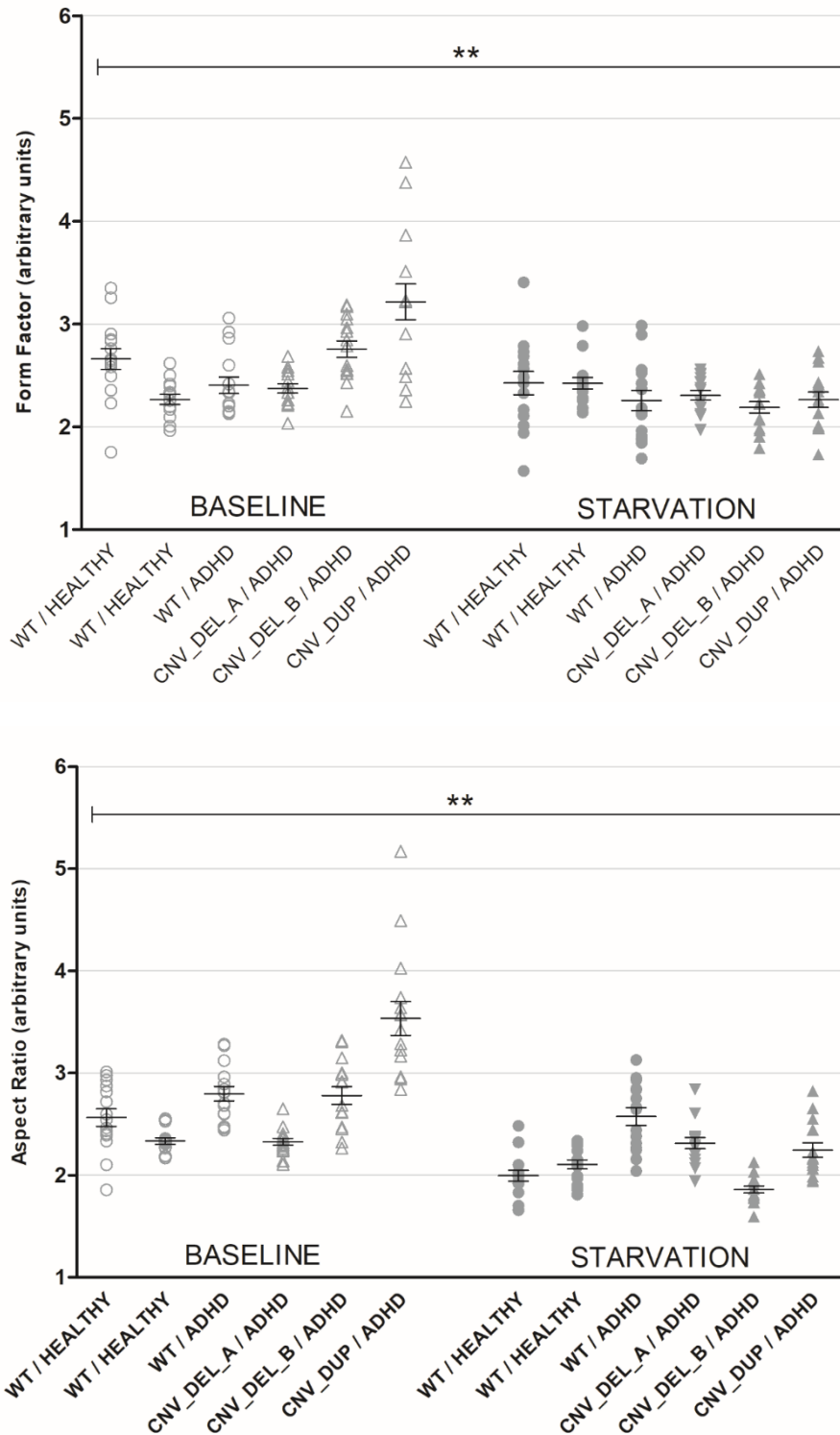


Figure 27 Mitochondrial network aspect ratio and form factor in HFD in baseline conditions and after starvation stress.

The form factor describes the morphological properties of the mitochondrial network (mitochondrial branching). It is calculated as: $[\text{perimeter}^2 / (4\pi \times \text{area})]$ and small values are indicative of a more fragmented-dotted network whereas higher values describe a more tubular, chain-like network. The aspect ratio describes mainly the shape of the mitochondria and is calculated as the ratio between the major axis and the minor axis of the ellipse equivalent to the object. A value of 1 describes a perfect circular shape whereas increased values are in relation with a more elongated shape. Univariate analysis of variance revealed a significant effect of treatment for both the indexes (AR: $F_{(1, 12)} = 14.318$, $p = .009$, $\eta_p^2 = .705$; FF: $F_{(1, 12)} = 16.532$, $p = .007$, $\eta_p^2 = .734$). 15 different selected

fibroblasts for each line/condition (90 cells total) from two independent experiments were analyzed. Data are shown as mean \pm SEM. Level of significance was set at $p=.05$. * $p \leq .05$, ** $p \leq .01$, and *** $p \leq .001$.

HiPSC were also tested for network morphology as described for the fibroblasts. As already reported in the literature (Bukowiecki, Adjaye, & Prigione, 2014), they showed a general low number and a perinuclear distribution of mitochondria (Figure 26 B). Mitochondria of HiPSCs do not form intricate networks like the mitochondria in fibroblasts, as described by low values for the form factor parameter (FF: $M=1.478$; $SD=.826$) and have a general round shape, consistent with values close to 1 for the aspect ratio parameter (AR: $M=1.473$; $SD=.027$). Statistical analysis did not reveal any significant effect of the genotype, treatment or interaction effects (AR: $F_{(2, 12)} = .407$, $p=.682$, $\eta_p^2=.120$; FF: $F_{(2, 12)} = .260$, $p=.779$, $\eta_p^2=.080$) suggesting that HiPSC might not show mitochondrial morphological rearrangement after stress condition, differently from what we have reported for the fibroblast lines (Figure 28). This result might be connected with the fact that HiPSC metabolisms, being different from fibroblasts, relies mostly on glycolysis rather than oxidative phosphorylation.

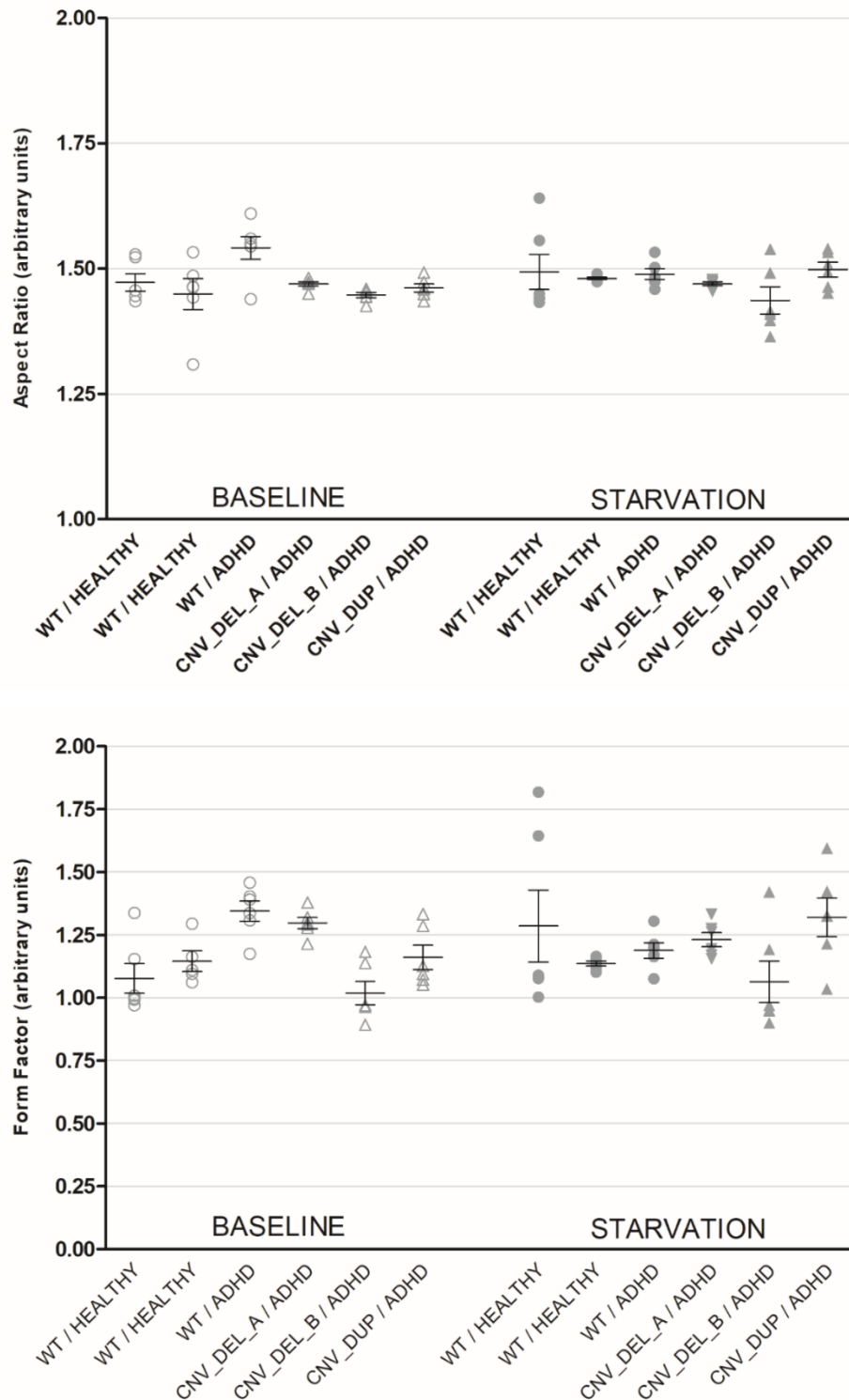


Figure 28 Mitochondrial network aspect ratio and form factor in HiPSC in baseline conditions and after starvation stress.

Statistical analysis did not reveal any significant effect of the genotype, treatment or interaction effects. Mitochondria of HiPSCs do not form intricate networks like the mitochondria in fibroblasts, as described by low values for the form factor parameter (FF: $M=1.478$; $SD=.826$) and have a general round shape, consistent with values close to 1 for the aspect ratio parameter (AR: $M=1.473$; $SD=.027$). Aspect ratio and form factor values were obtained from 6 whole pictures for each line/condition (36 in total). Data are shown as mean \pm SEM. Level of significance was set at $p=.05$. * $p \leq .05$, ** $p \leq .01$, and *** $p \leq .001$.

3.6 EVALUATION OF NICOTINE EFFECTS ON HiPSC-DERIVED DOPAMINERGIC NEURON FROM AADHD PATIENTS

3.6.1 Hypothesis free gene expression analysis (RNA sequencing)

The HiPSC-derived dopaminergic neurons were treated with nicotine in two different concentrations (namely “acute”: 5 μ M nicotine for 24hours prior harvesting, and “chronic”: 0.4 μ M nicotine for 7 days prior harvesting). Nicotine concentrations used in the study were previously reported to be smoking-relevant and close to concentrations related to “binging episodes” and “continuous consumption” (namely “acute” and “chronic” treatment) (Lomazzo et al., 2011) (Srinivasan et al., 2016). Additionally, samples from immature neurons (harvested at day 45) in baseline conditions and after acute treatment were included in the analysis. RNA samples were then sent to Novogene for RNA sequencing (Novogene, China). A summary of the lines investigated is reported in (Table 7).

	IMMATURE NEURONS (day 45)		MATURE NEURONS (day 60)		
	BASELINE	NICOTINE ACUTE	BASELINE	NICOTINE ACUTE	NICOTINE CHRONIC
	B27 complete medium	+ Nicotine 5 μ M 24h (day 44)	B27 complete medium	+ Nicotine 5 μ M 24 h (day 59)	+ Nicotine 0.4 μ M 7 days (day 53 to 60)
PARK2CNV_DEL_A / ADHD	DE1_I_B	DE1_I_NA	DE1_M_B	DE1_M_NA	DE1_M_NC
PARK2CNV_DEL_B / ADHD	DE2_I_B	DE2_I_NA	DE2_M_B	*	DE2_M_NC
PARK2CNV_DUP/ ADHD	DUP_I_B	DUP_I_NA	DUP_M_B	DUP_M_NA	DUP_M_NC
WT_B/ HEALTHY	W2_I_B	W2_I_NA	W2_M_B	W2_M_NA	W2_M_NC

Table 9 Summary of the samples used for RNA sequencing.

Each column represents the samples analyzed for each treatment. Sample naming used in the study and sample name used in the analysis are reported in the rows. Samples marked with * did not pass the initial RNA Quality Control and was therefore excluded from the analysis.

The analysis of the differentially expressed genes (DEGs) was performed comparing gene expression of the ADHD/*PARK2* CNVs carrier with the wild type controls for each of the five conditions taken into consideration. In all comparisons, a number of differentially expressed genes, either up- or down regulated was found (Figure 30). As reported by the Volcano plots, nicotine acute treatment in mature neurons seems to be the treatment with the biggest effect in terms of DEGs, with a total of 112 differentially regulated genes (62 up-regulated, 50 down-regulated).

To interpret the large amount of data a gene ontology approach was used (gene ontology enrichment analysis). The analysis showed that after nicotine acute treatment there was a significant enrichment in GO that falls under the biological processes “regulation of growth”, “regulation of cell growth”, “cell growth”, “growth” and under the molecular functions “insulin-like growth factor binding” “growth factor binding” (Figure 31). No significant differentially regulated GO were found in the other conditions.

We then decided to focus on the differential gene expression response due to nicotine treatments between ADHD/*PARK2* CNV carriers and wild types (Figure 32). We short-listed genes that were significantly up or down regulated after both nicotine acute and chronic treatment but not in baseline. We found 11 genes that were differentially regulated after both nicotine treatments, two of which were involved in energy production and oxidative stress response, three with extracellular matrix and cell adhesion.

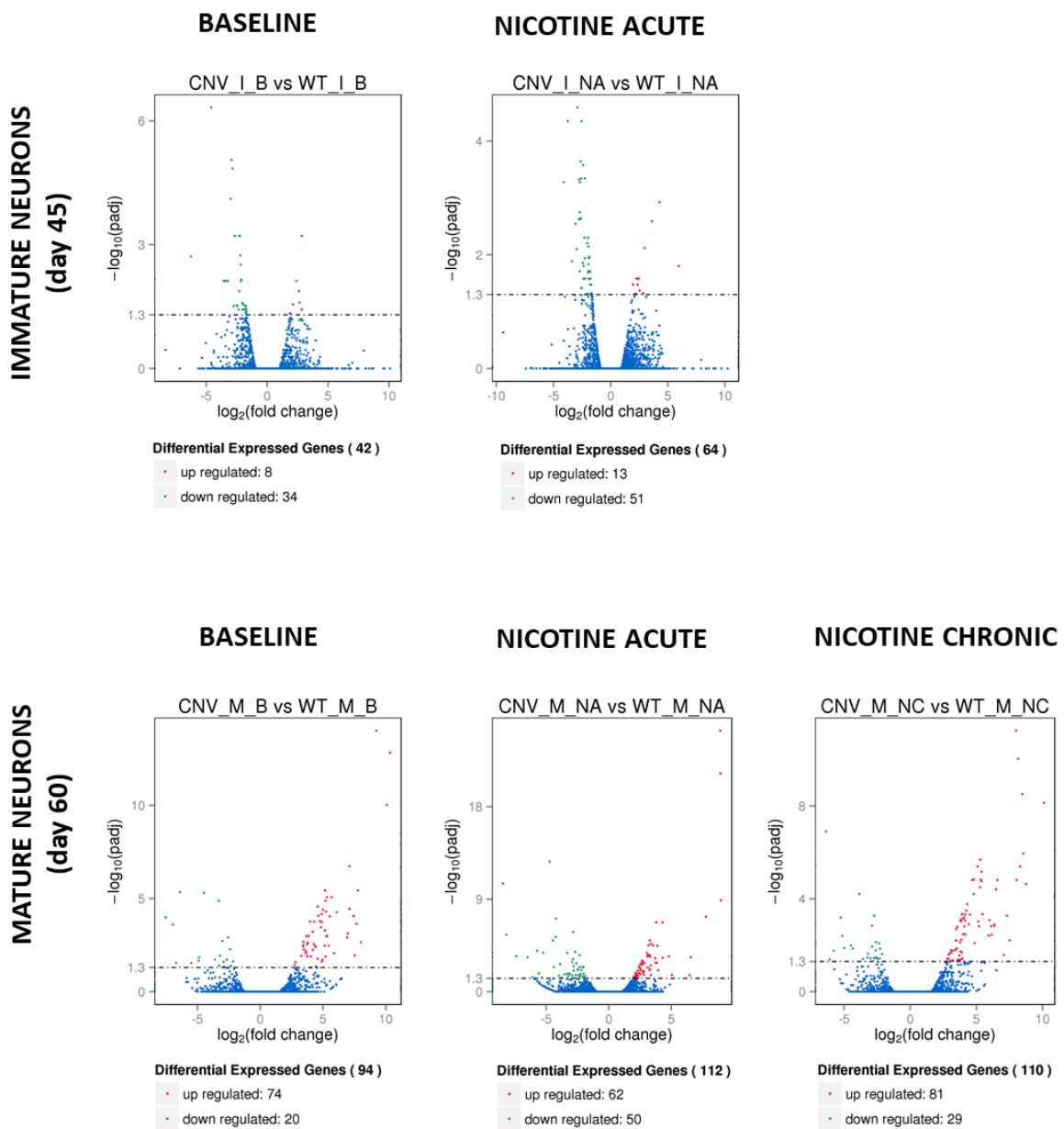


Figure 29 Volcano Plots of differentially regulated genes.

Volcano plots are used to infer the overall distribution of differentially expressed genes. The y-axis reports the negative logarithm of the adjusted p-value, significant values are reported as above threshold (1.3). The x-axis shows the logarithm of the fold change, significantly down regulated genes are shown in green whereas significantly up regulated genes are shown in red. Genes that were not expressed differently between treatment group and control group are shown in blue. Threshold is set as: $|\log_2(\text{fold change})| > 1$ and $q\text{-value} < .005$.

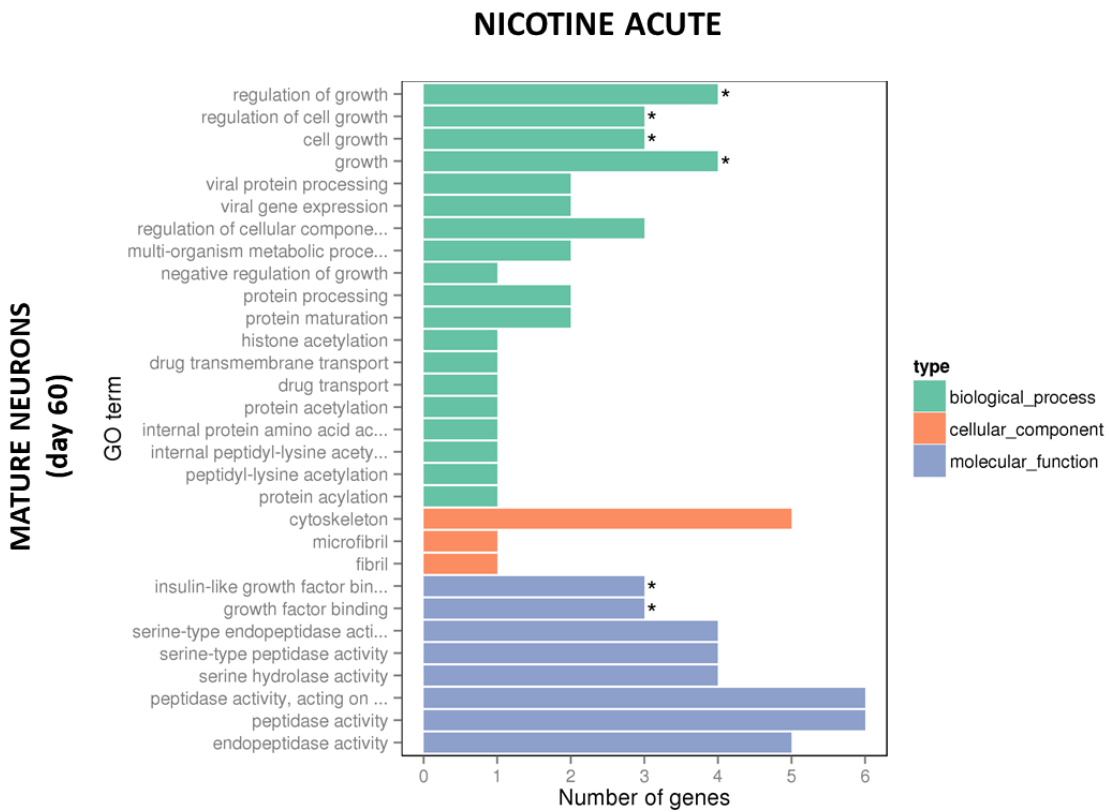


Figure 30 Gene ontology enrichment analysis of upregulated DEGs after acute nicotine treatment. The GO enrichment bar chart of DEGs presents the number of DEGs enriched in biological process (green), cellular component (orange) and molecular function (blue). The 30 most significant enriched terms are selected. The y-axis is the enriched GO term, x-axis is the number of DEGs enriched in this term. Significantly enriched terms are marked with “*”.

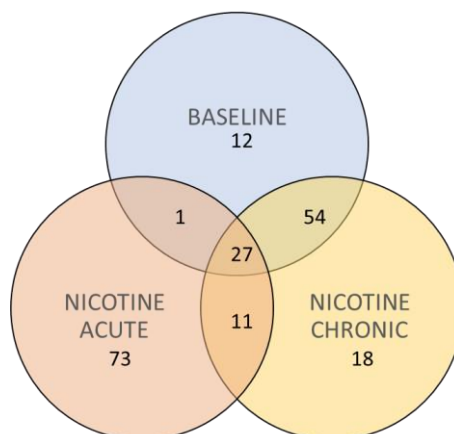


Figure 31 Venn diagram of DEGs. The diagram presents the number of genes that are differentially expressed between ADHD/PARK2 CNVs carriers and WT in baseline, nicotine acute and nicotine chronic conditions. The number in each circle is the number of genes differentially regulated in that condition whereas the number on the overlap represents the genes differentially expressed in common between the two conditions. Eleven genes were found to be differentially expressed after nicotine exposure.

Gene Name	Treatment	Log2 Fold Change	p-value adj	Involved in	
C1QTNF3	C1q and tumor necrosis factor related protein 3	NICOTINE ACUTE	3.361	0.00002	ENERGY PRODUCTION & OXIDATIVE STRESS
		NICOTINE CHRONIC	3.192	0.01749	
CARTPT	CART prepropeptide	NICOTINE ACUTE	-4.728	0.00000	ENERGY PRODUCTION & OXIDATIVE STRESS
		NICOTINE CHRONIC	-2.298	0.03753	
COL5A1	collagen, type V, alpha 1	NICOTINE ACUTE	1.971	0.04023	EXTRACELLULAR MATRIX/ CELL ADHESION
		NICOTINE CHRONIC	3.071	0.02083	
MFAP2	microfibrillar-associated protein 2	NICOTINE ACUTE	2.304	0.02697	EXTRACELLULAR MATRIX/ CELL ADHESION
		NICOTINE CHRONIC	2.911	0.03934	
PCDHGA6	protocadherin gamma subfamily A, 6	NICOTINE ACUTE	-2.193	0.00790	EXTRACELLULAR MATRIX/ CELL ADHESION
		NICOTINE CHRONIC	-2.603	0.00738	
CP	ceruloplasmin (ferroxidase)	NICOTINE ACUTE	3.269	0.00026	Fe PEROXIDATION
		NICOTINE CHRONIC	3.395	0.01626	
SLC30A8	solute carrier family 30, member 8	NICOTINE ACUTE	-4.456	0.00001	Zn EFFLUX TRANSPORTER
		NICOTINE CHRONIC	-2.997	0.03634	
ZNF208	zinc finger protein 208	NICOTINE ACUTE	Inf	0.00760	REGULATION OF TRANSCRIPTION
		NICOTINE CHRONIC	Inf	0.02337	
RP11-344E13.3		NICOTINE ACUTE	-2.451	0.00659	UNKNOWN
		NICOTINE CHRONIC	-2.725	0.03564	
RP11-469N6.1		NICOTINE ACUTE	-8.188	0.00000	UNKNOWN
		NICOTINE CHRONIC	-4.473	0.01026	

Table 10 List of genes differentially regulated after nicotine exposure.

For each gene we report the log2 of fold change (Log2 Fold Change) between ADHD/PARK2 CNVs carriers and WT (negative values correspond to a downregulation, positive values to an upregulation) and the adjusted p-value after correction for multiple testing (p-value adj).

3.6.2 *PARK2* gene expression

Data obtained from Illumina RNA sequencing were used to evaluate *PARK2* gene expression levels in HiPSC-derived dopaminergic neurons under basal condition and after two nicotine paradigms in mature and immature neurons (Table 9). We report the expected number of fragments per kilobase of transcript sequence per million base pairs sequenced (FPKM) which takes into account the effects of both sequencing depth and gene length on counting of fragments (Trapnell et al., 2010) for each cell line and the read counts values of *PARK2* CNVs carriers and wild type after normalization (Table 9). There was no significant difference between ADHD/*PARK2* CNVs carriers and WT healthy controls in *PARK2* gene expression in any of the conditions analyzed. This result confirms that, as already reported in HDF, there are no gene expression differences between CNV carriers and wild type and additionally suggests that the treatment does not affect the gene expression of *PARK2*.

SAMPLE ID	BASELINE IMMATURE	BASELINE MATURE	NICOTINE ACUTE IMMATURE	NICOTINE ACUTE MATURE	NICOTINE CHRONIC MATURE
PARK2CNV_DEL_A/ADHD	5.394	5.301	4.976	3.833	4.766
PARK2CNV_DEL_B/ADHD	4.204	3.361	3.911		2.789
PARK2CNV_DUP/ADHD	10.940	6.192	9.898	6.052	6.532
WT_B/HEALTHY	5.551	4.023	5.480	4.625	3.745
<hr/>					
<i>PARK2</i> CNV read count	350.978	297.368	326.088	256.643	254.939
<i>PARK2</i> WT read count	359.957	248.930	346.639	229.905	202.574
log2FoldChange (<i>PARK2</i> CNV vs <i>PARK2</i> WT)	-0.036	0.257	-0.088	0.159	0.332
p-value (<i>PARK2</i> CNV vs <i>PARK2</i> WT)	0.932	0.879	0.865	0.851	0.769
p- value adjusted (<i>PARK2</i> CNV vs <i>PARK2</i> WT)	1	1	1	1	1

Table 11 *PARK2* gene expression in baseline and after nicotine treatment in immature and mature HiPSC-derived dopaminergic neurons.

The upper part of the chart reports the expected number of Fragments Per Kilobase Of Transcript Sequence Per Million Base Pairs Sequenced (FPKM) for each cell line. The lower part of the chart reports the read count after normalization and the p-value after false discovery rate (FDR) estimation based on multiple hypothesis testing (method BH).

3.6.3 PARK2 protein expression

PARK2 protein abundance was measured in HiPSC-derived dopaminergic neurons under basal conditions and after nicotine acute and chronic treatment (Figure 32). We report results from one experiment with samples measured in duplicate. Our analysis did not reveal any significant difference between ADHD/*PARK2* CNVs carriers and wild types nor treatment effects ($F_{(2, 9)} = 1.252$, $p = \text{n.s.}$, $\eta_p^2 = .218$). Given the high standard deviation present in the samples, results from this experiment needs to be further replicated.

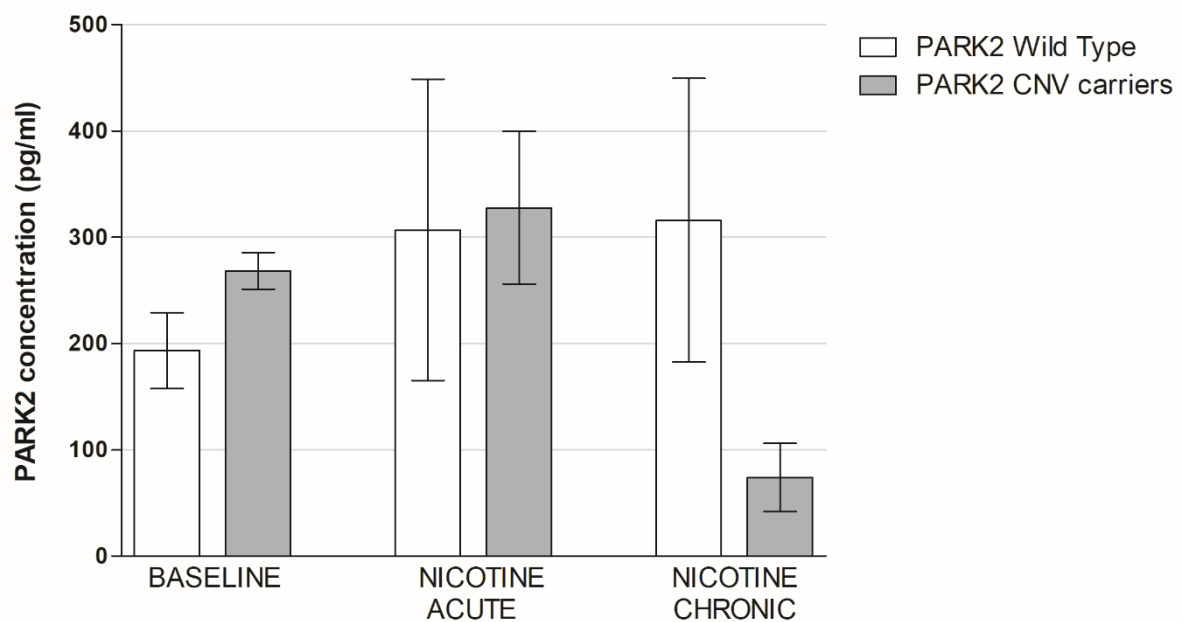


Figure 32 *PARK2* protein expression in HiPSC-derived dopaminergic neurons after nicotine treatment. *PARK2* protein concentration (pg/ml) in mature neurons (day 60) measured in basal conditions, after “acute” nicotine treatment (5 μM nicotine for 24hours prior harvesting) and “chronic” treatment (0.4 μM nicotine for 7 days prior harvesting). Statistical did not reveal any significant effect. Data refers to one experiment with samples measured in duplicate. Data are shown as mean protein concentration \pm SEM. Level of significance was set at $p = .05$.

4 DISCUSSION

Main goal of this doctoral thesis was to identify cellular patho-phenotypes related to rare CNV variants in *PARK2 locus* that have been associated with Attention-Deficit/Hyperactivity Disorder by genome wide association studies (Jarick et al., 2014).

4.1 ADHD/*PARK2* CNV CARRIERS USED IN THE STUDY DO NOT SHOW EARLY SIGNS OF PD

A cohort of 12 participants was initially chosen from a previous study (Jarick et al., 2014) and the absence or presence of rare variants was validated for the *PARK2 locus* genotype comprising 4 *PARK2* CNV carriers affected by ADHD, 4 *PARK2* wild types affected by ADHD and 4 *PARK2* wild types non-affected. All the ADHD patients were diagnosed both in adulthood and retrospectively in childhood. As mentioned in the introduction, *PARK2* mutations were first associated with an early onset autosomal form of Parkinson's Disease (PD) with an average age of symptoms onset around the early thirties (Brüggemann & Klein, 1993). Therefore, to exclude the possibility of a neurodegenerative disease co-morbidity in our cohort of adult ADHD patients carrying the *PARK2* CNVs, participants were also comprehensively and intensively neurologically tested. None of the diagnostic scales used for PD diagnosis and symptom severity measurement in every-day practice, such as UPDRS and PD NMS, revealed early symptoms of PD. Additionally, measurement of the volume of the *substantia nigra* by ultrasound revealed no size differences due to dopaminergic degeneration in ADHD/*PARK2* CNV carriers compared to controls. The loss of olfactory function is one of the earliest PD symptoms that can be assessed in the diagnostic process (Nielsen, Jensen, Stenager, & Andersen, 2018), therefore subjects were assessed by Sniffin' Sticks olfactory test that again revealed no significant differences. Taken together, these results hint that there is rather no co-occurrence of autosomal early onset PD form in the ADHD/*PARK2* CNVs carriers investigated in the study.

4.2 HiPSC AND HiPSC-DERIVED NEURONS WERE POSITIVE FOR ALL THE *BONA FIDE* CHARACTERIZATION TESTS PERFORMED WITHOUT GENOTYPE DIFFERENCES

The first part of the project was focused on the creation and validation of cellular model systems deriving from human adults ADHD patients carrying CNVs in the *PARK2 locus* and from *PARK2* WT healthy and ADHD affected donors.

Fibroblasts lines were generated from all the donors whereas a subset of this sample cohort was used both for generating HiPSC and HiPSC-derived neurons and to conduct most of the subsequent experiments included in the study. Therefore, 6 HiPSC and HiPSC-derived dopaminergic neurons lines were generated in this project, 3 *PARK2* CNV carriers affected by ADHD, one *PARK2* wild type affected by ADHD and two *PARK2* wild types non-affected by ADHD.

Fibroblasts source lines were chosen to be age and sex matched and showed no growth or viability variability between the lines. HiPSC obtained from fibroblast cultures were extensively and comprehensively characterized in order to prove the generation of *bona fide* HiPSC. As a good practice, we decided to validate 3 clones for each line generated in order to exclude any possible confounding effect due to the reprogramming (Martí et al., 2013). HiPSC showed a typical ES-like morphology on light microscope with round shaped and compact colonies presenting sharp and distinct borders, tightly packed cells with high nuclear-to-cytoplasm ratio and prominent nucleoli. A panel of biochemical and molecular markers associated with pluripotency has been identified to be specific for HiPSC physiology and fundamental to maintain an undifferentiated state. In humans, markers include *developmental pluripotency associated 5* (*DPPA5* also known as *ESG1*), *SRY-box 2* (*SOX2*), *Nanog homeobox* (*NANOG*), *POU class 5 homeobox 1* (*POU5F1* also known as *OCT3*; *OCT4*) cellular surface pluripotency markers such as podocalyxin like protein 1 (*TRA-1-60* also known as *PODXL*) and stage-specific embryonic antigen 4 (*SSEA4*) (Rony et al., 2015). All the tested clones were shown to express the selected pluripotency markers on both RNA and protein level. Pluripotent stem cells should be able to generate a plethora of different cell types by definition. Allowing the growth as spherical three dimensional aggregates, called embryoid bodies (EBs), is it possible to assess if the iPSC are able to spontaneously differentiate into all three germ layers (endoderm, ectoderm, mesoderm) that compose the embryo (Sheridan,

Surampudi, & Rao, 2012). All the EBs generated from our HiPSC lines expressed markers for mesodermal, ectodermal and endodermal lineage differentiation.

When working with HiPSC is of great importance to assess whether genetic variations occurred. In fact it has been repeatedly demonstrated that genomic alteration such as aneuploidy, copy number variation (CNV), and single nucleotide variations (SNVs) might occur during HiPSC generation and maintenance (Ronen & Benvenisty, 2012). This genetic alterations of the original genomic make-up might cause a phenotypic variation in the differentiated cells that might confer additional phenotypes and interfere with the disease modelling and drug discovery (G. Liang & Zhang, 2013). Therefore, all HiPSC clones generated were analyzed for genomic variations that showed that no additional CNVs were introduced in the genetic *locus* object of the study, there was no overall significant increase in CNVs in HiPSC clones compared to the fibroblast source and that there is a high degree of genetic proximity (relatedness) between HiPSC and fibroblast source. We thus can conclude that the HiPSC lines generated in this study have been confirmed to be *bona fide* HiPSCs and could be used to generate iPSC-derived dopaminergic neurons for ADHD disease modelling.

HiPSC-derived dopaminergic neurons generated in this project were also intensively characterized and proven to be *bona fide* HiPSC-derived neurons. During the neural induction strong morphological changes were observed: mature cultures were characterized by a multipolar cellular morphology, with extensive development of long and branched processes. Additionally, clustering of cell bodies and neurites was frequently observed. While maturing into dopaminergic neurons, cultures showed expression of markers consistent with the stage of maturation. In fact, immature neurons at day 45 and mature neurons at day 60 did not show expression of pluripotency associated markers such as *POU5F1* but expressed *LMX1B*, a transcription factor required in the early stages of DA progenitors (Deng et al., 2011; Andersson et al., 2006), *NEUROD1* a member of the family of pro-neural genes, which functions during embryonic neurogenesis as an essential neuronal differentiation factor (Pataskar et al., 2016) and *EN1* which expression normally starts early in the dopaminergic neurons maturation and is maintained throughout the adulthood (Hegarty et al., 2013). Therefore, the maturation was followed through a restriction of the pluripotency typical of HiPSC towards a dopaminergic fate. Moving to the protein level, HiPSC-derived neurons stained positive for a general neuron-specific marker TUBB3 and for another marker more

specifically expressed in DA neurons such as tyrosine hydroxylase (TH). Additionally, we evaluated the presence of dopamine (DA) both in the extracellular media and in the intracellular protein extract of mature neurons. Detectable levels of dopamine were reported in both cases that might additionally imply active exocytotic release of dopamine (Beaulieu & Gainetdinov, 2011; Sulzer, Cragg, & Rice, 2016). In none of the characterization assays performed we highlighted a genotype difference that implies, in contrast to what has been reported with some lines carrying various mutations in *PARK2* from PD patient's (Shaltouki et al., 2015), that the presence of ADHD/*PARK2* CNVs in our lines does not interfere with the dopaminergic differentiation. This provides proof that the phenotyping assays performed on HiPSC-dopaminergic neurons created in this study are not affected by differences due to the model itself.

4.3 EVALUATION OF PATHO-PHENOTYPES CONNECTED WITH ADHD/*PARK2* CNVs IN HDF AND HiPSC AFTER STRESS EXPOSURE

The validation of the cellular models created in this study allowed us to assess in parallel whether a patho-phenotype due to the different genetic background was discernible between ADHD/*PARK2* CNVs carriers and wild type lines. As mentioned in the introduction, the phenotypic effects of *PARK2* mutations have been extensively studied in Parkinson's disease patients but, to the best of our knowledge, no data are available regarding the functional consequences of rare *PARK2* CNVs associated with ADHD. Therefore, we decided to tailor our experiments to evaluate first, if differences were present in gene and protein expression regarding *PARK2* levels and second, investigating biological function that are believed to be connected with *PARK2* biological activity. *PARK2*, acting in concert with *PINK1*, is one of the main effectors of the so called mitochondrial quality control (MQC) system, that directs and regulates many mitochondrial functions such as mitochondrial fission and fusion dynamic events as well as mitochondria biogenesis itself, mitochondrial autophagy (mitophagy), transport, and contributes to regulating cellular apoptosis (Scarffe L.A., Stevens D.A., Dawson V.L., 2015). The MQC system functions already under normal basal conditions but exert a pivotal role especially after cellular homeostasis perturbations (Pickrell & Youle, 2015). Therefore, we decided to additionally evaluate if genotype differences were exacerbated

under cellular stress conditions. We thus applied a serum-deprivation paradigm, also known as nutrient deprivation paradigm (called “starvation” for brevity), a form of metabolic cellular stress that has been proven to induce an increase in *PARK2* expression both in human SH-SY5Y neuroblastoma cells and primary mouse neurons (Klinkenberg et al., 2012). Additionally we applied a pharmacological treatment with the ionophore carbonyl cyanide m-chlorophenyl hydrazine (CCCP) a substance that is known to depolarize the mitochondrial membrane potential and trigger PINK1 accumulation and therefore indirectly activating *PARK2* (Yamano et al., 2016).

4.3.1 ADHD/*PARK2* CNV carriers show different *PARK2* protein levels but not gene expression

The evaluation of *PARK2* gene expression in HDF cultures did not reveal a significant genotype difference, a result that was later replicated in HiPSC-derived dopaminergic neurons. *PARK2* transcript expression was found to be generally low in our HDF cultures, differently from what has been previously reported (Klinkenberg et al., 2012). Moving to the protein level, our data indicate a lower level of *PARK2* protein in CNVs carriers in fibroblasts after starvation stress. This result might suggest that the response to nutrient deprivation stress is differentially regulated in ADHD/*PARK2* CNV carriers in comparison to ADHD/wildtype and healthy control lines. *PARK2*, being a major regulator of the MQC system, this might imply that ADHD/*PARK2* CNV carriers could fail to set in place the cellular stress response mitochondrial-related mechanisms that usually help in buffering the increase of oxidative stress and in provide new molecular building blocks by mitophagy. Low levels of *PARK2* protein have been reported also in fibroblast from Parkinson’s disease patients harboring recessive mutations in *PARK2* (Zanellati et al., 2015) but no data are available for HiPSCs. Regarding the HiPSC lines, we report a higher amount of *PARK2* protein in CNVs carriers compared to controls in baseline conditions. To explain this and the subsequent results, it is important to point out that HiPSC metabolism is different from most of the adult cell types. In fact, differently from fibroblasts, HiPSC rely mostly on glycolysis rather than oxidative phosphorylation. This switch in metabolism occurs in parallel to strong mitochondria morphological changes: HiPSC mitochondria acquire a fragmented and globular shape, perinuclear localization and they become hyperpolarized (Lopes & Rego, 2016). The switch might be connected with the

PARK2/PINK1 MQC, as suggested by Vazquez-Martin and colleagues (Vazquez-Martin et al., 2016b). Although further analysis is required, our data might suggest that in *PARK2* CNV carriers this interplay could be deregulated leading to a PARK2 accumulation therefore explaining higher PARK2 protein levels in HiPSC from ADHD/*PARK2* CNV carriers.

Taken together our gene and protein expression analysis of PARK2 might suggest the presence of differences in ADHD/*PARK2* CNVs carriers in regulatory processes occurring after mRNA is made such as, post-transcriptional, translational and protein degradation regulation. In general it has been estimated that in eukaryotes only 40% of the variation in protein concentration can be explained by knowing mRNA abundances (Vogel & Marcotte, 2012). Multiple processes beyond transcript concentration contribute to establishing the expression level of a protein such as translation rates, translation rate modulation through the binding of non-coding RNAs, modulation of a protein's half-life by the complex ubiquitin-proteasome pathway or autophagy and protein synthesis delay (Y. Liu, Beyer, & Aebersold, 2016). In this regard, many recent works have underlined microRNAs (miRNAs) as prospective players in neuropsychiatric disorders and to date 19 different miRNAs have been identified as potentially playing a role in ADHD as reviewed in (Srivastav, Walitza, & Grünblatt, 2018). Among them we find miR-34c and miR-34b (Garcia-Martínez et al., 2016; Wu et al., 2017) that are also shown to be associated with autism spectrum disorder (Hicks and Middleton 2016), a disorder often comorbid with ADHD. Both the abovementioned miRNAs are linked with PARK2 regulation. In fact, decreased levels of miR-34c and miR-34b correspond to a decrease in PARK2 protein levels (Miñones-Moyano et al., 2011). Given the association of these miRNAs with ADHD and the fact that they could participate in the regulation of PARK2 expression, it might be an interesting point to further investigate the role of the abovementioned miRNA in our cellular models and therefore gather more understanding on additional processes that might be differentially regulated between ADHD/*PARK2* CNVs carrier and WT in regards of the regulation of protein abundance.

4.3.2 ADHD/*PARK2* CNV carriers show lower levels of cellular ATP and extracellular oxygen consumption rates compared to controls

Our investigation of mitochondrial-related features has yielded interesting results. In the last years, several studies have linked mitochondrial impairments to the etiology of many psychiatric and neurodevelopmental disorders (McCann & Ross, 2018). The brain, in fact, represents the organ with the highest energetic demand. Mitochondria, as well known, play a pivotal role in energy metabolism but also in metabolism of amino acids, lipids and steroids, all essential element for normal brain function (Manji et al., 2012). Moreover, at the neuronal synapsis, mitochondria contribute to maintaining the membrane potential, play a role in calcium dependent neurotransmitter release and activation of second messenger pathways (Sheng & Cai, 2012; Srivastava, Faust, Ramos, Ishizuka, & Sawa, 2018).

The biological function of mitochondria includes the production of several reactive oxygen species (ROS) and reactive nitrogen species (RNS) that are under normal conditions buffered by antioxidants balancing systems. Several studies have investigated the contribution of oxidative and nitrosative stress markers in ADHD patient derived tissues as reviewed by Lopresti and colleagues (Lopresti, 2015). Although most of the findings point out at an overall increase of oxidative stress and insufficient response to oxidative damage both in children and adults with ADHD (Joseph et al., 2015), investigation are sometimes contradictory most likely because of inconsistencies in markers tested, publication bias, sample collection and population used (Lopresti, 2015). The connection of this data with ADHD etiology is still in debate, on one hand it could be an artefact due to other factors (like diet or other concomitant medical conditions) on the other hand oxidative pathways could play an important role in affecting biological mechanisms associated with ADHD. It is widely accepted that the brain, having a great oxygen use and presenting a high lipid concentration, is one of the organs that could be mostly affected by oxidative damage. Moreover, dopamine, the neurotransmitter (besides norepinephrine) mostly connected with ADHD can be strongly influenced by oxidative stress and *vice versa* influence oxidative stress itself (Miyazaki & Asanuma, 2008). Interestingly, it has been reported that methylphenidate, the most widely used treatment in ADHD, might repair the oxidative balance by increasing antioxidant defense mechanisms (Guney et al., 2015) and overall antioxidant therapy seem to have a positive effect on ADHD symptoms (Bloch & Qawasmi, 2011; Garcia et al., 2013).

In this context we decided to evaluate the ATP total content in fibroblast cultures under baseline conditions and two stress paradigms. Our results indicate a significant difference between the genotypes both in baseline conditions and after 24h starvation. ADHD/*PARK2* CNV carriers show lower levels of cellular ATP compared to controls, a result that could suggest that the MQC system might be impaired and lead to an accumulation of damaged mitochondria, with ATP loss. This result is in line with data already reported in the literature from primary fibroblast cultures of PD patients with homozygous or compound heterozygous parkin mutations in baseline conditions (Mortiboys et al., 2009; Zanellati et al., 2015). Moreover, ADHD *PARK2* CNV carriers show lower extracellular oxygen consumption rates both in baseline conditions and after 24 hours nutrient deprivation. Our results sustain what was already reported in ADHD cybrids cells, a transgenic cell model that allows to study only the contribution of patient's derived mitochondria, that additionally describes lower levels of ATP production and oxygen consumption and increased levels of superoxide radicals (Verma et al., 2016).

4.3.3 The amount of reactive oxygen species (ROS) is influenced by the stressors but not by genotype

We thus decided to evaluate if the amount of reactive oxygen species (ROS) was also influenced by the genotype and treatment with the two stressors as was ATP production and oxygen consumption rate. As expected, our data suggest that the cells increase the ROS content after starvation stress and CCCP treatment compared to baseline, but the genotype did not seem to exert a role in the final ROS levels. This result is consistent with the findings from our hypothesis driven gene expression analysis. Fibroblasts from *PARK2* CNV carrier showed higher expression levels of *NAD(P)H Quinone Dehydrogenase1 (NQO1)* after starvation stress. NQO1 has a protective role in oxidative damage preventing the one electron reduction of quinones and thus the production of radical species (Ross & Siegel, 2017). From the same analysis we also report a genotype effect in the gene expression of *UBB* both for fibroblast and HiPSCs samples, also involved in stress response (Sarraf et al., 2013). In the HiPSCs samples the gene expression of *UBB* appears to be lower in ADHD *PARK2* CNV carriers after starvation stress compared to controls. The same analysis did not show any significant differences in blood samples. Although blood represents an easy-to obtain and cheap source

of biomaterial, it is composed of an heterogeneous pool of distinct cells with variable mRNA expression and, additionally, shows a high proportion of globin mRNA that might obscures the detection of transcripts expressed at low levels (Winn et al., 2011).

4.3.4 The mitochondrial network morphology is influenced by starvation stress but not by genotype

Finally, we investigated the mitochondrial morphology both in HDF and in HiPSC in basal and after nutrient deprivation stress, an assessment that can provide a picture of the mitochondrial fusion-fission events at a specific time. The deregulation of these events results in either a fragmented network characterized by a large number of small round-shape mitochondria or a hyperfused network with elongated and connected mitochondria (tubular network) (Tilokani, Nagashima, Paupe, & Prudent, 2018). Although it is still in debate which mitochondrial network form is more connected to a stress and results seems to be dependent to the line taken into exam, a balanced and dynamic transition between the two states is required for a proper mitochondrial function and response to cellular metabolic state (Wai & Langer, 2016). In our HDF lines, the application of starvation stress affected all the cell lines independently from the genotype resulting in a more fragmented mitochondrial network branching with single elements described by a more spherical shape. Although our results did not reach statistical significance, we can describe that ADHD/*PARK2* CNV duplication carrier in baseline conditions seems to show a more elongated mitochondrial shape and tubular branching compared to CNVs deletion carrier and WT. In this regard, other groups working with samples derived from PD patients with *PARK2* mutations, reported various different effects on the general mitochondrial network with both increased tubular branching (Mortiboys et al., 2009; Zanellati et al., 2015) and fragmented structure (Haylett et al., 2016). In connection with this topic, we could show an increased gene expression of *Mitofusin-2* (*Mfn2*) in all the genotypes after 24h starvation stress. *Mfn2* acts as a major regulator of mitochondrial fusion, maintenance and functionality of the mitochondrial network and is a well-known substrate of *PARK2* particularly in stress conditions (Kazlauskaite & Muqit, 2015). The mitochondrial morphology assessment on HiPSC lines confirmed the presence of a peculiar mitochondrial morphology that has been described by previous studies (Bukowiecki, Adjaye, & Prigione, 2014; Lopes & Rego, 2016) with few round-shaped mitochondria that

cluster closely to the nucleus and do not form intricate networks like in fibroblasts. We did not find genotype or treatment effects in the hiPSCs, a finding might be connected with the peculiar metabolisms of stem cells that, as described above, relies mostly on glycolysis rather than oxidative phosphorylation.

This phenotypic evaluation on HDF and hiPSC gave us insights whether alterations due to the genotype are visible already in cell types far from neurons but relatively easy to obtain and that might be used in order to clarify some patho-mechanism involved in the disease. Moreover, we could assess if alterations are already present in a pluripotent model that closely mirrors human embryonic stem cells. Most importantly these results allowed us to direct the experiments made with a model that more closely recapitulates the site of action of ADHD as a brain disease, the neurons.

4.4 EVALUATION OF NICOTINE EFFECTS ON hiPSC-DERIVED DOPAMINERGIC NEURONS FROM ADHD PATIENTS

The etiopathogenesis of both child and adult ADHD is still not fully understood. The genetic contribution to the etiology of the disorder has been estimated to be around 0.7 and 0.8 (Brikell et al., 2015; Nikolas & Burt, 2010) and therefore does not fully explain the risk for disorder. This “missing heritability” might be due to the effects of environmental factors that could either act independently or, more likely, interacting with the genetic makeup (GxE) and might explain about the 22% of ADHD variance (Faraone et al., 2005; Franke et al., 2018; Nikolas & Burt, 2010). Several studies have investigated the association of different risk factors with ADHD focusing mostly on the pre-, peri- and postnatal period and have indicated a number of substances or events that could affect the typical neurodevelopment (Banerjee et al., 2007). One of the best replicated risk factors for ADHD is smoking during pregnancy (Linnet et al., 2003; Tiesler & Heinrich, 2014). We therefore treated hiPSC-derived dopaminergic neurons with smoking-relevant nicotine concentrations mirroring “binging episodes” and “continuous consumption” (namely “acute” and “chronic” treatment)(Lomazzo et al., 2011; Srinivasan et al., 2016) focusing on gathering insights whether the presence of the

ADHD/*PARK2* CNVs genotype might convey a different susceptibility to this ADHD-risk associated factor.

To discern genotype differences specific to the nicotine treatment, we short listed genes that were significantly up- or downregulated after both nicotine acute and chronic treatment but not in baseline conditions. We found 11 genes that were differentially regulated after both nicotine treatments, two of which were involved in energy production and oxidative stress response (*C1QTNF3* and *CART*) and three with extracellular matrix and cell adhesion (*MAFAP1*, *PCDHGA6*, *COL5A1*).

As already mentioned, dysregulation of the energy production and oxidative stress response has been suggested play a role in the molecular pathomechanisms of ADHD (Guney et al., 2015; Joseph et al., 2015) and both biological processes are believed to be connected with *PARK2* function (Imaizumi et al., 2012b; Zanellati et al., 2015). ADHD/*PARK2* CNVs carriers showed a strong down-regulation of *CART*, a gene also involved in energy production and oxidative stress response. Cocaine- and amphetamine-regulated transcript (*CART*) peptides are believed to act both as an antioxidant hormone and as a neurotransmitter and influence diverse biological processes, including food intake, reward and addiction and stress response (Lau & Herzog, 2014). It has been demonstrated that *CART* protects the mtDNA, cellular proteins and lipids against oxidation and localize to mitochondria in cultured cells and mouse brain neuronal cells (Mao, Meshul, Thuillier, Goldberg, & Reddy, 2012). This effects are thought to be due to the interaction between *CART* and the subunit B of the mitochondrial enzyme succinate dehydrogenase (*SDHB*) that participates in two pivotal pathways in energy conversion: the citric acid cycle (or Krebs cycle) and oxidative phosphorylation (Mao et al., 2007). Low levels of *CART* gene expression in ADHD/*PARK2* CNVs carriers after nicotine exposure might suggest an increased susceptibility on an energetic level to this natural alkaloid compared to WT. Interesting, our data show a strong upregulation of *C1QTNF3* in ADHD/*PARK2* CNVs carriers compared to control after nicotine exposure. *C1QTNF3* (also known as *CTRP3*) has been demonstrated to play an important role in promoting mitochondrial energy production, mitochondrial biogenesis (C.-L. Zhang et al., 2017) and decreased oxidative stress by increasing *PKA* and decreasing *NOX-2* expression (Yang et al., 2017). Therefore, this result might suggest the presence of coexistent compensatory

mechanisms that increase the mitochondrial biogenesis, and therefore energy production, and simultaneously decreases the overall oxidative stress levels.

These results might provide further evidence of a bidirectional link both between ADHD and oxidative impairment and between the presence of *PARK2* CNVs and energy dysregulation.

The same short-listing analysis of genes differentially regulated after both nicotine treatments showed a differential regulation between ADHD/*PARK2* CNVs carriers and WT in three genes connected with extracellular matrix and cell adhesion (*MAFAP1*, *PCDHGA6*, *COL5A1*). Neuronal maturation and formation of proper neural connections and functional synapsis is orchestrated by a complex interplay between extracellular matrix glycoproteins and cell-adhesion molecules (Washbourne et al., 2004). Extracellular matrix (ECM) glycoproteins such as laminins, proteoglycans, tenascins, reelin, collagens are widely expressed in the developing and adult nervous system and provide a microenvironment that modulates neuron migration, axon formation, myelination and synaptogenesis (Barros, Franco, & Müller, 2011). ADHD/*PARK2* CNVs carriers show an upregulation of *MAFAP1* and *COL5A1* after nicotine exposure that might imply a deregulation of this microenvironment. Interestingly, the risk variant carriers also show lower expression levels of a member of the protocadherin family of cell-adhesion molecules, *PCDHGA6*. This is a member of the protocadherin gamma gene cluster, neural cadherin-like cell adhesion proteins that play a critical role in the establishment and function of specific cell-cell connections in the brain (Yagi & Takeichi, 2000) (Mountoufaris, Canzio, Nwakeze, Chen, & Maniatis, 2018). Specifically, protocadherins are involved in neural circuit assembly in regard of neurite self-avoidance and in neuronal tiling (Fan et al., 2018) and have been shown to regulate cortical neuron migration and cytoskeletal dynamics via Rac1 GTPase and WAVE complex in mice (Lu et al., 2018). It needs to be pointed out that an involvement of the protocadherin family has been suggested for various psychiatric disorders such as schizophrenia, bipolar disorder and autism spectrum disorder (Anitha et al., 2013; Ishizuka et al., 2016; Kalmady & Venkatasubramanian, 2009; Lachman et al., 2008).

It has been proven that addictive substances, such as nicotine, affects the proliferation, migration differentiation and survival of neural progenitors cells in different manners, resulting in modification of neurogenesis and circuit formation (Xu, Loh, & Law, 2016). Our analysis of differentially expressed genes (DEGs) between ADHD/*PARK2* CNVs carrier with the

wild type controls shows that there was a significant enrichment in GO that falls under the biological processes “regulation of growth”, “regulation of cell growth”, “cell growth”, “growth” after nicotine acute treatment. A deregulation of neuronal maturation and formation of proper neural connections at early developmental stages might have strong consequences and different works have underlined an abnormal brain connectivity in ADHD patients (Gehricke et al., 2017).

Taking advantage of HiPSC-derived dopaminergic neurons, a cellular model that closely mirrors the anatomical region connected with the disease, we showed preliminary evidences of patho-phenotypic characteristics connected with ADHD/*PARK2* CNVs genotype. Although further analysis are required, we could narrow down processes that might underline a different susceptibility of ADHD/*PARK2* CNV carriers to nicotine exposure.

4.5 LIMITATIONS OF THE STUDY AND FUTURE PERSPECTIVES

Although the models presented in this study are one of the few available cellular models for studying ADHD, we have to point out that the genetic variation object of the study, *PARK2* CNVs, represents a rare variation found just in a small subset of ADHD patients. Nevertheless, studying such rare variations can contribute in understanding the etiopathogenesis of the disease.

Furthermore, the scarce presence of evidences both of ADHD cellular models and of the connections between ADHD and *PARK2* CNVs variants, forced our study to be general and hypothesis oriented. In this manner we might have missed additional altered pathways and introduced a bias into the study.

Additionally, given on one hand that the *PARK2* CNVs associated with ADHD are rare genetic variants and therefore the biomaterial to start is scarce, and on the other hand that HiPSC technology and the generation of HiPSC-induced dopaminergic neurons has a great economic cost, these types of study rely on the generations of just few cellular lines. In the future we aim to increase the number of lines used in the study and therefore strengthen our results. Moreover, the creation of isogenic control lines, where the same cells are genetically

engineered, will provide additional information of the specific effect of CNV deletion and duplication in lines genetically matched with the ones investigated in this study.

HiPSC technology is still in development and a great variability of protocols is reported in the literature. Moreover, at the current state of the art, it is extremely hard to assess with which human embryonal developmental stage the HiPSC-derived neurons correspond. Therefore, although in our study we decided to test the effect of nicotine at two maturation points, it is difficult to state if the immature point represents early stages of *in vivo* neural maturation or not. Additionally, the study of molecules that act directly in the brain is complicated by the fact that it is not possible to have accurate data on the exact molecule concentration that reaches the human brain. Nicotine concentrations have been mostly measured in human peripheral blood, or in animal models and has been shown to be dependent on the route of administration (Benowitz, Hukkanen, Jacob, & III, 2009) and therefore the estimation of nicotine that reaches the brain might not exactly mirror the ones in the humans.

Finally, our results on the HiPSC-derived neurons need to be further investigated both by validating the results of the RNA sequencing and replicating the significant differences underlined by the experiments performed on HDF and HiPSC. This will lead us to a better understanding of the patho-phenotype of these cells and could be used to draw and test a possible therapeutic approach.

5 CONCLUSIONS

This study presents novel and fully validated cellular model systems to study the etiopathogenesis of ADHD. In the future, HiPSC of this cell model could be used to generate a plethora of different cell types whom investigation could lead to novel insight in the understanding of specific aspects of the disorder.

Additionally, this study provides an initial phenotyping with regard to the effects of *PARK2* CNVs in ADHD derived samples and will help to direction future experiments. Our work suggests that ADHD *PARK2* CNV carriers display a differential gene regulation, *PARK2* protein content and energy impairment. The energy impairment could be connected with the role of *PARK2* in diverse mitochondrial dynamics. The impairment at some level of the function of mitochondria could lead to the disruption of normal brain plasticity and cellular resilience. Additionally, our preliminary investigation of the effects of a well-known risk factor for ADHD, nicotine gestational exposure, point out a susceptibility of the *PARK2* CNVs carriers in processes involved in regulation of cell growth and in proteins connected with extracellular matrix composition and cell-adhesion molecules necessary for the formation of correct neural circuits. This hypothesis fits well with the neurodevelopmental origin of the disorder and might strengthens the idea of gene-environment-interaction playing a crucial role in ADHD.

6 APPENDIX

6.1 LIST OF ANTIBODIES USED IN THIS STUDY

Table 12: *List of antibodies used in this study*

	Antibody	Dilution	Company Cat # and RRID
Primary Antibodies			
Pluripotency markers (HiPSC)	Rabbit anti-OCT4	1:500	Thermo Fisher Scientific Cat# 710788, RRID: AB_2633097
	Mouse anti-SSEA4	1:200	Thermo Fisher Scientific Cat# MA1-021 RRID: AB_2536687
	Mouse anti-TRA-1-60	1:100	Novus Cat# NB100-730 RRID:AB_10001809
Three embryonic germ layers differentiation markers	Rabbit anti-TUJ1	1:700	Thermo Fisher Scientific Cat# A25532 RRID:AB_2651003
	Mouse anti-AFP	1:700	Thermo Fisher Scientific Cat# A25530 RRID:AB_2651004
	Mouse anti-SMA	1:200	Thermo Fisher Scientific Cat# A25531 RRID:AB_2651005
iPS-derived dopaminergic Neurons	Rabbit anti-TUBB3	1:100	Covance Research Products Inc Cat# PRB-435P-100 RRID:AB_291637
	Mouse anti-TH	1:500	Proteintech Cat# 66334-1-Ig CloneNo.: 2H7B7
Secondary antibodies			
	Alexa Fluor 594 donkey anti-rabbit	1:250	Thermo Fisher Scientific Cat# R37119, RRID:AB_2556547
	Alexa Fluor 488 goat anti-mouse IgG3	1:250	Thermo Fisher Scientific Cat# A-21151, RRID:AB_2535784
	Alexa Fluor 488 Goat anti-mouse IgM	1:250	Thermo Fisher Scientific Cat# A-21042, RRID:AB_2535711

	Alexa Fluor 488 goat anti-mouse IgG1	1:250	Thermo Fisher Scientific Cat# A25536, RRID:AB_2651011
	Alexa Fluor 555 goat anti-mouse IgG2a	1:250	Thermo Fisher Scientific Cat# A25533, RRID:AB_2651012
	Alexa Fluor 647 donkey anti-rabbit	1:250	Thermo Fisher Scientific Cat# A25535, RRID:AB_2651010
Direct staining			
	MitoTracker Red CMXRos	400 nM	Thermo Fisher Scientific Cat# M7512
	NucBlue Fixed Cell ReadyProbes Reagent	80 μl/ml	Thermo Fisher Scientific Cat# R37606
Live staining			
	Alkaline Phosphatase Live Stain	2 μl/ml	Thermo Fisher Scientific Cat#

6.2 LIST OF PRIMERS USED IN THIS STUDY

Table 13: List of Primers used in this study

Two steps Reverse Transcription PCR (RT-PCR)			
Pluripotency evaluation	hSOX2	AACCAGCGCATGGACAGTTA	GACTTGACCACCGAACCCAT
	hNANOG	ACCAGTCCCAAAGGCAAACA	AAAGGCTGGGGTAGGTAGGT
	hPOU5F1	GTTGATCCTCGGACCTGGCTA	GGTTGCCTCTCACTCGGTTCT
	hDPPA5	CGGCTGCTGAAAGCCATTTT	AGTTTGAGCATCCCTCGCTC
	hGAPDH	ATCACCATCTCCAGGAGCGA	AAGTGGTCGTTGAGGGCAAT
Viral vector (SeV) detection	SeV	GGATCACTAGGTGATATCGAGC	ACCAGACAAGAGTTTAAGAGATA TGTATC
	c-Myc	TAAGTACTGACTAGCAGGCTTGTCG	TCCACATACAGTCTGGATGATGATG
Quantitative RT-PCR (RT-qPCR)			
Reference genes	Hs_HPRT1	TGCTTTCTTGGTCAGGCAGT	TCCAACACTTCGTGGGGTCC
	Hs_SDHA	AACATCGGAACTGCGACTC	CTTCTTGAACACGCTTCCC
	Hs_ALAS1	CGGGATGGAGTCATGCCAAA	ATCAGAGAACTCGTGCTGGC
	Hs_TBP	GAGTTCAGCGCAAGGGTTT	GGGGTCAGTCCAGTGCCATA
Dopaminergic neuron markers	Hs_LMX1B	GTGTGTGAACGGCAGCTACG	CCGGCTTCATGTCCCATCT
	Hs_EN1	TCGACGAGCCTCTCGTATG	CCTGGAACCTCCGCTTGAGT
	Hs_POU5F1	CTTGCTGCAGAAGTGGGTGGAGGAA	CTGCAGTGTGGGTTTCGGGCA
	Hs_NEUROD1	GGAGGCCCCAGGGTTATGAG	GCCCACTCTCGCTGTACGAT
Hypothesis driven gene expression	Hs_RBFOX3	TACGACGCTACAGATACGCTC	TGTTCCAATGCTGTAGGTCGC
	Hs_ATG5	GCAACTCTGGATGGGATTGCAAAA	GCAGCCACAGGACGAAACAG
	Hs_MFN2	GTGACGCGCTTATCCAATTCC	TGTGTTGACTCCACCAGTCTC
	Hs_TP53	GACGGTGACACGCTTCCCT	GCTAGGATCTGACTGCGGCT
	Hs_NFE2L2	ATGCAGCTTTTGCGCAGAC	AGTGACTGAAACGTAGCCGAAG
	Hs_NQO1	AACCACGAGCCCAGCCAAT	TGGCATAGAGGTCCGACTCC
	Hs_PINK1	CCATCTGGTTCAACAGGGCA	AAATCTGCGATCACCAGCCA
	Hs_UBE3A	CGGTGGCTATACCAGGGACT	CTCTGTCTGTGCCGTTGTA
	Hs_UBB	GGAGCATTTAGGGGCGGTTG	ATCACCAACCACGTCCACCC
	Hs_UBC	CACAGCTAGTTCCGTCGACG	TCACGAAGATCTGCATTGTCAAG
Hs_ATXN3	GGAGTCCATCTTCCACGAGAA	TCATCCTCTCCTCCTCATCCA	
TaqMann gene expression assay	Hs_PARK2	Hs01038322	ThermoFisher Scientific
	Hs_POLR2A	Hs00172182	ThermoFisher Scientific
	Hs_YWHAZ	Hs03044281	ThermoFisher Scientific
	Hs_B2M	Hs00984230	ThermoFisher Scientific
	SDHA	Hs00188166	ThermoFisher Scientific

6.3 LIST OF ABBREVIATIONS

aADHD= adult Attention-Deficit/Hyperactivity Disorder

ADHD= Attention-Deficit/Hyperactivity Disorder

ASD= Autism Spectrum Disorder

cADHD= childhood Attention-Deficit/Hyperactivity Disorder

CCCP= Carbonyl cyanide m-chlorophenyl hydrazine

CD= Conduct Disorder

CDCV= common disease common variant

CDRV= common disease rare variant

CGH= comparative genomic hybridization

CNVs= Copy Number Variants

DA= Dopamine

DEGs= Differentially Expressed Genes

DSM= Diagnostic and Statistical Manual for Mental Disorders

EBs= Embryoid Bodies

ECM= Extracellular matrix

ER-M= endoplasmic reticulum-mitochondria interface

FPKM= Expected Number of Fragments Per Kilobase Of Transcript Sequence Per Million Base Pairs Sequenced

GWAS= genome-wide association study

GxE= gene-environment-interactions

HDF= Human Dermal Fibroblast

hESCs= Human Embryonic Stem Cells

hiPSC= Human Induced Pluripotent Stem Cells

ICD= International Classification of Diseases

MEF= Mouse Embryonic Fibroblasts

MPH= Methylphenidate

MQC= Mitochondria Quality Control

NE= noradrenaline

NI= Neural Induction

OCR= oxygen consumption rate

ODD= Oppositional Defiant Disorder

OMM= outer mitochondrial membrane

PD= Parkinson's disease

RFU= Relative Fluorescence Units

RLU= Relative Luminescence Units

RNAi= RNA interference

RNS= reactive nitrogen species

ROS= reactive oxygen species

siRNA= small interfering RNA

SNPs= Single Nucleotide Polymorphisms

SUD=Substance Use Disorder

TBI= Traumatic Brain Injury

UPR= Unfolded Protein Response

UPS= Ubiquitin Proteasome System

WHO= World Health Organization

7 BIBLIOGRAPHY

- Adegbola, A., Bury, L. A., Fu, C., Zhang, M., & Wynshaw-Boris, A. (2017). Concise Review: Induced Pluripotent Stem Cell Models for Neuropsychiatric Diseases. *Stem Cells Translational Medicine*, 6(12), 2062–2070. <https://doi.org/10.1002/sctm.17-0150>
- Aigner, S., Heckel, T., Zhang, J. D., Andreae, L. C., & Jagasia, R. (2014). Human pluripotent stem cell models of autism spectrum disorder: Emerging frontiers, opportunities, and challenges towards neuronal networks in a dish. *Psychopharmacology*, 231(6), 1089–1104. <https://doi.org/10.1007/s00213-013-3332-1>
- Altman, B. J., & Rathmell, J. C. (2012). Metabolic stress in autophagy and cell death pathways. *Cold Spring Harbor Perspectives in Biology*, 4(9), 1–16. <https://doi.org/10.1101/cshperspect.a008763>
- American Psychiatric Association. (2013). Diagnostic and Statistical Manual of Mental Disorders. 5th ed. *American Psychiatric Publishing; Arlington, VA, USA*.
- Anitha, A., Nakamura, K., Thanseem, I., Matsuzaki, H., Miyachi, T., Tsujii, M., ... Mori, N. (2013). Downregulation of the Expression of Mitochondrial Electron Transport Complex Genes in Autism Brains. *Brain Pathology*, 23(3), 294–302. <https://doi.org/10.1111/bpa.12002>
- Arcos-Burgos, M., Jain, M., Acosta, M. T., Shively, S., Stanescu, H., Wallis, D., ... Muenke, M. (2010). A common variant of the latrophilin 3 gene, LPHN3, confers susceptibility to ADHD and predicts effectiveness of stimulant medication. *Molecular Psychiatry*, 15(11), 1053–1066. <https://doi.org/10.1038/mp.2010.6>
- Asakawa, S., Tsunematsu, K., Takayanagi, A., Sasaki, T., Shimizu, A., Shintani, A., ... Shimizu, N. (2001). The Genomic Structure and Promoter Region of the Human Parkin Gene. *Biochemical and Biophysical Research Communications*, 286(5), 863–868. <https://doi.org/10.1006/bbrc.2001.5490>
- Ashrafi, G., Schlehe, J. S., LaVoie, M. J., & Schwarz, T. L. (2014). Mitophagy of damaged mitochondria occurs locally in distal neuronal axons and requires PINK1 and Parkin. *The Journal of Cell Biology*, 206(5), 655–670. <https://doi.org/10.1083/jcb.201401070>
- Auburger, G., Klinkenberg, M., Drost, J., Marcus, K., Morales-Gordo, B., Kunz, W. S., ... Jendrach, M. (2012). Primary skin fibroblasts as a model of Parkinson's disease. *Molecular Neurobiology*, 46(1), 20–27. <https://doi.org/10.1007/s12035-012-8245-1>
- Banerjee, T., Das, Middleton, F., & Faraone, S. V. (2007). Environmental risk factors for attention-deficit hyperactivity disorder. *Acta Paediatrica*, 96(9), 1269–1274. <https://doi.org/10.1111/j.1651-2227.2007.00430.x>
- Barkley, R. A., Murphy, K. R., Dupaul, G. I., & Bush, T. (2002). Driving in young adults with attention deficit hyperactivity disorder: knowledge, performance, adverse outcomes, and the role of executive functioning. *Journal of the International Neuropsychological Society : JINS*, 8(5), 655–672. Retrieved from <http://www.ncbi.nlm.nih.gov/pubmed/12164675>
- Barros, C. S., Franco, S. J., & Müller, U. (2011). Extracellular matrix: functions in the nervous system. *Cold Spring Harbor Perspectives in Biology*, 3(1), a005108. <https://doi.org/10.1101/cshperspect.a005108>
- Beaulieu, J.-M., & Gainetdinov, R. R. (2011). The physiology, signaling, and pharmacology of dopamine receptors. *Pharmacological Reviews*, 63(1), 182–217. <https://doi.org/10.1124/pr.110.002642>
- Benowitz, N. L., Hukkanen, J., Jacob, P., & III. (2009). Nicotine chemistry, metabolism, kinetics and biomarkers. *Handbook of Experimental Pharmacology*, (192), 29–60. https://doi.org/10.1007/978-3-540-69248-5_2
- Biederman, J., Faraone, S. V., Spencer, T. J., Mick, E., Monuteaux, M. C., & Alvardi, M. (2006). *The Journal of clinical psychiatry. The Journal of Clinical Psychiatry* (Vol. 67). [Physicians Postgraduate Press]. Retrieved from <https://www.psychiatrist.com/JCP/article/Pages/2006/v67n04/v67n0403.aspx>
- Bloch, M. H., & Qawasmi, A. (2011). Omega-3 Fatty Acid Supplementation for the Treatment of Children With Attention-Deficit/Hyperactivity Disorder Symptomatology: Systematic Review and Meta-Analysis. *Journal of the American Academy of Child & Adolescent Psychiatry*, 50(10), 991–1000. <https://doi.org/10.1016/j.jaac.2011.06.008>
- Bonvicini, C., Faraone, S. V., & Scassellati, C. (2016). Attention-deficit hyperactivity disorder in adults: A systematic review and meta-analysis of genetic, pharmacogenetic and biochemical studies. *Molecular Psychiatry*, 21(7), 872–884.

<https://doi.org/10.1038/mp.2016.74>

- Boonstra, A. M., Oosterlaan, J., Sergeant, J. A., & Buitelaar, J. K. (2005). Executive functioning in adult ADHD: a meta-analytic review. *Psychological Medicine, 35*(8), 1097–1108. Retrieved from <http://www.ncbi.nlm.nih.gov/pubmed/16116936>
- Brikell, I., Kuja-Halkola, R., & Larsson, H. (2015). Heritability of attention-deficit hyperactivity disorder in adults. *American Journal of Medical Genetics Part B: Neuropsychiatric Genetics, 168*(6), 406–413. <https://doi.org/10.1002/ajmg.b.32335>
- Brüggemann, N., & Klein, C. (1993). *Parkin Type of Early-Onset Parkinson Disease*. GeneReviews®. University of Washington, Seattle. Retrieved from <http://www.ncbi.nlm.nih.gov/pubmed/20301651>
- Bublitz, M. H., & Stroud, L. R. (2012). Maternal smoking during pregnancy and offspring brain structure and function: review and agenda for future research. *Nicotine & Tobacco Research : Official Journal of the Society for Research on Nicotine and Tobacco, 14*(4), 388–397. <https://doi.org/10.1093/ntr/ntr191>
- Buchmann, A. F., Schmid, B., Blomeyer, D., Becker, K., Treutlein, J., Zimmermann, U. S., ... Laucht, M. (2009). Impact of age at first drink on vulnerability to alcohol-related problems: Testing the marker hypothesis in a prospective study of young adults. *Journal of Psychiatric Research, 43*(15), 1205–1212. <https://doi.org/10.1016/J.JPSYCHIRES.2009.02.006>
- Bukowiecki, R., Adjaye, J., & Prigione, A. (2014). Mitochondrial function in pluripotent stem cells and cellular reprogramming. *Gerontology, 60*(2), 174–182. <https://doi.org/10.1159/000355050>
- Carvalho, C., Crespo, M. V., Bastos, L. F., Knight, A., & Vicente, L. (2016). Contribution of Animal models to contemporary understanding of Attention Deficit Hyperactivity Disorder. *Altex, 33*(3), 243–249. <https://doi.org/10.14573/altex.1507311>
- Castells, X., Blanco-Silvente, L., & Cunill, R. (2018). Amphetamines for attention deficit hyperactivity disorder (ADHD) in adults. *Cochrane Database of Systematic Reviews, 8*, CD007813. <https://doi.org/10.1002/14651858.CD007813.pub3>
- Caye, A., Spadini, A. V., Karam, R. G., Grevet, E. H., Rovaris, D. L., Bau, C. H. D., ... Kieling, C. (2016). Predictors of persistence of ADHD into adulthood: a systematic review of the literature and meta-analysis. *European Child & Adolescent Psychiatry, 25*(11), 1151–1159. <https://doi.org/10.1007/s00787-016-0831-8>
- Chambers, S. M., Fasano, C. A., Papapetrou, E. P., Tomishima, M., Sadelain, M., & Studer, L. (2009). Highly efficient neural conversion of human ES and iPS cells by dual inhibition of SMAD signaling. *Nature Biotechnology, 27*(3), 275–280. <https://doi.org/10.1038/nbt.1529>
- Chan, E. M., Ratanasirinawoot, S., Park, I.-H., Manos, P. D., Loh, Y.-H., Huo, H., ... Schlaeger, T. M. (2009). Live cell imaging distinguishes bona fide human iPS cells from partially reprogrammed cells. *Nature Biotechnology, 27*(11), 1033–1037. <https://doi.org/10.1038/nbt.1580>
- Chang, K. H., Lee-Chen, G. J., Wu, Y. R., Chen, Y. J., Lin, J. L., Li, M., ... Chen, C. M. (2016). Impairment of proteasome and anti-oxidative pathways in the induced pluripotent stem cell model for sporadic Parkinson's disease. *Parkinsonism Relat Disord, 24*, 81–88. <https://doi.org/10.1016/j.parkreldis.2016.01.001>
- Chang, Z., Lichtenstein, P., D'Onofrio, B. M., Sjölander, A., & Larsson, H. (2014). Serious Transport Accidents in Adults With Attention-Deficit/Hyperactivity Disorder and the Effect of Medication. *JAMA Psychiatry, 71*(3), 319. <https://doi.org/10.1001/jamapsychiatry.2013.4174>
- Charach, A., Yeung, E., Climans, T., & Lillie, E. (2011). Childhood Attention-Deficit/Hyperactivity Disorder and Future Substance Use Disorders: Comparative Meta-Analyses. *Journal of the American Academy of Child & Adolescent Psychiatry, 50*(1), 9–21. <https://doi.org/10.1016/J.JAAC.2010.09.019>
- Christiansen, H., Kis, B., Hirsch, O., Matthies, S., Hebebrand, J., Uekermann, J., ... Philipsen, A. (2012). German validation of the Conners Adult ADHD Rating Scales (CAARS) II: Reliability, validity, diagnostic sensitivity and specificity. *European Psychiatry, 27*(5), 321–328. <https://doi.org/10.1016/j.eurpsy.2010.12.010>
- da Costa, C. A., Sunyach, C., Giaime, E., West, A., Corti, O., Brice, A., ... Checler, F. (2009). Transcriptional repression of p53 by parkin and impairment by mutations associated with autosomal recessive juvenile Parkinson's disease. *Nature Cell Biology, 11*(11), 1370–1375. <https://doi.org/10.1038/ncb1981>
- Dalla Vecchia, E., Mortimer, N., Palladino, V. S., Kittel-Schneider, S., Lesch, K.-P., Reif, A., ... Norton, W. H. J. (2018). Cross-species models of attention-deficit/hyperactivity disorder and autism spectrum disorder: lessons from CNTNAP2, ADGRL3, and PARK2 Correspondence to. <https://doi.org/10.1097/YPG.0000000000000211>
- Dalsgaard, S., Ostergaard, S. D., Leckman, J. F., Mortensen, P. B., & Pedersen, M. G. (2015). Mortality in children, adolescents, and adults with attention deficit hyperactivity disorder: A nationwide cohort study. *The Lancet, 385*(9983), 2190–2196. [https://doi.org/10.1016/S0140-6736\(14\)61684-6](https://doi.org/10.1016/S0140-6736(14)61684-6)

- de la Peña, J. B., dela Peña, I. J., Custodio, R. J., Botanas, C. J., Kim, H. J., & Cheong, J. H. (2017). Exploring the Validity of Proposed Transgenic Animal Models of Attention-Deficit Hyperactivity Disorder (ADHD). *Molecular Neurobiology*, 55(5), 3739–3754. <https://doi.org/10.1007/s12035-017-0608-1>
- Demontis, D., Walters, R. K., Martin, J., Mattheisen, M., Als, T. D., Agerbo, E., ... Neale, B. M. (2017). Discovery Of The First Genome-Wide Significant Risk Loci For ADHD. *BioRxiv*, 145581. <https://doi.org/10.1101/145581>
- DiFranza, J. R., Aligne, C. A., & Weitzman, M. (2004). Prenatal and postnatal environmental tobacco smoke exposure and children's health. *Pediatrics*, 113(4 Suppl), 1007–1015. Retrieved from <http://www.ncbi.nlm.nih.gov/pubmed/15060193>
- Du Rietz, E., Coleman, J., Glanville, K., Choi, S. W., O'Reilly, P. F., & Kuntsi, J. (2018). Association of Polygenic Risk for Attention-Deficit/Hyperactivity Disorder With Co-occurring Traits and Disorders. *Biological Psychiatry: Cognitive Neuroscience and Neuroimaging*, 3(7), 635–643. <https://doi.org/10.1016/j.bpsc.2017.11.013>
- Elia, J., Gai, X., Xie, H. M., Perin, J. C., Geiger, E., Glessner, J. T., ... White, P. S. (2010). Rare structural variants found in attention-deficit hyperactivity disorder are preferentially associated with neurodevelopmental genes. *Molecular Psychiatry*, 15(6), 637–646. <https://doi.org/10.1038/mp.2009.57>
- Fagundes, A. O., Scaini, G., Santos, P. M., Sachet, M. U., Bernhardt, N. M., Rezin, G. T., ... Streck, E. L. (2010). Inhibition of mitochondrial respiratory chain in the brain of adult rats after acute and chronic administration of methylphenidate. *Neurochemical Research*, 35(3), 405–411. <https://doi.org/10.1007/s11064-009-0069-7>
- Fan, L., Lu, Y., Shen, X., Shao, H., Suo, L., & Wu, Q. (2018). Alpha protocadherins and Pyk2 kinase regulate cortical neuron migration and cytoskeletal dynamics via Rac1 GTPase and WAVE complex in mice. *ELife*, 7. <https://doi.org/10.7554/eLife.35242>
- Faraone, S. V. (2018). The pharmacology of amphetamine and methylphenidate: Relevance to the neurobiology of attention-deficit/hyperactivity disorder and other psychiatric comorbidities. *Neuroscience and Biobehavioral Reviews*, 87(January), 255–270. <https://doi.org/10.1016/j.neubiorev.2018.02.001>
- Faraone, S. V., & Biederman, J. (2016). Can Attention-Deficit/Hyperactivity Disorder Onset Occur in Adulthood? *JAMA Psychiatry*, 73(7), 655. <https://doi.org/10.1001/jamapsychiatry.2016.0400>
- Faraone, S. V., Biederman, J., & Mick, E. (2006, May 3). The age-dependent decline of attention deficit hyperactivity disorder: A meta-analysis of follow-up studies. *Psychological Medicine*. <https://doi.org/10.1017/S003329170500471X>
- Faraone, S. V., & Mick, E. (2010). Molecular Genetics of Attention Deficit Hyperactivity Disorder. *Psychiatric Clinics of North America*, 33(1), 159–180. <https://doi.org/10.1016/j.psc.2009.12.004>
- Faraone, S. V., Perlis, R. H., Doyle, A. E., Smoller, J. W., Goralnick, J. J., Holmgren, M. A., & Sklar, P. (2005). Molecular genetics of attention-deficit/hyperactivity disorder. *Biological Psychiatry*, 57(11), 1313–1323. <https://doi.org/10.1016/j.biopsych.2004.11.024>
- Fayyad, J., De Graaf, R., Kessler, R., Alonso, J., Angermeyer, M., Demyttenaere, K., ... Jin, R. (2007). Cross-national prevalence and correlates of adult attention-deficit hyperactivity disorder. *British Journal of Psychiatry*, 190(05), 402–409. <https://doi.org/10.1192/bjp.bp.106.034389>
- Ficks, C. A., & Waldman, I. D. (2009). Gene-environment interactions in attention-deficit/hyperactivity disorder. *Current Psychiatry Reports*, 11(5), 387–392. Retrieved from <http://www.ncbi.nlm.nih.gov/pubmed/19785980>
- Flaherty, E. K., & Brennand, K. J. (2017). Using hiPSCs to model neuropsychiatric copy number variations (CNVs) has potential to reveal underlying disease mechanisms. *Brain Research*, 1655, 283–293. <https://doi.org/10.1016/j.brainres.2015.11.009>
- Franx, W., Oldehinkel, M., Oosterlaan, J., Heslenfeld, D., Hartman, C. A., Hoekstra, P. J., ... Mennes, M. (2015). The executive control network and symptomatic improvement in attention-deficit/hyperactivity disorder. *Cortex*, 73, 62–72. <https://doi.org/10.1016/J.CORTEX.2015.08.012>
- Franke, B., Michelini, G., Asherson, P., Banaschewski, T., Bilbow, A., Buitelaar, J. K., ... Reif, A. (2018). Live fast, die young? A review on the developmental trajectories of ADHD across the lifespan. *European Neuropsychopharmacology*. <https://doi.org/10.1016/J.EURONEURO.2018.08.001>
- Galéra, C., Melchior, M., Chastang, J.-F., Bouvard, M.-P., & Fombonne, E. (2009). Childhood and adolescent hyperactivity-inattention symptoms and academic achievement 8 years later: the GAZEL Youth study. *Psychological Medicine*, 39(11), 1895. <https://doi.org/10.1017/S0033291709005510>
- García-Martínez, I., Sánchez-Mora, C., Pagerols, M., Richarte, V., Corrales, M., Fadeuilhe, C., ... Ribasés, M. (2016). Preliminary evidence for association of genetic variants in pri-miR-34b/c and abnormal miR-34c expression with

- attention deficit and hyperactivity disorder. *Translational Psychiatry*, 6(8), e879. <https://doi.org/10.1038/tp.2016.151>
- Garcia, R. J., Francis, L., Dawood, M., Lai, Z.-W., Faraone, S. V., & Perl, A. (2013). Attention deficit and hyperactivity disorder scores are elevated and respond to N-acetylcysteine treatment in patients with systemic lupus erythematosus. *Arthritis and Rheumatism*, 65(5), 1313–1318. <https://doi.org/10.1002/art.37893>
- Gautier, C. A., Erpapazoglou, Z., Mouton-Liger, F., Muriel, M. P., Cormier, F., Bigou, S., ... Corti, O. (2016). The endoplasmic reticulum-mitochondria interface is perturbed in PARK2 knockout mice and patients with PARK2 mutations. *Human Molecular Genetics*, 0(0), 1–13. <https://doi.org/10.1093/hmg/ddw148>
- Gehricke, J.-G., Kruggel, F., Thampipop, T., Alejo, S. D., Tatos, E., Fallon, J., & Muftuler, L. T. (2017). The brain anatomy of attention-deficit/hyperactivity disorder in young adults - a magnetic resonance imaging study. *PLoS One*, 12(4), e0175433. <https://doi.org/10.1371/journal.pone.0175433>
- Ghirardi, L., Brikell, I., Kuja-Halkola, R., Freitag, C. M., Franke, B., Asherson, P., ... Larsson, H. (2018). The familial co-aggregation of ASD and ADHD: a register-based cohort study. *Molecular Psychiatry*, 23(2), 257–262. <https://doi.org/10.1038/mp.2017.17>
- Giulivi, C., Zhang, Y.-F., Omanska-Klusek, A., Ross-Inta, C., Wong, S., Hertz-Picciotto, I., ... Pessah, I. N. (2010). Mitochondrial Dysfunction in Autism. *JAMA*, 304(21), 2389. <https://doi.org/10.1001/jama.2010.1706>
- Goldberg, M. S., Fleming, S. M., Palacino, J. J., Cepeda, C., Lam, H. A., Bhatnagar, A., ... Shen, J. (2003). Parkin-deficient Mice Exhibit Nigrostriatal Deficits but not Loss of Dopaminergic Neurons. *Journal of Biological Chemistry*, 278(44), 43628–43635. <https://doi.org/10.1074/jbc.M308947200>
- Greene, A. W., Grenier, K., Aguilera, M. A., Muise, S., Farazifard, R., Haque, M. E., ... Fon, E. A. (2012). Mitochondrial processing peptidase regulates PINK1 processing, import and Parkin recruitment. *EMBO Reports*, 13(4), 378–385. <https://doi.org/10.1038/embor.2012.14>
- Guney, E., Cetin, F. H., Alisik, M., Tunca, H., Tas Torun, Y., Iseri, E., ... Erel, O. (2015). Attention Deficit Hyperactivity Disorder and oxidative stress: A short term follow up study. *Psychiatry Research*, 229(1–2), 310–317. <https://doi.org/10.1016/j.psychres.2015.07.003>
- Guyatt, A. L., Stergiakouli, E., Martin, J., Walters, J., O'Donovan, M., Owen, M., ... Gaunt, T. R. (2018). Association of copy number variation across the genome with neuropsychiatric traits in the general population. *American Journal of Medical Genetics. Part B, Neuropsychiatric Genetics: The Official Publication of the International Society of Psychiatric Genetics*, 177(5), 489–502. <https://doi.org/10.1002/ajmg.b.32637>
- Halmøy, A., Klungsoyr, K., Skjærven, R., & Haavik, J. (2012). Pre- and Perinatal Risk Factors in Adults with Attention-Deficit/Hyperactivity Disorder. *Biological Psychiatry*, 71(5), 474–481. <https://doi.org/10.1016/j.biopsych.2011.11.013>
- Hamshere, M. L., Langley, K., Martin, J., Agha, S. S., Stergiakouli, E., Anney, R. J. L., ... Thapar, A. (2013). High Loading of Polygenic Risk for ADHD in Children With Comorbid Aggression. *American Journal of Psychiatry*, 170(8), 909–916. <https://doi.org/10.1176/appi.ajp.2013.12081129>
- Hang, L., Thundiyil, J., & Lim, K. L. (2015). Mitochondrial dysfunction and Parkinson disease: a Parkin-AMPK alliance in neuroprotection. *Annals of the New York Academy of Sciences*, 1350, 37–47. <https://doi.org/10.1111/nyas.12820>
- Hänzelmann, S., Beier, F., Gusmao, E. G., Koch, C. M., Hummel, S., Charapitsa, I., ... Wagner, W. (2015). Replicative senescence is associated with nuclear reorganization and with DNA methylation at specific transcription factor binding sites. *Clinical Epigenetics*, 7(1), 19. <https://doi.org/10.1186/s13148-015-0057-5>
- Hartman, C. A., Geurts, H. M., Franke, B., Buitelaar, J. K., & Rommelse, N. N. J. (2016). Changing ASD-ADHD symptom co-occurrence across the lifespan with adolescence as crucial time window: Illustrating the need to go beyond childhood. *Neuroscience & Biobehavioral Reviews*, 71, 529–541. <https://doi.org/10.1016/j.neubiorev.2016.09.003>
- Hattori, N., & Mizuno, Y. (2017). Twenty years since the discovery of the parkin gene. *Journal of Neural Transmission*, 124(9), 1037–1054. <https://doi.org/10.1007/s00702-017-1742-7>
- Hawi, Z., Cummins, T. D. R., Tong, J., Johnson, B., Lau, R., Samarrai, W., & Bellgrove, M. A. (2015). The molecular genetic architecture of attention deficit hyperactivity disorder. *Molecular Psychiatry*, 20(3), 289–297. <https://doi.org/10.1038/mp.2014.183>
- Haylett, W., Swart, C., van der Westhuizen, F., van Dyk, H., van der Merwe, L., van der Merwe, C., ... Bardien, S. (2016). Altered Mitochondrial Respiration and Other Features of Mitochondrial Function in Parkin -Mutant Fibroblasts from Parkinson's Disease Patients. *Parkinson's Disease*, 2016, 1–11. <https://doi.org/10.1155/2016/1819209>
- Heal, D. J., Smith, S. L., Gosden, J., & Nutt, D. J. (2013). Amphetamine, past and present—a pharmacological and clinical perspective. *Journal of Psychopharmacology (Oxford, England)*, 27(6), 479–496.

<https://doi.org/10.1177/0269881113482532>

- Hegarty, S. V., Sullivan, A. M., & O'Keefe, G. W. (2013). Midbrain dopaminergic neurons: A review of the molecular circuitry that regulates their development. *Developmental Biology*, *379*(2), 123–138. <https://doi.org/10.1016/j.ydbio.2013.04.014>
- Héron, C., Costentin, J., & Bonnet, J. J. (1994). Evidence that pure uptake inhibitors including cocaine interact slowly with the dopamine neuronal carrier. *European Journal of Pharmacology*, *264*(3), 391–398. Retrieved from <http://www.ncbi.nlm.nih.gov/pubmed/7698180>
- Hirota, Y., Yamashita, S. ichi, Kurihara, Y., Jin, X., Aihara, M., Saigusa, T., ... Kanki, T. (2015). Mitophagy is primarily due to alternative autophagy and requires the MAPK1 and MAPK14 signaling pathways. *Autophagy*, *11*(2), 332–343. <https://doi.org/10.1080/15548627.2015.1023047>
- Hollville, E., Carroll, R. G., Cullen, S. P., & Martin, S. J. (2014). Bcl-2 Family Proteins Participate in Mitochondrial Quality Control by Regulating Parkin/PINK1-Dependent Mitophagy. *Molecular Cell*, *55*(3), 451–466. <https://doi.org/10.1016/j.molcel.2014.06.001>
- Imaizumi, Y., Okada, Y., Akamatsu, W., Koike, M., Kuzumaki, N., Hayakawa, H., ... Okano, H. (2012a). Mitochondrial dysfunction associated with increased oxidative stress and α -synuclein accumulation in PARK2 iPSC-derived neurons and postmortem brain tissue. *Molecular Brain*, *5*(1), 35. <https://doi.org/10.1186/1756-6606-5-35>
- Imaizumi, Y., Okada, Y., Akamatsu, W., Koike, M., Kuzumaki, N., Hayakawa, H., ... Okano, H. (2012b). Mitochondrial dysfunction associated with increased oxidative stress and α -synuclein accumulation in PARK2 iPSC-derived neurons and postmortem brain tissue. *Molecular Brain*, *5*(1), 35. <https://doi.org/10.1186/1756-6606-5-35>
- International Schizophrenia Consortium, I. S., Purcell, S. M., Wray, N. R., Stone, J. L., Visscher, P. M., O'Donovan, M. C., ... Sklar, P. (2009). Common polygenic variation contributes to risk of schizophrenia and bipolar disorder. *Nature*, *460*(7256), 748–752. <https://doi.org/10.1038/nature08185>
- Ishizuka, K., Kimura, H., Wang, C., Xing, J., Kushima, I., Arioka, Y., ... Ozaki, N. (2016). Investigation of Rare Single-Nucleotide PCDH15 Variants in Schizophrenia and Autism Spectrum Disorders. *PLOS ONE*, *11*(4), e0153224. <https://doi.org/10.1371/journal.pone.0153224>
- Itier, J. M., Ibáñez, P., Mena, M. A., Abbas, N., Cohen-Salmon, C., Bohme, G. A., ... García de Yébenes, J. (2003). Parkin gene inactivation alters behaviour and dopamine neurotransmission in the mouse. *Human Molecular Genetics*, *12*(18), 2277–2291. <https://doi.org/10.1093/hmg/ddg239>
- Jacob, C. P., Romanos, J., Dempfle, A., Heine, M., Windemuth-Kieselbach, C., Kruse, A., ... Lesch, K.-P. (2007). Co-morbidity of adult attention-deficit/hyperactivity disorder with focus on personality traits and related disorders in a tertiary referral center. *European Archives of Psychiatry and Clinical Neuroscience*, *257*(6), 309–317. <https://doi.org/10.1007/s00406-007-0722-6>
- Jacob, L., Haro, M., & Koyanagi, A. I. (2018). Relationship between attention-deficit hyperactivity disorder symptoms and problem gambling: A mediation analysis of influential factors among 7,403 individuals from the UK. <https://doi.org/10.1556/2006.7.2018.72>
- Jansch, C., Günther, K., Waider, J., Ziegler, G. C., Forero, A., Kollert, S., ... Lesch, K. P. (2018). Generation of a human induced pluripotent stem cell (iPSC) line from a 51-year-old female with attention-deficit/hyperactivity disorder (ADHD) carrying a duplication of SLC2A3. *Stem Cell Research*, *28*, 136–140. <https://doi.org/10.1016/j.scr.2018.02.005>
- Jarick, I., Volckmar, A.-L., Pütter, C., Pechlivanis, S., Nguyen, T. T., Dauvermann, M. R., ... Hinney, A. (2014). Genome-wide analysis of rare copy number variations reveals PARK2 as a candidate gene for attention-deficit/hyperactivity disorder. *Molecular Psychiatry*, *19*(1), 115–121. <https://doi.org/10.1038/mp.2012.161>
- Jauniaux, E., Gulbis, B., Acharya, G., Thiry, P., & Rodeck, C. (1999). Maternal tobacco exposure and cotinine levels in fetal fluids in the first half of pregnancy. *Obstetrics & Gynecology*, *93*(1), 25–29. [https://doi.org/10.1016/S0029-7844\(98\)00318-4](https://doi.org/10.1016/S0029-7844(98)00318-4)
- Jin, S. M., & Youle, R. J. (2013). The accumulation of misfolded proteins in the mitochondrial matrix is sensed by PINK1 to induce PARK2/Parkin-mediated mitophagy of polarized mitochondria. *Autophagy*, *9*(11), 1750–1757. <https://doi.org/10.4161/auto.26122>
- Joseph, N., Zhang-James, Y., Perl, A., & Faraone, S. V. (2015). Oxidative Stress and ADHD: A Meta-Analysis. *Journal of Attention Disorders*, *19*(11), 915–924. <https://doi.org/10.1177/1087054713510354>
- Kalmady, S. V., & Venkatasubramanian, G. (2009). Evidence for positive selection on Protocadherin Y gene in Homo sapiens: Implications for schizophrenia. *Schizophrenia Research*, *108*(1–3), 299–300. <https://doi.org/10.1016/j.schres.2008.09.015>

- Kálmán, S., Garbett, K. A., Janka, Z., & Mirnics, K. (2016). Human dermal fibroblasts in psychiatry research. *Neuroscience*, *320*, 105–121. <https://doi.org/10.1016/j.neuroscience.2016.01.067>
- Katzman, M. A., Bilkey, T. S., Chokka, P. R., Fallu, A., & Klassen, L. J. (2017). Adult ADHD and comorbid disorders: clinical implications of a dimensional approach. *BMC Psychiatry*, *17*(1), 302. <https://doi.org/10.1186/s12888-017-1463-3>
- Kazlauskaite, A., & Muqit, M. M. K. (2015). PINK1 and Parkin - Mitochondrial interplay between phosphorylation and ubiquitylation in Parkinson's disease. *FEBS Journal*, *282*(2), 215–223. <https://doi.org/10.1111/febs.13127>
- Kitada, T., Asakawa, S., Hattori, N., Matsumine, H., Yamamura, Y., Minoshima, S., ... Shimizu, N. (1998). Mutations in the parkin gene cause autosomal recessive juvenile parkinsonism. *Nature*, *392*(6676), 605–608. <https://doi.org/10.1038/33416>
- Klinkenberg, M., Gispert, S., Dominguez-Bautista, J. A., Braun, I., Auburger, G., & Jendrach, M. (2012). Restriction of trophic factors and nutrients induces PARKIN expression. *Neurogenetics*, *13*(1), 9–21. <https://doi.org/10.1007/s10048-011-0303-8>
- Kooij, S. J., Bejerot, S., Blackwell, A., Caci, H., Casas-Brugué, M., Carpentier, P. J., ... Asherson, P. (2010). European consensus statement on diagnosis and treatment of adult ADHD: The European Network Adult ADHD. *BMC Psychiatry*, *10*(1), 67. <https://doi.org/10.1186/1471-244X-10-67>
- Krain, A. L., & Castellanos, F. X. (2006). Brain development and ADHD. *Clinical Psychology Review*, *26*(4), 433–444. <https://doi.org/10.1016/J.CPR.2006.01.005>
- Kriks, S., Shim, J.-W., Piao, J., Ganat, Y. M., Wakeman, D. R., Xie, Z., ... Studer, L. (2011). Dopamine neurons derived from human ES cells efficiently engraft in animal models of Parkinson's disease. *Nature*, *480*(7378), 547–551. <https://doi.org/10.1038/nature10648>
- La Cognata, V., Iemmolo, R., D'Agata, V., Scuderi, S., Drago, F., Zappia, M., & Cavallaro, S. (2014). Increasing the Coding Potential of Genomes Through Alternative Splicing: The Case of PARK2 Gene. *Current Genomics*, *15*(3), 203–216. <https://doi.org/10.2174/1389202915666140426003342>
- Lachman, H. M., Petruolo, O. A., Pedrosa, E., Novak, T., Nolan, K., & Stopkova, P. (2008). Analysis of protocadherin alpha gene deletion variant in bipolar disorder and schizophrenia. *Psychiatric Genetics*, *18*(3), 110–115. <https://doi.org/10.1097/YPG.0b013e3282fa1838>
- LaMarca, E. A., Powell, S. K., Akbarian, S., & Brennand, K. J. (2018). Modeling Neuropsychiatric and Neurodegenerative Diseases With Induced Pluripotent Stem Cells. *Frontiers in Pediatrics*, *6*, 82. <https://doi.org/10.3389/fped.2018.00082>
- Lau, J., & Herzog, H. (2014). CART in the regulation of appetite and energy homeostasis. *Frontiers in Neuroscience*, *8*, 313. <https://doi.org/10.3389/fnins.2014.00313>
- Lesch, K.-P., Selch, S., Renner, T. J., Jacob, C., Nguyen, T. T., Hahn, T., ... Ullmann, R. (2011). Genome-wide copy number variation analysis in attention-deficit/hyperactivity disorder: association with neuropeptide Y gene dosage in an extended pedigree. *Molecular Psychiatry*, *16*(5), 491–503. <https://doi.org/10.1038/mp.2010.29>
- Lew, A. R., Kellermayer, T. R., Sule, B. P., & Szigeti, K. (2018). Copy Number Variations in Adult-onset Neuropsychiatric Diseases. *Current Genomics*, *19*(6), 420–430. <https://doi.org/10.2174/1389202919666180330153842>
- Li, J., Olsen, J., Vestergaard, M., & Obel, C. (2011). Low Apgar Scores and Risk of Childhood Attention Deficit Hyperactivity Disorder. *The Journal of Pediatrics*, *158*(5), 775–779. <https://doi.org/10.1016/j.jpeds.2010.10.041>
- Liang, G., & Zhang, Y. (2013). Genetic and epigenetic variations in iPSCs: potential causes and implications for application. *Cell Stem Cell*, *13*(2), 149–159. <https://doi.org/10.1016/j.stem.2013.07.001>
- Liang, N., Trujillo, C. A., Negraes, P. D., Muotri, A. R., Lameu, C., & Ulrich, H. (2017). Stem cell contributions to neurological disease modeling and personalized medicine. *Progress in Neuro-Psychopharmacology and Biological Psychiatry*, (May), 1–9. <https://doi.org/10.1016/j.pnpbp.2017.05.025>
- Lim, C.-S., Yang, J.-E., Lee, Y.-K., Lee, K., Lee, J.-A., & Kaang, B.-K. (2015). Understanding the molecular basis of autism in a dish using hiPSCs-derived neurons from ASD patients. *Molecular Brain*, *8*(1), 57. <https://doi.org/10.1186/s13041-015-0146-6>
- Linnet, K. M., Dalsgaard, S., Obel, C., Wisborg, K., Henriksen, T. B., Rodriguez, A., ... Jarvelin, M.-R. (2003). Maternal Lifestyle Factors in Pregnancy Risk of Attention Deficit Hyperactivity Disorder and Associated Behaviors: Review of the Current Evidence. *American Journal of Psychiatry*, *160*(6), 1028–1040. <https://doi.org/10.1176/appi.ajp.160.6.1028>
- Liu, S., Sawada, T., Lee, S., Yu, W., Silverio, G., Alapatt, P., ... Lu, B. (2012). Parkinson's disease-associated kinase PINK1 regulates miro protein level and axonal transport of mitochondria. *PLoS Genetics*, *8*(3), 15–17.

<https://doi.org/10.1371/journal.pgen.1002537>

- Liu, Y., Beyer, A., & Aebersold, R. (2016). On the Dependency of Cellular Protein Levels on mRNA Abundance. *Cell*, *165*(3), 535–550. <https://doi.org/10.1016/j.cell.2016.03.014>
- Ljung, T., Chen, Q., Lichtenstein, P., & Larsson, H. (2014). Common Etiological Factors of Attention-Deficit/Hyperactivity Disorder and Suicidal Behavior. *JAMA Psychiatry*, *71*(8), 958. <https://doi.org/10.1001/jamapsychiatry.2014.363>
- Lomazzo, E., Hussmann, G. P., Wolfe, B. B., Yasuda, R. P., Perry, D. C., & Kellar, K. J. (2011). Effects of chronic nicotine on heteromeric neuronal nicotinic receptors in rat primary cultured neurons. *Journal of Neurochemistry*, *119*(1), 153–164. <https://doi.org/10.1111/j.1471-4159.2011.07408.x>
- Lopes, C., & Rego, A. C. (2016). Revisiting Mitochondrial Function and Metabolism in Pluripotent Stem Cells: Where Do We Stand in Neurological Diseases? *Molecular Neurobiology*, 1–16. <https://doi.org/10.1007/s12035-016-9714-8>
- Lopresti, A. L. (2015). Oxidative and nitrosative stress in ADHD: possible causes and the potential of antioxidant-targeted therapies. *ADHD Attention Deficit and Hyperactivity Disorders*, *7*(4), 237–247. <https://doi.org/10.1007/s12402-015-0170-5>
- Lu, W., Zhou, Y., Qiao, P., Zheng, J., Wu, Q., & Shen, Q. (2018). The protocadherin alpha cluster is required for axon extension and myelination in the developing central nervous system. *Neural Regeneration Research*, *13*(3), 427. <https://doi.org/10.4103/1673-5374.228724>
- Maier, A. B., le Cessie, S., de Koning-Treurniet, C., Blom, J., Westendorp, R. G. J., & van Heemst, D. (2007). Persistence of high-replicative capacity in cultured fibroblasts from nonagenarians. *Aging Cell*, *6*(1), 27–33. <https://doi.org/10.1111/j.1474-9726.2006.00263.x>
- Malik, N., & Rao, M. S. (2013). A Review of the Methods for Human iPSC Derivation. *Methods in Molecular Biology (Clifton, N.J.)*, *997*, 23. https://doi.org/10.1007/978-1-62703-348-0_3
- Manji, H., Kato, T., Di Prospero, N. A., Ness, S., Beal, M. F., Krams, M., & Chen, G. (2012). Impaired mitochondrial function in psychiatric disorders. *Nature Reviews Neuroscience*, *13*(5), 293–307. <https://doi.org/10.1038/nrn3229>
- Mao, P., Ardeshiri, A., Jacks, R., Yang, S., Hurn, P. D., & Alkayed, N. J. (2007). Mitochondrial mechanism of neuroprotection by CART. *European Journal of Neuroscience*, *26*(3), 624–632. <https://doi.org/10.1111/j.1460-9568.2007.05691.x>
- Mao, P., Meshul, C. K., Thuillier, P., Goldberg, N. R. S., & Reddy, P. H. (2012). CART Peptide Is a Potential Endogenous Antioxidant and Preferentially Localized in Mitochondria. *PLoS ONE*, *7*(1), e29343. <https://doi.org/10.1371/journal.pone.0029343>
- Marazziti, D., Baroni, S., Picchetti, M., Landi, P., Silvestri, S., Vatteroni, E., & Catena Dell’Osso, M. (2012). Psychiatric disorders and mitochondrial dysfunctions. *European Review for Medical and Pharmacological Sciences*, *16*(2), 270–275.
- Marín, I. (2009). RBR ubiquitin ligases: Diversification and streamlining in animal lineages. *Journal of Molecular Evolution*, *69*(1), 54–64. <https://doi.org/10.1007/s00239-009-9252-3>
- Martí, M., Mulero, L., Pardo, C., Morera, C., Carrió, M., Laricchia-Robbio, L., ... Belmonte, J. C. I. (2013). Characterization of pluripotent stem cells. *Nature Protocols*, *8*(2), 223–253. <https://doi.org/10.1038/nprot.2012.154>
- Martin, J., Hamshere, M. L., Stergiakouli, E., O’Donovan, M. C., & Thapar, A. (2014). Genetic risk for attention-deficit/hyperactivity disorder contributes to neurodevelopmental traits in the general population. *Biological Psychiatry*, *76*(8), 664–671. <https://doi.org/10.1016/j.biopsych.2014.02.013>
- Martin, J., O’Donovan, M. C., Thapar, A., Langley, K., & Williams, N. (2015). The relative contribution of common and rare genetic variants to ADHD. *Translational Psychiatry*, *5*(December 2014), e506. <https://doi.org/10.1038/tp.2015.5>
- Martin, J., Walters, R. K., Demontis, D., Mattheisen, M., Lee, S. H., Robinson, E., ... Neale, B. M. (2018). A Genetic Investigation of Sex Bias in the Prevalence of Attention-Deficit/Hyperactivity Disorder. *Biological Psychiatry*, *83*(12), 1044–1053. <https://doi.org/10.1016/j.biopsych.2017.11.026>
- Matsumine, H., Saito, M., Shimoda-Matsubayashi, S., Tanaka, H., Ishikawa, A., Nakagawa-Hattori, Y., ... Mizuno, Y. (1997). Localization of a gene for an autosomal recessive form of juvenile Parkinsonism to chromosome 6q25.2-27. *American Journal of Human Genetics*, *60*(3), 588–596. Retrieved from <http://www.ncbi.nlm.nih.gov/pubmed/9042918>
- Matthies, S. D., & Philipsen, A. (2014). Common ground in Attention Deficit Hyperactivity Disorder (ADHD) and Borderline Personality Disorder (BPD)-review of recent findings. *Borderline Personality Disorder and Emotion Dysregulation*, *1*, 3. <https://doi.org/10.1186/2051-6673-1-3>

- McCann, R. F., & Ross, D. A. (2018). So Happy Together: The Storied Marriage Between Mitochondria and the Mind. *Biological Psychiatry*, *83*(9), e47–e49. <https://doi.org/10.1016/j.biopsych.2018.03.006>
- McClernon, F. J., & Kollins, S. H. (2008). ADHD and smoking: from genes to brain to behavior. *Annals of the New York Academy of Sciences*, *1141*, 131–147. <https://doi.org/10.1196/annals.1441.016>
- McWilliams, T. G., & Muqit, M. M. (2017). PINK1 and Parkin: emerging themes in mitochondrial homeostasis. *Current Opinion in Cell Biology*, *45*, 83–91. <https://doi.org/10.1016/j.CEB.2017.03.013>
- Meinzer, M. C., Lewinsohn, P. M., Pettit, J. W., Seeley, J. R., Gau, J. M., Chronis-Tuscano, A., & Waxmonsky, J. G. (2013). ATTENTION-DEFICIT/HYPERACTIVITY DISORDER IN ADOLESCENCE PREDICTS ONSET OF MAJOR DEPRESSIVE DISORDER THROUGH EARLY ADULTHOOD. *Depression and Anxiety*, *30*(6), 546–553. <https://doi.org/10.1002/da.22082>
- Meissner, C., Lorenz, H., Weihofen, A., Selkoe, D. J., & Lemberg, M. K. (2011). The mitochondrial intramembrane protease PARL cleaves human Pink1 to regulate Pink1 trafficking. *Journal of Neurochemistry*, *117*(5), 856–867. <https://doi.org/10.1111/j.1471-4159.2011.07253.x>
- Mick, E., Biederman, J., Faraone, S. V., Sayer, J., & Kleinman, S. (2002). Case-control study of attention-deficit hyperactivity disorder and maternal smoking, alcohol use, and drug use during pregnancy. *Journal of the American Academy of Child and Adolescent Psychiatry*, *41*(4), 378–385. <https://doi.org/10.1097/00004583-200204000-00009>
- Mill, J., & Petronis, A. (2008). Pre- and peri-natal environmental risks for attention-deficit hyperactivity disorder (ADHD): the potential role of epigenetic processes in mediating susceptibility. *Journal of Child Psychology and Psychiatry*, *49*(10), 1020–1030. <https://doi.org/10.1111/j.1469-7610.2008.01909.x>
- Miller, S. A., Dykes, D. D., & Polesky, H. F. (1988). A simple salting out procedure for extracting DNA from human nucleated cells. *Nucleic Acids Research*, *16*(3), 1215. Retrieved from <http://www.ncbi.nlm.nih.gov/pubmed/3344216>
- Minde, K., Eakin, L., Hechtman, L., Ochs, E., Bouffard, R., Greenfield, B., & Looper, K. (2003). The psychosocial functioning of children and spouses of adults with ADHD. *Journal of Child Psychology and Psychiatry, and Allied Disciplines*, *44*(4), 637–646. Retrieved from <http://www.ncbi.nlm.nih.gov/pubmed/12751853>
- Miñones-Moyano, E., Porta, S., Escaramís, G., Rabionet, R., Iraola, S., Kagerbauer, B., ... Martí, E. (2011). MicroRNA profiling of Parkinson's disease brains identifies early downregulation of miR-34b/c which modulate mitochondrial function. *Human Molecular Genetics*, *20*(15), 3067–3078. <https://doi.org/10.1093/hmg/ddr210>
- Miyazaki, I., & Asanuma, M. (2008). Dopaminergic neuron-specific oxidative stress caused by dopamine itself. *Acta Medica Okayama*, *62*(3), 141–150. <https://doi.org/10.18926/AMO/30942>
- Moffitt, T. E., Houts, R., Asherson, P., Belsky, D. W., Corcoran, D. L., Hammerle, M., ... Caspi, A. (2015). Is Adult ADHD a Childhood-Onset Neurodevelopmental Disorder? Evidence From a Four-Decade Longitudinal Cohort Study. *American Journal of Psychiatry*, *172*(10), 967–977. <https://doi.org/10.1176/appi.ajp.2015.14101266>
- Morris, G., & Berk, M. (2015). The many roads to mitochondrial dysfunction in neuroimmune and neuropsychiatric disorders. *BMC Medicine*, *13*, 68. <https://doi.org/10.1186/s12916-015-0310-y>
- Mortiboys, H., Thomas, K. J., Koopman, W. J. H., Abou-sleiman, P., Olpin, S., Wood, N. W., ... Cookson, M. R. (2009). Mitochondrial function and morphology are impaired in parkin mutant fibroblasts, *64*(5), 555–565. <https://doi.org/10.1002/ana.21492>. Mitochondrial
- Motlagh, M. G., Sukhodolsky, D. G., Landeros-Weisenberger, A., Katsoyich, L., Thompson, N., Scahill, L., ... Leckman, J. F. (2011). Adverse effects of heavy prenatal maternal smoking on attentional control in children with ADHD. *Journal of Attention Disorders*, *15*(7), 593–603. <https://doi.org/10.1177/1087054710374576>
- Moukhtarian, T. R., Mintah, R. S., Moran, P., & Asherson, P. (2018). Emotion dysregulation in attention-deficit/hyperactivity disorder and borderline personality disorder. *Borderline Personality Disorder and Emotion Dysregulation*, *5*, 9. <https://doi.org/10.1186/s40479-018-0086-8>
- Mountoufaris, G., Canzio, D., Nwakeze, C. L., Chen, W. V., & Maniatis, T. (2018). Writing, Reading, and Translating the Clustered Protocadherin Cell Surface Recognition Code for Neural Circuit Assembly. *Annual Review of Cell and Developmental Biology*, *34*(1), 471–493. <https://doi.org/10.1146/annurev-cellbio-100616-060701>
- Mowinckel, A. M., Pedersen, M. L., Eilertsen, E., & Biele, G. (2015). A Meta-Analysis of Decision-Making and Attention in Adults With ADHD. *Journal of Attention Disorders*, *19*(5), 355–367. <https://doi.org/10.1177/1087054714558872>
- Müller-Rischart, A. K., Pilsl, A., Beaudette, P., Patra, M., Hadian, K., Funke, M., ... Winklhofer, K. F. (2013). The E3 Ligase Parkin Maintains Mitochondrial Integrity by Increasing Linear Ubiquitination of NEMO. *Molecular Cell*, *49*(5), 908–921. <https://doi.org/10.1016/j.molcel.2013.01.036>

- Murphy, M. P. (2009). How mitochondria produce reactive oxygen species. *The Biochemical Journal*, 417(1), 1–13. <https://doi.org/10.1042/BJ20081386>
- Narendra, D., Tanaka, A., Suen, D.-F., & Youle, R. J. (2008). Parkin is recruited selectively to impaired mitochondria and promotes their autophagy. *The Journal of Cell Biology*, 183(5), 795–803. <https://doi.org/10.1083/jcb.200809125>
- Nielsen, T., Jensen, M. B., Stenager, E., & Andersen, A. D. (2018). The use of olfactory testing when diagnosing Parkinson's disease - a systematic review. *Danish Medical Journal*, 65(5). Retrieved from <http://www.ncbi.nlm.nih.gov/pubmed/29726318>
- Nikolas, M. A., & Burt, S. A. (2010). Genetic and environmental influences on ADHD symptom dimensions of inattention and hyperactivity: A meta-analysis. *Journal of Abnormal Psychology*, 119(1), 1–17. <https://doi.org/10.1037/a0018010>
- Ossmann, J. M., & Mulligan, N. W. (2003). Inhibition and attention deficit hyperactivity disorder in adults. *The American Journal of Psychology*, 116(1), 35–50. Retrieved from <http://www.ncbi.nlm.nih.gov/pubmed/12710221>
- Pastrakuljic, A., Schwartz, R., Simone, C., Derewlany, L. O., Knie, B., & Koren, G. (1998). Transplacental transfer and biotransformation studies of nicotine in the human placental cotyledon perfused in vitro. *Life Sciences*, 63(26), 2333–2342. [https://doi.org/10.1016/S0024-3205\(98\)00522-0](https://doi.org/10.1016/S0024-3205(98)00522-0)
- Perez, F. A., & Palmiter, R. D. (2005). Parkin-deficient mice are not a robust model of parkinsonism. *Proceedings of the National Academy of Sciences of the United States of America*, 102(6), 2174–2179. <https://doi.org/10.1073/pnas.0409598102>
- Peterson, C., & Goldman, J. E. (1986). Alterations in calcium content and biochemical processes in cultured skin fibroblasts from aged and Alzheimer donors. *Proceedings of the National Academy of Sciences of the United States of America*, 83(8), 2758–2762. Retrieved from <http://www.ncbi.nlm.nih.gov/pubmed/3458236>
- Philipsen, A., Jans, T., Graf, E., Matthies, S., Borel, P., Colla, M., ... Comparison of Methylphenidate and Psychotherapy in Adult ADHD Study (COMPAS) Consortium. (2015). Effects of Group Psychotherapy, Individual Counseling, Methylphenidate, and Placebo in the Treatment of Adult Attention-Deficit/Hyperactivity Disorder. *JAMA Psychiatry*, 72(12), 1199. <https://doi.org/10.1001/jamapsychiatry.2015.2146>
- Pickrell, A. M., & Youle, R. J. (2015). The Roles of PINK1, Parkin, and Mitochondrial Fidelity in Parkinson's Disease. *Neuron*, 85(2), 257–273. <https://doi.org/10.1016/j.neuron.2014.12.007>
- Polanczyk, G. V., Willcutt, E. G., Salum, G. A., Kieling, C., & Rohde, L. A. (2014). ADHD prevalence estimates across three decades: an updated systematic review and meta-regression analysis. *International Journal of Epidemiology*, 43(2), 434–442. <https://doi.org/10.1093/ije/dyt261>
- Prilutsky, D., Palmer, N. P., Smedemark-Margulies, N., Schlaeger, T. M., Margulies, D. M., & Kohane, I. S. (2014). iPSC-derived neurons as a higher-throughput readout for autism: promises and pitfalls. *Trends in Molecular Medicine*, 20(2), 91–104. <https://doi.org/10.1016/j.molmed.2013.11.004>
- Ramos-Quiroga, J.-A., Sánchez-Mora, C., Casas, M., Garcia-Martínez, I., Bosch, R., Nogueira, M., ... Ribasés, M. (2014). Genome-wide copy number variation analysis in adult attention-deficit and hyperactivity disorder. *Journal of Psychiatric Research*, 49, 60–67. <https://doi.org/10.1016/J.JPSYCHIRES.2013.10.022>
- Ramos-Quiroga, J. A., Nasillo, V., Fernández-Aranda, F., Casas, M., & Casas, M. (2014). Addressing the lack of studies in attention-deficit/hyperactivity disorder in adults. *Expert Review of Neurotherapeutics*, 14(5), 553–567. <https://doi.org/10.1586/14737175.2014.908708>
- Razoki, B. (2018). Neurofeedback versus psychostimulants in the treatment of children and adolescents with attention-deficit/hyperactivity disorder: a systematic review. *Neuropsychiatric Disease and Treatment*, Volume 14, 2905–2913. <https://doi.org/10.2147/NDT.S178839>
- Reif, A., Nguyen, T. T., Weißflog, L., Jacob, C. P., Romanos, M., Renner, T. J., ... Schäfer, H. (2012). DIRAS2 is Associated with Adult ADHD, Related Traits, and Co-Morbid Disorders. *Neuropsychopharmacology*, 37(4), 1076–1076. <https://doi.org/10.1038/npp.2011.305>
- Retz-Junginger, P., Retz, W., Blocher, D., Weijers, H.-G., Trott, G.-E., Wender, P. H., & Rössler, M. (2002). Wender Utah Rating Scale (WURS-k) Die deutsche Kurzform zur retrospektiven Erfassung des hyperkinetischen Syndroms bei Erwachsenen. *Der Nervenarzt*, 73(9), 830–838. <https://doi.org/10.1007/s00115-001-1215-x>
- Retz, W., Stieglitz, R.-D., Corbisiero, S., Retz-Junginger, P., & Rössler, M. (2012). Emotional dysregulation in adult ADHD: what is the empirical evidence? *Expert Review of Neurotherapeutics*, 12(10), 1241–1251. <https://doi.org/10.1586/ern.12.109>
- Rial, D., Castro, A. A., Machado, N., Garção, P., Gonçalves, F. Q., Silva, H. B., ... Prediger, R. D. (2014). Behavioral

- phenotyping of Parkin-deficient mice: looking for early preclinical features of Parkinson's disease. *PLoS One*, 9(12), e114216. <https://doi.org/10.1371/journal.pone.0114216>
- Riddle, E. L., Hanson, G. R., & Fleckenstein, A. E. (2007). Therapeutic doses of amphetamine and methylphenidate selectively redistribute the vesicular monoamine transporter-2. *European Journal of Pharmacology*, 571(1), 25–28. <https://doi.org/10.1016/J.EJP.2007.05.044>
- Rodriguez, A., & Bohlin, G. (2005). Are maternal smoking and stress during pregnancy related to ADHD symptoms in children? *Journal of Child Psychology and Psychiatry*, 46(3), 246–254. <https://doi.org/10.1111/j.1469-7610.2004.00359.x>
- Rommelse, N. N. J., Geurts, H. M., Franke, B., Buitelaar, J. K., & Hartman, C. A. (2011). A review on cognitive and brain endophenotypes that may be common in autism spectrum disorder and attention-deficit/hyperactivity disorder and facilitate the search for pleiotropic genes. *Neuroscience & Biobehavioral Reviews*, 35(6), 1363–1396. <https://doi.org/10.1016/J.NEUBIOREV.2011.02.015>
- Ronen, D., & Benvenisty, N. (2012). Genomic stability in reprogramming. *Current Opinion in Genetics & Development*, 22(5), 444–449. <https://doi.org/10.1016/j.gde.2012.09.003>
- Rony, I. K., Baten, A., Bloomfield, J. a, Islam, M. E., Billah, M. M., & Islam, K. D. (2015). Inducing pluripotency in vitro : recent advances and highlights in induced pluripotent stem cells generation and pluripotency reprogramming. *Cell Proliferation*, 48(2), 140–156. <https://doi.org/10.1111/cpr.12162>
- Rösler, M., Retz, W., Retz-Junginger, P., Hengesch, G., Schneider, M., Supprian, T., ... Thome, J. (2004). Prevalence of attention deficit-/hyperactivity disorder (ADHD) and comorbid disorders in young male prison inmates*. *European Archives of Psychiatry and Clinical Neuroscience*, 254(6), 365–371. <https://doi.org/10.1007/s00406-004-0516-z>
- Rösler, M., Retz, W., Thome, J., Schneider, M., Stieglitz, R.-D., & Falkai*, P. (2006). Psychopathological rating scales for diagnostic use in adults with attention-deficit/hyperactivity disorder (ADHD). *European Archives of Psychiatry and Clinical Neuroscience*, 256(S1), i3–i11. <https://doi.org/10.1007/s00406-006-1001-7>
- Ross, D., & Siegel, D. (2017). Functions of NQO1 in Cellular Protection and CoQ10 Metabolism and its Potential Role as a Redox Sensitive Molecular Switch. *Frontiers in Physiology*, 8, 595. <https://doi.org/10.3389/fphys.2017.00595>
- Rossignol, D. A., & Frye, R. E. (2012). Mitochondrial dysfunction in autism spectrum disorders: a systematic review and meta-analysis. *Molecular Psychiatry*, 17(3), 290–314. <https://doi.org/10.1038/mp.2010.136>
- Ruderfer, D. M., Hamamsy, T., Lek, M., Karczewski, K. J., Kavanagh, D., Samocha, K. E., ... Purcell, S. M. (2016). Patterns of genic intolerance of rare copy number variation in 59,898 human exomes. *Nature Genetics*, 48(10), 1107–1111. <https://doi.org/10.1038/ng.3638>
- Sagiv, S. K., Epstein, J. N., Bellinger, D. C., & Korrick, S. A. (2013). Pre- and Postnatal Risk Factors for ADHD in a Nonclinical Pediatric Population. *Journal of Attention Disorders*, 17(1), 47–57. <https://doi.org/10.1177/1087054711427563>
- Salmasi, G., Grady, R., Jones, J., & McDonald, S. D. (2010). Environmental tobacco smoke exposure and perinatal outcomes: a systematic review and meta-analyses. *Acta Obstetrica et Gynecologica Scandinavica*, 89(4), 423–441. <https://doi.org/10.3109/00016340903505748>
- Sarraf, S. A., Raman, M., Guarani-Pereira, V., Sowa, M. E., Huttlin, E. L., Gygi, S. P., & Harper, J. W. (2013). Landscape of the PARKIN-dependent ubiquitylome in response to mitochondrial depolarization. *Nature*, 496(7445), 372–376. <https://doi.org/10.1038/nature12043>
- Scarffe L.A., Stevens D.A., Dawson V.L., D. T. M. (2015). Parkin and PINK1: Much More than Mitophagy, 19(2), 161–169. <https://doi.org/10.3851/IMP2701.Changes>
- Schachar, R. J., Park, L. S., & Dennis, M. (2015). Mental Health Implications of Traumatic Brain Injury (TBI) in Children and Youth. *Journal of the Canadian Academy of Child and Adolescent Psychiatry = Journal de l'Academie Canadienne de Psychiatrie de l'enfant et de l'adolescent*, 24(2), 100–108. Retrieved from <http://www.ncbi.nlm.nih.gov/pubmed/26379721>
- Schwenke, E., Fasching, P. A., Faschingbauer, F., Pretscher, J., Kehl, S., Peretz, R., ... Schneider, M. (2018). Predicting attention deficit hyperactivity disorder using pregnancy and birth characteristics. *Archives of Gynecology and Obstetrics*, 1–7. <https://doi.org/10.1007/s00404-018-4888-0>
- Scuderi, S., La Cognata, V., Drago, F., Cavallaro, S., & D'Agata, V. (2014). Alternative splicing generates different parkin protein isoforms: Evidences in human, rat, and mouse brain. *BioMed Research International*, 2014. <https://doi.org/10.1155/2014/690796>
- Seo, J.-Y., Lee, C.-S., Park, C.-S., Kim, B.-J., Cha, B.-S., Lee, S.-J., & Ahn, I.-Y. (2014). Mediating Effect of Depressive Symptoms

- on the Relationship between Adult Attention Deficit Hyperactivity Disorder and Quality of Life. *Psychiatry Investigation*, 11(2), 131–136. <https://doi.org/10.4306/pi.2014.11.2.131>
- Shaltouki, A., Sivapatham, R., Pei, Y., Gerencser, A. A., Mom??ilovi??, O., Rao, M. S., & Zeng, X. (2015). Mitochondrial alterations by PARKIN in dopaminergic neurons using PARK2 patient-specific and PARK2 knockout isogenic iPSC lines. *Stem Cell Reports*, 4(5), 847–859. <https://doi.org/10.1016/j.stemcr.2015.02.019>
- Shaw, P., Sudre, G., Wharton, A., Weingart, D., Sharp, W., & Sarlls, J. (2015). White Matter Microstructure and the Variable Adult Outcome of Childhood Attention Deficit Hyperactivity Disorder. *Neuropsychopharmacology*, 40(3), 746–754. <https://doi.org/10.1038/npp.2014.241>
- Sheng, Z.-H., & Cai, Q. (2012). Mitochondrial transport in neurons: impact on synaptic homeostasis and neurodegeneration. *Nature Reviews Neuroscience*, 13(2), 77–93. <https://doi.org/10.1038/nrn3156>
- Sheridan, S. D., Surampudi, V., & Rao, R. R. (2012). Analysis of Embryoid Bodies Derived from Human Induced Pluripotent Stem Cells as a Means to Assess Pluripotency. *Stem Cells International*, 2012, 1–9. <https://doi.org/10.1155/2012/738910>
- Shin, J.-H., Ko, H. S., Kang, H., Lee, Y., Lee, Y.-I., Pletinkova, O., ... Dawson, T. M. (2011). PARIS (ZNF746) Repression of PGC-1 α Contributes to Neurodegeneration in Parkinson's Disease. *Cell*, 144(5), 689–702. <https://doi.org/10.1016/j.cell.2011.02.010>
- Silva, D., Colvin, L., Hagemann, E., & Bower, C. (2014). Environmental Risk Factors by Gender Associated With Attention-Deficit/Hyperactivity Disorder. *Pediatrics*, 133(1), e14–e22. <https://doi.org/10.1542/peds.2013-1434>
- Simon, V., Czobor, P., Bálint, S., Mészáros, Á., & Bitter, I. (2009). Prevalence and correlates of adult attention-deficit hyperactivity disorder: meta-analysis. *British Journal of Psychiatry*, 194(03), 204–211. <https://doi.org/10.1192/bjp.bp.107.048827>
- Singh, V. K., Kalsan, M., Kumar, N., Saini, A., & Chandra, R. (2015). Induced pluripotent stem cells: applications in regenerative medicine, disease modeling, and drug discovery. *Frontiers in Cell and Developmental Biology*, 3(February), 1–18. <https://doi.org/10.3389/fcell.2015.00002>
- Skogli, E. W., Teicher, M. H., Andersen, P. N., Hovik, K. T., & Øie, M. (2013). ADHD in girls and boys--gender differences in co-existing symptoms and executive function measures. *BMC Psychiatry*, 13, 298. <https://doi.org/10.1186/1471-244X-13-298>
- Sobanski, E., Brüggemann, D., Alm, B., Kern, S., Deschner, M., Schubert, T., ... Rietschel, M. (2007). Psychiatric comorbidity and functional impairment in a clinically referred sample of adults with attention-deficit/hyperactivity disorder (ADHD). *European Archives of Psychiatry and Clinical Neuroscience*, 257(7), 371–377. <https://doi.org/10.1007/s00406-007-0712-8>
- Sochacki, J., Devalle, S., Reis, M., Mattos, P., & Rehen, S. (2016). Generation of urine iPSC cell lines from patients with Attention Deficit Hyperactivity Disorder (ADHD) using a non-integrative method. *Stem Cell Research*, 17(1), 102–106. <https://doi.org/10.1016/j.scr.2016.05.015>
- Spencer, T. J., Biederman, J., & Mick, E. (2007). Attention-Deficit/Hyperactivity Disorder: Diagnosis, Lifespan, Comorbidities, and Neurobiology. *Ambulatory Pediatrics*, 7(1), 73–81. <https://doi.org/10.1016/j.ambp.2006.07.006>
- Spiers, H., Hannon, E., Schalkwyk, L. C., Smith, R., Wong, C. C. Y., O'Donovan, M. C., ... Mill, J. (2015). Methylomic trajectories across human fetal brain development. *Genome Research*, 25(3), 338–352. <https://doi.org/10.1101/gr.180273.114>
- Sprenger, A., Küttner, V., Biniossek, M. L., Gretzmeier, C., Boerries, M., Mack, C., ... Dengjel, J. (2010). Comparative quantitation of proteome alterations induced by aging or immortalization in primary human fibroblasts and keratinocytes for clinical applications. *Molecular BioSystems*, 6(9), 1579. <https://doi.org/10.1039/c003962d>
- Srinivas, N. R., Hubbard, J. W., Korchinski, E. D., & Midha, K. K. (1993). Enantioselective pharmacokinetics of dl-threo-methylphenidate in humans. *Pharmaceutical Research*, 10(1), 14–21. Retrieved from <http://www.ncbi.nlm.nih.gov/pubmed/8430051>
- Srinivasan, R., Henley, B. M., Henderson, B. J., Indersmitten, T., Cohen, B. N., Kim, C. H., ... Lester, H. A. (2016). Smoking-Relevant Nicotine Concentration Attenuates the Unfolded Protein Response in Dopaminergic Neurons. *Journal of Neuroscience*, 36(1), 65–79. <https://doi.org/10.1523/JNEUROSCI.2126-15.2016>
- Srivastav, S., Walitza, S., & Grünblatt, E. (2018). Emerging role of miRNA in attention deficit hyperactivity disorder: a systematic review. *ADHD Attention Deficit and Hyperactivity Disorders*, 10(1), 49–63. <https://doi.org/10.1007/s12402-017-0232-y>

- Srivastava, R., Faust, T., Ramos, A., Ishizuka, K., & Sawa, A. (2018). Dynamic Changes of the Mitochondria in Psychiatric Illnesses: New Mechanistic Insights From Human Neuronal Models. *Biological Psychiatry*, *83*(9), 751–760. <https://doi.org/10.1016/j.biopsych.2018.01.007>
- Stankiewicz, P., & Lupski, J. R. (2010). Structural Variation in the Human Genome and its Role in Disease. *Annual Review of Medicine*, *61*(1), 437–455. <https://doi.org/10.1146/annurev-med-100708-204735>
- Stergiakouli, E., Hamshere, M., Holmans, P., Langley, K., Zaharieva, I., Hawi, Z., ... Thapar, A. (2012). Investigating the Contribution of Common Genetic Variants to the Risk and Pathogenesis of ADHD. *American Journal of Psychiatry*, *169*(2), 186–194. <https://doi.org/10.1176/appi.ajp.2011.11040551>
- Stichel, C. C., Zhu, X.-R., Bader, V., Linnartz, B., Schmidt, S., & Lubbert, H. (2007). Mono- and double-mutant mouse models of Parkinson's disease display severe mitochondrial damage. *Human Molecular Genetics*, *16*(20), 2377–2393. <https://doi.org/10.1093/hmg/ddm083>
- Subcommittee on Attention-Deficit/Hyperactivity Disorder, Steering Committee on Quality Improvement and Management, Wolraich, M., Brown, L., Brown, R. T., DuPaul, G., ... Visser, S. (2011). ADHD: Clinical Practice Guideline for the Diagnosis, Evaluation, and Treatment of Attention-Deficit/Hyperactivity Disorder in Children and Adolescents. *PEDIATRICS*, *128*(5), 1007–1022. <https://doi.org/10.1542/peds.2011-2654>
- Sudre, G., Mangalmurti, A., & Shaw, P. (2018). Growing out of attention deficit hyperactivity disorder: Insights from the 'remitted' brain, *94*(August), 198–209. <https://doi.org/10.1016/j.neubiorev.2018.08.010>
- Sulzer, D., Cragg, S. J., & Rice, M. E. (2016). Striatal dopamine neurotransmission: regulation of release and uptake. *Basal Ganglia*, *6*(3), 123–148. <https://doi.org/10.1016/j.baga.2016.02.001>
- Suzuki, S., Akamatsu, W., Kisa, F., Sone, T., Ishikawa, K.-I., Kuzumaki, N., ... Okano, H. (2016). Efficient induction of dopaminergic neuron differentiation from induced pluripotent stem cells reveals impaired mitophagy in PARK2 neurons. *Biochemical and Biophysical Research Communications*, *483*(1), 88–93. <https://doi.org/10.1016/j.bbrc.2016.12.188>
- Takahashi, K., Tanabe, K., Ohnuki, M., Narita, M., Ichisaka, T., Tomoda, K., & Yamanaka, S. (2007). Induction of Pluripotent Stem Cells from Adult Human Fibroblasts by Defined Factors. *Cell*, *131*(5), 861–872. <https://doi.org/10.1016/j.cell.2007.11.019>
- Takahashi, K., & Yamanaka, S. (2006). Induction of Pluripotent Stem Cells from Mouse Embryonic and Adult Fibroblast Cultures by Defined Factors. *Cell*, *126*(4), 663–676. <https://doi.org/10.1016/j.cell.2006.07.024>
- Takumi, T., & Tamada, K. (2018). CNV biology in neurodevelopmental disorders. *Current Opinion in Neurobiology*, *48*, 183–192. <https://doi.org/10.1016/J.CONB.2017.12.004>
- Tanida, I., Ueno, T., & Kominami, E. (2008). LC3 and Autophagy. In *Methods in molecular biology (Clifton, N.J.)* (Vol. 445, pp. 77–88). https://doi.org/10.1007/978-1-59745-157-4_4
- Tiesler, C. M. T., & Heinrich, J. (2014). Prenatal nicotine exposure and child behavioural problems. *European Child & Adolescent Psychiatry*, *23*(10), 913–929. <https://doi.org/10.1007/s00787-014-0615-y>
- Tilokani, L., Nagashima, S., Paupe, V., & Prudent, J. (2018). Mitochondrial dynamics: overview of molecular mechanisms. *Essays in Biochemistry*, *62*(3), 341–360. <https://doi.org/10.1042/EBC20170104>
- Torgersen, T., Gjervan, B., & Rasmussen, K. (2008). Treatment of adult ADHD: is current knowledge useful to clinicians? *Neuropsychiatric Disease and Treatment*, *4*(1), 177–186. Retrieved from <http://www.ncbi.nlm.nih.gov/pubmed/18728815>
- Van den Bergh, B. R. H., & Marcoen, A. (2004). High Antenatal Maternal Anxiety Is Related to ADHD Symptoms, Externalizing Problems, and Anxiety in 8- and 9-Year-Olds. *Child Development*, *75*(4), 1085–1097. <https://doi.org/10.1111/j.1467-8624.2004.00727.x>
- Vangipuram, M., Ting, D., Kim, S., Diaz, R., & Schüle, B. (2013). Skin Punch Biopsy Explant Culture for Derivation of Primary Human Fibroblasts. *Journal of Visualized Experiments*, (77), e3779. <https://doi.org/10.3791/3779>
- Vazquez-Martin, A., Van den Haute, C., Cufí, S., Corominas-Faja, B., Cuyàs, E., Lopez-Bonet, E., ... Menendez, J. A. (2016a). Mitophagy-driven mitochondrial rejuvenation regulates stem cell fate. *Aging*, *8*(7), 1330–1352. <https://doi.org/10.18632/aging.100976>
- Vazquez-Martin, A., Van den Haute, C., Cufí, S., Corominas-Faja, B., Cuyàs, E., Lopez-Bonet, E., ... Menendez, J. A. (2016b). Mitophagy-driven mitochondrial rejuvenation regulates stem cell fate. *Aging*, *8*(7), 1330–1352. <https://doi.org/10.18632/aging.100976>

- Verma, P., Singh, A., Nthenge-Ngumbau, D. N., Rajamma, U., Sinha, S., Mukhopadhyay, K., & Mohanakumar, K. P. (2016). Attention deficit-hyperactivity disorder suffers from mitochondrial dysfunction. *BBA.Clin.*, *6*, 153–158. <https://doi.org/10.1016/j.bbaci.2016.10.003>
- Vogel, C., & Marcotte, E. M. (2012). Insights into the regulation of protein abundance from proteomic and transcriptomic analyses. *Nature Reviews. Genetics*, *13*(4), 227–232. <https://doi.org/10.1038/nrg3185>
- Wai, T., & Langer, T. (2016). Mitochondrial Dynamics and Metabolic Regulation. *Trends in Endocrinology and Metabolism: TEM*, *27*(2), 105–117. <https://doi.org/10.1016/j.tem.2015.12.001>
- Wai, T., Saita, S., Nolte, H., Müller, S., König, T., Richter-Dennerlein, R., ... Langer, T. (2016). The membrane scaffold SLP2 anchors a proteolytic hub in mitochondria containing PARL and the i-AAA protease YME1L. *EMBO Reports*, *17*(12), 1844–1856. <https://doi.org/10.15252/embr.201642698>
- Waldera-Lupa, D. M., Kalfalah, F., Florea, A.-M., Sass, S., Kruse, F., Rieder, V., ... Stuhler, K. (2014). Proteome-wide analysis reveals an age-associated cellular phenotype of <i>in situ</i> aged human fibroblasts. *Aging*, *6*(10), 856–872. <https://doi.org/10.18632/aging.100698>
- Walton, E., Pingault, J.-B., Cecil, C. A. M., Gaunt, T. R., Relton, C. L., Mill, J., & Barker, E. D. (2017). Epigenetic profiling of ADHD symptoms trajectories: a prospective, methylome-wide study. *Molecular Psychiatry*, *22*(2), 250–256. <https://doi.org/10.1038/mp.2016.85>
- Wang, X., Winter, D., Ashrafi, G., Schlehe, J., Wong, Y. L., Selkoe, D., ... Thomas, L. (2012). PINK1 and Parkin Target Miro for Phosphorylation and Degradation to Arrest Mitochondrial Motility, *147*(4), 893–906. <https://doi.org/10.1016/j.cell.2011.10.018>.PINK1
- Wang, Y., Nartiss, Y., Steipe, B., McQuibban, G. A., & Kim, P. K. (2012). ROS-induced mitochondrial depolarization initiates PARK2/PARKIN-dependent mitochondrial degradation by autophagy. *Autophagy*, *8*(10), 1462–1476. <https://doi.org/10.4161/auto.21211>
- Washbourne, P., Dityatev, A., Scheiffele, P., Biederer, T., Weiner, J. A., Christopherson, K. S., & El-Husseini, A. (2004). Cell adhesion molecules in synapse formation. *The Journal of Neuroscience : The Official Journal of the Society for Neuroscience*, *24*(42), 9244–9249. <https://doi.org/10.1523/JNEUROSCI.3339-04.2004>
- Wauer, T., Simicek, M., Schubert, A., & Komander, D. (2015). Mechanism of phospho-ubiquitin-induced PARKIN activation. *Nature*, *524*(7565), 370–374. <https://doi.org/10.1038/nature14879>
- Wilens, T. E., & Dodson, W. (2004). A clinical perspective of attention-deficit/hyperactivity disorder into adulthood. *The Journal of Clinical Psychiatry*, *65*(10), 1301–1313. Retrieved from <http://www.ncbi.nlm.nih.gov/pubmed/15491232>
- Williams, N. M., Zaharieva, I., Martin, A., Langley, K., Mantripragada, K., Fossdal, R., ... Thapar, A. (2010). Rare chromosomal deletions and duplications in attention-deficit hyperactivity disorder: a genome-wide analysis. *Lancet (London, England)*, *376*(9750), 1401–1408. [https://doi.org/10.1016/S0140-6736\(10\)61109-9](https://doi.org/10.1016/S0140-6736(10)61109-9)
- Willner, P. (1986). Validation criteria for animal models of human mental disorders: learned helplessness as a paradigm case. *Progress in Neuro-Psychopharmacology & Biological Psychiatry*, *10*(6), 677–690. Retrieved from <http://www.ncbi.nlm.nih.gov/pubmed/3809518>
- Wilmot, B., Fry, R., Smeester, L., Musser, E. D., Mill, J., & Nigg, J. T. (2016). Methylomic analysis of salivary DNA in childhood ADHD identifies altered DNA methylation in *VIPR2*. *Journal of Child Psychology and Psychiatry*, *57*(2), 152–160. <https://doi.org/10.1111/jcpp.12457>
- Winn, M. E., Shaw, M., April, C., Klotzle, B., Fan, J.-B., Murray, S. S., & Schork, N. J. (2011). Gene expression profiling of human whole blood samples with the Illumina WG-DASL assay. *BMC Genomics*, *12*, 412. <https://doi.org/10.1186/1471-2164-12-412>
- Wu, L. H., Cheng, W., Yu, M., He, B. M., Sun, H., Chen, Q., ... Wu, X. Z. (2017). Nr3C1-Bhlhb2 Axis Dysregulation Is Involved in the Development of Attention Deficit Hyperactivity. *Molecular Neurobiology*, *54*(2), 1196–1212. <https://doi.org/10.1007/s12035-015-9679-z>
- Xia, N., Zhang, P., Fang, F., Wang, Z., Rothstein, M., Angulo, B., ... Reijo Pera, R. A. (2016). Transcriptional comparison of human induced and primary midbrain dopaminergic neurons. *Scientific Reports*, *6*(1), 20270. <https://doi.org/10.1038/srep20270>
- Xu, C., Loh, H. H., & Law, P. Y. (2016). Effects of addictive drugs on adult neural stem/progenitor cells. *Cellular and Molecular Life Sciences*, *73*(2), 327–348. <https://doi.org/10.1007/s00018-015-2067-z>
- Yagi, T., & Takeichi, M. (2000). Cadherin superfamily genes: functions, genomic organization, and neurologic diversity. *Genes & Development*, *14*(10), 1169–1180. <https://doi.org/10.1101/GAD.14.10.1169>

- Yamano, K., Matsuda, N., & Tanaka, K. (2016). The ubiquitin signal and autophagy: an orchestrated dance leading to mitochondrial degradation. *EMBO Reports*, *17*(3), 300–316. <https://doi.org/10.15252/embr.201541486>
- Yamano, K., & Youle, R. J. (2013). PINK1 is degraded through the N-end rule pathway. *Autophagy*, *9*(11), 1758–1769. <https://doi.org/10.4161/auto.24633>
- Yang, B., Wang, S., Yu, S., Chen, Y., Li, L., Zhang, H., & Zhao, Y. (2017). C1q/tumor necrosis factor-related protein 3 inhibits oxidative stress during intracerebral hemorrhage via PKA signaling. *Brain Research*, *1657*, 176–184. <https://doi.org/10.1016/j.brainres.2016.11.016>
- Yin, C.-L., Chen, H.-I., Li, L.-H., Chien, Y.-L., Liao, H.-M., Chou, M. C., ... Gau, S. S.-F. (2016). Genome-wide analysis of copy number variations identifies PARK2 as a candidate gene for autism spectrum disorder. *Molecular Autism*, *7*(1), 23. <https://doi.org/10.1186/s13229-016-0087-7>
- Zanellati, M. C., Monti, V., Barzaghi, C., Reale, C., Nardocci, N., Albanese, A., ... Garavaglia, B. (2015). Mitochondrial dysfunction in Parkinson disease: Evidence in mutant PARK2 fibroblasts. *Frontiers in Genetics*, *6*(MAR). <https://doi.org/10.3389/fgene.2015.00078>
- Zhang, C.-L., Feng, H., Li, L., Wang, J.-Y., Wu, D., Hao, Y.-T., ... Wu, L.-L. (2017). Globular CTRP3 promotes mitochondrial biogenesis in cardiomyocytes through AMPK/PGC-1 α pathway. *Biochimica et Biophysica Acta (BBA) - General Subjects*, *1861*(1), 3085–3094. <https://doi.org/10.1016/j.bbagen.2016.10.022>
- Zhang, C., Lee, S., Peng, Y., Bunker, E., Giaime, E., Shen, J., ... Liu, X. (2014). PINK1 triggers autocatalytic activation of Parkin to specify cell fate decisions. *Current Biology : CB*, *24*(16), 1854–1865. <https://doi.org/10.1016/j.cub.2014.07.014>
- Zheutlin, A. B., & Ross, D. A. (2018). Polygenic Risk Scores: What Are They Good For? *Biological Psychiatry*, *83*(11), e51–e53. <https://doi.org/10.1016/j.biopsych.2018.04.007>
- Zhu, J., Fan, F., McCarthy, D. M., Zhang, L., Cannon, E. N., Spencer, T. J., ... Bhide, P. G. (2017). A prenatal nicotine exposure mouse model of methylphenidate responsive ADHD-associated cognitive phenotypes. *International Journal of Developmental Neuroscience*, *58*, 26–34. <https://doi.org/10.1016/j.ijdevneu.2017.01.014>
- Zhu, J., & Reith, M. E. A. (2008). Role of the dopamine transporter in the action of psychostimulants, nicotine, and other drugs of abuse. *CNS & Neurological Disorders Drug Targets*, *7*(5), 393–409. Retrieved from <http://www.ncbi.nlm.nih.gov/pubmed/19128199>
- Zhu, J., Zhang, X., Xu, Y., Spencer, T. J., Biederman, J., & Bhide, P. G. (2012). Prenatal nicotine exposure mouse model showing hyperactivity, reduced cingulate cortex volume, reduced dopamine turnover, and responsiveness to oral methylphenidate treatment. *The Journal of Neuroscience : The Official Journal of the Society for Neuroscience*, *32*(27), 9410–9418. <https://doi.org/10.1523/JNEUROSCI.1041-12.2012>

8 ACKNOWLEDGMENTS

I would like to take this opportunity to thank and express my deep appreciation to whom has supported me during my Ph.D. work.

Firstly, I would like to express my deep appreciation to Prof. Andreas Reif and Prof. Michaela Müller-McNicoll, my Ph.D. supervisors, for their guidance, encouragement and useful critiques of this research work.

I would like to express my sincere gratitude to my research group leader, Dr. Sarah Kittel-Schneider, for her continuous support of my Ph.D. study. Without her precious encouragement and constructive suggestions, it would have not been possible to conduct this research.

I would like to express my very great appreciation to all the professors of the MiND project and my fellow ESRs with whom I shared so much during these years.

My special thanks to all the people that compose the Translational Psychiatry group and the Biomarker and Cell Models Research Group with whom I have had the pleasure to work and share benches during these years.

Last but not the least, I would like to thank my family and my friends. No matter how geographically far we are, they have always been on my side.

9 CURRICULUM VITAE

Personal Information

First name: Viola Stella

Surname: Palladino

Telephone: 0039 329 1227385 0049 15207509815

E-mail: viola.stella.palladino@outlook.it

violastella.palladino@kgu.de

Date of Birth: 25/02/1989

Place of Birth: Assisi (Perugia) ITALY

Nationality: Italian



Education

March 2016, ongoing

Enrolment as a PhD candidate at the Faculty of Biological Sciences - Goethe University Frankfurt

May 2015

Position as an Early Stage Researcher (ESR) within the EU Marie Skłodowska-Curie project Innovative Training Network (ITN) MiND <https://mind-project.eu>

July 2014

Master's degree in Neurobiology. Two-year MSc program at Sapienza University of Rome, Italy (Corso di Laurea Magistrale in Neurobiologia).

Graduation score: 110 cum laude / 110 (First class honours). Thesis title: "Effects of a post-natal treatment with oxytocin in a murine model of Autism Spectrum Disorders (ASD)". Supervisors: prof. Andrea Mele; Francesca R. D'Amato.

July 20, 2012

Bachelor's Degree in Biology. Three-year bachelor's degree program at Sapienza University of Rome, Italy (Corso di Laurea Triennale in Scienze Biologiche).

Thesis title: "Nutritional enrichment in Omega-3 and Behavioural Development in Mouse". Supervisors: prof. Andrea Mele; Francesca R. D'Amato.

2003-2008

High School Diploma in Foreign languages (Liceo Linguistico) "Giordano Bruno", Perugia, Italy. Graduation score: 100/100.

Professional Training

November 2018

one week Industrial training on IPs-derived dopaminergic neurons handling at LIFE&BRAIN Gmbh, Bonn, Germany

June 2018

FENS-SfN Summer School 2018 on Neural stem cells, brain organoids and brain repair, Bertinoro, Italy

May 2018

Training course "Intellectual property rights and patenting", Vall d'Hebron Research Institute (VHIR), Barcelona, Spain

November 2017

Training course "Human Genome", University of Barcelona, Spain

July 2017

Training course "Model systems in science" University of Leicester, UK

May 2017

Training course "Professional Skills Development Programme", Imperial College London, UK

June 2017

one week Industrial training for researcher at Prestwick Chemical Pc, Strasbourg, France

July 2016

Training course "Clinical aspects of psychiatry" Goethe University Hospital Frankfurt, Germany

November 2015

Training course "Introduction in Neuroscience" University of Bergen, Norway

August 1st 2015, ongoing

Experimental activity as Early Stage Researcher (ESR) in the Laboratory of Translational Psychiatry at the Department of Psychiatry, Psychosomatics and Psychotherapy of the University Hospital of Frankfurt under professor Andreas Reif's supervision. Object: development of a new cellular model systems (human induced pluripotent stem cells, dopaminergic neurons) to investigate the pathomechanism of Attention deficit hyperactivity disorder (ADHD).

June 2014

Training course "Use of statistics in biomedical research", Italian Association for Laboratory animals science (AISAL), Rome, Italy

2012-2014

Experimental activity for the Master thesis. Doctor D'Amato laboratory of Psychobiology (Cellular Biology and Neurobiology Institute, National Centre of Research IBCN- CNR), Rome,

Italy. Main occupation: planning and bibliographical research, tests execution, data analysis, mouse colony maintenance.

January- July 2012

Experimental activity for the Bachelor thesis. Doctor D'Amato laboratory of Psychobiology (Cellular Biology and Neurobiology Institute, National Centre of Research IBCN- CNR), Rome, Italy. Main occupation: planning and bibliographical research, tests execution, data analysis, mouse colony maintenance.

Conferences and Meetings

July 7-11, 2018

11th FENS Forum of Neuroscience, Berlin, Germany.

Poster presentation: *"Investigation of PARK2 copy number variations associated with ADHD in different patient-derived cell models."* Palladino VS, Cipta NO, Frank L, Grein A, Chiocchetti A, Reif A, Kittel-Schneider S

June 13-15, 2018

5th Rhine main neuroscience network rmn² Biennial Meeting, Oberwesel, Germany.

Poster presentation: *"Modelling ADHD in a dish: evaluation of PARK2 copy number variations in different patient-derived cell models"* Palladino VS, Cipta NO, Frank L, Grein AJ, Chiocchetti A, Reif A, Kittel-Schneider S

May 31 and June 1, 2018

MiND International Conference, Barcelona, Spain.

March 9-12 2017

ECNP Workshop for Junior Scientists in Europe

Poster presentation *"Creation of a new cellular model system: modelling attention deficit hyperactivity disorder in a dish"* Palladino VS, Kittel-Schneider S, Auer J, Leish M, Reif A

Language Skills

Italian: Mother tongue

English: Proficient user

French: Independent user

Spanish: Independent user

German: Basic User

Professional Expertise's

Molecular techniques

Expert user of the most used molecular techniques: RT-PCR, RT-qPCR, primer design, ELISA, Western Bot, luminescence and fluorescence assays, gDNA extraction, RNA extraction, protein extraction.

Skilled user of Immunofluorescence techniques and Microscope handling.

Cell culture

Maintenance, propagation and preservation of different cell types cultures (Fibroblasts, PBMC, HEK, Human Induced Pluripotent Stem Cells, HiPSC-derived neurons).
Cell-fate reprogramming by viral transfection for staminality induction and dopaminergic neuron induction.

Electrophysiology

Basic competence in patch clamp intracellular recording.

Animal behaviour and Pharmacology

Experience in mouse handling and manipulation
Practical ability in the most used behavioural and social tests in rodents during infancy and adulthood. Proficient user of several behavioural data analysis programs.
Drug administration in adult mouse and pups

Statistical analysis

Good statistical knowledge and command of IBM SPSS Software.

Computer skills

Proficient with most Microsoft Office tools (Microsoft Word, Excel, PowerPoint).
Expert user of Fiji-ImageJ for image analysis and Genex ver6 (Biomcc) for RT-qPCR data analysis.

Scholarships

From 2015 to 2018: Winner of a scholarship as an Early Stage Researcher (ESR) within the EU Marie Skłodowska-Curie project MiND

From 2008 till 2014 LazioDisu scholarship (Ente Per il Diritto allo Studio nel Lazio).

10 LIST OF PUBLICATIONS

PUBLISHED

Cross-species models of Attention Deficit/Hyperactivity Disorder and autism spectrum disorder: lessons from CNTNAP2, ADGRL3, and PARK2.

Elisa Dalla Vecchia*, Niall Mortimer*, **Viola Stella Palladino***, Sarah Kittel-Schneider, Klaus-Peter Lesch, Andreas Reif, Annette Schenck and William H.J. Norton (2018).

Psychiatric Genetics. <https://doi.org/10.1097/YPG.0000000000000211>

* shared first authorship

Generation of human induced pluripotent stem cell lines (HiPSC) from one bipolar disorder patient carrier of a DGKH risk haplotype and one non-risk-variant-carrier bipolar disorder patient.

Viola Stella Palladino, Nadia Omega Cipta Subrata, Andreas Geburtig-Chiocchetti, Rhiannon McNeill, Per Hoffmann, Andreas Reif and Sarah Kittel-Schneider (2018).

Stem Cell Research, 32, 104–109. <https://doi.org/10.1016/j.scr.2018.09.008>

Region specific up-regulation of oxytocin receptors in the opioid oprm1^(-/-) mouse model of autism.

Valentina Gigliucci, Marianna Leonzino, Marta Busnelli, Alessandra Luchetti, **Viola Stella Palladino**, Francesca R. D'Amato and Bice Chini (2014).

Frontiers in Pediatrics, 2, 91. <https://doi.org/10.3389/fped.2014.00091>

ONGOING

The role of pre-, peri- and postnatal risk factors in bipolar disorder and adult ADHD.

Franziska Tole, Juliane Kopf, Katrin Schröter, **Viola Stella Palladino**, Christian Jacob, Andreas Reif and Sarah Kittel-Schneider

Revised version submitted to Journal of Neural Transmission

Genetic risk factors and gene-environment interactions in adult and childhood attention deficit hyperactivity disorder.

Viola Stella Palladino, Rhiannon McNeill, Andreas Reif, Sarah Kittel-Schneider

Revised version submitted to Psychiatric Genetics

Investigation of PARK2 Copy Number Variations in blood, fibroblasts and human Induced pluripotent stem cells from aADHD patients.

Viola Stella Palladino, Andreas Geburtig-Chiocchetti, Lukas Frank, Heike Weber, Katharina Günther, Frank Edenhofer, Andreas Reif and Sarah Kittel-Schneider

IN PREPARATION expected submission February 2019

Effects of Nicotine exposure on HiPSC- derived dopaminergic neurons from aADHD patients PARK2 CNVs carriers.

Viola Stella Palladino, Lukas Frank, Schumacher Nina, Andreas Reif and Sarah Kittel-Schneider

IN PREPARATION expected submission May 2019